Electrochemical Society

New York Meeting Program Issue

Better cell operations

The technical skills and experienced know-how of the men who operate mercury cells, are most important factors in low cost chlorine-caustic production.

Equally important is the superior performance of GLC anodes, which are "custom made" to individual cell requirements.

FREE - This illustration of cell building has been handsomely reproduced with no advertising text. We will be pleased to send you one of these reproductions with our compliments. Simply write to Dept. J-3.

ELECTRODE
GLC®
DIVISION

GREAT LAKES CARBON CORPORATION

18 EAST 48TH STREET, NEW YORK 17, N.Y. OFFICES IN PRINCIPAL CITIES

EDITORIAL STAFF

R. J. McKay, Chairman, Publication Committee

Cecil V. King, Editor

Norman Hackerman, Technical Editor

Ruth G. Sterns, Managing Editor

U. B. Thomas, News Editor

H. W. Salzberg, Book Review Editor

Natalie Michalski, Assistant Editor

DIVISIONAL EDITORS

W. C. Vosburgh, Battery

J. E. Draley, Corrosion, I

R. T. Foley, Corrosion, II

John J. Chapman, Electric Insulation

Abner Brenner, Electrodeposition

H. C. Froelich, Electronics

D. H. Baird, Electronics—Semiconductors

Sherlock Swann, Jr., Electro-Organic

John M. Blocher, Jr., Electrothermics and Metallurgy, I

A. U. Seybolt, Electrothermics and Metallurgy, II

W. C. Gardiner, Industrial Electrolytic

C. W. Tobias, Theoretical Electrochemistry, I

A. J. de Bethune, Theoretical Electrochemistry, II

REGIONAL EDITORS

Howard T. Francis, Chicago

Joseph Schulein, Pacific Northwest

J. C. Schumacher, Los Angeles

G. W. Heise, Cleveland

G. H. Fetterley, Niagara Falls

Oliver Osborn, Houston

Earl A. Gulbransen, Pittsburgh

A. C. Holm, Canada

J. W. Cuthbertson, Great Britain

T. L. Rama Char, India

ADVERTISING OFFICE

ECS
1860 Broadway, New York 23, N. Y.

ECS OFFICERS

Norman Hackerman, President
University of Texas, Austin, Texas

Sherlock Swann, Jr., Vice-President
University of Illinois, Urbana, Ill.

W. C. Gardiner, Vice-President
Olin Mathieson Chemical Corp., Niagara Falls, N. Y.

R. A. Schaefer, Vice-President
Cleveland Graphite Bronze Div., Clevite Corp., Cleveland, Ohio

Lyle I. Gilbertson, Treasurer
Air Reduction Co., Murray Hill, N. J.

Henry B. Linford, Secretary
Columbia University, New York, N. Y.

Robert K. Shannon, Assistant Secretary
National Headquarters, The ECS, 1860 Broadway, New York 23, N. Y.

Journal of the Electrochemical Society

MARCH 1958 **VOL. 105 • NO. 3**

CONTENTS

Editorial

Educational Standards 35C

Technical Papers

Convection and Film Instability; Copper Anodes in Hydrochloric Acid. *R. S. Cooper and J. H. Bartlett* 109

A Reaction Rate Study of the Corrosion of Low-Hafnium Zirconium in Aqueous Hydrofluoric Acid Solutions. *T. Smith and G. R. Hill* 117

Metal-Water Reactions, VI. Kinetics of the Reactions of Water Vapor with Strontium and Barium. *H. J. Svec and H. G. Staley* 121

Phase Equilibria in the System ZnO-P_2O_5. *F. L. Katnack and F. A. Hummel* 125

The Luminescence of Self-Coactivated ZnS:Cu. *M. H. Aven and R. M. Potter* 134

Conductivity and Energy Gap Measurements of Some Relatives of Phthalocyanine. *W. Felmayer and I. Wolf* 141

The Concentration of Hydrogen in Nickel under Hydrogen Ion Bombardment. *J. Morrison and J. J. Lander* 145

Iron and Phosphate Slag from Byproduct Ferrophosphorus. *J. M. Potts, W. C. Scott, Jr., J. U. Campbell, and J. A. Wilbanks* 148

Electrolytic Production of Sodium Perchlorate Using Lead Dioxide Anodes. *J. C. Schumacher, D. R. Stern, and P. R. Graham* 151

Dissolution of Metals in Aqueous Acid Solutions. II. Depolarized Dissolution of Mild Steel. *A. C. Makrides and N. Hackerman* 156

Anodic Polarization of Titanium in Nonaqueous Base Etching Solutions. *M. Eisenberg and R. E. DeLaRue* 162

Technical Note

Junction Delineation in Silicon by Gold Chemiplating. *S. J. Silverman and D. R. Benn* 170

Technical Review

A Review of the Measurement of the Quantum Efficiency of Inorganic Phosphors. *J. Tregellas-Williams* 173

Current Affairs

Complete New York Meeting Program 37C

Perkin Medal Award to W. J. Kroll 58C

ECS Future Meeting Dates 34C
Section News 59C
Division News 60C
New Members 61C
Personals 62C
News Items 64C
ECS Membership Statistics 64C
Announcements from Publishers 66C
Book Reviews 66C
Literature from Industry 68C
Employment Situations 68C

Published monthly by The Electrochemical Society, Inc., from Manchester, N. H., **Executive Offices, Editorial Office** and **Circulation Dept.**, and **Advertising Office** at 1860 Broadway, New York 23, N. Y., combining the JOURNAL and TRANSACTIONS OF THE ELECTROCHEMICAL SOCIETY. Statements and opinions given in articles and papers in the JOURNAL OF THE ELECTROCHEMICAL SOCIETY are those of the contributors, and The Electrochemical Society assumes no responsibility for them. Nondeductible subscription to members $5.00; subscription to nonmembers $18.00. Single copies $1.25 to members, $1.75 to nonmembers.

Copyright 1958 by The Electrochemical Society, Inc.

Entered as second-class matter at the Post Office at Manchester, N. H., under the act of August 24, 1912.

Where does progress begin?

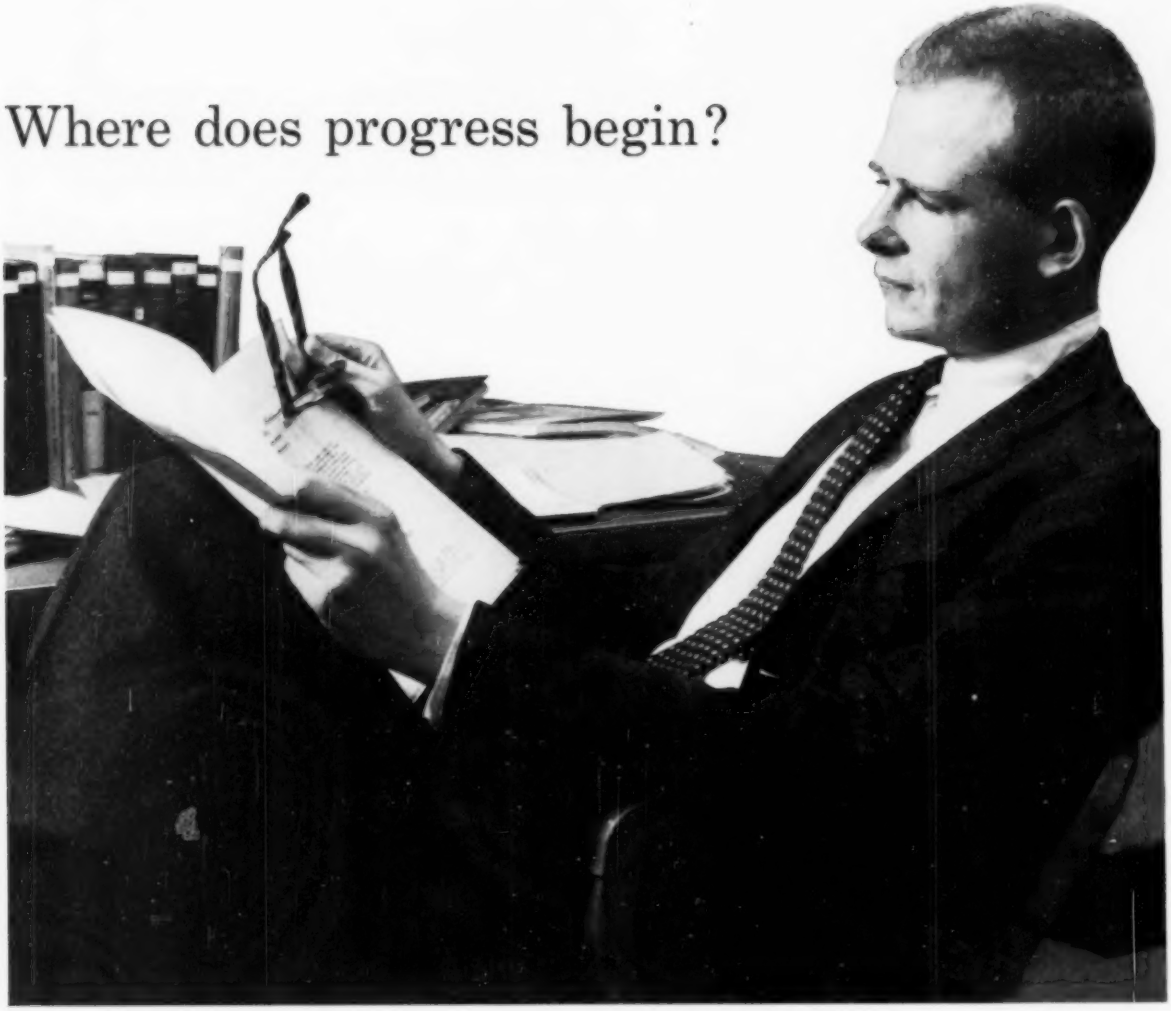

Kendall Preston Jr., S.M. in engineering from Harvard University . . .
graduate of the Laboratories' Communications Development Training Program.

Progress begins in the mind—in the perception and appreciation of new ideas. In the past the ideas that sparked progress too often had to wait on the random interest of genius. Today more and more new ideas come from men trained to an awareness of that which is yet to be accomplished.

At Bell Laboratories, communications science is entering upon its most challenging era in history. As never before, progress will depend upon men who have acquired the special training needed to think creatively in this exciting field.

Bell Laboratories provides the young college graduate with unique opportunities to develop his creative abilities. During his first two years, he spends two or three days a week as part of his job, taking postgraduate courses in basic mathematics, physics and electronics. This he does at a graduate study center which has been established at the Laboratories by New York University. As he gathers a broad fundamental knowledge which will enable him to tackle every type of communications problem, he also gathers credits toward advanced degrees. To round out his education, he spends a third year on special phases of communications technology.

By helping scientists and engineers to reach their top development, Bell Laboratories has helped to make your telephone system the world's best—and will keep it so.

BELL TELEPHONE LABORATORIES

WORLD CENTER OF COMMUNICATIONS RESEARCH AND DEVELOPMENT

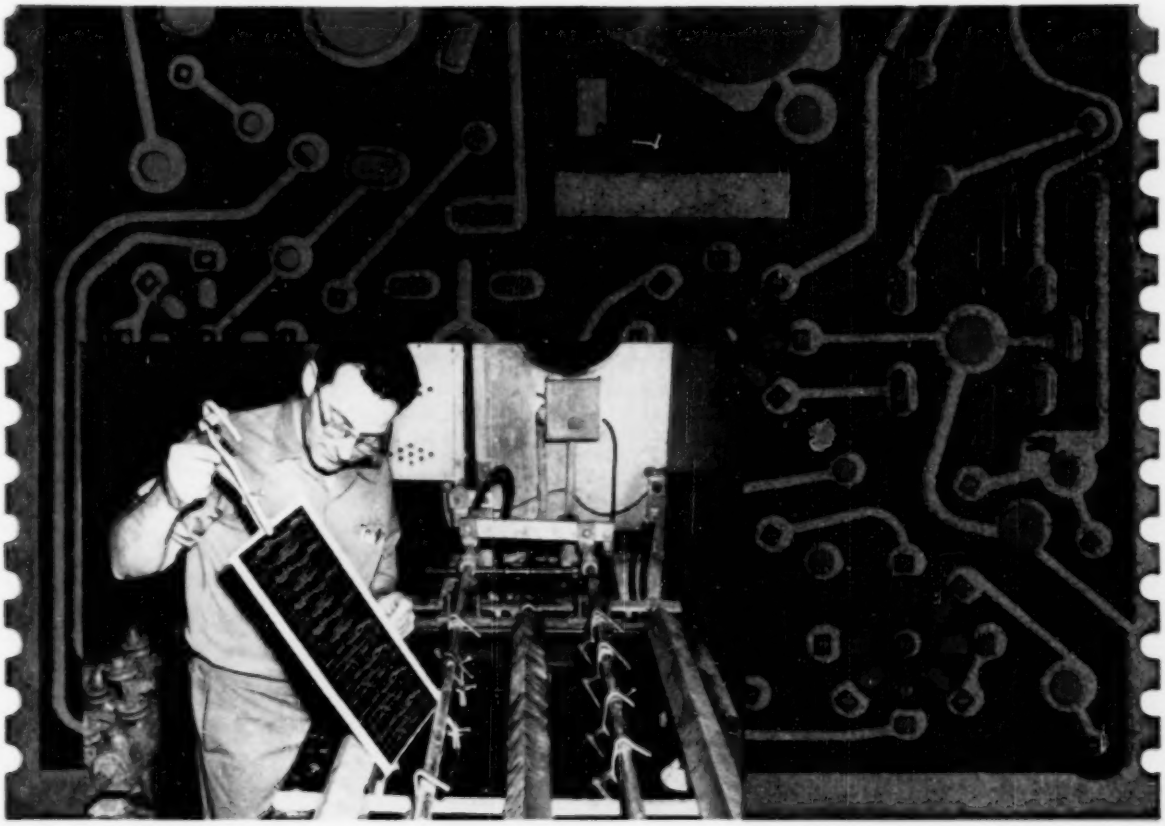

HOW TO PLATE PRINTED CIRCUITS

FASTER, BETTER, AT LOWER COST

...with B&A Fluoborates

First step—use B&A copper fluoborate for high-speed copper plating of thick, high quality circuits.

Second step—use B&A lead-tin fluoborate for maximum solderability (60:40 tin-lead deposit).

Advantages: Both of these high purity fluoborate plating solutions come in concentrated solution form. They give you easy bath make-up and easy control. Since anode and cathode efficiencies approximate 100%, you get easy maintenance, too. They require no mixing or dissolving, and offer excellent bath stability, good anode corrosion.

Result: You produce *better* printed circuits, *faster* and *at lower cost—more easily*, too!

Mail coupon now for comprehensive technical bulletins giving complete information on these improved plating techniques for printed circuits.

BAKER & ADAMSON®
Fine Chemicals

GENERAL CHEMICAL DIVISION
ALLIED CHEMICAL & DYE CORPORATION
40 Rector Street, New York 6, N. Y.

BAKER & ADAMSON PRODUCTS
GENERAL CHEMICAL DIVISION
ALLIED CHEMICAL & DYE CORPORATION
40 Rector Street, New York 6, N. Y.

Please send technical bulletins on the use of B&A Fluoborates in the production of printed circuits.

Name_____

Title_____

Company_____

Address_____

City_____ Zone____ State_____ JE-3

FUTURE MEETINGS OF
The Electrochemical Society

New York, N. Y., April 27, 28, 29, 30, and May 1, 1958

Headquarters at the Statler Hotel

Sessions will be scheduled on
Electric Insulation, Electronics (Luminescence and Semiconductors), Electrothermics and Metallurgy, Electrothermics and Metallurgy—Semiconductors Joint Symposium, Electrothermics and Metallurgy—Corrosion Joint Symposium, Industrial Electrolytics, and Theoretical Electrochemistry (including a symposium on "Electrokinetic and Membrane Phenomena")

* * *

Ottawa, Canada, September 28, 29, 30, October 1, and 2, 1958

Headquarters at the Chateau Laurier

Sessions probably will be scheduled on
Batteries, Corrosion, Electrodeposition (including symposia on "Electrodeposition on Uncommon Metals" and "Chemical and Electropolishing"), Electronics (Semiconductors), Electro-Organics, and Electrothermics and Metallurgy

* * *

Philadelphia, Pa., May 3, 4, 5, 6, and 7, 1959

Headquarters at the Sheraton Hotel

* * *

Columbus, Ohio, October 18, 19, 20, 21, and 22, 1959

Headquarters at the Deshler-Hilton Hotel

* * *

Chicago, Ill., May 1, 2, 3, 4, and 5, 1960

Headquarters at the Lasalle Hotel

* * *

Houston, Texas, October 9, 10, 11, 12, and 13, 1960

Headquarters at the Shamrock Hotel

* * *

Papers are now being solicited for the meeting to be held in Ottawa, Canada, September 28-October 2, 1958. Triplicate copies of each abstract (*not exceeding 75 words in length*) are due at the Secretary's Office, 1860 Broadway, New York 23, N. Y., *not later than June 2, 1958* in order to be included in the program. *Please indicate on abstract for which Division's symposium the paper is to be scheduled.* Complete manuscripts should be sent in triplicate to the Managing Editor of the JOURNAL at 1860 Broadway, New York 23, N. Y.

Editorial

Educational Standards

FIFTY years ago many American children went to small elementary schools where one teacher, or perhaps two, handled the entire eight-year curriculum. The teachers had no college diplomas, perhaps a term or a year in a nearby "Normal School," but, at least ideally, they were sincere and devoted and had the ability to handle children. They could insist that the children learn the limited daily textbook assignments and give them the opportunity to learn much more. Disciplinary problems were not serious and the teacher had a rather free hand when necessary. The schoolroom was quiet during school hours; bedlam broke loose at the recess signal and the teacher joined wholeheartedly in the fun.

The day was not long enough for a full program of classes, and two or three grades were combined for each recitation. A pupil could be assigned according to his ability. If he were weak in arithmetic he could get a review with the younger children while trying to keep up in his own class. The Friday afternoon spelling and "ciphering" contests created keen competition and a resolve to improve. The brighter pupil could finish the curriculum and be certified for high school in six or seven years instead of the usual eight.

We do not advocate a return to the little red brick school house, but we do welcome the present searching inquiries into the aims and operations of the entire American school system. Many educators and capable public men do not believe that the schools have lived up to the standards we should expect of them. Possibly some people raised their standards suddenly when the Russian satellites went up. Still, there is no doubt that many children do graduate from elementary school and high school without the knowledge, the rigorous training, or the discipline which should be the products of acceptable standards. It is even rumored that many college students profit more from growing older than from what they learn.

Many reasons are given for this unsatisfactory state of affairs, all of them probably valid in selected areas. A most important factor, it seems to us, is that the school system of a nation reflects that nation's way of life. If discipline is poor at home and on the street, then it must be poor in the schools. If good writing and accurate arithmetic are unimportant in living, then they are neglected in the schools. If we were an austere, disciplined, self-denying people dedicated to something like, for example, the maximum attainment of knowledge, then our schools would be operated quite differently.

The solution to our present difficulties and desires is not an attempt at quick reform throughout the school system, which cannot be accomplished anyway. If we decide that more scientists are needed, the short-range solution is to enlarge and intensify the effort, which has been made to some extent for many years, to find the young people with scientific ability and interest and offer them inducements to study science. Part of the longer-range solution is to encourage more and sounder teaching of scientific principle and disciplines at every school level. Efforts are being made in this direction, but they can be really successful only if the population as a whole understands and accepts them.

—CVK

NOW!

...Greatly Reduced Clogging of Diaphragms

...Lower Cell Maintenance Costs

...Longer Anode Life

Costly, troublesome clogging of diaphragms due to the oil impregnant in conventional anodes, is materially lessened by the new Stackpole *"GraphAnodes."* Cell maintenance costs are reduced accordingly.

Better results are achieved because Stackpole *GraphAnodes* present a uniform, low-porosity surface to the electrolyte. The graphite is consumed slowly and evenly. It does not slough off to clog the diaphragm or contaminate the cell.

Let Stackpole arrange for a convincing demonstration of these new anodes on your own equipment. You be the judge—and, by way of convincing proof we suggest that you pay particular attention to the reduced frequency of diaphragm renewals.

STACKPOLE CARBON COMPANY
St. Marys, Pa.

STACKPOLE GraphAnodes

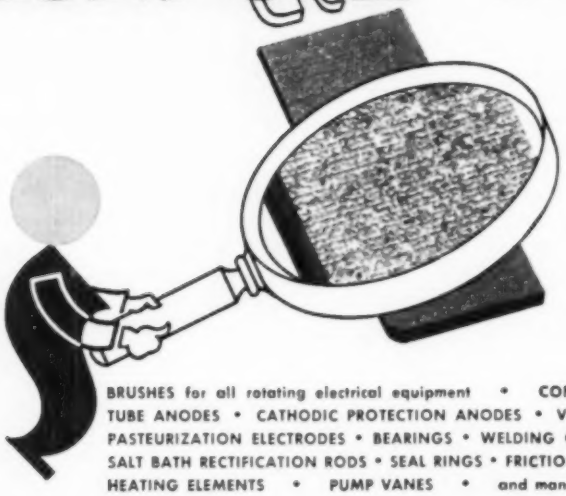

MAGNIFIED, UNRETOUCHED PHOTO... shows uniform structure of Stackpole *GraphAnodes*. The low-porosity surface assures that electrolyte will act on the surface, not below to cause premature anode deterioration and cell contamination by droppings of unconsumed graphite particles.

BRUSHES for all rotating electrical equipment • CONTACTS (carbon-graphite and metal powder types) TUBE ANODES • CATHODIC PROTECTION ANODES • VOLTAGE REGULATOR DISCS • WATER HEATER and PASTEURIZATION ELECTRODES • BEARINGS • WELDING CARBONS • MOLDS AND DIES • POROUS CARBON SALT BATH RECTIFICATION RODS • SEAL RINGS • FRICTION SEGMENTS • CLUTCH RINGS • ELECTRIC FURNACE HEATING ELEMENTS • PUMP VANES • and many other carbon, graphite, and electronic components.

Convection and Film Instability

Copper Anodes in Hydrochloric Acid

R. S. Cooper and J. H. Bartlett

Department of Physics, University of Illinois, Urbana, Illinois

ABSTRACT

In the Cu/HCl system, when natural convection occurs, there are two steady-state current plateaus. On the first of these ($-0.28<V<-0.05$), copper dissolves only in the cuprous form, and the value of the current agrees with that predicted by the Tobias theory of natural convection. On the second plateau, up to 30% of the copper is dissolved as cupric ions. When the circuit is interrupted, the resistance of the CuCl layer decays primarily due to opening of its pores, the pore area increasing linearly with time. Oscillations are found at the anode voltage region below which there is no layer and above which the layer can remain on the electrode indefinitely. A kinetic explanation of oscillations is proposed, and is in accord with the observations.

In the study of the anodic behavior of Cu in HCl, it has been shown (1) that the phenomena of overshoot and oscillation, as well as the existence of a nonzero steady-state current, are possible only if convection is allowed to take place.

The process of convection is a complicated one, and at first sight one might suppose that quantitative conclusions would be difficult to obtain. Nevertheless, progress has been made in the theory (2), at least as regards the steady-state behavior. If the composition of the convection layer is known, perhaps by deduction from schlieren and other information, then the rate at which the reaction products are removed by diffusion and convection may be calculated, and thus the value of the steady-state current. In the present paper, it is shown that theory and experiment agree well.

The manner of approach to the steady state is more difficult to explain, but even here one can at least clarify some aspects of it. Initially the main process is the deposition of Cl^- from solution to form a cuprous chloride layer, and this has precedence until the layer is complete. Any material which has been convected downward during this stage (time less than 3 sec) is not sufficient to form a stream from the bottom of the anode. However, once the layer is complete, or almost so, the current is reduced by the layer resistance, and the bulk removal process becomes predominant. The initial thickness of the CuCl layer is a function of the plateau current i_p. If this thickness is greater than the steady-state value, one may expect an adjustment to occur such that the thickness decreases, with pore area constant, and the current will rise from a minimum value. On the assumption that the thickness decreases at a rate proportional to the excess of removal current over actual current, it is possible, as will be shown, to account for the shape of the current vs. time curve after the minimum.

It had previously been a puzzle as to what is responsible for the higher current on the second steady-state plateau. Accordingly, weight-loss determinations were made, and showed that a new reaction involving cupric ions comes in. On the basis of a simple model, it now seems possible to account for the value of the above-mentioned current.

Also, previous measurements (3) of the decay of layer resistance had not been made for times sufficiently short so that one could draw good conclusions about the mechanism. This has now been remedied, and it seems certain that the process which is most important electrically is the opening of the pores.

The mechanism underlying oscillations has been uncertain. Bonhoeffer and Gerischer (4) tried to construct a theory in which a Cu_2O layer was involved. In the previous work (1), the second current-time plateau was found to be much more prominent at lower concentrations, and it seemed therefore that the OH^- ion is involved. Subsequent observations reveal that CuCl is also deposited during this plateau, and there still is no direct evidence for Cu_2O formation, even though electron diffraction techniques allow the detection of very small quantities. The above theory remains, therefore, very much in doubt, especially since our observations show the oscillations to be confined to the boundary region between where a layer exists and where it does not. Hence the present article contains a discussion of how one can expect oscillations even in the absence of a Cu_2O layer.

Experimental arrangement.—The experimental apparatus and methods, as well as the associated nomenclature, are the same as described in previous studies (1,3,5). These consisted of a simple cell with an 0.1*N* calomel reference electrode and the necessary equipment for applying and measuring voltages and currents. Circular anodes (0.02 cm^2) were

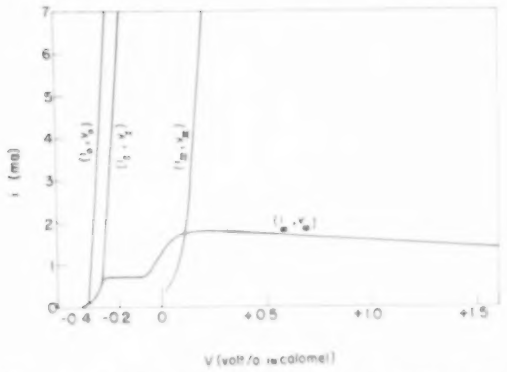

Fig. 1. Characteristic curves for an unshielded anode (0.02 cm²) with exposed face vertical, in 2N HCl, showing locus of initial current and voltage (i_0,V_0), of stationary values of current and voltage for the first plateau (i_1,V_1), for the second plateau (i_{11},V_{11}), and for the steady state (i_∞,V_∞).

used for the most part, the electrolyte being 2*N* HCl.

Results

The Steady State

As may be seen from Fig. 1, the steady-state current-voltage curve is similar in shape to a polarogram, having two plateaus,[1] i.e., regions where the current is approximately independent of voltage. The steady state (indicated by the subscript ∞) is usually reached in from 1 to 5 min, except at high voltages where the time may be longer. The curve for i_∞ vs. V_∞ does not depend on the choice of external parameters (E and R), nor on the values of the initial current or initial layer thickness.

The low-voltage region. — The region below −0.24 v is governed by a polarization equation of the form

$$V = a + b \log i \qquad \text{(I)}$$

This is the form expected according to the reaction rate theory of Glasstone, Laidler, and Eyring (6), applied to anodic dissolution of a metal; with

[1] These are not to be confused with the current-time plateaus of ref. (1).

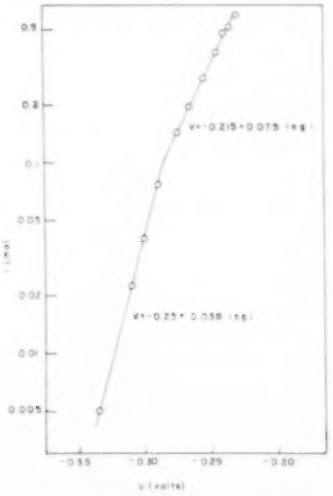

Fig. 2. Current vs. voltage in the steady state, at low voltages for a Cu anode (0.02 cm²) in 2N HCl.

$$b = \frac{0.059}{Z\,\alpha} \qquad \text{(II)}$$

where Z is the charge transferred and α is a constant lying between 0 and 1. Alpha is sometimes found to be greater than one, and this has been interpreted as due to mechanisms involving more than one ion (7). The results (Fig. 2) show a break in the curve at −0.28 v, corresponding to the potential of Cu in CuCl-saturated 2*N* HCl (1). Below −0.28 v, $b = 0.038$, and above that voltage b abruptly doubles, becoming 0.075. The value for b below −0.28 v yields a value for α (= 1.55) greater than 1, which indicates a mechanism involving at least two ions, and thus favors the reaction

$$Cu + 2Cl^- \rightarrow CuCl_2^- + e^- \qquad \text{(III)}$$

as a mechanism rather than direct formation of Cu^+ ion, followed by complex ion formation in solution. The fact that b exactly doubles may mean that the effective α is the same in both cases, and that the larger value of b (corresponding to $\alpha = 0.785$) is associated with a reaction involving only one ion. The reaction

$$Cu + Cl^- \rightarrow CuCl + e^- \qquad \text{(IV)}$$

is such a reaction, and all our available evidence indicates that it is the one which occurs.

The first steady-state plateau.—For $V \geq -0.28$ v, an anodic film, which was identified as CuCl by means of electron diffraction, was observed on the electrode. On the first plateau, i.e., for the range $-0.28 \leq V_\infty \leq -0.05$, no Cu^+ enters the solution (shown by weight-loss determinations). In the steady state, the current is thus accounted for wholly by the entrance of cuprous ions into solution in the form of the complex $CuCl_2^-$, which is removed from the anode region by convection and diffusion. If one assumes reasonable values for viscosity and density of the convection layer, then, as is shown below, it is possible to calculate from theory a value for the steady-state current, as well as a value for the maximum thickness of the convection layer, which is in good agreement with the experimental value.

Application of convection theory.—Tobias and coworkers (2) and Wagner (8)[2] have recently developed a theory of natural convection control at electrodes and soluble slabs, treating the mass transfer problem in the same fashion as the well-studied problem of heat transfer. A relation is developed in terms of three dimensionless groups, which written out in familiar terms is

$$\frac{i}{S} = 0.66\,\frac{zFD\,\Delta c}{y(1-t_-)}\left(\frac{\mu}{\rho D}\right)^{1/4}\left(\frac{gy^3\,\Delta\rho}{\mu^2}\right)^{1/4} \qquad \text{(V)}$$

where S is the anode area, μ is the average viscosity of the solution in the convection layer, and is approximately that of 2*N* HCl (= 10^{-2} poise); g is the acceleration of gravity; and ρ is the average density, 1.045 g/cc. Δc and $\Delta\rho$ are the differences between the bulk and interphase concentrations and densities, respectively. (These two quantities serve as

[2] In the author's case, the condition of Wagner that $|\Delta c| \ll c_0$ is not met. Instead, $|\Delta c|$ is about Δc_{max} and this leads to $x^{-1/4}$ dependence, where x is the distance from the leading edge of the electrode.

the driving force of the mass transfer process). F is the Faraday, and z the valence (= 1 here). The concentration referred to is that of the $CuCl_2^-$ complex ion. It is zero in the bulk phase and $0.24N$ at the CuCl layer surface, if there is saturation in the approximately $2N$ Cl^- solution. [That the Cl^- concentration is close to the bulk value can be seen from the schlieren photos of the steady state (11), and from a calculation (Appendix I) which shows that even under pure diffusion a small Cl^- gradient (about $0.2N$ across the layer) is sufficient to supply the steady-state Cl^- demand.] From solubility data (9), and using the densities as determined by Engle (10), $\Delta\rho = 0.026$ g/cm. y is the height of the electrode, and must be suitably averaged for one with a circular cross section. The precise evaluation is made in Appendix II and the result is $y = 0.121$ cm for the case considered here. t^- is the transport number of the $CuCl_2^-$ ion, and may be taken as zero, since the $CuCl_2^-$ ion must move against the current, and is at most one-tenth as numerous as the Cl^- and H^+ ions. D, the diffusion coefficient of $CuCl_2^-$, is estimated to be 1×10^{-5} cm²/sec, from the value for similar ions. Putting these values in Eq. (V) one obtains 32.7 ma/cm² as the limiting current density, which falls in the observed range of 30-35 ma/cm². This is strong evidence that the current on the first plateau is controlled by natural convection of the $CuCl_2^-$ away from the electrode. It is to be noted that this process is almost entirely independent of electrochemical influences, being mainly mass transfer from a solid slab of a soluble material. When the circuit is opened, this process continues unchanged as long as there is a CuCl layer on the anode surface, as is proven by schlieren observations. This fact, that the removal process is relatively independent of current fluctuations, will prove to be important for subsequent discussions of oscillations and overshoot.

The thickness of the convection layer varies along the height of the electrode, being zero at the top and a maximum at the bottom. The maximum thickness was found to be independent of current density once convection had become stabilized, and was of the order of 0.02 mm as measured from schlieren photographs (11). This agrees with the recent theoretical result of Keulegen (12) for the maximum convection layer thickness:

$$\delta_c = 3.33 \left(\frac{\mu D y}{g \Delta\rho} \right)^{1/4} \qquad \text{(VI)}$$

which yields a value for δ_c of 0.185 mm, for an electrode 2.5 mm high in $2N$ HCl.

The Second Steady-State Plateau.—Electrochemical experiments show that the increase in current above −0.05 v is at least partially due to the formation of Cu^{++} ions, which go directly into solution through the pores in the CuCl layer. Weight loss determinations were carried out at −0.02, 0.4, 0.5, and 0.96 v, and the fractions of cupric ion formed were found to be 13%, 29%, 32%, and 28%, respectively. The first result corresponds to a point about half-way up on the rise between −0.05 and +0.1 v (Fig. 1), and the following three to points on the second plateau. Thus the relative Cu^{++} formation reaches a limiting value of approximately 30% of the Cu lost (equivalent to 46% of the current).

Since Cu^{++} is highly favored in concentrated solutions of copper ion, one might expect Cu^{++} formation exclusively, instead of its being limited to 30%. However, a closer analysis shows how this limiting current may come about. Assume that in the steady state there exists a porous CuCl layer with pore area S_p, that the production of more CuCl occurs according to Eq. (IV) at the Cu surface, the Cl^- passing in through the pores, and that the CuCl layer dissolves by a purely chemical action at the interface of the layer and the solution. Under these conditions the Cl^- flux through the pores will be equal to the current due to Eq. (IV). Because there is a source of Cu^{++} at the anode surface the H^+ ions (being 8 times as mobile as the Cu^{++}) will tend to migrate out of the pores, which will then be filled with a solution consisting mainly of $CuCl_2^-$. If the concentration of the $CuCl_2^-$ in the pores is uniform (molarity = c) which is reasonable on the grounds that there are appropriate sources and sinks at the end of the pores and that the mobilities, μ, are comparable, then the currents carried by the respective ions are due only to migration and are:

$$i_{Cu^{++}} = i_{Cl^-} = eS_pF\left(\frac{dN}{dt}\right)_{Cl^-} = eS_pF\mu_{Cl^-}E\,2c \qquad \text{(VII)}$$

$$i_{Cu^{++}} = 2eS_pF\left(\frac{dN}{dt}\right)_{Cu^{++}} = 2eS_pF\mu_{Cu^{++}}Ec \qquad \text{(VIII)}$$

where dN/dt is the ion flux and E is the electric field. Thus the ratio of the currents due to Cu^{++} and Cu^+ formation is equal to the ratio of the Cu^{++} and Cl^- ion mobilities (or ionic conductances). Using values at infinite dilution from Conway (13),

$$\frac{i_{Cu^{++}}}{i} = \frac{\lambda_{Cu^{++}}}{\lambda_{Cu^{++}} + \lambda_{Cl^-}} = 41.5\%$$

$$\frac{[Cu^{++}]}{[Cu^{++}] + [Cu^+]} = 26\%$$

compared to 46% and 30% experimentally, which is very good agreement considering the crude assumptions and approximations involved.

It may be possible to account for the magnitude of the current increase from the first plateau to the second. Adding the percentage of current due to Cu^{++} would increase the 0.65 ma to only 1.2 ma. If Eq. (V) is used uncritically, the added Cu^{++} (estimated to be at least 0.2 molar from schlieren data from preceding papers) approximately doubles the density difference ($\Delta\rho$) and consequently increases the convection current to about 1.4 ma, as against the observed value of 1.8 ma. However, Eq. (V) only holds for one current-carrying ionic species, so that the agreement is reasonably good.

Resistance and potential.—By breaking the circuit and observing the voltage change one can determine the open-circuit electrode potential and the electrode resistance associated with the steady state. At voltages below −0.05 v, it was found (3) that the electrode resistance is small compared to the solution resistance of about 14 ohms, and that the electrode potential varies, adjusting to the applied

voltage. The anode film is so thin or porous as to have a resistance negligible as compared to that of the solution. The variation in electrode potential is due to concentration polarization of the Cl^- ions in the pores of the layer, as was shown for the first temporal plateau (1). For applied voltages above −0.05 v the resistance increases with V_a, while the electrode potential remains constant, being in the range of −0.05 to −0.03 v. The resistance increase is associated partly with the observed (3) increase in the steady-state layer thickness (δ_s). That the electrode potential remains near the standard potential of the $Cu|Cu^{++}$ half-cell (−0.05 v) indicates that the Cu^{++} is the potential determining ion. A twofold increase of Cu^{++} concentration is equivalent to a polarization of only 0.01 v, and the maximum solubility of $CuCl_2$ (7M) limits the total polarization to 0.03 v above the standard potential. Thus, until the initiation of a new reaction with a higher electrode potential, the electrode potential must remain below −0.02 v.

Break transients.—The decay of layer resistance has been studied previously (3), but most of the data were for times greater than 30 msec, when the resistance has already dropped to less than one-tenth of its steady-state value. To obtain the missing information, it was found convenient to use the rapid-acting interruption switch (1) to obtain data for short off-times. This switch, which was motor driven, would operate from 2 to 6 times/sec, opening the circuit for periods of from 0.4 to 10 msec. Since the period between interruptions was sufficiently long for the electrode to recover completely, a complete resistance decay curve could be obtained during one run. The result for V = 2.5 v (Fig. 3) shows σ, the conductance of solution plus layer, to be a linear function of time in the early stages of the decay, namely,

$$\sigma = 0.36 \times 10^{-3} + 0.24t \qquad \text{(IX)}$$

Extrapolating this to the end of the −0.05 v potential plateau (0.29 sec) gives 14 ohms, which is the value of the solution resistance alone. Thus the linear relation for σ holds throughout the resistance decay.

It is to be noted that, while the data cover only 2% of the time of the decay, this corresponds to 75% of the resistance drop, after which the percentage uncertainty in σ becomes high. The fact that the layer resistance becomes of the order of r_s (14 ohms) or smaller does not mean that the layer has dissolved to any great extent, but rather that the pores have widened. Assuming the layer in question to be 10^{-3} cm thick, then the resistance would be 14 Ω if the pore area were as much as only 1% of the surface. Furthermore the rate of solution is not sufficient to dissolve an appreciable portion of the layer in the short times associated with the resistance decay. The film resistance (r_f) is given by:

$$r_f = \frac{\delta}{\kappa S_p} \qquad \text{(X)}$$

Since δ cannot change so rapidly and κ cannot be expected to vary much (in going from that for a $CuCl_2$ solution to that for HCl) then the major change in r_f must be due to variation in S_p, the pore area. Comparing (IX) and (X) one sees that S_p increases linearly with time. Therefore

$$S_p(t) = (S_p)_0 + kt \qquad \text{(XI)}$$

where k is a constant.

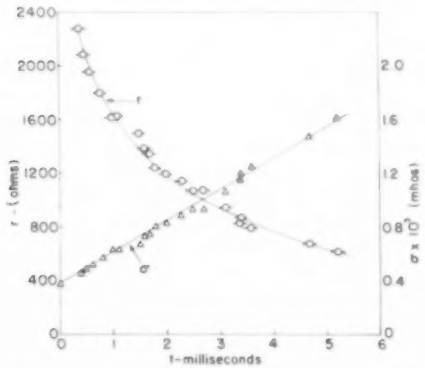

Fig. 3. Resistance and conductance vs. time for a break from the steady state (V = 2.5v). Copper anode (0.02 cm^2) in 2N HCl.

Overshoot

Overshoot is defined to be the situation where the current or voltage passes beyond its steady-state value before finally arriving there. For definiteness, the following discussion will be confined to the case where the current goes through a minimum after the completion of a plateau.

Shielded electrodes with no convection display no minimum, but rather a monotonically decreasing current. Also, unshielded vertical electrodes in low acid concentrations (small removal currents) do not show appreciable overshoot. Finally, such current minima never occur before 3 sec have passed, regardless of the duration of the plateau. Since this is approximately the time required for the initiation of convective fluid flow, this type of overshoot appears to be associated with the convection process, which removes material from the layer.

Several examples, taken with an unshielded electrode in 2*N* HCl, are reproduced in Fig. 4. The transient in Fig. 4a is typical of those with low applied voltages such that the steady state lies on the first plateau, between −0.27 and −0.05 v. As the applied voltage is increased the overshoot, $(i_s - i_{min})$, becomes at first greater, and then smaller, finally disappearing altogether (Fig. 4d).

The thickness (δ_1) of the layer originally formed during the first current plateau *depends only on the value of the current on the plateau* (i_1), and may be larger[a] than the steady-state layer thickness (δ_s) which depends only on V_a. If there were no convection, the thickness would increase indefinitely once the pore area had reached its lowest value. Obviously, if $\delta_1 > \delta_s$, the steady state will be approached only if the thickness decreases due to dissolution of the layer.

[a] The value of δ_1 is a function of i_1, and ranges from 10^{-2} cm at low current densities to 10^{-4} cm or less at high current densities. δ_s varies with V_a and has been estimated (3) to be of the order of 2×10^{-4} cm in the steady state.

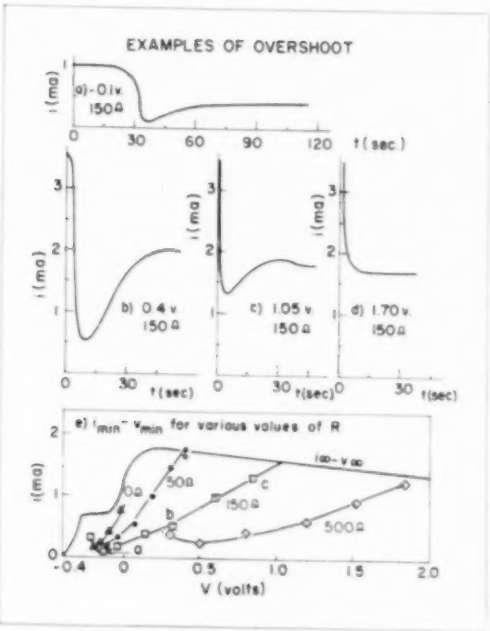

Fig. 4. (a) — (d) Current vs. time curves for a Cu anode (0.02 cm²) in 2N HCl. R = 150Ω and E is indicated on each graph. (e) Curves showing i_{min} vs. V_{min} for various values of R. The steady-state curve i_s vs. V_s is also shown, and an unshielded Cu anode (0.02 cm²) is used, in 2N HCl.

To obtain a quantitative relation for the current rise after the minimum, assume that the transient has reached the current minimum through the process of layer formation, and that sufficient time has passed for the solution and removal of the layer by convection to reach its steady-state value of i_s ($= i_\infty$). The layer will be removed by solution at a net rate proportional to $(i_s - i)$, the difference between formation and removal, assuming no complication due to varying rate of formation of Cu^{++}. If any Cu^{++} is formed, its rate of formation may vary during the overshoot, and its appearance in solution will alter the removal rate of the CuCl. Thus the following analysis is strictly valid only for $V < -0.05$ v, where $CuCl_2^-$ and CuCl are the only reaction products. The rate of solution of the layer is given by

$$\frac{d\delta}{dt} = \frac{-M(i_s - i)}{\rho SF} \qquad \text{(XI)}$$

The layer thickness may be approximated by:

$$\delta(t) = \delta_{min} - \frac{M(i_s - i)\,(t - t_{min})}{\rho SF} \quad (t \geq t_{min}) \qquad \text{(XII)}$$

The symbols δ_{min}, r_{min}, i_{min}, and t_{min} refer to those quantities at the current minimum. The current at any time is given by:

$$i = \frac{E - \epsilon}{R + r_0 + r_l} \qquad \text{(XIII)}$$

where $r_l = \dfrac{\delta(t)}{\kappa S_p}$, the layer resistance, and ϵ is the open-circuit potential. Combining Eqs. (XII) and (XIII) we have the behavior of the current after the minimum:

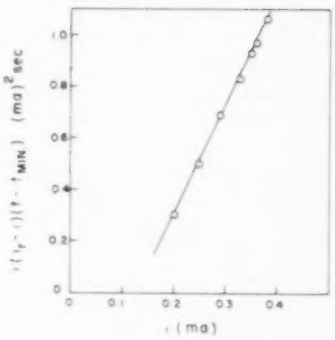

Fig. 5. Plot of $i\,(i_s - i)\,(t - t_{min})$ vs. i to test Eq. (XV). Cu anode, 0.02 cm², 2N HCl, E = −0.1 v, R = 150Ω, and $t - t_{min}$ ranges from 6 sec to 40 sec. Data from curve 4(a).

$$i = \frac{E - \epsilon}{R + r_0 + \dfrac{\delta\,\max}{\kappa S_p} - \dfrac{M(i_s - i)\,(t - t_{min})}{S_p\,\kappa\rho\,SF}} \qquad \text{(XIV)}$$

According to Eq. (XIV) i will increase with time, asymptotically approaching i_s. To compare Eq. (XIV) with experiment it is most convenient to rearrange it to

$$i(i_s - i)(t - t_{min}) = \frac{F\rho\kappa SS_p}{M}\,[(E - \epsilon) + (R + r_{min})i] \qquad \text{(XV)}$$

This is of the form $f\,(i, t) = a + bi$, and thus a plot of $i(i_s - i)\,(t - t_{min})$ vs. i must be a straight line if Eq. (XIV) is correct, and ϵ, κ, and S_p are constant during the overshoot. In the example of Fig. 4a no cupric ion is formed and it may be used as a test of Eq. (XIV). The result (Fig. 5) was a line with a slope of 4.2×10^{-4} amp-sec and an intercept of -0.6×10^{-4} amp² sec. a and b can be estimated only to an order of magnitude because of the lack of precise knowledge of $(E - \epsilon)$, κ, and S_p. Assuming values of 10^{-1} v, 10^{-2} (ohm-cm)$^{-1}$, and 10^{-4} cm², respectively, for these quantities gives $a = -0.7 \times 10^{-4}$ amp²-sec and $b = 5.4 \times 10^{-3}$ amp-sec, in good agreement with experiment. Thus the model, which pictures overshoot as due to the reduction of the initial layer thickness (δ_i) to a value determined by steady-state condition, appears to be applicable in certain cases.

Although the model used above based on the relative values of δ_i and δ_s is not quantitatively accurate in the cases involving Cu^{++} ion, it is consistent with the observed behavior of overshoot. On this model one would expect that the value of the minimum current would increase with decreasing δ_i, for at the current minimum the pore area has reached its minimum value, and the resistance of the layer is proportional to its thickness. The expected result is observed to be the case for R constant and $i_i > 2$ ma (Fig. 6), as can be seen from the fact that δ_i varies inversely with i_i. That the trend is reversed for $i_i < 2$ ma may be due to the partial solution of the layer which takes place (1) during the long plateaus associated with the low values of i_i. The dependence of i_{min} upon R at constant i_i may be related in part to the variations in amount of current carried by Cu^{++}; e.g., at $i_i = 4$ ma (Fig. 6) the lowest value of i_{min} is for a transient with no

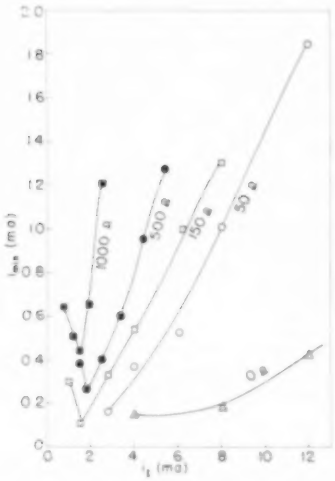

Fig. 6. Minimum current vs. current on first plateau, for various values of the external resistance R (shown on curve). Cu anode, 0.02 cm², 2N HCl.

Cu^{++} formed, and the higher values of i_{min} are associated with voltage in the range of increasing percentage of Cu^{+}. Next consider the limiting cases of overshoot (Fig. 4d) where the current assumes its steady-state value immediately after the current drop. This implies that δ_1 plus the growth in depth (1) is equal to δ_s, the steady-state layer thickness. The limiting cases of overshoot associated with larger values of δ_1 correspond to larger values of δ_s, as would be expected if the growth in depth is relatively independent of δ_1. Finally, with very high initial currents, and consequently extremely thin initial layers, no overshoot is observed.

Oscillations

Under certain conditions, with a fixed d-c voltage applied, the cell current and electrode potential undergo periodic fluctuations after approaching a quasi-stationary state, which is called here the steady state. Such oscillations have been observed and studied by Hedges (14) and Bonhoeffer (4) using large applied voltages (6 to 200 v). In this work, oscillations have been observed for low applied voltages, (Fig. 7) in the region below Cu^{++} or O_2 formation and apparently below that for oxide production. These oscillations have a period which varies in the Cu|HCl system from 10 sec to 1 min or more, and may continue indefinitely, damp out slowly, or cease abruptly after a number of cycles. Usually they have the form of relaxation oscillations, with periods of relatively constant current interrupted by sudden changes. After the current rises from the initial minimum and approaches the steady-state value, it may suddenly rise to i_1, the current on the first plateau, remain there for a time shorter than the duration of the first plateau, and fall to a minimum in a manner similar to the drop after the plateau. After passing through this minimum the current rises at a rate more rapid than that from the first overshoot, until it again becomes approximately equal to the steady-state value. The interval when $i < i_s$ is denoted by Bonhoeffer as the passive phase (Fig. 7), although considerable current is flowing. Following the passive period the current rises rapidly to i_1 (active phase) and the cycle repeats. In certain cases each phase is distinctly separate, while in others the oscillations appear almost sinusoidal. Periodic phenomena do not appear if the electrode is shielded to prevent convection, but are found in systems with natural convection or stirring. The major condition necessary for the occurrence of oscillations in this geometry and concentration is that the steady-state voltage lies in the range of −0.27 to −0.25 v, which is at the beginning of the first current-voltage plateau (Fig. 1). This is the voltage at which a solid layer of CuCl first appears. Subject to this very restrictive condition, oscillations have been found with any value of applied voltage $E > -0.26$ and external resistance $R \geq 20$. The current fluctuates above and below the steady-state current, and when the potential is too low for the production of Cu^{++} ions, the average current is exactly i_s ($V_a = -0.26$). In any one period the amount of CuCl removed during the passive period will be equal to the amount deposited during the active period. When no Cu^{++} is produced, this means area 'a' (Fig. 7) will be equal to area 'b', as is found experimentally for $E < 0$ v.

Interruption experiments were performed to observe the variation of electrode resistance and potential during the oscillations. The results (Fig. 8)

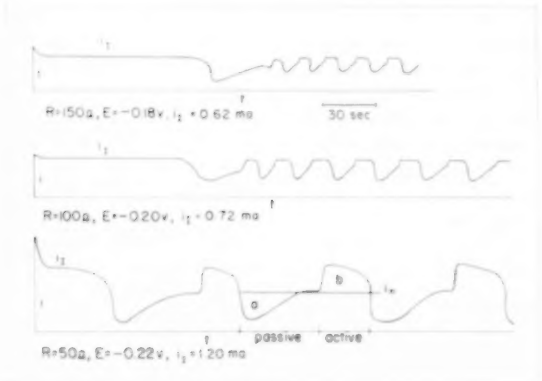

Fig. 7. Current vs. time oscillations for a Cu anode 0.02 cm² in 2N HCl.

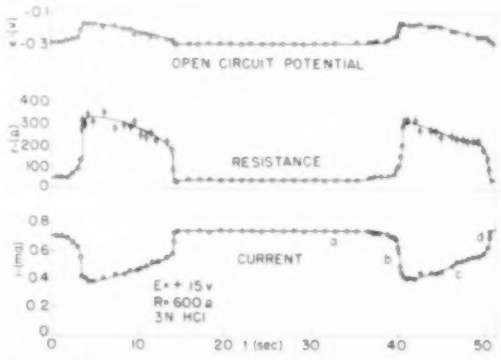

Fig. 8. Open-circuit potential, layer resistance, and current vs. time for a Cu anode 0.02 cm² in 3N HCl.

indicate that the major portion of the current change is due to variations in electrode resistance, while the potential alters by a small amount.

Discussion

The role of natural convection in determining the steady-state current-voltage characteristic has been demonstrated for a case involving a solid anode film. This process is apparently effective in controlling the current even in the presence of an additional, soluble, reaction product. Convective removal of the CuCl layer also alters the duration of current-time plateaus, which has been discussed elsewhere (1).

Overshoot has been explained on the basis of a model which assumes the completion of a relatively thick initial layer and the subsequent reduction of this layer to one with thickness determined by the steady-state conditions. This model is in general qualitative agreement with the experimental results, and quantitatively predicts the form of the current rise after the minimum. [Its general quantitative applicability is limited by the appearance of Cu^{++}, which not only adds to the current directly but also increases the rate of solution of the CuCl layer (by altering the density in the convection layer). It should be possible to investigate overshoot without this complication by choosing a suitable singly-valent system (involving a moderately soluble salt), such as Ag H_2SO_4.] The difficulty in developing a single equation which gives the current both before and after the minimum is that there apparently are at least two distinct processes occurring. The first process is that of layer formation, which usually involves both sideways growth and growth in depth, even when there is only one reaction product. The process tending to increase the current is the solution of the layer, which is strongly dependent on the removal of the dissolved salt by natural convection. The calculation of the steady-state configuration of a natural convection layer is a very complicated mathematical problem, and that of its development in time is even more complex, and so analysis from first principles will have to await further work.

An examination of the shape of the oscillations can yield important clues as to the processes which are taking place. At first, there is a current plateau followed by a drop, which has been identified as due to the formation of a CuCl layer. The current rises from the minimum and levels off. During this interval the resistance decreases, which is to be expected when the layer is being removed. At the same time, the open-circuit potential decreases, as would be the case if the Cl^- concentration should increase. This continues rather slowly for a time, and then there is a small but rapid change in the potential, which occurs because the Cu surface is suddenly exposed to Cl^- with concentration roughly the bulk value. The simultaneous rapid decrease in resistance is probably due to widening of the pores. Since the duration of the active phase is not as great as that of the first plateau, it is probable that not all of the solid layer is removed. (A similar breakdown of the layer occurs for Fe in H_2SO_4, at the lower limit for stability of the passive layer. After the minimum, the current rises slowly for a long time, and then the potential drops suddenly, as does the resistance. Current flows at a high rate, and it is some time before the passive layer is restored.)

It is now in order to consider the variation in concentration of Cl^-, the potential-determining ion. As the CuCl surface layer is formed, this concentration decreases, as is evidenced by schlieren observations. Upon completion of the layer, ϵ increases suddenly and by a large amount, indicating that the concentration at the base of the pores has decreased still more. Since the total current is now much less, the gradient of the anolyte concentration must decrease, and the concentration at the layer-solution interface must increase (to a value about that in bulk). The current density, however, is presumably just a function of ϵ and stays relatively constant, as does the gradient in the pores. Consequently, the concentration at the base of the pores rises to keep pace with that outside, and the value of ϵ goes down. When it becomes les than ϵ_0, layer can no longer be formed. However, the removal continues until the layer has been eaten away, and the cycle repeats itself.

Oscillations occur when the system can exist in two possible states neither one of which is permanently stable. The current cannot remain at its minimum value because the initial thickness of the layer is more than needed to maintain a balance between the processes of formation and removal, when the Cl^- concentration has reached its steady-state value. After the overshoot, the current can maintain a steady-state value only if enough new layer is being formed to offset the amount removed by dissolution. No new layer can be formed below $V = -0.28$ v, and it can be presumed that, in a limited range above this potential, the rate of formation is not sufficient to keep pace with the removal. Under these circumstances, the layer cannot stay on the electrode and no steady state is possible. Hence, sustained oscillations will take place.

The above oscillations represent only one extreme case of nonlinear oscillations, namely, where there are practically discontinuous jumps between two possible states. The other extreme is characterized by oscillations which are sinusoidal and of small amplitude (15), and has been found with the systems Cu|KCl and Fe|H_2SO_4. It would seem that it represents a situation where there is a more delicate balance between the two states, but further work is necessary in order to elucidate the details.

Summary

Natural convection, which aids in the solution of the layer, causes the appearance of a nonzero steady-state current, overshoot, and oscillations.

The steady state is characterized by two regions where the current is independent of voltage. In the first of these ($-0.28 < V < -0.05$) CuCl and $CuCl_2^-$ have been found to be the only reaction products, and the current is in agreement with that predicted by Tobias' theory of mass transfer by natural con-

vection. The removal process is that of a solution of a soluble slab, the CuCl being chemically dissolved by formation of the $CuCl_2^-$ complex ion, which is convected away due to the increased density of the solution. The dependence of i_c on anode area and on bulk acid concentration, as well as the diffusion layer thickness, is given correctly by the convection theory.

For $V > -0.05$, the current increases, with V, corresponding to increasing proportions of Cu^{++} ion formed, up to a limit of 30% at $V = +0.1$ v. At higher voltages the current is approximately independent of voltage. The limiting current and proportion of cupric ion has been explained on the basis of the mass transfer rate of CuCl and the relative mobilities of the Cu^{++} and Cu^{+} ions.

The steady-state electrode potential was found to be given by the same conditions holding for transients (1), i.e., for ϵ is given by the $Cu|CuCl_2^-$ potential; for $-0.28 \leq V \leq -0.05$, ϵ is determined by the chloride ion polarization. For $V > -0.05$, Cu^{++} is observed as a product and ϵ is within 0.03 v of the $Cu-Cu^{++}$ standard potential. The decay of the layer resistance has been found to be due to the opening of the pores, a process different from the bulk removal of the layer. Overshoot has been explained by noting that the initial layer thickness may be greater than that in the steady state, and thus that the current flowing on completion of the initial layer will then be less than i_c. Convection acts to reduce the layer thickness and thus increase the current. Using this model it has been possible to account quantitatively for the current rise after the minimum in certain cases, and to understand qualitatively other features of overshoot.

The oscillations which are found in the Cu HCl system have been investigated and most phases of the oscillations are understood in terms of events occurring during the ordinary transients. After the layer is complete, the decrease of total current causes an increase in anolyte concentration. This drags up the concentration at the base of the pores and lowers the electrode potential there. Below the critical value, layer formation will cease and the existing layer will continue to dissolve until the surface is bare enough for the cycle to begin again.

Acknowledgment

This reasearch was supported by the Office of Ordnance Research under Contract DA-11-022-ORD-939 to whom the authors are sincerely grateful.

Manuscript received June 6, 1957.

Any discussion of this paper will appear in a Discussion Section to be published in the December 1958 JOURNAL.

REFERENCES

1. R. S. Cooper, *This Journal*, **103**, 307 (1956).
2. C. W. Tobias, C. R. Wilke, and M. Eisenberg, *Chem. Eng. Progr.*, **49**, 663 (1953); C. R. Wilke, M. Eisenberg, and C. W. Tobias, *This Journal*, **100**, 513 (1953).
3. J. H. Bartlett and L. P. Stephenson, *This Journal*, **101**, 571 (1954).
4. K. F. Bonhoeffer and H. Gerischer, *Z. Elektrochem.*, **52**, 149 (1948).
5. J. H. Bartlett and L. P. Stephenson, *This Journal*, **99**, 504 (1952).
6. S. Glasstone, J. Laidler, and H. Eyring, "The Theory of Rate Processes," Chap. 10, McGraw Hill Book Co., New York (1941).
7. S. Glasstone, "Introduction to Electrochemistry," p. 461, D. Van Nostrand Co., New York (1951).
8. C. Wagner, *This Journal*, **104**, 129 (1957).
9. H. Le Chatelier, *Compt. rend.*, **98**, 814 (1884).
10. M. Engle, *Ann. Chem. et Phys.*, (6), **17**, 372 (1889).
11. R. S. Cooper, To be published.
12. G. Keulegan, *J. Research Nat. Bur. Standards*, **47**, 156 (1951).
13. B. E. Conway, "Electrochemical Data," Elsevier Publishing Co., Amsterdam (1955).
14. E. S. Hedges, *J. Chem. Soc.*, **1926**, 1533.
15. B. van der Pol, *Phil. Mag.*, **2**, 978 (1926).

APPENDIX I

The upper limit for the chloride ion concentration difference across the convection layer may be estimated by applying Fick's law to a stagnant diffusion layer of the same thickness. This gives

$$\Delta c = \frac{lo}{SFDZ}$$

where l is the convection layer thickness which is approximately 0.02 cm from schlieren observations (3) or a current density of 30 ma/cm^2, as found in the steady state, this gives $\Delta c = 0.2N$, which is small compared to the bulk acid concentration ($2N$). In the presence of convective flow the actual value of Δc will be even less.

APPENDIX II

In order to compute the average current density for a circular electrode using Eq. (XIV), it is only necessary to average the dependence of the current density on the anode height (y) over a circle. Since i varies as $y^{1/3}$ we want

$$y^{1/3} = \frac{1}{R} \int_0^R (2\sqrt{R^2 - x^2})^{1/3}\, dx$$

$$= (2R)^{1/3} \frac{\sqrt{\pi}\,\Gamma(7/8)}{2\,\Gamma(11/8)} = 1.08\,(2R)^{1/3}$$

For the anodes used in this study this results in $y = 0.121$ cm.

A Reaction Rate Study of the Corrosion of Low-Hafnium Zirconium in Aqueous Hydrofluoric Acid Solutions

Tennyson Smith[1] **and George Richard Hill**

Department of Fuel Technology, University of Utah, Salt Lake City, Utah

ABSTRACT

Zirconium dissolves readily in HF solutions leaving a smooth unpitted surface. The rate of dissolution of Zr in aqueous HF solutions has been studied over a temperature range of 7°-78°C using a radioactive tracer Zr^{95}. The rate was found to be directly proportional to the un-ionized HF concentration. In order to control the equilibrium concentrations of un-ionized HF, HF^-_2, H^+, and F^- ions, most of the solutions contained another component such as HCl, HNO_3, KF, or $HClO_4$. For a given un-ionized HF concentration, the rate was independent of the HF^-_2, H^+, F^-, Cl^-, NO^-_3, K^+, or ClO^-_4 concentrations over a wide range.

A discussion of the Zr complex ions in solution is given. The gaseous product of the reaction between Zr and aqueous HF with HCl is H_2. When HNO_3 is used in place of HCl the gaseous products are H_2 and N_2O. The diffusion of un-ionized HF from the bulk solution through a diffusion film to the solid surface is postulated as the slow step, the energy of activation being 3.3 kcal/mole. At 25°C the rate constant for the case of rapid stirring is 5.19×10^{-4} g cm^{-2} min^{-1} (moles HF)$^{-1}$ liter.

The wide interest in research and development of Zr is a result of its favorable properties as a construction material in nuclear reactors. Some of these properties are: low neutron absorption cross section of 0.18 barn; corrosion resistance to acids, bases, and water; ductility and ability to be fabricated.

The literature consists of reports concerned primarily with corrosion rates useful as engineering data. This work was undertaken to study the corrosion of Zr from a fundamental point of view, i.e., to determine the mechanism of the corrosion of Zr in acid solutions. Two systems have been studied: Zr in HF solutions, which is reported in this paper, and Zr in H_2SO_4 solutions which will be reported in a later paper.

Baumrucher (1) studied the possibility of using dissolution of Zr by HF for analysis of diffusion specimens requiring handling by remote control. A rough estimate of the activation energy from runs made at two temperatures by Baumrucher is 4 kcal/mole, as compared to 3.3 kcal/mole reported here. He found a linear relation between the weight of Zr dissolved and time, also as reported here. Since he made all of his runs at one concentration and did not report rates of stirring of the solution, no further correlation could be made.

Experimental

The Zr samples supplied by the Atomic Energy Commission were 5 cm x 5 cm x 0.32 cm. Four samples were irradiated to an activity of 10 millicuries each. The irradiation was accomplished by neutron bombardment at the Oak Ridge National Laboratory.

[1] Present address: Atomics International, Canoga Park, Calif.

The isotope Zr^{95} with a half life of 65 days, emits a β particle to become Nb^{95}, the Nb^{95} emits a 0.73 mev γ and then a β particle to become stable Mo. The decay scheme is more complicated than this, but the fairly strong γ rays can be detected easily with a scintillometer. Specimens were tested for uniformity of activity by taking samples at various depths through the specimen thickness and measuring the activity of each sample with the counting equipment. The activity proved constant within experimental error through three-eighths of the specimen thickness from either side, then rose to a maximum at the center. The activity at the center was about twice that at the surface. Only the outer part of the specimen was used in these runs.

In order to detect any change in the true surface area, control runs were made periodically as the specimens were used. Since the rate of reaction remained constant within experimental error, under the same experimental conditions each time, it was concluded that the ratio of the true to the apparent surface area remained constant.

The AEC supplied the analysis (Table I) and the following history with the samples. The Zr was

Table I. Analysis of zirconium samples

Concentration of contaminants in parts per million					
Hf	80-100	Fe	300	Si	50
B	0.5	Mn	20	Sn	20
Cd	1.0	Al	30	Ti	50
Co	10.0	C	100-200	V	20
Cr	50.0	N	48	Zn	50
Ca	50.0	Ni	5	Mo	50
Mg	20.0	Pb	50		

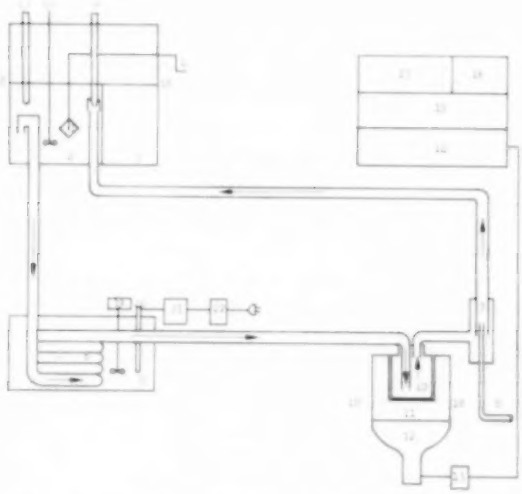

Fig. 1. Schematic diagram of the apparatus: 1, zirconium sample; 2, reaction cell; 3, cleaning cell; 4, sample manipulator; 5, constant temperature bath; 6, heat exchanger coil; 7, air lift pumps; 8, gas intake; 9, baffle filler tube; 10, sample cell; 11, scintillation solution; 12, photomultiplier tube; 13, preamplifier; 14, amplifier; 15, scaler; 16, recorder; 17, counting rate computer; 18, lead shielding (not shown); 19, stirring motor; 20, thermoregulator; 21, current reducer; 22, relay; 23, thermocouple well; 24, stirring rod.

fabricated from 300 to 500 lb, double-arc melted ingots. They were then: forged at 1800°F, blasted to remove oxide, hot-rolled to size, cold-rolled to about 25% reduction, annealed in air at 1550°F, and pickled in a HF solution.

In this study all solutions were made with conductivity water and reagent grade chemicals.

Apparatus

The equipment had to comply with a number of requirements due to the nature of this work. The samples, being radioactive, had to be shielded to protect the investigators and to keep the background count to a minimum. Since HF, H_2SO_4, and other acids were to be used, a material resistant to these was needed. Polyethylene fulfilled this requirement very well. The temperature of the solution had to be controlled and numbers 5, 6, 20, 21, and 22 in Fig. 1 indicate the apparatus used for this purpose. Although a temperature drop existed between the reaction cell and the constant temperature bath, the temperature in the cell remained constant within ±0.1°C during a run.

The reaction cell (No. 2, Fig. 1) was approximately 11 cm long by 6 cm wide by 11 cm high, and had an inlet and outlet tube by which the solution could be circulated through a constant temperature bath (No. 5 Fig. 1), through a scintillation counter unit (Nos. 10, 11, 12, Fig. 1) and back to the cell with the help of the airlift pump (No. 7, Fig. 1). The other cell shown was for the purpose of cleaning and storing the sample. Although Fig. 1 is not to scale, it gives a close description of the way each part of the equipment was arranged relative to each other part. The container for the reaction cell was made of Lucite and was surrounded by lead bricks. Number 4, Fig. 1, is a rod covered with polyethylene used as a manipulator. It allowed the radioactive sample to be transferred from one cell to another without exposing the operator. The Lucite container was made air tight so that the desired atmosphere of air, oxygen, or argon could be maintained in contact with the solution in order to test the effect of oxygen partial pressure on the reaction rate. Lead was also placed around the scintillation unit (Nos. 10, 11, 12, Fig. 1) to lower the background.

The sample cell (No. 10, Fig. 1) was placed in a specially made container filled with scintillation fluid (toluene + 4 g/liter of 2, 5 diphenyloxazole). This container was attached to a 5 in. diameter Dumont photomultiplier tube No. 6365. The Dumont tube was connected to a preamplifier which was in series with an amplifier, scaler, count rate computer, and recorder in that order. As the solution containing the radioactive Zr^{95} passed through the cell, a permanent record of the activity was made on the recorder. To determine the weight of Zr dissolved in the solution from the counts per minute as read on the recorder at any given time, a standard was made for each specimen. This was done by taking a small representative sample from each specimen, weighing it, dissolving it in HF solution, and placing it in a polyethylene bottle the same size as that used for circulating the solution through the scintillometer (No. 10, Fig. 1). A correction factor to account for any change in the efficiency of the counting equipment, or the activity of the specimens, was determined by counting the radiation from the standard before and after each run.

The reaction cell (No. 2, Fig. 1) held 600 ml of solution, the sample cell (in the scintillometer) contained 140 ml and the rest of the system contained 160 ml, making a total of 900 ml.

Reactant Solutions

The stoichiometric concentrations, the concentration of undissociated hydrofluoric acid, $(HF)_{un}$, and the observed dissolution rates per mole of hydrofluoric acid, Rate/$(HF)_{un}$, for a few of the runs at 33° and 34°C, are given in Table II. The concentra-

Table II. Observed rates of dissolution of Zr at 33° and 34°C with stirring 1200 rpm

Stoichiometric conc., *M*			Initial rate*, g cm^{-2} min^{-1} divided by $(HF)_{un}$
HF	Other	$(HF)_{un}$	× 10^5
0.27	1.5 HCl	0.27	4.30
0.27	0.61 KF	0.05	3.57
0.27	1.0 HNO_3	0.27	4.12
0.27	0.5 $HClO_4$	0.27	4.02
0.27	—	0.248	3.40
0.27	—	0.248	4.12
HF × 10^5		$(HF)_{un}$ × 10^5	
6.0	1.25 HNO_3	6.0	4.49
1.1	1.52 HNO_3	1.1	4.40
0.275	1.52 HNO_3	0.275	2.84
—	1.52 HNO_3	— Rate = 3.2 × 10^{-5}	

* Multiply (g cm^{-2} min^{-1}) by 1.44 × 10^6 to get mdd (milligrams per dm^2 per day).
Multiply (g cm^{-2} min^{-1}) by 3.23 × 10^4 to get ipy (inches penetration per year).

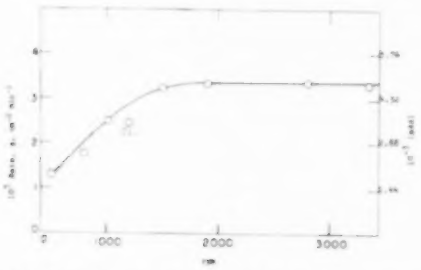

Fig. 2. Relationship between the rate of stirring in rpm and the rate of dissolution of Zr. The molarity of HF is 0.00613 and H^+ is 1.50M; T, 33°C.

tions of undissociated HF, fluoride and hydrogen bifluoride ions were calculated by interpolating and extrapolating equilibrium constants from the following data of Broene and deVries (2).

	Temperature °C	12	15	25	35
$HF \rightleftharpoons H^+ + F^-$	$K_1 \times 10^4 =$	8.3	7.9	6.7	5.6
$HF + F^- \rightleftharpoons HF_2^-$	$K_2 =$		3.92	3.96	4.33

With foreign acids present and in very dilute solutions, fluoride and hydrogen bifluoride ion concentrations are small, and, in some cases, difficult to calculate. Their values were estimated until it became obvious that they bore no relation to the rate.

At 0°C the activity coefficient for $(HF)_{aq}$ is essentially unity to 0.1M HF, increasing to 1.06 at 1M HF (3). Similar values are to be expected at higher temperatures and no attempt was made to substitute the activity for the concentration of HF. While the concentrations of H^+ ion and accompanying (NO_3^-, Cl^-, F^-, HF_2^-, ClO_4^-) ions were varied over a wide range, the values of, Rate/$(HF)_{aq}$ remained essentially constant. It was concluded that at constant temperature the rate is a function of nothing but the HF_{aq} concentration.

Results

Stirring effect.—Figure 2 shows a pronounced effect of stirring on the rate, with a leveling off above 2,000 rpm. This is typical for transport-controlled heterogeneous reactions, with the type of stirring used; the rate is proportional to a fractional power of the rpm. The absolute velocity of the solution past the Zr sample was not measured.

Effect of various ions on the rate.—Analysis of 32 runs at about 33°C (rpm 1200) gave an average value for the Rate/$(HF)_{aq}$ as 4.11×10^{-4} g cm^{-2} min^{-1} per mole liter^{-1} with or without the use of foreign acids. The average error is 0.46×10^{-4} g cm^{-2} min^{-1} per mole liter^{-1}.

As shown in Table II, a run made in 1.52M HNO_3 gave a rate of 3.2×10^{-4} g cm^{-2} min^{-1} which was appreciable when the most dilute HF solutions were used. It is concluded that the variations in the Rate/$(HF)_{aq}$ are due to a combination of experimental errors, error in calculating the concentration of $(HF)_{aq}$ in some cases, lack of correction for HNO_3, etc.

Effect of hydrofluoric acid on the rate.—A plot of all the rates at ca. 33°C and 1200 rpm vs. the concentration of $(HF)_{aq}$ is given in Fig. 3. The circles

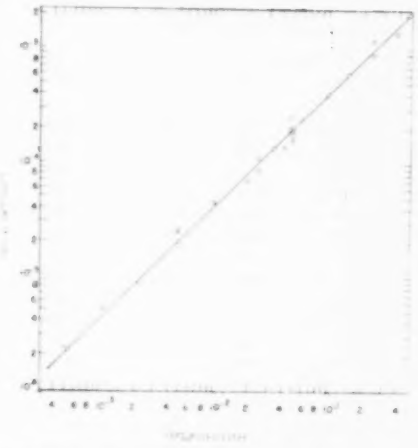

Fig. 3. Relationship between the equilibrium concentration of un-ionized HF and the rate of dissolution of Zr. T=33°C, rpm = 1200.

are experimental values, the curve is drawn with a slope of 1 on the log-log scale, corresponding to a first order reaction with respect to $(HF)_{aq}$. These are initial rates determined from the slopes of plots of g (Zr dissolving) per cm^2 (of surface area) vs. time.

Effect of oxygen on the rate.—In order to determine the effect of oxygen on the reaction rate, a number of runs were made with a Zr, aqueous HF, HCl system in which the partial pressure of oxygen in equilibrium with the solution was varied. The oxygen partial pressure ranged from one to zero atmospheres in a series of experiments, the partial pressure being varied by mixing oxygen with purified argon. No variation in the rate was observed as the oxygen partial pressure was changed from run to run. The remainder of the runs were made with air to pump the solution.

Effect of temperature on the rate.—Figure 4 is an Arrhenius plot; the circles represent the data tabulated in Table III and the line is the best eye fit of these points. The symbol k is the rate constant defined by $k = R/(HF)_{aq}$, where R is the rate in g cm^{-2} min^{-1} and $(HF)_{aq}$ is the concentration of un-ionized HF in moles/liter. All of the runs in Table III were made with stirring greater than 2000 rpm, where the stirring effect had reached its limit. The

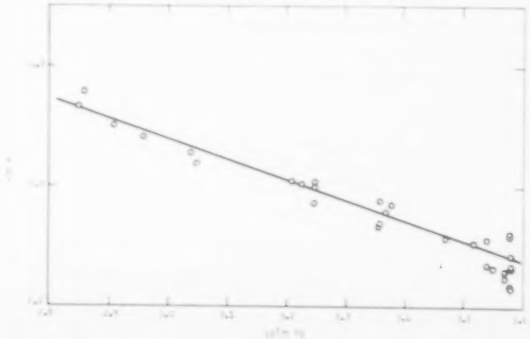

Fig. 4. Plot of ln k vs. 1/T, showing the temperature coefficient of the rate constant, (rpm > 2000).

Table III. Variation of the rate constant with HF concentration* and temperature, (rpm > 2000, (HCl) = 0.5-1.5)

t°C	$(HF)_{ss}$	−lnk	t°C	$(HF)_{ss}$	−lnk
6.0	0.0005	5.42	24.0	0.050	5.22
7.0	0.0005	5.69	25.0	0.0005	5.34
7.0	0.0010	5.58	25.0	0.0050	5.30
7.0	0.0050	5.40	25.0	0.0050	5.11
7.0	0.050	5.69	35.0	0.0005	5.15
7.0	0.050	5.85	35.0	0.0050	4.96
7.0	0.50	5.84	35.0	0.50	5.02
7.5	0.50	5.76	37.0	0.050	4.99
7.5	1.00	5.71	38.5	0.0005	4.96
8.5	0.50	5.68	55.3	0.0005	4.73
9.0	0.050	5.66	55.0	0.050	4.81
9.0	0.50	5.43	65.0	0.0005	4.00
11.0	0.0090	5.48	71.0	0.0090	4.50
15.0	0.050	5.43	73.0	0.0050	4.21
23.0	0.0090	5.16	78.0	0.0090	4.35

* The stoichiometric HF concentration is essentially equal to $(HF)_{ss}$ at (HCl) 0.5M or greater.

temperature coefficient is seen to be small; the activation energy was calculated to be 3.34 kcal/mole.

Reaction products.—There has been some question as to whether the majority of the Zr complex ions in aqueous HF is ZrF_3^+, ZrF_4 or ZrF_5^-. A qualitative determination of the complex ions in solution can be made as follows: let A be the initial concentration of HF and X be the moles of HF per liter that have reacted at time t. Consider the over-all reaction:

$$Zr + (4-b)H^+ + bHF \rightarrow ZrF_b^{(4-b)+} + 2H_2$$

where b is the average number of fluorine atoms associated with a Zr atom in solution. The number of moles of Zr per liter that have reacted at time t is just X/b. Since in the experiments the rate that Zr enters the solution is measured and not the rate that HF is depleted, the rate equation is written, $R = d(Zr)/dt = k(HF)_{ss} = k(A-X) = -d(X/b)/dt$. Although b varies slowly with X, if one makes the approximation that b is constant, and makes the well-known integration of the first order rate expression, one gets: $\ln(1 - X/A) = bkt$ if $X = 0$ at $t = 0$. The $\ln(1-X/A)$ plotted vs. t gives a straight line only with the proper choice of b, and therefore suggested a method of evaluating b. A plot of the $\ln(1 - X/A)$ vs. t for various choices of b is given in Fig. 5. It is seen that a choice of $b = 3.3$ gives a straight line. However, rather than remain constant as was assumed, b must decrease as the HF is used up. This is shown by the following equilibrium constants at 25°C reported by Connick and McVey (4):

$$Zr^{+4} + HF \rightleftharpoons ZrF^{+3} + H^+ \qquad K_1 = 6.3 \times 10^5$$
$$ZrF^{+3} + HF \rightleftharpoons ZrF_2^{+2} + H^+ \qquad K_2 = 2.1 \times 10^4$$
$$ZrF_2^{+2} + HF \rightleftharpoons ZrF_3^+ + H^+ \qquad K_3 = 6.7 \times 10^2$$

Consequently, the concentration of ZrF_4, ZrF_5^-, or ZrF_6^{-2} must be very small in this particular solution, the majority of the complex being ZrF_3^+. Plots similar to Fig. 5 for runs in which higher concentrations of HF were used showed a shift to higher values of b as was expected. For example, a run with an aqueous solution 0.009M in HF, 0.5M in hydrogen ion and at 71°C gave $b = 4.5$.

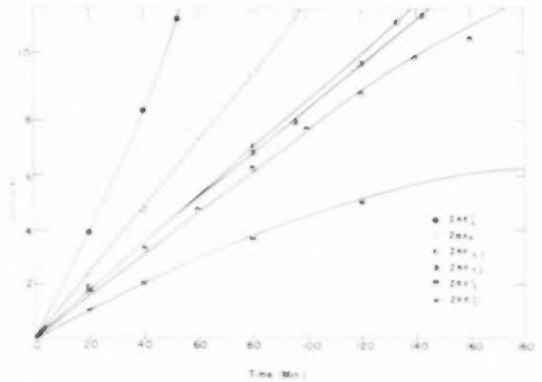

Fig. 5. Curves to determine the correct formula for the Zr complex ion in solution.

Gas samples for the reaction of Zr in aqueous HF were analyzed by infrared spectroscopy and with an Orsat gas analyzer. For the system Zr, aqueous HF, and HCl, only H_2 was detected. For the system Zr, aqueous HF, and HNO_3, H_2 and N_2O were detected, the majority being hydrogen. Comparing the amount of gas evolved with the weight of Zr dissolved showed that just enough H^+ ions were reduced to oxidize Zr to the +4 state.

Discussion

The following observations have been made: The amount of hydrogen evolved is that which is expected if Zr is oxidized to the +4 state. The over-all reaction is: $Zr + (4-b)H^+ + bHF \rightarrow ZrF_b^{(4-b)+} + 2H_2$ or $Zr + 4HF \rightarrow ZrF_4^{(4-b)+} + 2H_2 + (4-b)F^-$ when no excess H^+ ion is available. The reaction is first order with respect to un-ionized HF. The rate does not drop off at high HF concentrations as might be expected if the slow step was one of adsorption. The stirring rate greatly influences the rate of reaction, but does come to a limit as shown in Fig. 2. The activation energy for the reaction is 3.34 kcal/mole.

From Fig. 2 one would expect that above 2000 rpm the diffusion step would be eliminated as the slow step. However, this is not necessarily true. The effect of stirring, in Fig. 2, is very similar to that for the dissolution of Fe in solution recorded by King (5). It would appear that a diffusion film is established very close to the surface, the thickness of which reaches a limit as the turbulence in the bulk liquid is increased. A great deal of study (6-8) has been made concerning the nature of such a boundary layer.

Assuming the diffusion of un-ionized HF across a boundary layer of thickness δ to be rate controlling, a comparison of the rate equation with Fick's first low (S1C), for the case of steady state, can be made.

Consider the equations: $-d(HF)/dt = bk(HF)_{ss}$ and $-J = Ddc/dx$, where J is the flux (mass passing unit area per second) and dc/dx is the differential concentration gradient at the plane the particles are diffusing across. The term $d(HF)/dt$ is the moles of

HF reaching 1 cm² of the Zr surface/sec. Then, $J = d(HF)/dt$ and $bk(HF)_{ss} = Ddc/dx$. Assuming D to be a constant, it follows that the concentration gradient dc/dx is constant, since J is constant for steady state. Therefore, dc/dx can be written $\Delta c/\Delta x$ or $(c - c_s)/\delta$, where c is the concentration in the bulk solution, c_s is the concentration at the metal surface and δ is the boundary layer thickness. Since the reaction at the surface is probably much faster than the rate the HF diffuses to the surface, it may be assumed that $c_s = 0$, then $\delta = D/bk$. From Fig. 4, at 298°K, $k = 5.19 \times 10^{-3}$ g cm^{-2} min^{-1} moles^{-1} liter or $k = 0.95 \times 10^{-5}$ cm sec^{-1}. The diffusion coefficients for most small molecules in water vary between 1×10^{-5} and 5×10^{-5} cm^2 sec^{-1} at room temperature. Assuming $D = 1 \times 10^{-5}$ cm^2 sec^{-1} for HF in water, and $b = 3$, it is seen that $\delta = 3.5 \times 10^{-3}$ cm. From calculations for typical runs given in King's (5) data (S1C), δ varies between 3×10^{-3} cm and 5×10^{-3} cm.

From these facts and the observation that the rate constant and activation energy are of the same magnitude as many other dissolution reactions that are diffusion (5, 9) controlled, it was concluded that the slow step is the diffusion of un-ionized HF through an effective diffusion layer to the metal surface.

Manuscript received March 22, 1956. This paper was prepared for delivery before the Cleveland Meeting, Sept. 30-Oct. 4, 1956.

Any discussion of this paper will appear in a Discussion Section to be published in the December 1958 JOURNAL.

REFERENCES

1. J. E. Baumrucker, AEC Report ANL 5020.
2. H. H. Broene and T. de Vries, *J. Am. Chem. Soc.*, **69**, 1644 (1947).
3. D. J. Anthony and L. J. Hudleston, *J. Chem. Soc.* **127**, 1122 (1925).
4. R. E. Connick and W. H. McVey, *J. Am. Chem. Soc.* **72**, 3182 (1949).
5. C. V. King, *ibid.*, **57**, 828 (1935); **59**, 63 (1937); **61**, 2290 (1939).
6. Kamenetskii, D. A. Frank, "Diffusion and Heat Exchange in Chemical Kinetics," Princeton University Press, Princeton (1955).
7. J. Laufer, *Nat. Advisory Comm. Aeronaut., Repts, Tech Note* 2945, June (1953).
8. R. G. Deissler and C. S. Eian, *Nat. Advisory Comm. Aeronaut., Repts. Tech. Note* 2629, Feb. (1952).
9. R. G. Van Name and G. Edgar, *Am. J. Sci.*, **29**, 237 (1910); R. S. Bosworth and R. G. Van Name, *ibid.*, **32**, 207 (1911); D. U. Hill and R. G. Van Name, *ibid.*, **42**, 307 (1916).

Metal-Water Reactions

VI. Kinetics of the Reactions of Water Vapor with Strontium and Barium

Harry J. Svec and H. Gene Staley

Institute for Atomic Research and Department of Chemistry, Iowa State College, Ames, Iowa

ABSTRACT

Strontium and barium were reacted with water vapor and the kinetics determined in the temperature range 40°-66°C for water vapor pressures from 17.5 to 92.5 mm Hg. The stoichiometry varied according to the reaction conditions. For the strontium reactions the products were H_2 and $Sr(OH)_2$. For vapor pressures below 44 mm the products of the barium reactions were H_2 and $Ba(OH)_2$ while for pressures above 44 mm they were H_2 and $Ba(OH)_2 \cdot H_2O$.

Manometric and gravimetric methods were employed in the kinetic studies. Both the Sr and lower vapor pressure Ba reactions followed the parabolic rate law. At higher pressures the Ba reaction followed a linear law. An activation energy of -5.2 ± 0.2 kcal/mole was found for the Sr reactions. The activation energy for the Ba reactions was found to depend on reaction conditions.

Higher temperature studies of the reactions between water vapor and Sr, Ba, and Ca indicated that in certain temperature ranges above 100°C completely protective coatings were formed similar to those observed in the oxidation of Al or Cr.

The kinetics of gas-metal reactions involving N_2, O_2, and H_2 have been studied for many years and numerous references are available (1). In recent years there has been interest in reactions between metals and water vapor. It has been shown that lithium (2), thorium (3), and calcium (4) follow a logarithmic rate law and that magnesium (5) follows the linear rate law.

Strontium and barium were studied in order to compare the other alkaline earth metals with calcium. Because of the nature of the reaction and the products, the rate was followed by observing the evolution of H_2 and/or the weight gain of a specimen of the reacting metal as a function of time. Conditions of temperature and water vapor pressures were regulated carefully to determine their effect on the rate of reaction.

Experimental

Strontium and barium rods were obtained from the Mackay Company of New York. Spectrographic analysis showed that the impurities totalling ap-

proximately 1% occurred in the Sr mainly as a mixture of Ca, Ba, Mn, Mg, Fe, and Al; in the Ba, 1% occurred mainly as Sr, Mn, Fe, Mg, and Al. Cylindrical specimens of the metals were prepared in the manner described (4) for Ca. Because of the greater reactivity of Sr and Ba, special care was required in handling and transporting the specimens in their final prepared form from the controlled atmosphere box, in which the machining was done, to the reaction apparatus. Flushing the apparatus with purified argon or helium prevented contamination with atmospheric CO_2. The apparatus used in this work has already been described (3, 4).

Results for Strontium

The reactions between Sr and water vapor were carried out in the temperature range 40°-66°C and water vapor pressures of 17.5-92.5 mm Hg. During some of the kinetic experiments careful measurements were made of the amounts of Sr and H_2O consumed and the amounts of $Sr(OH)_2$ and H_2 formed. As a result of these measurements, which attained a precision of ±1%, the stoichiometry of the reaction was established to be according to the equation

$$Sr + 2H_2O \rightarrow Sr(OH)_2 + H_2$$

The uniqueness and the identity of the products were determined by chemical, x-ray, and mass spectrometric methods.

The weight of water consumed in mg H_2O/cm^2 of Sr was plotted against various functions of time in order to determine the rate law. In all cases, the data indicated that the reaction follows the parabolic rate law more nearly than any other law. Several plots of the reaction data obtained at various temperatures and a water vapor pressure of 55 mm Hg are shown in Fig. 1.

The rate constant k, [mg $H_2O/cm^2Sr)^2hr$] was determined for each reaction condition. A plot of k vs. temperature is shown in Fig. 2, where the k's obtained at different but constant water vapor pressures are plotted against the reaction temperature. As is indicated, the value of the rate constants decreased as the temperature increased. At about 51°-56°C the rate constants of the reactions at 17.5 and 32 mm Hg water vapor pressure appear to become independent of temperature.

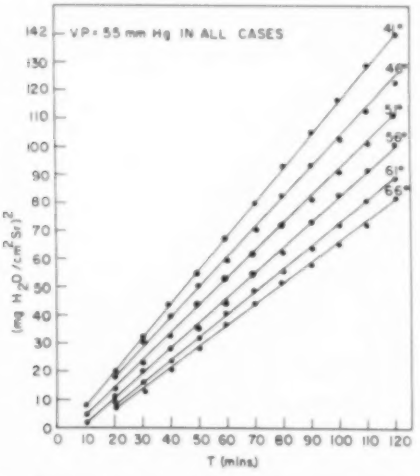

Fig. 1. Parabolic plots of strontium-water vapor data at 55 mm water vapor pressure in the low temperature range 41°-66°C.

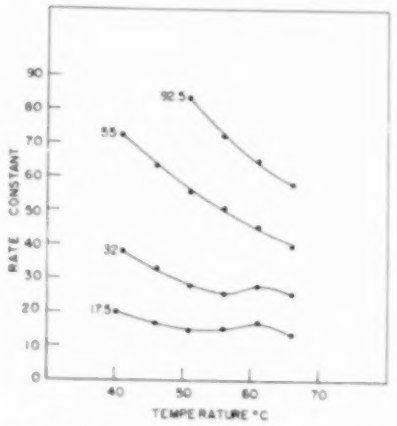

Fig. 2. Effect of temperature on the rate constants of the strontium-water vapor reaction. The units of k are [mg $H_2O/cm^2Sr]^2/hr$. The plotted points represent the average of several runs under each experimental condition. The general precision obtained was from ± 5 to 10% with the higher range generally applying to low pressure, low temperature experiments.

Arrhenius plots were made for each isobar over the temperature dependent range. The plots were linear with positive slopes, indicating an apparent negative energy of activation. The calculated activation energy was independent of water vapor pressure and had a value of -5.2 ± 0.2 kcal/mole.

Results for Barium

The reactions between Ba and water vapor were observed in the temperature range 41°-66°C and at water vapor pressures of 17.5, 32, 55, and 92.5 mm Hg. Two different reaction stoichiometries were observed. These were established by measuring the liquid water consumed and the hydrogen formed, in addition to x-ray diffraction analysis of the solid product. For water vapor pressures of 17.5 and 32 mm Hg, the stoichiometry is according to the equation

$$Ba + 2H_2O \rightarrow Ba(OH)_2 + H_2$$

At water vapor pressures of 55 and 92.5 mm Hg the stoichiometry is according to the equation

$$Ba + 3H_2O \rightarrow Ba(OH)_2 \cdot H_2O + H_2$$

Both manometric and gravimetric procedures indicated that the reactions at 17.5 and 32 mm Hg pressure followed the parabolic rate law. Manometric reactions at 55 and 92.5 mm pressure did not follow any of the known rate laws. The general pattern of these reactions is shown in Fig. 3. When the reactions were observed in the gravimetric apparatus (3) at 55 and 92.5 mm Hg, after an initial period of very rapid reaction rate during which time no law was determinable by the method available, the kinetics approached the linear rate law. A typical

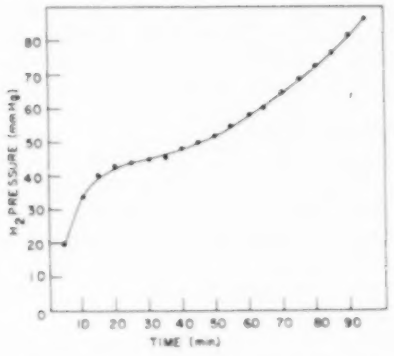

Fig. 3. General pattern of the manometric data for the barium-water vapor reaction. The curve illustrated is from data at 55 mm water vapor pressure and 56°C.

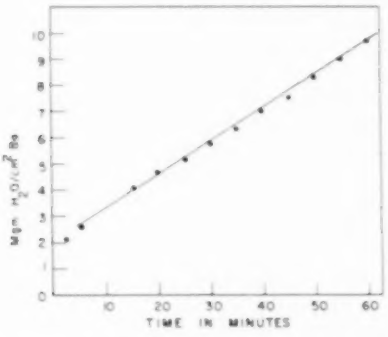

Fig. 4. Linear plot of the gravimetric data for the barium-water vapor data obtained at 55 mm water vapor pressure and 41°C. Other data at 55 mm and 92.5 mm and other temperatures cited here follow the same general pattern as these data.

gravimetric reaction is plotted in Fig. 4. It is significant that flaking occurred after 4 or 5 min in the reactions at 55 and 92.5 mm Hg water vapor pressure.

The vapor pressure at which water combines with $Ba(OH)_2$ to form the monohydrate is 44 ± 2 mm Hg. This was measured by following the weight gained by anhydrous $Ba(OH)_2$ in contact with water vapor at known pressures. It was also shown that formation of the octahydrate also takes place in this vapor pressure range, but only after all of the anhydrous $Ba(OH)_2$ has been converted to the monohydrate.

The rate constants for both manometric and gravimetric reactions are plotted against temperature of reaction in Fig. 5 and 6. Arrhenius plots of the data for the reactions at 32 mm in the temperature range 41°-56°C indicated an apparent activation energy of -5.1 ± 0.3 kcal/mole. At 17.5 mm the apparent activation energy is zero. Similar plots of the linear data for the 55 mm reaction indicate no linear relationship in the temperature range 41°-56°C; so, no activation energy was deduced. If such were possible, however, it would be negative in sign. The data at 55 mm from 56° to 66°C give a linear plot and the activation energy is 9.5 ± 1.0 kcal/mole.

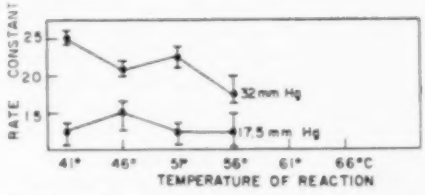

Fig. 5. Effect of temperature on the rate constants of the barium-water vapor reaction where kinetics are described by the parabolic rate law. Data were obtained manometrically. Units of k are [mg $H_2O/cm^2Ba]^2/hr$.

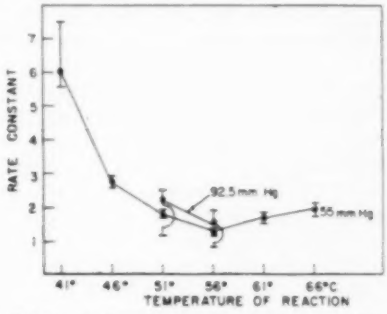

Fig. 6. Effect of temperature on the rate constants of the barium-water vapor reaction where kinetics are described by the linear rate law. Data were obtained gravimetrically. The units of k are [mg $H_2O/cm^2Ba]/hr$.

High Temperature Reactions of Ca, Sr, and Ba with Water Vapor

Calcium, strontium, and barium reactions were carried out at higher temperatures in an apparatus similar to the one used above but modified to permit higher reaction temperatures. The reactions were carried out at vapor pressures of 25 ± 1.5 mm Hg. It was found that in certain temperature ranges these reactions would start and then apparently stop, due to the formation of protective coatings similar to those involved in the air oxidation of Al or Cr. In all the reactions described below, in which there was a protective coating formed, the hydrogen pressure increased steadily for about 15 min after the initiation of the reaction and then the increase stopped. No further evolution of H_2 took place, even after 5 hr of contact between the metal specimens and water vapor.

It was observed that for Ca the reaction was of this type in two temperature ranges, one from 100° to 255°C and the second from 400° to 500°C, above which temperature no observations were made. The reaction below 100°C is that reported by Svec and Apel (4). The reaction rate as determined manometrically went through a maximum at around 85°C and then apparently decreased to zero at 100°C. Similar behavior was again observed between 255° and 330°C. From 330° to 400°C the reaction was approximately the same as described by Gibbs and Svec (6). The differences of temperature range described here and those obtained in the earlier work are probably due to the fact that the Ca used in these experiments was the redistilled material (4) prepared in the Ames Laboratory of the A.E.C., while that used by Gibbs and Svec was ordinary commercial metal.

In the 100°-250°C range, the specimens maintained their original shiny, metallic luster. In the 400°-500°C range, the specimens were covered by a thin whitish coating. X-ray diffraction studies of the protective coatings in both upper and lower regions indicated the presence of Ca, $Ca(OH)_2$, and CaO with possible small amounts of CaH_2 at the higher temperatures. The x-ray lines were very sharp compared to those produced by the reaction product formed at temperatures below 70°C (4). The presence of strong lines due to Ca reflections in the x-ray diffraction patterns was taken as *a priori* evidence that the reaction product coating was very thin, although no attempt was made to measure its thickness.

Reactions involving Sr and Ba showed only one temperature range for each metal in which the completely protective type of coating was formed. For Sr this range was 175°-375°C while for Ba it was 100°-400°C. The upper limit in both cases coincides with the mp of the respective anhydrous hydroxides. Both Sr and Ba specimens maintained their metallic appearance.

Discussion of Results

The separation of the reactants in the metal-water vapor reaction by the solid product indicates some diffusion process must take place within the coating. In both the Sr and Ba reactions, under each set of conditions, markers, which were small chips of Mg incorporated into the metal surfaces during the machining of the sample, stayed flush with the surface of the coating being displaced from the Sr and Ba metal after reaction by a layer of hydroxide. This is strong evidence that inward diffusion of some species takes place in both reactions. Similar observations with marker experiments have been made for the reactions of water vapor with Ca and with Th which follow a logarithmic rate law. The same observation was made in marker experiments with the Mg reactions although it was expected since the rate of reaction is linear. These limited observations suggest that inward diffusion of some species may be a general characteristic of water vapor-metal reactions. Experiments with less active metals than the alkaline earths will be necessary to record these phenomena microphotographically.

A comparison of the reaction rates of Ca, Sr, and Ba cannot include the Ca reaction because of the logarithmic nature of the kinetic law. However, comparison of Sr and Ba at 17.5 mm and 32 mm water vapor pressure where both reactions appear to be parabolic indicates (Fig. 5 and 2) that Sr is more reactive than Ba, which is contrary to general observations and expectations. This apparent difference based only on manometric data might be explained on the basis of hydride formation. However, comparison of gravimetric data still indicated that the Sr reaction is faster than the corresponding Ba reaction. No evidence for hydride was obtained by x-ray diffraction analyses. No reasonable explanation is apparent at this time.

In an exact comparison of the gravimetric with the manometric data, some difficulty was first observed due to the change in size of the cylindrical specimens for the two types of experimental conditions. In order to gain greater sensitivity in the manometric experiments a larger sample was used. All data were consistent and reproducible as long as the size did not change appreciably. In the gravimetric experiments the diameter of the sample specimens was about ½ that of the manometric samples. Despite the fact that no changes were made in tool position on the lathe used to prepare the samples, the data, which were again consistent and reproducible, indicated a rate of reaction higher than in the manometric experiments. Comparative data between the two types of experiments were obtained only after experiments were made using samples with similar dimensions.

The assumption was always made in the past that a reproducible surface was obtained by close control of the machining operations. Reaction rates given in weight of H_2O reacted/cm² of metal surface were assumed to be minimum rates. Now it appears that in order to reproduce a machined surface, the dimensions of the machined specimen must be comparable. This is probably related to the exact tool-to-metal angle which changes as the diameter of the machined bar is reduced. As the diameter is decreased, the surface roughness increases, thereby causing an increase in available metal surface. It was fortuitous that during the Li(2), Ca(4), Th(3), and Mg(5) work the specimen size was kept constant, thereby accounting for the consistency of these data.

The apparent negative activation energy observed for the Sr reactions can be explained in the same manner as that observed for Ca(4) as involving a heat of desorption. Except for the change in rate law, Sr reactions follow a pattern similar to that of Ca throughout the temperature range in which kinetics were studied. In the heterogeneous reactions of concern here, this presumes that a prior fast equilibrium exists in a chain of reactions. This is then followed by a slow, rate-governing reaction. For example, if the equilibrium involves some interaction of H_2O vapor with the surface, one can write

$$H_2O_{(g)} + S \underset{\text{fast}}{\overset{K_{eq}}{=}} H_2O \cdot S \qquad (I)$$

where K_{eq} is the equilibrium constant and S some property of the surface. The slow step might then follow according to some relationship as

$$\frac{d(H_2O)}{dt} = k\,[H_2O \cdot S] \qquad (II)$$

or

$$\frac{d(H_2O)}{dt} = k\,K_{eq}[H_2O_{(g)}][S] \qquad (III)$$

If the value of K_{eq} is temperature sensitive and decreases in value sufficiently to make the product $k \cdot K_{eq}$ become smaller as the temperature increases, then the apparent activation energy, computed from the Arrhenius relationship, becomes negative. This condition is attained when the forward reaction in (I) is slower than the reverse reaction. In the case of water vapor-metal systems it involves desorption

of H_2O molecules from the coating surface. That this has not been observed in oxidation reactions involving O_2 or N_2 is probably due to the difference in the character of the adsorption compared to water molecules.

The apparent negative activation energies observed for the Ba reactions are also explainable as involving heats of desorption. The value of −5.1 kcal/mole found for the 32 mm Ba reactions indicates that the processes in this and the Sr reactions are similar. The apparent zero value for the activation energy at 17.5 mm is similar to the same Sr reaction at temperatures above 51°C and can be explained on the basis of a change in the predominant character of the rate-limiting processes. If the constants in equations (I) and (II) are decreasing and increasing at such a rate as to make their product remain at a fixed value, the rate of reaction then appears to be independent of temperature. As the temperature increases further, the product $k \cdot K_{ad}$ increases in value and the apparent activation energy should become positive. This was observed in the 55 mm reactions from 56° to 66°C. It is significant that the activation energy of 9.5 kcal/mole for this linear Ba-H_2O reaction is the same as that for the Mg-H_2O reaction (5) at 425°-500°C and 208 mm (11.1 ± 2.7 kcal/mole) which appears to depend on the rate of adsorption of gas molecules on the reacting surface.

The high temperature reactions were followed only by the manometric technique. The observations of Svec and Gibbs (6) on Ca made the appearance of a completely protective coating in these reactions unexpected, especially at the high temperatures. It was not possible to deduce what rate law was followed during the initial stages of these high temperature reactions. The experimental difficulties of characterizing precisely the coatings at the elevated temperatures involved make it impossible to educe an explanation for these phenomena based on experimental fact. The most significant observation remains the sharpening of the x-ray diffraction patterns of the high temperature coating compared to the low temperature coatings.

Manuscript received June 4, 1957.

Any discussion of this paper will appear in a Discussion Section to be published in the December 1958 JOURNAL.

REFERENCES

1. O. Kubaschewski and B. E. Hopkins, "Oxidation of Metals and Alloys," Academic Press Inc., New York (1953).
2. H. J. Svec and B. E. Deal, *J. Am. Chem. Soc.*, **75**, 6173 (1953).
3. H. J. Svec and B. E. Deal, *This Journal*, **103**, 421 (1956).
4. H. J. Svec and C. A. Apel, *ibid.*, **104**, 346 (1957).
5. H. J. Svec and D. S. Gibbs, *ibid.*, **104**, 434 (1957).
6. H. J. Svec and D. S. Gibbs, *J. Am. Chem. Soc.*, **75**, 6052 (1953).

Phase Equilibria in the System ZnO-P_2O_5

Fred L. Katnack and F. A. Hummel

College of Mineral Industries, Pennsylvania State University, University Park, Pennsylvania

ABSTRACT

Phase relationships in the system ZnO-P_2O_5 were determined in air in the range between ZnO and $Zn(PO_3)_2$, using solid state and quenching methods. Three congruently melting compounds exist, $Zn_3(PO_4)_2$, $Zn_2P_2O_7$, and $Zn(PO_3)_2$. The orthophosphate has a sluggish, reversible inversion at 942° and melts at 1060° ±8°C. The pyrophosphate undergoes a rapid, reversible inversion at 132° and melts at 1017°C. The irreversible inversion in the metaphosphate takes place in air in the range between 600° and 700°C, depending on the rate of heating of the sample. The low temperature form of the metaphosphate cannot be obtained by heating the high temperature form in air, but glass of the metaphosphate composition will yield a mixture of low and high temperature forms if held at 550°C for 16 hr. $Zn(PO_3)_2$ melts at 872°C. Simple eutectic relationships exist between ZnO and $Zn_3(PO_4)_2$, $Zn_3(PO_4)_2$ and $Zn_2P_2O_7$, and $Zn_2P_2O_7$ and $Zn(PO_3)_2$.

The phase relationships in the system ZnO-P_2O_5 were investigated because the system was known to contain at least two compounds of interest as host lattices for luminescent preparations, and it was thought that a determination of the properties of the crystals and glasses in the system might be of some interest to allied fields.

Numerous references to hydrated and anhydrous zinc phosphate minerals and synthetic preparations are available, e.g., (1), but the paper by Smith (2) on luminescence of zinc phosphates appears to be the only high temperature study which is closely related to the present work. Smith claimed three forms of $Zn_3(PO_4)_2$, α, β, and γ. The α form was said to be stable up to the fusion point if no Mn was present. To produce a pure β form, 1% Mn and temperatures above 800°C were required. Therefore, it was inferred that the β form would not appear if less than 1% Mn were present. The γ form was produced by the addition of 2 mole % $Mg_3(PO_4)_2$ with or without the addition of Mn. Gamma could be produced by the addition of $Zn_2P_2O_7$ to $Zn_3(PO_4)_2$. It was not clear whether or not Mn was present in the latter experiment. Pyrophosphates were said to prevent the formation of β-$Zn_3(PO_4)_2$.

It was felt that a detailed study of the phase relationships in the systems ZnO-P_2O_5, ZnO-MnO-P_2O_5, and ZnO-MgO-MnO-P_2O_5 would be necessary

in order to understand the luminescent properties of these compositions. This paper is confined to a clarification of the relationships between ZnO and P_2O_5. The other systems will be dealt with in a later paper.

Experimental Procedure

Techniques, Equipment, and Materials

Quench technique.—The quench technique followed essentially that described by Hill, Faust, and Reynolds (3) in the system P_2O_5-$2CaO \cdot P_2O_5$. Since their work was concerned with the P_2O_5-rich end of the system, elaborate methods of minimizing P_2O_5 volatilization were used. Such techniques did not appear necessary in the ZnO-P_2O_5 system, since chemical analyses of some of the zinc phosphate glasses did not indicate a significant loss of P_2O_5 through volatilization.

The quench furnace consisted of a Pt wound tube furnace. Temperature was controlled by a Tagliabue Celectray indicating potentiometer controller. A separate Pt-Pt 10% Rh thermocouple for the controller was inserted inside the tube so that this control thermocouple could be positioned manually near the quench packet.

Actual quench packet temperatures were measured by a L&N portable precision potentiometer using a second Pt-Pt 10% Rh thermocouple placed next to the quench packet. The accuracy of the second thermocouple was checked periodically against the melting point of gold at 1063°C.

X-ray diffraction.—Room temperature x-ray diffraction data were recorded with a Norelco Geiger counter diffractometer. Nickel-filtered CuKα radiation was used with the x-ray tube operating at 40 kv at 15 ma current. For routine identification, a scanning rate of 1 deg/min was used while the initial patterns used as a reference throughout this work were recorded at ½ deg/min.

High temperature x-ray diffraction data were obtained on a General Electric XRD-3 Geiger counter diffractometer also using Ni-filtered CuKα radiation. The x-ray furnace[1] was of ceramic construction with Pt heating elements and sample holder. An Al foil window in the furnace served as an entrance and exit for the x-radiation. The temperature of the specimen was maintained at ±5°C.

Differential thermal analyses.—Differential thermal analyses were done on an apparatus described by Gruver (4).

Polarizing microscope.—A Bausch and Lomb polarizing microscope was used to examine the crystalline and glass phases in the ZnO-P_2O_5 system. Index oils accurate to 0.004 were used for the index of refraction measurements of the glasses.

Heat treating furnaces.—All heat treatment other than quench work was done in electrically heated furnaces using silicon carbide heating elements. The temperature was controlled manually by an autotransformer. Because of the large size of the heating chamber, temperatures were considered accurate to only ±10°C. Such processes as formation of large amounts of glass, dehydration of zinc phosphate crystalline materials, weight loss measurements, and the preliminary work in determining the phase equilibrium relationships were done in these furnaces.

Raw materials.—The ZnO used in this investigation was obtained from the Chemical Products Plant of the General Electric Company. It is manufactured by the New Jersey Zinc Company and is a luminescent grade raw material with a purity comparable to a C.P. grade in commercially available chemicals. The ZnO was used as received with no weight loss correction.

The phosphoric acid used was a Baker Analyzed Reagent of C.P. grade. This acid contained approximately 85% orthophosphoric acid, H_3PO_4, the remaining 15% being water. To determine exactly the amount of P_2O_5 in the acid, gravimetric quantitative analysis of P_2O_5 described by Pierce and Haenisch (5) was used. This analysis consisted briefly of precipitation of the P_2O_5 as $MgNH_4PO_4 \cdot 6H_2O$ and finally weighing as $Mg_2P_2O_7$. Two 7-lb bottles of H_3PO_4 were analyzed separately. The following results were obtained:

Bottle #1 (g of P_2O_5/ml of acid)		Bottle #2 (g of P_2O_5/ml of acid)	
1.0665		1.0305	
1.0660		1.0340	
1.0665		1.0325	
Average analysis	1.066±.001	Average analysis	1.032±.002

Compositions and Heat Treatments

Compound preparation.—Zinc orthophosphate was prepared by reacting ZnO with H_3PO_4. The acid was slowly added to a water slurry of the ZnO. To insure homogeneity the resulting batch was hand mixed in a glass mortar for 1 hr. The acid reacted quite readily with the ZnO and water had to be added continually as the $Zn_3(PO_4)_2$ that was formed became hydrated. The final material was then dried at 110°C.

A sample of the dried batch which was heated to 640°C for 5 hr underwent a 9.14% weight loss. The theoretical weight loss in dehydrating $Zn_3(PO_4)_2 \cdot 2H_2O$ is 9.34%; therefore, it was concluded that this material was zinc orthophosphate dihydrate, and the x-ray data presented in Table IV as $Zn_3(PO_4)_2 \cdot 2H_2O$ were recorded from this material.

This $Zn_3(PO_4)_2 \cdot 2H_2O$ was then fired to 800-950°C for 12 hr. X-ray analysis indicated that the fired material consisted mainly of α-$Zn_3(PO_4)_2$ with some β-$Zn_3(PO_4)_2$ present. Further heat treatment of this mixture of α and β $Zn_3(PO_4)_2$ produced the pure forms of this compound. Refiring to 750°C for 4 hr produced all α-$Zn_3(PO_4)_2$, while refiring to 1000°C for 12 hr produced all β-$Zn_3(PO_4)_2$ (Table IV).

Three chemical analyses were run on each of two samples of the $Zn_3(PO_4)_2$. The average value obtained was 36.59±0.2% P_2O_5 compared to the theoretical value of 36.79% P_2O_5 in $Zn_3(PO_4)_2$. An independent analysis[2] gave a value of 36.48% P_2O_5.

[1] Furnace designed by H. A. McKinstry of the Mineral Constitution Laboratory of the Pennsylvania State University.

[2] Chemical Products Plant, General Electric Co., Cleveland, Ohio.

Zinc pyrophosphate was made by the well-known analytical procedure used for both ZnO and P_2O_5 analysis. A C.P. grade of $ZnCl_2$ was reacted with C.P. $(NH_4)_2PO_4$ to form $ZnNH_4PO_4$. The Zn NH_4PO_4 produced in this manner was fired to 900°C for 12 hr. A P_2O_5 analysis[2] indicated 47.3% P_2O_5 present compared to the theoretical amount of 46.59%. This indicated that a small amount of $Zn(PO_3)_2$ was present in the $Zn_2P_2O_7$.

Zinc metaphosphate could not be made by the reaction of ZnO with H_3PO_4. $Zn_3(PO_4)_2$ would form preferentially and even at elevated temperatures would not react readily with the remainder of the acid.

The $Zn(PO_3)_2$ finally used in the phase equilibrium investigation was obtained from the Monsanto Chemical Company. A chemical analysis[2] gave a value of 63.34±0.07% P_2O_5 as compared with the theoretical amount of 63.58% P_2O_5 in $Zn(PO_3)_2$.

Intermediate compositions and glasses.—The intermediate compositions between ZnO and $Zn_2P_2O_7$ were made by reacting ZnO with H_3PO_4 while the compositions between $Zn_2P_2O_7$ and $Zn(PO_3)_2$ were made from ZnO and $Zn(PO_3)_2$.

All solid-state reactions were done in Pt crucibles. The batches were given an initial low temperature firing between 600° and 700°C and then stored for later use.

Since the batches in the composition range between $Zn_2P_2O_7$ and $Zn(PO_3)_2$ were made from ZnO and $Zn(PO_3)_2$, $Zn_3(PO_4)_2$ rather than $Zn_2P_2O_7$ formed in some cases during the low temperature firing. This nonequilibrium existence of $Zn_3(PO_4)_2$ in this composition range did not affect the over-all chemical compositions or the glasses that were later made from these batches. As firing temperatures increased the $Zn_3(PO_4)_2$ disappeared.

After the intermediate compositions were made, portions of these batches were used to determine the extent of glass formation in this system. About 10-g samples were melted between 1100° and 1200°C for 30 min in a Pt crucible and quenched to a glass. The glass was removed from the crucible and crushed to −100 mesh particle size with a steel mortar and pestle. A magnet was used to remove any Fe particles introduced by the grinding. Table I lists the compositions made in the study of the $ZnO-P_2O_5$ system.

Chemical analyses.—To check the accuracy of the compositions made in the $ZnO-P_2O_5$ system, P_2O_5 analyses were run on various crystalline samples and glasses. Table II lists these analyses, some of which were mentioned previously in the section on compound formation.

Heat treatment of compositions.—All crystalline and glass compositions used for the phase equilibrium study in the $ZnO-P_2O_5$ system were heat treated in quench furnaces. This assured accurate temperature control and a minimum of P_2O_5 volatilization because of the sealed quench packet.

The preliminary investigations in the system were done using only crystalline batches as starting materials. Glasses were later used for liquidus and solidus determinations and for checking various points in the system.

One group of glasses in the composition range between $Zn_2P_2O_7$ and $Zn(PO_3)_2$ was devitrified in a Globar furnace. The purpose of this study was to crystallize the low form of $Zn(PO_3)_2$ from the

Table I. Compositions used for investigation of the system $ZnO-P_2O_5$

No.	Weight % ZnO	Weight % P_2O_5	Mole ratio	Initial heat treatment Time, hr	Initial heat treatment Temp, °C
1	74.12	25.88	5:1	12	924
2	72.00	28.00		19	700
3*	69.62	30.38	4:1	12	836
4*	68.00	32.00		19	700
5*	66.00	34.00		24	700
6	64.50	35.50		18	700
7	63.22	36.78	3:1		
8	62.00	38.00		19	700
9*	61.00	39.00		48	712
10	60.00	40.00		18	700
11*	58.89	41.11	5:2		
12*	58.00	42.00		24	600
13*	57.00	43.00		12	750
14*	55.00	45.00		12	710
15*	53.40	46.60	2:1		
16*	51.00	49.00		12	650
17*	48.85	51.15	5:3	24	650
18*	46.22	53.78	3:2	12	650
19*	43.31	56.69	4:3	24	650
20*	41.73	58.27	5:4	24	650
21	40.4	59.6		24	600
22*	39.00	61.00		24	650
23	37.6	62.4		24	650
24	36.42	63.58	1:1		

* Composition melted to glasses for use in quench determinations.

Table II. Chemical analyses of $ZnO-P_2O_5$ compositions

Sample No.	Description of sample	Weight per cent P_2O_5 Calculated	Analyzed Sample No. 1	Analyzed Sample No. 2
1	ZnO and P_2O_5 reacted in a 5:1 molar ratio and fired to 924°C/12 hr.	25.88	25.21	25.21
2	ZnO and P_2O_5 reacted in a 3:1 molar ratio and fired to 900°C/12 hr.	36.78	36.51	36.32
3	ZnO and P_2O_5 reacted and fired to 700°C/19 hr.	38.00	37.20	37.26
4	ZnO and P_2O_5 reacted and melted to a glass at 1200°C/30 min.	43.00	42.96	42.89
5	$Zn_2P_2O_7$ made from zinc ammonium phosphate and fired to 900°C/12 hr.	46.60	46.18	46.17
6	$Zn_2P_2O_7$ made from ZnO and H_3PO_4, fired to 800°C/12 hr.	46.60	45.66	45.62
7	$Zn_2P_2O_7$ melted to a glass at 1200°C/30 min.	46.60	47.10	47.12
8	ZnO and $Zn(PO_3)_2$ reacted in solid state at 650°C/24 hr.	62.40	62.30	62.37
9	Monsanto Chemical Company zinc metaphosphate, dried 110°C.	63.58	63.27	63.41

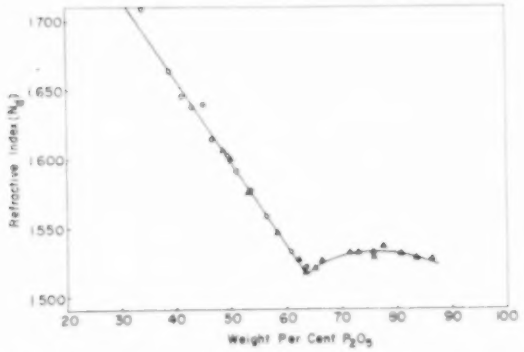

Fig. 1. Refractive indices of zinc phosphate glasses (sodium D light).

glasses. Since temperatures were not critical, the quench furnaces were not used in this investigation.

Experimental Results and Discussion

Zinc Phosphate Glasses

The index of refraction curve of the zinc phosphate glasses for sodium light is presented in Fig. 1. A break in the curve occurs at the $Zn(PO_3)_2$ composition according to the data of Kordes (11). Since the present work was concerned only with compositions ranging from ZnO to $Zn(PO_3)_2$, no glasses were made with a higher P_2O_5 content, and the data of Kordes were not checked.

The composition of $Zn_3(PO_4)_2$, 63.22% ZnO and 36.78% P_2O_5, could not be quenched to a glass. However, glasses could be formed on the ZnO side of $Zn_3(PO_4)_2$. This presents an unusual situation, since glasses could be formed on both sides of a compound composition, but not exactly on the compound composition.

The glasses with a P_2O_5 content greater than that in the $Zn_2P_2O_7$ composition, 53.40% ZnO and 46.60% P_2O_5, were attacked by the moisture in the air after a two month period.

Zinc Phosphate Compounds

Zinc orthophosphate.—The differential thermal analyses of the low and high forms of $Zn_3(PO_4)_2$ are presented in Fig. 2.

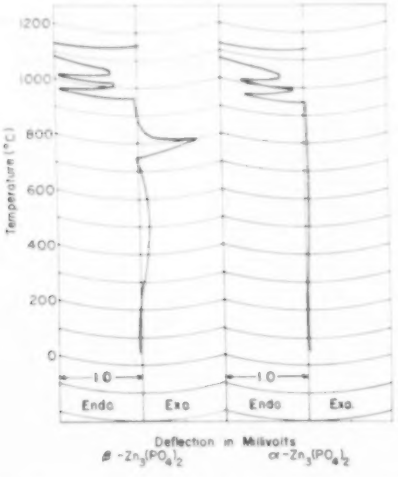

Fig. 2. Typical differential thermal analysis curves for β-$Zn_3(PO_4)_2$ and α-$Zn_3(PO_4)_2$.

The DTA of the α-$Zn_3(PO_4)_2$ showed three endothermic peaks. The first peak was due to an inversion in this compound. High temperature x-ray diffraction data indicated that this was the change from the α to the β form.

The inversion temperature was measured exactly by inserting samples of both α- and β-$Zn_3(PO_4)_2$ together in the quench furnace and examining the samples after heat treatment by x-ray analysis. At 938°C α-$Zn_3(PO_4)_2$ was stable and the β-$Zn_3(PO_4)_2$ was partially converted to α-$Zn_3(PO_4)_2$. This conversion was not complete even after 27 hr at this temperature. After 20 hr at 942°C, both the samples of α- and β-$Zn_3(PO_4)_2$ remained in their original form. At 944°C for 4 hr β-$Zn_3(PO_4)_2$ was stable, and the α-$Zn_3(PO_4)_2$ was partially converted to β-$Zn_3(PO_4)_2$. An inversion temperature of 942°C was concluded on the basis of these data.

The second endothermic peak in α-$Zn_3(PO_4)_2$ was due to the formation of some liquid in the sample. The chemical analysis indicated that the P_2O_5 content was about 0.3% low, indicating that the composition lies between the ZnO and $Zn_3(PO_4)_2$ end members. The eutectic temperature in this region is 1005°C. Above this temperature $Zn_3(PO_4)_2$ would be in equilibrium with a small amount of liquid phase if the composition deviated from the exact $3ZnO:P_2O_5$ ratio.

The third peak was due to the melting of $Zn_3(PO_4)_2$. Since $Zn_3(PO_4)_2$ could not be quenched completely to a glass, the melting point was measured by examining the material with a binocular microscope after heat treatment. As indicated, a small amount of liquid formed below the melting point. The effect of this liquid was to form the sample into a hard, dense mass. Above the melting point the $Zn_3(PO_4)_2$ flowed completely to the bottom of the quench packet. This difference in appearance above and below the melting temperature was used to determine the melting point. At a temperature of 1062°C, the sample had definitely melted, and there was a trace of glass present, while at 1056°C the sample was unmelted. A melting point of 1060°C was concluded from these data with an error of ±8°C because of the relatively poorer accuracy obtainable by this technique as compared to the regular quench technique using a glass.

The DTA of the high form of $Zn_3(PO_4)_2$ showed the three peaks present in the low form plus a fourth exothermic peak. The three endothermic peaks correspond to the three peaks in the α-$Zn_3(PO_4)_2$ DTA curve and are caused by the α-β inversion, eutectic liquid formation, and melting. However, the exothermic peak was unique for the DTA of the high form. Numerous runs showed that the temperature at which this peak occurred was not consistent and varied between 800° and 900°C. This peak is due to the return of β-$Zn_3(PO_4)_2$, which is unstable in this temperature range, to α-$Zn_3(PO_4)_2$.

Thermal expansion curves of α-$Zn_3(PO_4)_2$ indicated that the compound undergoes a substantial contraction during the inversion to β-$Zn_3(PO_4)_2$.

Conversely, the β form expands as it returns to the stable α form.

It was concluded that $Zn_3(PO_4)_2$ has a sluggish inversion at 942°C. The β form which is desired as a phosphor is metastable at room temperature which explains its poor chemical and thermal stability.

The x-ray diffraction data for α and β-$Zn_3(PO_4)_2$ shown in Table III reveal some differences when compared to those of Smith (2). It is believed that the data given in Table III are for pure phases, not contaminated with each other, or with "γ zinc phosphate."

Table III. X-ray diffraction patterns for the compounds in the system $ZnO-P_2O_5$

$Zn_3(PO_4)_2 \cdot 2H_2O$ (dried 110°C)*

2θ	d	I/I_o	2θ	d	I/I_o
9.8°	9.03	10	38.6°	2.33	—
11.3°	7.83	100	39.5°	2.28	—
17.1°	5.19	—	41.3°	2.19	—
18.6°	4.77	5	42.9°	2.11	—
19.5°	4.55	10	43.2°	2.09	—
20.9°	4.25	10	46.4°	1.96	15
22.7°	3.92	75	47.0°	1.93	15
24.6°	3.62	5	48.4°	1.88	5
25.5°	3.49	—	50.4°	1.81	5
25.9°	3.44	—	53.3°	1.72	—
26.4°	3.38	—	54.2°	1.69	—
27.9°	3.20	30	55.3°	1.66	—
29.2°	3.06	5	56.6°	1.63	—
29.6°	3.02	10	58.1°	1.59	5
30.5°	2.93	15	59.0°	1.57	10
31.5°	2.84	5	60.9°	1.52	5
32.2°	2.78	—	62.7°	1.48	—
32.7°	2.74	—	65.7°	1.42	—
34.4°	2.61	5	68.5°	1.37	5
34.9°	2.57	—	69.5°	1.35	—
35.8°	2.51	5	70.9°	1.33	5
36.9°	2.44	—	Other reflections		
37.5°	2.40	5			

* Pattern recorded at 1°/min.

Low (α) $Zn_3(PO_4)_2$

2θ	d	I/I_o	2θ	d	I/I_o
12.4°	7.14	5	44.6°	2.03	5
19.5°	4.55	40	45.1°	2.01	10
21.3°	4.17	35	46.2°	1.96	10
22.7°	3.92	40	46.5°	1.95	10
24.8°	3.59	90	47.1°	1.93	5
28.6°	3.12	75	49.2°	1.85	10
29.2°	3.06	100	50.0°	1.82	20
31.9°	2.81	15	50.8°	1.80	10
32.5°	2.75	10	51.3°	1.78	10
33.9°	2.64	10	54.9°	1.67	10
34.3°	2.61	25	55.6°	1.65	10
36.9°	2.44	40	57.9°	1.59	5
37.4°	2.40	35	59.8°	1.55	20
37.9°	2.37	5	60.9°	1.52	15
38.4°	2.34	5	61.5°	1.51	10
39.4°	2.29	40	63.2°	1.47	5
40.3°	2.24	25	64.6°	1.44	15
40.8°	2.21	20	66.2°	1.41	10
42.7°	2.12	10			
43.6°	2.07	10	Other reflections		

High (β) $Zn_3(PO_4)_2$

2θ	d	I/I_o	2θ	d	I/I_o
20.6°	4.31	5	38.1°	2.36	5
21.3°	4.17	15	39.1°	2.30	5
22.2°	4.00	10	39.6°	2.28	—
22.6°	3.93	15	41.0°	2.20	5
22.8°	3.90	10	41.5°	2.18	—
23.3°	3.82	—	42.0°	2.15	10
24.2°	3.68	10	43.3°	2.09	15
25.2°	3.53	—	44.7°	2.03	5
27.1°	3.29	100	45.1°	2.01	5
28.4°	3.14	20	45.5°	1.99	5
28.9°	3.09	60	46.4°	1.96	5
29.1°	3.07	35	47.2°	1.93	—
29.6°	3.02	20	47.6°	1.91	15
30.5°	2.93	15	48.7°	1.87	15
31.2°	2.87	75	48.9°	1.86	15
31.5°	2.84	60	50.4°	1.81	15
31.9°	2.81	5	51.4°	1.78	5
32.4°	2.76	—	53.7°	1.71	—
33.7°	2.66	—	54.7°	1.68	10
34.1°	2.63	5	55.5°	1.66	5
35.0°	2.56	10	56.0°	1.64	5
35.3°	2.54	5	57.4°	1.61	15
36.0°	2.49	20	58.8°	1.57	5
36.6°	2.46	5			
37.6°	2.39	20	Other reflections		

Low (α) $Zn_2P_2O_7$

2θ	d	I/I_o	2θ	d	I/I_o
9.2°	9.61	—	35.3°	2.54	45
15.8°	5.61	10	36.2°	2.48	—
17.4°	5.10	10	38.1°	2.36	—
18.4°	4.82	—	39.1°	2.30	10
18.8°	4.72	—	41.2°	2.19	5
19.4°	4.58	—	42.8°	2.11	20
19.8°	4.48	—	43.2°	2.09	45
20.3°	4.37	15	43.5°	2.08	5
21.3°	4.17	15	45.0°	2.01	10
22.5°	3.95	—	47.0°	1.93	5
23.3°	3.82	—	47.6°	1.91	—
23.7°	3.75	5	48.5°	1.88	10
24.7°	3.60	5	51.6°	1.77	—
25.4°	3.51	—	52.1°	1.76	—
25.8°	3.45	—	53.5°	1.71	5
26.5°	3.36	—	54.1°	1.70	5
26.8°	3.33	—	55.0°	1.67	5
27.7°	3.22	—	55.8°	1.65	5
28.3°	3.15	—	56.8°	1.62	5
28.9°	3.09	5	57.2°	1.61	10
29.5°	3.03	60	57.4°	1.61	10
29.7°	3.01	100	58.7°	1.57	25
31.2°	2.87	5	59.6°	1.55	5
31.4°	2.85	10	60.0°	1.54	5
31.8°	2.81	—	61.8°	1.50	5
32.9°	2.72	5	63.1°	1.47	15
34.6°	2.59	—	Other reflections		

High (β) $Zn_2P_2O_7$*

2θ	d	I/I_o	2θ	d	I/I_o
17.5°	5.07	—	57.0°	1.62	10
20.3°	4.34	5	58.4°	1.58	15
24.7°	3.60	—	59.8°	1.55	5
27.3°	3.27	—	61.5°	1.51	5
28.7°	3.11	—	62.0°	1.50	—
29.6°	3.02	100	62.8°	1.48	10
34.9°	2.57	—	63.6°	1.46	—
35.2°	2.55	30	70.0°	1.34	5
39.0°	2.31	5	70.7°	1.33	5
41.1°	2.20	5	71.4°	1.32	—
43.0°	2.10	25	71.7°	1.32	5
43.6°	2.08	5	75.4°	1.26	5
44.9°	2.02	5	78.3°	1.22	—
46.8°	1.94	5	78.9°	1.21	—
48.5°	1.88	15			
51.9°	1.76	5	Other reflections		
53.5°	1.71	5			
54.1°	1.70	5			

* Pattern recorded at 1°/min with specimen at 850°C.

Low (α) $Zn(PO_3)_2$

2θ	d	I/I_o	2θ	d	I/I_o
13.5°	6.56	5	38.2°	2.36	25
13.7°	6.46	15	42.4°	2.13	10
13.8°	6.42	55	42.9°	2.11	10
14.4°	6.15	5	43.8°	2.07	25
19.3°	4.60	5	45.1°	2.01	10
20.0°	4.44	55	45.4°	2.00	10
20.8°	4.27	50	46.8°	1.94	5
25.2°	3.53	5	47.9°	1.90	20
25.8°	3.45	55	50.1°	1.82	—
26.4°	3.38	5	50.6°	1.80	—
27.1°	3.29	—	51.0°	1.79	10
27.6°	3.23	5	52.0°	1.76	—
28.1°	3.18	5	52.4°	1.75	5
29.3°	3.05	15	53.5°	1.71	5
30.1°	2.97	95	56.6°	1.63	10
30.7°	2.91	100	56.9°	1.62	10
31.2°	2.87	5	57.5°	1.60	10
31.7°	2.82	20	59.6°	1.55	10
34.8°	2.58	5	60.1°	1.54	50
35.5°	2.53	5	60.7°	1.53	5
37.3°	2.41	45			
37.7°	2.39	10	Other reflections		

Table III. X-ray diffraction patterns for the compounds in the system ZnO-P_2O_5 (Cont.)

		High (β) $Zn_3(PO_4)_2$			
2θ	d	I/I_o	2θ	d	I/I_o
16.5°	5.37	5	35.4°	2.54	—
17.3°	5.13	5	36.3°	2.47	5
17.6°	5.04	5	37.4°	2.40	10
19.6°	4.53	10	37.7°	2.39	10
20.1°	4.42	10	39.6°	2.28	10
21.8°	4.08	40	40.0°	2.25	5
23.1°	3.85	10	40.8°	2.21	5
23.4°	3.80	30	41.2°	2.19	10
24.0°	3.71	15	41.5°	2.18	5
25.5°	3.49	45	44.1°	2.05	5
25.8°	3.45	100	44.3°	2.04	15
26.2°	3.40	25	47.8°	1.90	5
27.2°	3.28	10	48.2°	1.89	5
27.8°	3.21	15	48.7°	1.87	5
29.8°	3.00	—	49.6°	1.84	5
31.8°	2.81	10	51.4°	1.78	5
32.5°	2.75	10	53.9°	1.70	10
33.6°	2.67	10	Other reflections		

Zinc pyrophosphate.—The differential thermal analysis curve of $Zn_2P_2O_7$ is given in Fig. 3. The curve showed two peaks, one at about 130° and the other at about 1020°C.

The first peak was due to an inversion in $Zn_2P_2O_7$. Duplicate runs on the same sample indicated that this inversion was reversible. Quenches of $Zn_2P_2O_7$ heated to temperatures above the inversion temperature did not freeze in a high form of the material. These data indicated that the inversion was very rapidly reversible.

High temperature x-ray methods were used to measure the inversion temperature. A sample was heated above the inversion temperature and then cooled in 10°C increments until the x-ray pattern showed a change to another form. This change took place between 127° and 137°C. An inversion temperature of 132°±8°C was concluded from these data.

The major peaks in the x-ray data of the high form of $Zn_2P_2O_7$ closely resembled those for the low form, Table III. The inversion to the high form was accompanied by the disappearance of about one-half of the x-ray peaks present in the low form. This suggests that the inversion of $Zn_2P_2O_7$ was due to a change from a lower to a higher symmetry structure. The low form of $Zn_2P_2O_7$ gave biaxial interference figures under the polarizing microscope.

The second peak at 1020°C in the DTA curve was due to the melting of $Zn_2P_2O_7$. The melting point of $Zn_2P_2O_7$ as determined accurately by quench techniques is 1017°C.

Zinc metaphosphate.—The differential thermal analysis curve of $Zn(PO_3)_2$ is presented in Fig. 3. This curve showed two peaks, one at approximately 780° and the other at 900°C.

The first peak is due to a polymorphic inversion in $Zn(PO_3)_2$. This peak has an unusual contour showing a slow rounding effect after the initial sharp peak. This rounding effect was probably due to the formation of a very small amount of liquid in the sample. The chemical analysis indicated the P_2O_5 content was about 0.3% below that of pure $Zn(PO_3)_2$, or that the actual composition of this material lies between $Zn_2P_2O_7$ and $Zn(PO_3)_2$. The eutectic temperature in this region is 834°C which is approximately where this rounding effect takes place. This peak is about 120°C above the inversion temperature of 650°C as measured by quench techniques. This is to be expected since differential thermal analysis is a dynamic measurement and this inversion is sluggish.

The second peak was due to the melting of $Zn(PO_3)_2$ and corresponds roughly to the melting point of 872°C as measured by quench techniques.

A sample of α-$Zn(PO_3)_2$ was heated to 630°-650°C for 54 hr to confirm the stability of the low form in this temperature range. X-ray analysis of the above sample indicated that only the low form of $Zn(PO_3)_2$ was present.

Since heating the high form of $Zn(PO_3)_2$ at a temperature below its inversion at 650°C did not produce the low form, an attempt was made to form α-$Zn(PO_3)_2$ by devitrifying a glass of the $Zn(PO_3)_2$ composition. The first experimental run consisted of heating a sample of $Zn(PO_3)_2$ glass for 1, 4, and 16 hr at 650°C. X-ray analysis indicated that these glasses divitrified to only the high form. A second set of glasses heated for 1, 4, and 16 hr at 550°C devitrified to a mixture of the high and low forms of $Zn(PO_3)_2$. Temperatures below 450°C were found to be not high enough to produce devitrification. This study indicated that the low form of $Zn(PO_3)_2$ could be formed by devitrifying $Zn(PO_3)_2$ glass. However, complete devitrification to the low form could not be obtained. This eliminated the technique of measuring the inversion temperature by devitrifying glasses. Consequently, the inversion temperature measurement was determined only by going from the low to the high form.

It was concluded that $Zn(PO_3)_2$ has an irreversible inversion when heated in air. This inversion is reasonably slow in a temperature range near the inversion. Temperatures 90°-140°C above the arbitrarily selected inversion temperature of 650°C produce complete transition to the higher form in about a one-hour firing time.

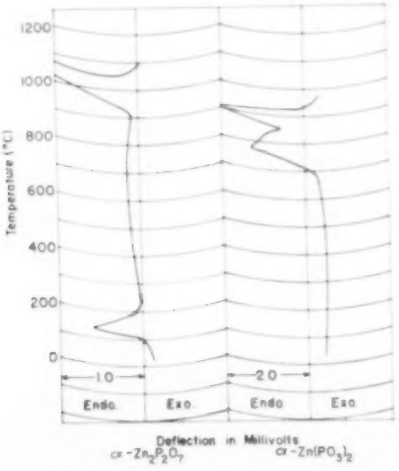

Fig. 3. Typical differential thermal analysis curves for α-$Zn_2P_2O_7$ and α-$Zn(PO_3)_2$.

Phase Equilibrium Relationships

Quench data.—The experimental data obtained by quench method are presented in Table IV. The

Table IV. Quench data for the system ZnO-P_2O_5

No.	Composition weight % ZnO	Composition weight % P_2O_5	Mole ratio	Starting material	Heat treatment Time, hr	Heat treatment Temp. °C	Phases present	Method of direction
1	74.12	25.88	5:1	CR	1	1015	GL + CR	M
				CR	1	1004	CR	M
				CR	3	1012	ZnO (+GL)	X
				CR	20	941	ZnO + α3:1	X
				CR	2	932	ZnO + α3:1	X
				CR	4	916	ZnO + α3:1	X
3	69.62	30.38	4:1	GL	½	1179	GL	M
				GL	½	1170	GL + CR	M
				CR	1	1003	GL + CR	M
				CR	1	992	CR	M
				CR	15	1028	ZnO (+GL)	X
				CR	3	959	ZnO + β3:1	X
				CR	2	948	ZnO + β3:1	X
				CR	2	932	ZnO + α3:1	X
				CR	20	892	ZnO + α3:1	X
4	68.00	32.00	—	GL	½	1110	GL	M
				GL	½	1104	CR	M
5	66.00	34.00	—	CR	4	1013	GL	M
				CR	4	1008	GL + CR	M
7	63.22	36.78	3:1	CR	14	1062	GL + CR	M
				CR	3	1056	CR	M
				CR	15	1030	β3:1	X
				CR	15	990	β3:1	X
				CR	15	954	β3:1	X
				CR	21	949	β3:1	X
				CR	20	942	β3:1	X
				CR	20	942	α3:1	X
				CR	27	938	α3:1	X
				CR	24	928	α3:1	X
8	62.00	38.00	—	CR	2	954	α3:1 + β2:1	X
				CR	2	900	α3:1 + β2:1	X
				CR	2	850	α3:1 + β2:1	X
9	61.00	39.00	—	CR	1½	1045	GL	M
				CR	2	1041	GL + CR	M
				CR	8	1024	β3:1 (+GL)	X
				CR	8	990	β3:1 (+GL)	X
				GL	2	954	α3:1 + β2:1	X
				CR	15	948	α3:1 + β2:1	X
				GL	2	897	α3:1 + β2:1	X
				GL	2	849	α3:1 + β2:1	X
11	58.89	41.11	5:2	CR	½	1026	GL	M
				CR	½	1016	GL + CR	M
				CR	12	1032	(GL)	X
				CR	15	989	β3:1 (+GL)	X
				GL	2	954	α3:1 + β2:1	X
				CR	15	948	α3:1 + β2:1	X
				GL	2	897	α3:1 + β2:1	X
				GL	2	849	α3:1 + β2:1	X
12	58.00	42.00	—	CR	½	1007	GL	M
				CR	½	995	GL + CR	M
				CR	1½	958	β3:1 + β2:1	X
13	57.00	43.00	—	CR	½	982	GL	M
				CR	½	972	GL + CR	M
				CR	20	1029	(GL)	X
				CR	20	939	α3:1 + β2:1	X
14	55.00	45.00	—	CR	½	1006	GL	M
				CR	½	997	GL + CR	M
				CR	12	976	β2:1 (+GL)	X
				CR	1½	967	β3:1 + β2:1	X
15	53.40	46.60	2:1	CR	2	1018	GL	M
				CR	2	1015	CR	M
16	51.00	49.00	—	GL	2½	1006	GL	M
				GL	2½	1001	GL + CR	M
				CR	10	902	β2:1 (+GL)	X
				CR	16	820	β2:1 + β1:1	X
17	48.85	51.15	5:3	CR	½	1020	GL	M
				CR	½	1014	GL + CR	M
				GL	3	837	β2:1 (+GL)	X
				GL	1	827	β2:1 + β1:1	X
				GL	2½	818	β2:1 + β1:1	X

Table IV. Quench data for the system ZnO-P_2O_5 (Cont.)

18	46.22	53.78	3:2	GL	½	1004	GL	M
				GL	½	997	GL + CR	M
				CR	6	895	β2:1 (+GL)	X
				CR	22	836	β2:1 (+GL)	X
				CR	8	820	β2:1 + β1:1	X
				CR	22	755	β2:1 + β1:1	X
				CR	9	711	β2:1 + α1:1	X
19	43.31	56.69	4:3	GL	½	962	GL	M
				GL	½	957	GL + CR	M
				GL	3	837	β2:1 (+GL)	X
				GL	1	827	β2:1 + β1:1	X
				GL	2½	818	β2:1 + β1:1	X
				GL	1½	717	β2:1 + α1:1	X
20	41.73	58.27	5:4	CR	½	938	GL	M
				CR	½	932	GL + CR	M
				CR	4	859	β2:1 (+GL)	X
				CR	6	818	β2:1 + β1:1	X
				CR	15	722	β2:1 + α1:1	X
				CR	6	699	β2:1 + α1:1	X
22	39.00	61.00	—	GL	½	844	GL	M
				GL	½	840	GL + CR	M
				GL	1	827	β2:1 + β1:1	X
				GL	2½	818	β2:1 + β1:1	X
				CR	19	707	β2:1 + β1:1	X
24	36.42	63.58	1:1	CR	2	874	GL	M
				CR	1	870	CR	M
				CR	16	745	β1:1	X
				CR	22	694	β1:1 (Trace α1:1)	X
				CR	9	690	β1:1 + α1:1	X
				CR	20	687	α1:1	X
				CR	20	676	α1:1	X
				CR	20	658	α1:1	X

α3:1 = Low (α) $Zn_3(PO_4)_2$
β3:1 = High (β) $Zn_3(PO_4)_2$
β2:1 = High (β) $Zn_2P_2O_7$
α1:1 = Low (α) $Zn(PO_3)_2$
β1:1 = High (β) $Zn(PO_3)_2$

GL = Glass
CR = Crystals
M = Microscope
X = X-ray

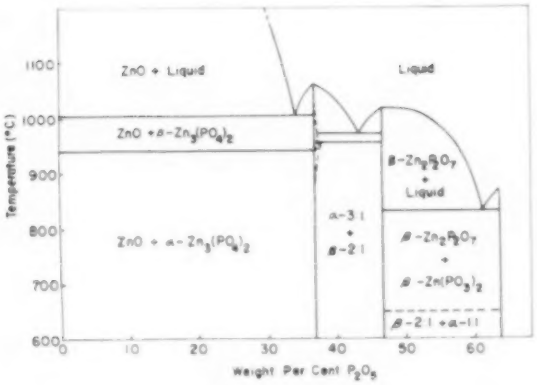

Fig. 4. Phase equilibrium diagram for the system ZnO-$Zn(PO_3)_2$.

phase diagram of the ZnO-$Zn(PO_3)_2$ portion of the ZnO-P_2O_5 system was drawn from these data and is presented in Fig. 4.

The five crystalline modifications of the zinc phosphates obtainable at room temperature all produced biaxial interference figures under the polarizing microscope. The high and low forms of $Zn_3(PO_4)_2$ particularly resembled one another under the light microscope. Since all these materials produced distinct and characteristic x-ray diffraction patterns, x-ray diffraction techniques were used for all crystal indentification. This single method of identification proved to be completely adequate throughout the system.

ZnO-$Zn_3(PO_4)_2$ *portion.*—The presence of excess ZnO with $Zn_3(PO_4)_2$ had no effect on the inversion temperature of the pure $Zn_3(PO_4)_2$, indicating no solubility of ZnO in the orthophosphate.

The eutectic temperature is 1005°C, and the eutectic composition is approximately 66% ZnO and 34% P_2O_5. No experimental difficulty was experienced in obtaining ZnO in equilibrium with α-$Zn_3(PO_4)_2$, β-$Zn_3(PO_4)_2$ or glass.

$Zn_3(PO_4)_2$-$Zn_2P_2O_7$ *portion.*— An enlarged view of the $Zn_3(PO_4)_2$-$Zn(PO_3)_2$ portion of the system is presented in Fig. 5. The presence of $Zn_2P_2O_7$ with $Zn_3(PO_4)_2$ had a definite effect on the inversion temperature of $Zn_3(PO_4)_2$. The quenched compositions in this portion showed that α-$Zn_3(PO_4)_2$ was stable in the presence of $Zn_2P_2O_7$ to at least 955°C, 13° above the inversion temperature of pure $Zn_3(PO_4)_2$. This increase in inversion temperature implies the existence of a solid solution of $Zn_2P_2O_7$ in $Zn_3(PO_4)_2$ to the extent of approximately 5% $Zn_2P_2O_7$. A composition with a chemical analysis of 37.23% P_2O_5, which is about 0.5% more P_2O_5 than the pure $Zn_3(PO_4)_2$, always showed the presence of two phases when heat treated.

There was no difficulty in obtaining α-$Zn_3(PO_4)_2$ in equilibrium with $Zn_2P_2O_7$. However, it was very difficult to obtain β-$Zn_3(PO_4)_2$ in equilibrium with $Zn_2P_2O_7$. Only two quenches presented in Table IV

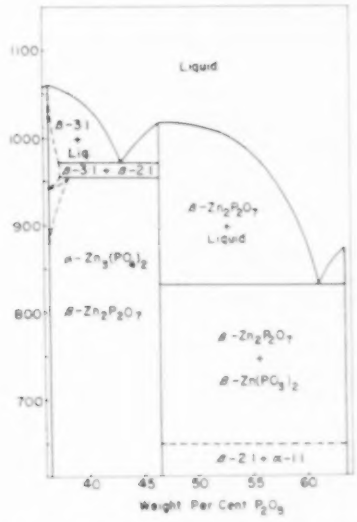

Fig. 5. Enlarged diagram of the equilibrium relationships in the range between $Zn_3(PO_4)_2$ and $Zn(PO_3)_2$.

contain these two phases. Numerous other quenches in this very small temperature range usually showed the nonequilibrium existence of three phases, α-$Zn_3(PO_4)_2$, β-$Zn_3(PO_4)_2$, and $Zn_2P_2O_7$. The eutectic temperature in this region is at 972°C, and the eutectic composition is approximately 57% ZnO and 43% P_2O_5.

$Zn_2P_2O_7$-$Zn(PO_3)_2$ *portion.*—Since glasses in this portion of the system could not be devitrified completely to the low form, the $Zn(PO_3)_2$ inversion in the presence of $Zn_2P_2O_7$ was measured using crystalline starting material.

The $Zn(PO_3)_2$ inversion appeared to be inhibited by the presence of $Zn_2P_2O_7$ and occurred at temperatures of 65°-80°C above the 650° observed for the pure $Zn(PO_3)_2$. Since the lowest temperature at which pure α-$Zn(PO_3)_2$ crystallized from glass was 650°C, the inversion is shown at this temperature in Fig. 4 and 5. The actual equilibrium inversion temperature may be considerably below 650°C.

The eutectic temperature is 832°C, and the eutectic composition is approximately 39% ZnO and 61% P_2O_5.

Summary and Conclusions

1. Equilibrium relationships have been established for the system ZnO-$Zn(PO_3)_2$.

2. The conclusion of Smith that $Zn_3(PO_4)_2$ does not show any phase change up to the point of fusion has been proven incorrect. A relatively sluggish reversible inversion of α-$Zn_3(PO_4)_2$ to β-$Zn_3(PO_4)_2$ occurs at 942°C.

3. $Zn_2P_2O_7$ and $Zn(PO_3)_2$ exist in two polymorphic forms.

Acknowledgment

The authors wish to thank members of the analytical laboratory of the Chemical Products Plant of the General Electric Co., Cleveland, Ohio for their assistance with the chemical analyses. The financial support of the General Electric Company during the course of the work was deeply appreciated.

Manuscript received July 15, 1957. Contribution No. 57-1 from the College of Mineral Industries, The Pennsylvania State University.

Any discussion of this paper will appear in a Discussion Section to be published in the December 1958 JOURNAL.

REFERENCES

1. H. Insley, G. W. Morey, F. D. Rossini, and A. Silverman, Editors, *Bull. Nat. Research Council. (U. S.)*, No. 118, U. of Pittsburgh (1949).
2. A. L. Smith, *This Journal*, **98**, 363 (1951).
3. W. L. Hill, G. T. Faust, and D. S. Reynolds, *Am. J. Sci.*, **242**, 457 (1944).
4. R. M. Gruver, *J. Am. Ceram. Soc.*, **31**, 323 (1948).
5. W. C. Pierce and E. L. Haenisch, "Quantitative Analysis," 2nd ed., John Wiley & Sons, Inc., New York (1937).

The Luminescence of Self-Coactivated ZnS:Cu

M. H. Aven and R. M. Potter

Lamp Development Department, General Electric Company, Nela Park, East Cleveland, Ohio

ABSTRACT

Phosphors prepared by firing ZnS with Cu in purified H_2S show a simple orange emission band, with no other bands in evidence even at 90°K. Excitation by ultraviolet, cathode rays, and electric field gives identical emission spectra. The emission band peaks at the same wave length for samples with either hexagonal or cubic crystal structure, but is shifted to longer wave lengths by addition of CdS. The orange luminescence is strongly decreased by traces of H_2O in the H_2S firing atmosphere, but quite stable to firing in oxidizing or reducing atmospheres.

Addition of Al to ZnS:Cu gives a series of phosphors showing various proportions of orange, blue, and green emission. Firing ZnS with Ag in pure H_2S gives a new yellow-emitting phosphor with properties very similar to the orange Cu-activated phosphor. Possible models for the orange center are discussed.

A few years ago, Froelich (1) described a new ZnS:Cu phosphor exhibiting a yellow-red emission under ultraviolet or electroluminescent excitation. It was prepared by firing mixes containing from 10^{-3} to 10^{-2} atom fraction Cu at temperatures above 1000°C in an H_2S atmosphere which was free of oxygenous impurities. The emission spectra of Froelich's products varied somewhat with the firing conditions, and also with the mode of excitation. The emission occurred in a broad band peaking around 6500A, and was believed to consist of a strong red band at 6700A, and a weaker yellow band at 5800A. The relative intensity of the latter under ultraviolet depended on the wave length of the exciting radiation.

Recently Bowers and Melamed (2) reported that a blue (4400A) emission band was always found in their ZnS:Cu phosphors showing the 6700A band (referred to by them as the "red" emission), although in some of their products, the blue band showed up only at liquid air temperatures. Since they found no temperature-dependent magnetic susceptibility in these products they concluded that the "red" centers did not involve any unpaired electrons. They therefore proposed that the "red" center was an interstitial copper coactivated by a zinc vacancy, which in turn was responsible for the 4400A band.

In the present work it was possible, by scrupulous elimination of oxygenous and coactivator type impurities from the H_2S firing atmosphere, to prepare "self-coactivated" ZnS:Cu with only the 6700A band present with all types of excitation used. This band is referred to in this paper as the "orange band" because "orange" describes the color of its luminescent emission as perceived by the eye better than "red".

Preparation of Phosphors

The phosphors were prepared from precipitated ZnS which had been prefired in pure H_2S to remove oxygen and halide impurities. Froelich (1) had found that, in preparing the orange phosphors, comparable results were obtained with pure H_2S gas directly from a cylinder and with gas that was first washed with $Ba(OH)_2$ solution and then freed from water vapor. In the present work, however, it was found to be impossible to obtain bright orange phosphors, using the best available grade H_2S gas directly from a cylinder. Therefore the above-mentioned method of purification was employed in all H_2S firings. The residual quantity of oxygenous and coactivator impurities after such treatment was estimated to be less than 10 ppm (possibly much less than 10 ppm).

The phosphors were fired in small bottle-shaped tubes in an arrangement very similar to that described by Froelich (1). In this set-up, fresh H_2S gas is passed continually over the phosphor sample, thus sweeping out any gaseous reaction products.

The phosphor mixes were prepared by adding Cu or Al as dilute solutions of the nitrate or sulfate to ZnS powder, along with enough deionized water to give a stiff paste. This paste was dried, sieved, and transferred to the firing tube. The firing tubes were inserted into the furnace at 600°C, and the temperature raised quickly to the firing temperature, usually 1100°C. After the firing period, usually 1 hr, the tube was removed from the furnace and allowed to cool to room temperature. The flow of pure H_2S was maintained from the time before inserting the tube into the furnace until the time the firing tube had cooled to room temperature. The cooled phosphors were removed from the firing tube and washed in NaCN solution to remove free Cu_2S.

It is of theoretical interest to know the minimum temperature needed to form a phosphor. When attempts were made to prepare the orange phosphor by the method described above, but using firing temperatures lower than 1000°C, the products showed very weak or no luminescence. It was sus-

pected that these lower temperature firings failed to remove the oxygen which was present in the starting materials. This residual oxygen then prevented the formation of orange centers. Therefore a preparation method was developed in which oxygen was removed from the starting materials. A portion of ZnS, prefired as described above, was further fired for ½ hr at 1100°C in pure H_2S. A sample of Cu_2S was prefired for 20 min at 600°C in H_2S. With H_2S passing through both tubes, the Cu_2S was shaken into the tube containing the ZnS, avoiding contact with air. After mixing by rotating the tube, the mix was put back into the furnace at 900°C for 1 hr. This experiment was repeated except that the final firing was (*a*) 2 hr at 800°C, (*b*) 2 hr at 700°C. In each case the orange luminescence appeared, although not as bright as in normally prepared samples. A sample fired for 2 hr at 600°C did not fluoresce. Thus it appears that orange centers can form at comparatively low temperatures provided oxygen is carefully excluded.

In some preparations, the phosphor mix was fired in H_2S to which H_2O had purposely been added in certain proportions. This wet H_2S was prepared by passing pure H_2S through water or over ice maintained at a series of temperatures to give the desired vapor pressure of H_2O. In these products, the orange emission was much weaker than in samples fired in dry H_2S. The intensity of the orange band could be brought back to normal by refiring at 1100°C for approximately 1 hr in dry H_2S. However, once this good phosphor was formed, firing for several hours at 1100°C in wet H_2S caused very little dimming of the fluorescence. Refiring at 1200°C or higher in wet H_2S again destroyed the orange luminescence. Apparently, the activation energy for destroying orange centers with H_2O is appreciably higher than that for forming them from nonluminescing material.

Some experiments were carried out which indicated stability of the orange centers to firing in oxidizing atmospheres. Some preformed (unwashed) ZnS:10^{-4} Cu orange phosphor was placed in a thick-walled quartz tube and fired in H_2S at 1100°C for ½ hr to remove any adsorbed air or water. After cooling, enough pure sulfur was added to give about 15 atm of S_2 at 1100°C (assuming perfect gas laws), and the tube was sealed off under vacuum. It was then placed in a furnace and brought up to 1100°C for 1 hr, cooled slowly, and removed. The product appeared essentially unchanged in fluorescent color and brightness from the starting material.

In order to determine the stability of the orange centers to reducing atmospheres, some firings were performed in H_2 and in Zn vapor. Firings of ZnS:10^{-4} Cu carried out in a flow of pure H_2 (similar to H_2S firing technique) gave a product showing the orange emission. However the fluorescent color depended, at least in part, on the number of similar firings carried out in the same quartz tube. A series of three firings in one tube gave products which were in time sequence, blue (with some weak orange), pink (blue plus orange), and pink (even less blue). The part of the sample next to the walls was blue in each case. The blue fluorescence probably corresponds to under-coactivated Cu blue emission (*see* Fig. 3). A single firing in another tube gave a green-fluorescing product. Analogous experiments, using enough pure Zn to give 15 atm, gave nonuniform products which were sometimes quite green, but sometimes largely pink under u.v. excitation. Apparently some coactivating impurity, like Al, is present in the quartz walls of the firing tube, and a reducing atmosphere like Zn or H_2 causes it to leach out into the ZnS:Cu. Repeated firings seem to deplete this impurity from the walls and allow the normal orange fluorescent color to develop. It was difficult to reproduce these results, apparently because of a variability in the quartz firing tubes.

These results indicate that orange centers are stable to reducing or oxidizing conditions. They suggest a different interpretation of the results of Riehl and Ortmann (3), who reported a green-fluorescing product from firing ZnS:Cu in H_2. It seems quite possible that their product was contaminated with a coactivator impurity.

Methods of Spectral Measurements

The emission spectra were measured with a Perkin-Elmer Double Pass Monochromator, Model 99. The detector used for the visible region of the spectrum was a 1P22 photomultiplier tube. In one special measurement, a DuMont infrared photomultiplier tube, which gives response out to about 1.1μ was used. For 3650A excitation, the output of an AH4 mercury lamp, passed through a 7-37 Corning filter, was focussed on the sample. For 3000-3500A excitation, an erythemal fluorescent lamp was used; the intensity of excitation was much lower with this source. The electroluminescent excitation was produced by a 60 cps 500 v rms field across a 0.005 in. phosphor-dielectric layer. The cathode ray spectrum was measured using a 16 kv, 510μ nonfocussed raster (130 cm^2). The spectrometer used here was not calibrated beyond 7000Å.

The monochromator (used for all spectra except the cathode ray spectrum) was calibrated with an incandescent lamp whose spectral distribution was known. The calibration was expressed in a form to give fluorescent emission spectra as a plot of the relative energy per unit photon energy interval vs. photon energy rather than the conventional relative energy per unit wave-length interval vs. wave length. When simple fluorescent emission spectra are plotted in the former units, they usually assume, to a good degree of accuracy, a symmetrical bell-shape or Gaussian form (4, 5). Complex emission spectra can be resolved usually into a set of Gaussian curves. The positions of the emission peaks of spectra plotted in this fashion are, of course, slightly shifted relative to their positions on conventional plots. For example, the emission peak of the orange phosphor occurs at 1.84 e.v. (6750A) on the energy per unit photon energy interval plot and at 1.91 e.v. (6500A) on the energy per unit wavelength interval plot.

The excitation spectrum of the orange phosphor was determined by mounting the sample as a thin layer in front of the photomultiplier detector of the

Perkin-Elmer spectrophotometer. A red filter next to the photomultiplier transmitted only the fluorescent emission. A projection lamp was focussed on the entrance slit. First pass and stray radiation were eliminated at the exit slit by means of suitable filters. Two runs were made; in the first, the radiation from the exit slit was deflected to the internal thermocouple detector by means of a mirror. The signal from the thermocouple as the spectral region of interest was scanned gave the intensity I_E of the exciting radiation. In the second run, the light from the exit slit was allowed to fall on the sample. The signal from the photomultiplier gave the intensity I_F of the fluorescent emission. The excitation spectrum is a plot of I_F/I_E vs. photon energy.

Results

In Fig. 1 is shown the emission spectrum of ZnS:1.5 x 10^{-4} Cu[1] (fired at 1100°C for ½ hr) under four different methods of excitation. The solid line is the Gaussian fitting the equation $I = I_0 \exp[-C(E - E_0)^2]$, where I is the emitted energy per unit photon energy interval, E is the photon energy, E_0 is the photon energy at the peak of the emission band, I_0 is a normalization constant, and C is related to the half-width, $2(E_{1/2} - E_0)$, of the band by the relation

$$C = \frac{\ln 2}{(E_{1/2} - E_0)^2}$$

For the emission band in Fig. 1, $E_0 = 1.84$ e.v. and $2(E_{1/2} - E_0) = 0.62$ e.v. The experimental points for 3650Å, 3000-3500Å, cathode ray, and electroluminescent excitation are plotted to show the accuracy of fit to a Gaussian curve and to show the near identity of results for different methods of excitation. The portion of the 3650Å plot for photon energies less than 1.7 e.v. was obtained in a separate measurement with the infrared sensitive photomultiplier tube.

[1] In all formulas in this paper, the number preceding the impurity symbol refers to the atom fraction of added impurity; in the case of ZnS:Cu with no Al, the atom fraction retained in the phosphor after the NaCN wash is about 30-40% of that added.

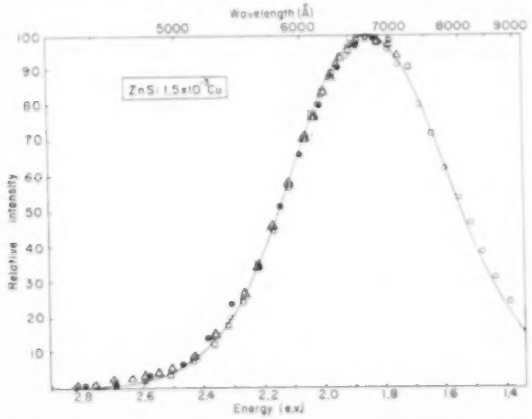

Fig. 1. Emission spectrum of orange fluorescing ZnS:1.5 x 10^{-4} Cu, fired at 1100°C. Solid line, Gaussian function fitted through the experimental points; open circles, 3650 Å u.v. excitation; full circles, cathode ray excitation; squares, electroluminescent excitation; triangles, 3000-3500Å u.v. excitation.

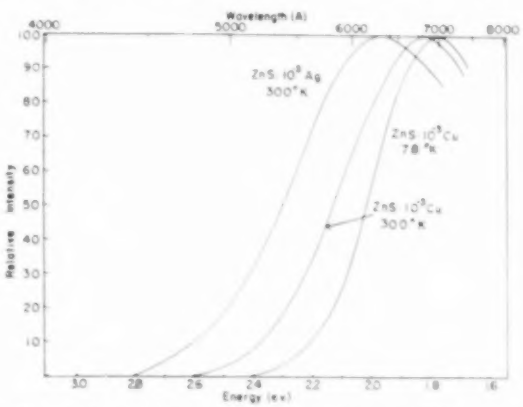

Fig. 2. Emission spectra of ZnS:10^{-3} Cu at 78°K and at 300°K, and the emission spectrum of ZnS:10^{-3} Ag at 300°K.

There is no detectable change in emission spectrum when the frequency of electroluminescent excitation is changed from 60 to 5000 cps. The electroluminescent emission spectra of a few samples with higher than average electroluminescent response showed a shift of the whole orange emission band by a few hundredths of an electron volt toward higher energies compared to the u.v. excited spectrum. This effect is due presumably to a perturbation of the energy levels in the activator centers by the high local electric fields present during electroluminescent excitation.

The spectrum of ZnS:Cu at 78°K is shown in Fig. 2. This, as well as all other spectra discussed below, was obtained under 3650Å u.v. excitation. Here the peak is shifted to 1.78 e.v. and the half-width is decreased from 0.62 e.v. to 0.48 e.v. It still approximates a single Gaussian band and no blue emission band is observed.

Since ZnS phosphors activated with Ag and Au and coactivated with Al or Cl exist and are similar to coactivated Cu phosphors, it was decided to attempt to prepare self-coactivated ZnS:Ag and ZnS:Au. The ZnS:Ag firing produced a yellow-emitting phosphor with a weak afterglow, whose spectrum is shown in Fig. 2. It is seen that the half-width of the band is about the same as that of the ZnS:Cu band, but the emission peak occurs at a higher photon energy (1.97 e.v.). This shift of the peak to higher photon energies is analogous to the shift from green to blue in coactivated ZnS:Cu and ZnS:Ag phosphors, and indicates that the Cu and Ag atoms are integral parts of the emission centers. The ZnS:Au firing produced a nonluminescent product.

The series ZnS:10^{-4} Cu, x Al was prepared in order to investigate the action of various concentrations of Al when these are below that of the Cu. The emission spectra are presented in Fig. 3. The sample without Al shows emission only in the orange band. The addition of as little as 10^{-4} Al is sufficient to give a blue band of greater peak intensity than the orange. Further addition of Al almost completely eliminates the orange band and produces a green band in addition to the blue. With equivalent Al or greater, both the orange and blue bands become negligible compared to the green band.

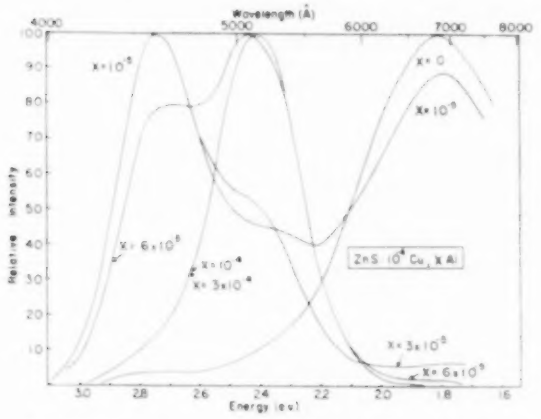

Fig. 3. Emission spectra of ZnS: 10^{-4} Cu x Al, with x ranging from 0 to 3×10^{-4}.

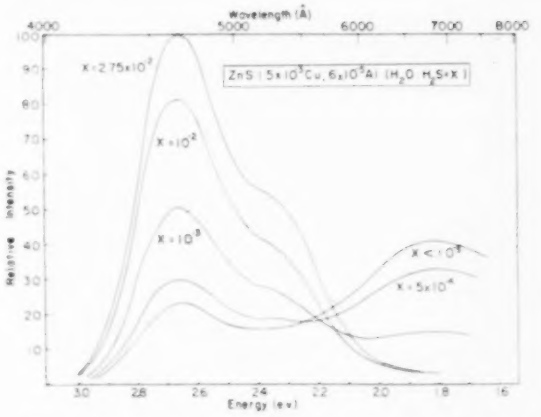

Fig. 5. Emission spectra of ZnS: 1.5×10^{-5} Cu, 6×10^{-5} Al fired in H_2S containing variable amounts of H_2O.

In Fig. 4, the spectra of ZnS: 9×10^{-4} Cu fired in H_2S containing an increasing mole fraction of water are shown. It can be seen that the presence of water strongly inhibits the orange emission. This action of water on the orange centers might be due to one of two causes: the water may somehow inhibit the formation of orange centers, or it may introduce a large concentration of killer centers. The choice between these two hypotheses will become clear in the light of the results reported next.

In Fig. 5, the emission spectra of ZnS: 1.5×10^{-5} Cu, 6×10^{-5} Al fired in H_2S containing an increasing mole fraction of water are shown. These plots are drawn so that the area under each curve is proportional to the relative total emitted energy. Several things are apparent from the plots. First, with increasing water content, the orange emission band is strongly reduced, while the blue and green bands are increased. Second, the total emitted energy increases somewhat with increasing water content. A replot of these data on the basis of number of photons vs. photon energy showed that the total number of photons emitted remains constant, indicating a constant quantum efficiency. Third, the ratio of blue to green emission remains constant. Apparently the inhibiting effect of water is specific for orange centers; the hypothesis of water causing the formation of killer centers, which should lower the over-all quantum efficiency, must be ruled out.

The excitation spectrum of ZnS: 10^{-3} Cu, shown in Fig. 6, peaks around 3.3 e.v. (3750Å), thus falling between that of self-coactivated blue at 3.65 e.v. (3400Å) (6) and green-emitting ZnS:Cu, Cl at 3.1 e.v. (4000Å).

The diffuse reflection spectra of two samples of ZnS: 10^{-4} Cu, one fired in dry H_2S and the other fired in H_2S saturated with water at room temperature are shown in Fig. 7. Both products show a very broad absorption band extending to about 2.1 e.v. (6000Å); this band is broader in the wet-fired sample. The dry-fired sample shows in addition a narrower absorption band extending to about 3.0 e.v. (4200Å). This band seems to correspond to the excitation band for dry-fired ZnS: 10^{-3} Cu, which indicates that absorption in the narrower band leads to the excitation of orange centers. The absorption between 3.0 e.v. (4200Å) and 2.1 e.v. (6000Å) cannot be explained at present. The absence of the narrower absorption band in wet-fired samples further supports the idea that wet H_2S firing inhibits the formation of the orange centers. The presence of killer centers would not be expected to destroy an absorption band.

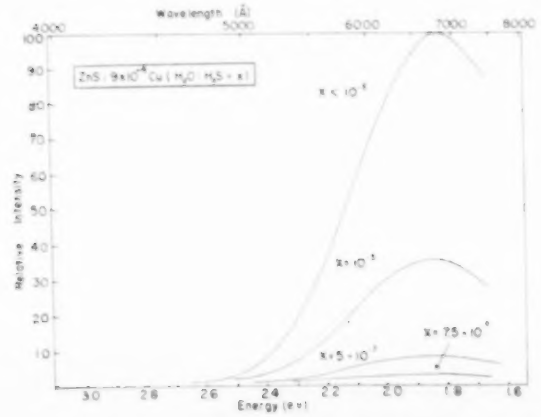

Fig. 4. Emission spectra of ZnS: 9×10^{-4} Cu fired in H_2S containing variable amounts of H_2O.

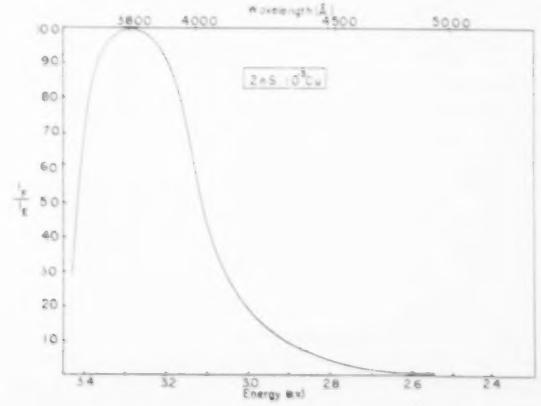

Fig. 6. Excitation spectrum of ZnS: 10^{-3} Cu

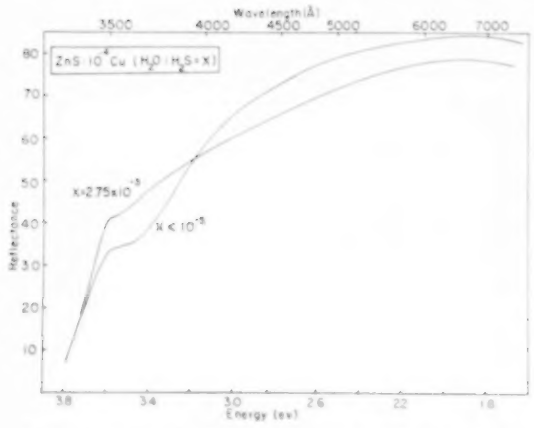

Fig. 7. Diffuse reflectance spectra of ZnS:10^{-4} Cu fired in pure H_2S and in H_2S saturated with water vapor at room temperature.

Orange-fluorescing ZnS:Cu shows no afterglow but does show moderate infrared stimulability (1). Preliminary glow curve work (7) reveals a principal peak at around 400°K (about 0.5 e.v.), which is shifted to lower temperatures by the addition of CdS. In under-coactivated ZnS:Cu, Al phosphors with the main emission in the green band but with some orange band emission, the phosphorescence is much stronger than in over-coactivated ZnS:Cu, Al showing only the green band. This phosphorescence is presumably due to the 400°K trap associated with the orange centers.

Investigation of the crystal structure of the orange phosphors showed that samples of ZnS:Cu with high (around 10^{-3} or more) Cu, fired at 1100°C and cooled normally are largely cubic in crystal structure. This is in contrast to samples containing low (10^{-4}) Cu or those with high Cu in which the Cu is completely coactivated by Cl or Al, which are hexagonal (8). Preparations of ZnS:10^{-4} Cu, which are almost pure hexagonal, show a fluorescent emission spectrum which is almost identical to that of cubic ZnS:10^{-3} Cu (compare Fig. 1 and 3). This absence of a shift in emission peak with change in crystal structure from cubic to hexagonal is in contrast to the well-known shift of about 150Å to shorter wave lengths found for the blue and green Cu emission bands. The fact that ZnS:Cu with high Cu is largely cubic in spite of being fired above the hexagonal-cubic transition point (1040°C) is believed due to the excess Cu_2S promoting the hexagonal-cubic transition during the cooling of the sample.

A shift of the orange band to longer wave lengths has been found for ZnS:10^{-3} Cu prepared under very special conditions, i.e., cooled rapidly from 1300°C. The shift amounts to about 0.1 e.v. (400Å). The sample was fired in a special firing tube with a thin bottom, which was held in the hot zone of a vertical tube furnace. To achieve the high cooling rate (about 1000°C/sec.) the firing tube was released and fell out of the furnace onto a metal point just above the surface of a container of water. The tube shattered, allowing the powdered phosphor to disperse rapidly into the water. The origin of this shift is not yet known.

Discussion

The variance of emission spectrum with method of excitation, the nonappearance of more than one band at low temperature, and the good fit to a Gaussian curve strongly support the idea that the orange band is due to a single species of emission center. An additional piece of evidence was provided by measuring the buildup and decay of the 3650A u.v. excited emission of ZnS:Cu with and without a deep red filter at the detector. With the filter in place, only the long wave-length part of the emission band could reach the detector, while without the filter the entire emission band was passed. The time constants for buildup and decay were found to be nearly identical for the two cases, which would not be expected if the orange band were a composite of two bands due to two species of emission center.

The temperature dependence of brightness of the orange emission was measured and found to be about the same as that of self-activated blue emission (9). In terms of the Schön-Klasens (10) theory of hole migration, this can be interpreted as meaning that the ground states of the self-activated blue centers and of the orange centers must have about the same position with respect to the top of the filled band (about 0.4 e.v. above it). The excitation spectrum qualitatively supports this conclusion, the peak lying about 0.4 e.v. from the ZnS absorption edge.

In forming a theory of the orange center, it is reasonable to compare the properties of the orange phosphor with those of the class of ZnS phosphors produced by "indirect activation", discussed by Klasens (11). Self-coactivated ZnS:Cu and ZnS:Ag resemble this class in certain aspects. The relatively small difference of 0.13 e.v. between their emission peaks suggests that the emission is more a property of the lattice itself than of the activator. Also, a preliminary experiment showed that the emission peak of ZnS:Cu is shifted from 1.84 e.v. to 1.71 e.v. by addition of 10% CdS. This shift of 0.13 e.v. for the first 10% of added CdS is very close to that observed in the well-known indirectly activated phosphors. However, the self-coactivated phosphors differ from this class in other respects. The half-width of the emission band is unusually great, as is the energy difference between excitation and emission peaks. Also, there is no difference in the position of the emission peak between essentially hexagonal and essentially cubic products, as is found for the better known indirect activators. It is concluded that the self-activated phosphors can be considered to be indirectly activated but to differ in some details from the better-known members of this class of ZnS phosphors.

The specific effect of H_2O (and other oxygenous agents) in inhibiting the formation of orange centers is not completely understood. Some preliminary observations indicate that the H_2O actually prevents the Cu_2S from dissolving in the ZnS. Careful comparison of a sample of ZnS:10^{-4} Cu fired in dry H_2S with one fired in wet H_2S showed the latter to have

a lower reflectance to visible light, presumably because of the presence of a greater amount of undissolved Cu_2S. When the two samples were ground in NaCN solution to remove excess Cu_2S and refired at 1100°C in dry H_2S, the sample originally fired in wet H_2S was the dimmer, indicating less Cu available for formation of orange centers. The wet-fired sample was found by chemical analysis to contain only about half as much Cu as the dry-fired sample. Thus at least part of the decrease in orange emission in wet-fired samples can be correlated with a decrease in the concentration of dissolved Cu.

It is probable that a small amount of ZnO is formed in solid solution in the ZnS during a wet H_2S firing. A semiquantitative chemical analysis of wet-fired ZnS:10^{-3} Cu indicated that the concentration of ZnO must amount to less than 10^{-4} mole fraction. Since the concentration of orange centers, while being unknown, is expected to be of the order of 10^{-4}, it is conceivable that this amount of dissolved oxygen may associate with the Cu or the coactivating species so as to prevent the formation of orange centers. A better oxygen analysis should help clear up this question.

There is not yet sufficient evidence to decide on the identity of the orange center in ZnS:Cu. It may be of some value, however, to list all the models which seem reasonably likely; this has been done below. Models (II) and (IV) have been suggested previously by Kröger (12), and model (I), by Bowers and Melamed (2). All the models will here be assumed to adhere to the rule that no species may have unpaired electrons. This rule is based on the conclusion of Bowers and Melamed (2) that no unpaired electrons are involved in the orange centers.

(I) $Cu_i^{\cdot} \cdot V_c^{\cdot\cdot} \cdot Cu_i^{\cdot}$
(II) $Cu_i^{\cdot} \cdot V_s^{\cdot\cdot} \cdot Cu_i^{\cdot}$
(III) $Cu_i^{\cdot} \cdot Zn_i^{\cdot\cdot} \cdot Cu_i^{\cdot}$
(IV) $Cu_s^{\cdot} \cdot Cu_i^{\cdot}$
(V) $Cu_s^{\cdot} \cdot Cu_s^{\cdot}$

The convention used in the above list for labeling imperfection or impurity centers in ZnS is as follows: subscripts s and i are used to designate substitutional and interstitial positions. Zinc and sulfur vacancies are written as V_c and V_s, respectively. The superscript is the excess charge in the region of the species arising from donor or acceptor action in the sense used by Prener and Williams (13) or Bowers and Melamed (2). For instance, substitutional Cu, having one less electron than Zn, must act as a single acceptor. It accepts one electron from the donor and thus takes on a single negative charge compared to substitutional Zn. A sulfur vacancy or an interstitial Zn acts as a doubly ionized donor and therefore takes on a double positive charge, while interstitial Cu acts as a singly ionized donor. The positive charge on a substitutional Cu in model (V) will be explained in a later paragraph.

In all the above models, the different species are considered as associated, that is, occupying positions in the close neighborhood of each other. This comes out of the following reasoning.

It is generally agreed that the green center in coactivated ZnS:Cu is $Cu_s^{\cdot}$, with the coactivator, such as $Cl_s^{\cdot}$ or $Al_s^{\cdot}$, (*a*) randomly distributed with respect to the $Cu_s^{\cdot}$, or (*b*) associated with it (11). The former has been tacitly assumed in the past. A model in which the $Cu_s^{\cdot}$ and $Cl_s^{\cdot}$ occupy second or third nearest neighbor positions was proposed by Prener and Williams (13). This association was predicted on the basis of the electrostatic attraction between the $Cu_s^{\cdot}$ and the $Cl_s^{\cdot}$. It will be shown that whichever case is the truth, the species of the orange center must be associated.

Now models (II) to (V) each involve a $Cu_s^{\cdot}$. Therefore, if the species are not associated, each model would yield $Cu_s^{\cdot}$, with the positively charged species randomly distributed. According to postulate (*a*), this $Cu_s^{\cdot}$ should then behave as a green center. Since self-coactivated ZnS:Cu does not emit in a green band, one would conclude that the species are associated.

If, however, it is true that electrostatic attraction between $Cu_s^{\cdot}$ and the coactivator leads to association, then the species in models (II) to (V) should also be associated for the same reason. In this case, the peculiar nature of the self-coactivator must account for the emission spectrum differing so radically from the green band found for the usual coactivators.

An analogous argument can be developed for model (I), where the $V_c^{\cdot\cdot}$ could lead to blue emission band like self-activated ZnS, if postulate (*a*) is true.

Theoretically, it should be possible to choose among the models by predicting the free energies of formation of the various species and choosing the model which represents the smallest (positive) free energy charge. This would entail a careful estimation of the energy associated with interstitial atoms, vacancies, missing bonds, coulombic terms, entropy, etc. The ZnS lattice can probably be considered as largely covalent in these estimates, although an ionic contribution may be important. The concept of donors and acceptors can be borrowed from semiconductor theory to help understand some of the relationships (2). However, a limited exploration of this method indicates no very great energy differences among the different models.

It does seem that model (I) can be eliminated because of the following considerations. Model (I) involves the same species as that proposed by Bowers and Melamed (2), but is associated, whereas they apparently assumed a completely dissociated model with the $V_c^{\cdot\cdot}$ accounting for the blue emission band they found in their samples. Since the blue band has been shown by this work to be due to impurities, their argument for this dissociated model is unsatisfactory. This model also seems improbable because it is likely that energy could be gained by the reaction

$$Cu_i^{\cdot} \cdot V_c^{\cdot\cdot} \cdot Cu_i^{\cdot} \rightarrow Cu_s^{\cdot} \cdot Cu_i^{\cdot}$$

Here the energy of the system can be decreased by a Cu atom moving from an interstitial position (which may represent a strain) into a vacancy

where it can form bonds to the surrounding S atoms.

Model (V) involves oxidation of the ZnS as can be seen by writing the formal steps necessary to convert model (II) into model (V).

$$2Cu_s^- \cdot V_s^{++} \rightarrow 2Cu_s^\circ \cdot V_s \xrightarrow{\frac{1}{2}S_2} 2Cu_s^\circ \rightarrow Cu_s^- + Cu_s^+$$

In the first step, each Cu_s^- acceptor transfers its electron back to the V_s^{++} donor. A neutral S atom from the atmosphere then fills the V_s. Then one of the Cu_s° atoms acts as a donor, giving an electron to the other Cu_s°, which acts as an acceptor. The Cu_s^+ then is a substitutional Cu (with d shell filled), with both electrons missing from one of its bonds to a neighboring S atom. This model is attractive because no vacancies or interstitial atoms are necessary. In addition, when associated in neighboring positions, the pair of Cu atoms may lower the energy of the system by the resonance represented by the equation

$$Cu_s^- \cdot Cu_s^+ \rightleftharpoons Cu_s^+ \cdot Cu_s^-$$

This resonance might result in a set of energy levels quite different from those of a hypothetical system with Cu_s^+ and Cu_s^- separated, with no resonance occurring. These levels might account for the peculiar properties of the orange center. The weakness of this model is the fact that the orange centers are stable to firing in a reducing atmosphere, a condition which should inhibit the necessary oxidation step shown above.

Conclusions

1. The emission of self-coactivated ZnS:Cu consists of a single broad band peaking at 1.84 e.v.; the presence of other emission bands can be attributed to coactivator type impurities.
2. An analogous silver-activated phosphor can be prepared with an emission peak at 1.97 e.v.
3. The position of the self-coactivated ZnS:Cu emission peak does not change with crystal structure, but does shift with CdS addition.
4. Orange centers are insensitive to oxidizing and reducing atmospheres.
5. Orange centers do not form in the presence of traces of oxygenous impurities in the firing atmosphere; once formed at 1100°C, however, they are stable to these impurities at 1100° or lower.
6. The orange center is probably completely associated, has a ground level about 0.4 e.v. from the top of the filled band and a trapping level about 0.5 e.v. below the bottom of the conduction band.

Acknowledgments

The authors wish to acknowledge the contribution of Miss M. Brines of the General Electric Chemical Products Plant, who measured the cathode ray spectrum, of Miss J. R. Cooper of this laboratory, who carried out the crystal structure investigation, and of Dr. F. F. Morehead, also of this laboratory, who performed the buildup and decay measurements.

Manuscript received Aug. 19, 1957. This paper was prepared for delivery before the Washington Meeting, May 12-16, 1957.

Any discussion of this paper will appear in a Discussion Section to be published in the December 1958 JOURNAL.

REFERENCES

1. H. C. Froelich, *This Journal*, **100**, 280 (1953).
2. R. Bowers and N. T. Melamed, *Phys. Rev.*, **99**, 1781 (1955).
3. N. Riehl and H. Ortmann, *J. phys. radium*, **17**, 620 (1956).
4. Brinkman and Vlam, *Physica*, **14**, 650 (1949).
5. P. W. Ranby, *et al.*, *Brit. J. Appl. Phys.*, Supplement No. 4, S18 (1954).
6. H. W. Leverenz, "Luminescence of Solids," p. 163, John Wiley & Sons, Inc., New York (1950).
7. F. F. Morehead, Extended Abstracts of the Electronics Division, ECS, Washington Meeting, p. 2 (1957).
8. H. C. Froelich, *This Journal*, **100**, 496 (1953).
9. H. W. Leverenz, *loc. cit.*, p. 344.
10. M. Schön, *Z. Physik*, **119**, 463 (1942); H. A. Klasens, *Nature*, **158**, 306 (1946).
11. H. A. Klasens, *This Journal*, **100**, 72 (1953).
12. F. A. Kröger, *Brit. J. Appl. Phys.*, Supplement No. 4 S58 (1954).
13. J. S. Prener and F. E. Williams, *J. phys. radium*, **17**, 667 (1956); *Phys. Rev.*, **101**, 1427 (1956); *This Journal*, **103**, 342 (1956).

Conductivity and Energy Gap Measurements of Some Relatives of Phthalocyanine

Wolfgang Felmayer and Irving Wolf

Materials and Processes Laboratory, General Electric Company, Syracuse, New York

ABSTRACT

The electrical resistance of samples of powdered copper-phythalocyanine, platinum phthalocyanine, highly chlorinated copper-phthalocyanine, and of two polymers of copper-phthalocyanine were measured at various temperatures in a nitrogen atmosphere.

All of the compounds showed semiconductive behavior. The highly chlorinated copper-phthalocyanine and the platinum-phthalocyanine had approximately the same resistance as the copper-phthalocyanine, whereas both polymers had lower resistances—one of the polymers having a resistance of about 10^{-4} that of copper-phthalocyanine at various temperatures. Some theoretical implications of the above facts are mentioned in this report.

In 1935 and 1936 Robertson (1) reported the crystal structure of several metal substituted phthalocyanines, as well as phthalocyanine itself. These compounds are well-known pigments which are structurally related to the naturally occurring porphyrins. The structures of phthalocyanine and copper phthalocyanine are shown in Fig. 1.

Vartanyan (2) and Eley (3), working independently, found the exponential relationship between conductivity and the reciprocal of the temperature for phthalocyanines; from this and other observations, they each concluded that phthalocyanines act like intrinsic semiconductors.

Kleitman (4) reported temperature-conductivity measurements for single crystals of phthalocyanine and copper phthalocyanine, as well as absorption spectra and photoconductivity measurements of "smeared films" of phthalocyanine. He compared "energy gaps" determined from the different measurements, in addition to making a photosensitive point contact rectifier from a pressed pill of phthalocyanine.

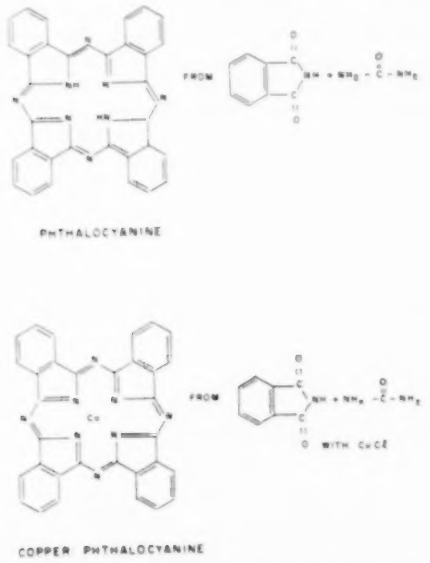

Fig. 1. Structural formulas and starting compounds

Many, Harnik, and Gerlich (5) made rough calculations of the "mobility" of the carriers in phthalocyanine, copper phthalocyanine, and many other polynuclear organic materials. The values they estimated were 1 $cm^2/v/sec$ for phthalocyanine and 10 $cm^2/v/sec$ for the copper substituted compound.

In this work, temperature-conductivity measurements have been made on powder samples of copper phthalocyanine and a number of relatives of these compounds differing only in crystalline arrangement or molecular structure.

The results on each material can be expressed by a relation of the form

$$\sigma = \sigma_\infty e^{-\epsilon/kT}$$

where ϵ may be considered the apparent energy gap and σ_∞ the conductivity extrapolated to infinite temperature which may be presumed to depend on the total carrier concentration and on the carrier mobility. The various materials are thus conveniently compared in terms of these parameters.

The compounds studied besides copper phthalocyanine were chlorinated copper phthalocyanine, platinum phthalocyanine, and the two polymers of copper phthalocyanine. This was done in an attempt to discover what effect the differences between the compounds might have on the "energy gap" and "relative mobility" of the carriers. It was felt that through this, some insight into the nature of the conductivity might be gained.

Chlorinated copper phthalocyanine.—The chlorinated copper phthalocyanine molecule has chlorine in place of the hydrogens which surround the molecule. On the average, 15 out of the 16 hydrogens were replaced by chlorine. If the energy gap or mobility depends on activity at the edges of the molecule, the replacement of the hydrogen should vastly affect it.

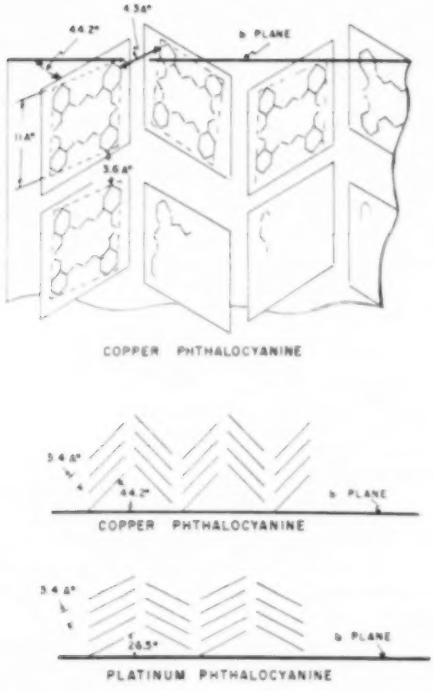

Fig. 2. Geometric positioning of molecular planes in crystal

Platinum phthalocyanine.—The platinum phthalocyanine differs in crystalline arrangement from the copper compound in that the angle with the b plane (*see* Fig. 2) differs from that of the latter considerably. Thus, if the energy gap or mobility depends on specific atoms in one molecule in a "stack" being lined up with specific atoms of a neighbor in front of or behind it, the variation in angle should greatly affect it.

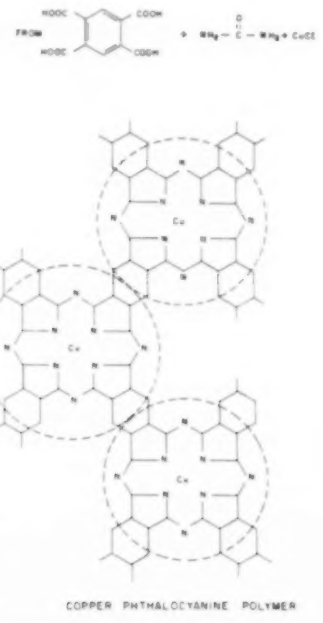

Fig. 3. Structure of polymer and starting compounds

Polymers.—The polymers (*see* Fig. 3) differed from the monomer in size; the molecules of the former probably "stacking" just as the latter. As in the chlorinated compound, if the activity were edge to edge, some very substantial effects should be noted on energy gap and mobility.

Thus, it was felt that the comparisons described above would provide some early indications of the nature of the charge motion from molecule to molecule.

Experimental Results

Copper-phthalocyanine.—The first step was to take resistance vs. temperature measurements on multiply vacuum-sublimed copper-phthalocyanine crystal powder. The purpose of this measurement was to compare the results with existing measurements and thus test the procedure and equipment used in this work (*see* Fig. 4). The samples measured were all loose powders under low compaction pressure (about 8 psi). It was noted that the resistance did not vary appreciably with minor pressure variations. The resistances given throughout were for samples 20 mm in diameter and approximately 1 mm thick. The electrodes were gold disks. To avoid irregularities of measurements during the first run (4), the samples were heated directly up to 340°C in a nitrogen atmosphere; then the resistances were measured while the temperature was decreasing constantly at a rate of about 10°C/min in intervals of 10°C (Fig. 5, curve a). Measurements taken during constantly increasing temperature showed slightly higher resistances (Fig. 5, curve b). For final data the samples were reheated to at least three different temperatures—for the sake of accuracy each of these temperatures was maintained for approximately half an hour before the resistance was measured. This method led to readings (Fig. 5 curve c) which lay between those of the first two runs. Graphically all linear curves in the log Ω vs. $1/T$ diagram showed the same slope, while their resistances differed by a constant factor due to temperature lags in the sample. Therefore, the middle curve was considered to be the most accurate one.

It should be mentioned that copper-phthalocyanine synthesized from different materials (phthalic acid, phthalamide, phthalonitrile) showed the same semiconductive behavior. The only deviations were due

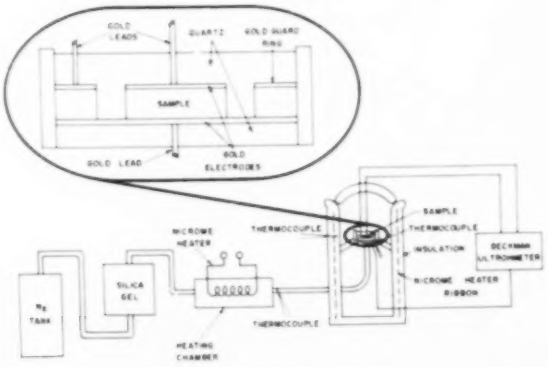

Fig. 4. Measurement apparatus

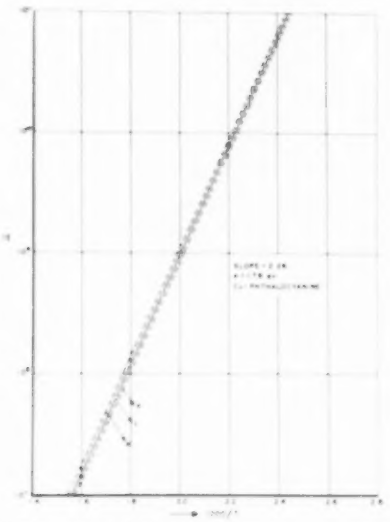

Fig. 5. Resistance of Cu-phthalocyanine vs. reciprocal of temperature

to poor purity of the pigment. Even after the first vacuum sublimation certain irregularities were sometimes found, while the results after a second and third sublimation were always in good agreement.

In order to study the most effective purification methods for nonsublimable phthalocyanines, a series of purification experiments were performed on nonsublimed copper-phthalocyanine. Even multiple reprecipitation or recrystallization from concentrated sulfuric acid proved to be insufficient. Bringing the sample up to 400°C and holding it there for several hours in nitrogen atmosphere resulted in a product, of which the resistance vs. temperature measurements were in good agreement with those of sublimed copper-phthalocyanine. Hourly checks showed a constant approach to the ideal curve, which was reached after 5 hr. A further heating of up to 10 hr brought no change.

Chlorinated copper-phthalocyanine.—Highly chlorinated (about 15 Cl-atoms per phthalocyanine molecule) copper-phthalocyanine (du Pont Monastral Fast Green G) was purified carefully at first by treatments with HCl and NaOH. In addition, the product was extracted with boiling alcohol. A treatment at 350°C in vacuum still gave some sublimation of a white material. After some hours the first resistance vs. temperature measurements were taken (Fig. 6, curve a). Further heat treatment in vacuum up to 500°C, however, resulted in an approach of this curve toward the normal copper-phthalocyanine log Ω over $1/T$ curve. (Fig. 6, curve b, c). Since a sublimation of copper-phthalocyanine was found in the tube, it is assumed that chlorinated copper-phthalocyanine splits off some or all of its chlorine atoms. The residue, also, looked much bluer than the original sample and had characteristics given in curve d of Fig. 6.

Thus, for this compound, indications were that decomposition accompanied purification and the data obtained should be understood to be that of a partially dechlorinated molecule. In general, it may be

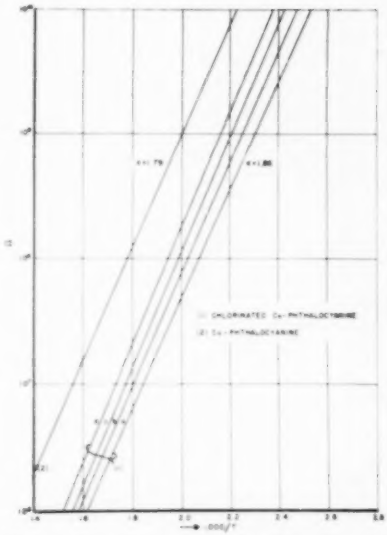

Fig. 6. Comparison of results for Cu-phthalocyanine with its chlorinated counterpart.

said that chlorinated copper-phthalocyanine shows the same activation energy as copper-phthalocyanine itself and about 1/10 the resistance (*see* Fig. 6).

Platinum-phthalocyanine.—By x-ray examination of platinum-phthalocyanine crystals, Robertson (1) found that the molecular structure of platinum-phthalocyanine is very similar to the other phthalocyanines. As for its crystalline structure, however, even though the molecules are arranged in a similar "stacked" fashion, they are at an angle to the (b) plane of only 26.5° instead of 44.2° as in copper-phthalocyanine. All the other phthalocyanines examined were similar to the copper in this respect.

In order to study the effect of the crystal structure on semiconductive properties of phthalocyanines, some resistance vs. temperature measurements on multiply sublimed platinum-phthalocyanine were made. Results are given in Fig. 7 and compared with

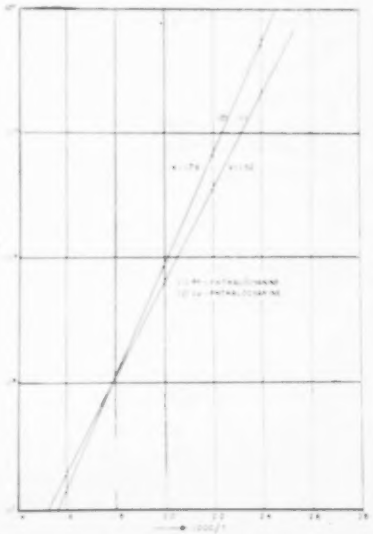

Fig. 7. Comparison of results for Cu-phthalocyanine with Pt-phthalocyanine.

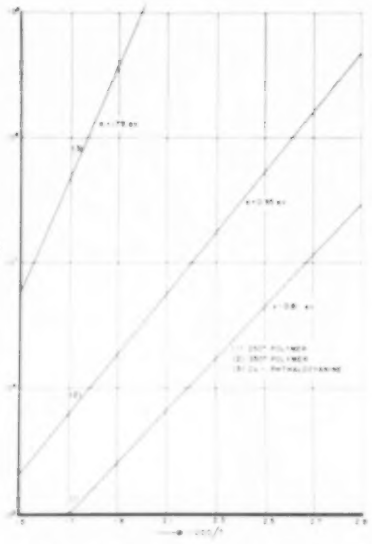

Fig. 8. Comparison of results for Cu-phthalocyanine monomer with two polymers

those of copper-phthalocyanine. As the difference in absolute resistance values is small, the conclusion was reached that the angle with the (b) plane—which governs the way atoms in one molecule line up with those in another, behind or in front of it—has no important influence on the mobility of the charge carriers.

A slight difference in slope of both curves is not very surprising, as the same effect was known for phthalocyanine, magnesium-phthalocyanine, and similar compounds when compared with each other or with copper-phthalocyanine. Thus, a certain influence of the central atom on the band gap is to be expected.

Polymer copper-phthalocyanine.—Although it is not possible to give definite statements about the structure of the polymer phthalocyanines, chemical and physical examinations indicate that the four carboxyl groups of pryomellitic acid react with molten urea in a way similar to the reaction of the two carboxyl groups of phthalic acid when phthalocyanine is formed. In this way a polymer phthalocyanine is built up. A combination of elementary analysis and theoretical calculations lead to the indication of a model of at least ten closely packed phthalocyanine molecules.

Since former experiments have shown that the reaction temperature has considerable influence on this kind of phthalocyanine condensation and also affects the polymolecularity, two parallel condensations were started, one at 250°C and the other at 350°C.

Comparison of the 250° polymer and the 350° polymer.—All of the experiments led to the conclusion that the 250° polymer had a higher molecular weight than the 350° polymer. The chief indications were resistance vs. temperature measurements, viscosity measurements in solution, and copper-analyses. A further confirmation might be expected from total elementary analysis. The importance of the latter, however, is rather small since the data for C, H, N, and O show smaller changes with the polymolecularity than the copper data.

Table I

Compound	ϵ (e.v.)	Ω_∞ (ohms)	σ_∞ (ohm-cm)$^{-1}$ $\times 10^{-6}$
Copper phthalocyanine	1.79	0.83	3.82
Platinum phthalocyanine	1.52	13.92	0.229
Chlorinated copper phthalocyanine	1.86	0.09	35.0
Lower polymer (350°C)	0.95	31.9	0.10
Higher polymer (250°C)	0.81	50.2	0.063

Resistance vs. temperature measurements.—Figure 8 shows that both the slope and conductivity for the 350° polymer lie between respective data for the 250° polymer and the monomer copper-phthalocyanine. The comparison of the band gaps of the three compounds shows that they are subject to an expected decreasing sequence (7-10).

According to the results of the copper analysis, the two polymers should be considered as tight molecular nets. This configuration results in a number of new resonance possibilities which are responsible for the compound's extremely dark color.

Results indicate that the energy gaps of such polymers decrease as the number of condensed rings and hence the resonance possibilities increase. A similar result has been obtained in studies by Akamatu and Inokuchi (7-10) who found lower activation energies for such higher condensed aromatics as violanthrons and isoviolanthrone than for anthracene. It appears that the increase in the number of condensed rings results, in general, in a decreasing energy gap.

Comparative Results

In Table I are listed for each of the materials the values of ϵ and σ_∞, together with Ω_∞, the extrapolated sample resistance corresponding to $t = \infty$. A comparison of these values indicates no vast difference in σ_∞. It is true that the chlorinated substituted compound has about 10 times the σ_∞ of the unsubstituted, and the high polymer a value 60 times lower than the monomer, but these differences are thought to be much smaller than would be expected if the actual mechanism of charge transfer were altered.

Since the carriers are probably pi-electrons, whose density is roughly proportional to the density of the materials, and since these densities vary only slightly compared to the variation of σ_∞'s observed, the relative values for σ_∞ might also be considered a good indication of the relative values of carrier mobility.

Manuscript received Jan. 11, 1957. This paper was prepared for delivery before the San Francisco Meeting, May 1-5, 1956.

Any discussion of this paper will appear in a Discussion Section to be published in the December 1958 JOURNAL.

REFERENCES

1. J. M. Robertson, *J. Chem. Soc.*, **1935**, 615; **1936**, 1195.
2. A. T. Vartanyan, *Zhur. Fiz. Khim.* **22**, 769 (1948).

3. D. D. Eley, *Nature*, **162**, 819 (1948).
4. D. Kleitman, Electrical Properties of Phthalocyanine, U. S. Dept. of Commerce, Office of Technical Services, Report PB111419 (1953).
5. A. Many, E. Harnik, D. Gerlich, *J. Chem. Phys.*, **23**, 1733 (1955).
6. W. Felmayer, Dissertation, University of Vienna, (1954).
7. H. Akamatu and H. Inokuchi, *J. Chem. Phys.*, **20**, 1481 (1952).
8. H. Akamatu, H. Inokuchi, T. Handa, *Nature*, **168**, 520 (1951).
9. H. Akamatu and H. Inokuchi, *J. Chem. Phys.*, **18**, 810 (1950).
10. H. Inokuchi, *Bull. Chem. Soc. Japan*, **24**, 222 (1951).
11. H. Inokuchi, *ibid.*, **24**, 28 (1952).

The Concentration of Hydrogen in Nickel under Hydrogen Ion Bombardment

J. Morrison and J. J. Lander

Bell Telephone Laboratories, Inc., Murray Hill, New Jersey

ABSTRACT

Concentrations of hydrogen dissolved in nickel under hydrogen ion bombardment have been measured using a nickel diffusion tube as the cathode in a glow discharge. No increase above the normal was observed when clean nickel was bombarded. Increases of several orders of magnitude were obtained in the range near 200°C when the nickel was coated with nickel oxide or barium oxide. It is believed that energetic ions penetrate the outer surfaces of these materials efficiently and are then trapped in the interior by surface barriers. These data show that normal values of concentration cannot be applied to nickel and probably many other metals operating under hydrogen ion bombardment if their surfaces are contaminated.

It has been found that high concentrations of hydrogen can be produced in ZnO by hydrogen ion bombardment (1). For example, bombardment at 200°C with hydrogen ions can produce a concentration five orders of magnitude higher than the concentration obtained when an equal number of normal hydrogen molecules strike the surface. This behavior results from two factors: *(a)* ions of sufficient velocity penetrate efficiently a surface barrier to normal reaction, and *(b)* the barrier to escape of dissolved hydrogen is high. In general it is expected that in systems where such surface barriers are high, relatively large internal pressures of hydrogen can be generated by hydrogen ion bombardment.

In the work on ZnO concentrations of hydrogen were determined by measurements of conductivity. This was possible because hydrogen forms a donor with convenient properties. In this work steady-state diffusion rates of hydrogen through a Ni tube under hydrogen ion bombardment were measured.

In the steady state the quantity of hydrogen flowing through such a tube is

$$Q = CDtA/d \qquad (1)$$

where Q is the quantity in cc mm (a cc mm is 1 cc at 1 mm pressure), C is the concentration in cc mm/cc of Ni, D the diffusion coefficient in cm²/sec, t the time in seconds, A the area of the tube in cm², and d the thickness of the tube in cm. The concentration at the exit side is assumed to be relatively low. Bombardment by hydrogen ions was accomplished by using the Ni tube as cathode in a glow discharge.

This work has shown the importance of oxide films on Ni under hydrogen ion bombardment. Large increases in concentration of hydrogen in Ni were obtained with NiO on Ni and with BaO on Ni. Following the previous work on ZnO, it is proposed that the surfaces of these oxides are easily penetrated by energetic ions, but they act as effective barriers to the escape of hydrogen molecules. No increase in concentration was detected when the Ni was "clean."

Apparatus

The work was carried on with the system shown schematically in Fig. 1. Hydrogen from a tank was introduced through a stop-cock to a spiraled tube of Ni. This Ni spiral was formed of six turns of approximately 3 cm diameter from tubing measuring 45 mils outside diameter and 2 mils wall thickness. An electrode of 60 mil Ni rod was mounted parallel to the spiral and about 1 cm distant from the top of the spiral. An oil manometer using Octoil S and a Pirani gauge were used to measure the hydrogen pressure. A small cold trap was in the line near the

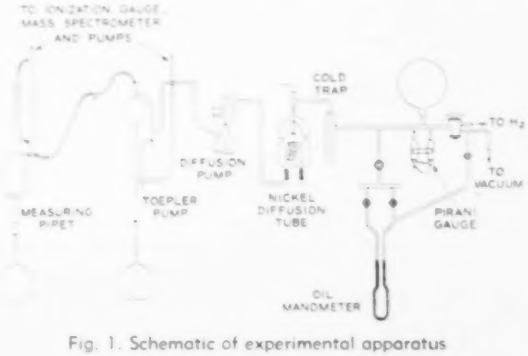

Fig. 1. Schematic of experimental apparatus

Fig. 2. Diffusion coefficient and normal concentration of hydrogen in Ni as a function of temperature.

tube containing the Ni spiral. This part of the system could be evacuated to a good fore pump pressure before flushing and filling with hydrogen.

One of the ends of the spiral was sealed and the other end connected to the gas measuring system in which a small Hg diffusion pump was used to evacuate the inside of the Ni tubing. The gas removed was pumped by a Toepler pump into a calibrated volume.

Techniques of Measurement

Quantity of gas.—The quantity of gas collected in a 3-min interval was measured in the calibrated volume. After measurement it was pumped away through a system to which a mass spectrometer and an ionization gauge were sealed. The background pressure in this vacuum system was 2-3 x 10^{-7} mm.

Temperature.—Change in the average temperature of the Ni spiral was determined by measuring its change in resistance with a calibrated ammeter and voltmeter. A curve was drawn using data obtained from the International Critical Tables for the temperature coefficient of resistivity and the observed value of resistance of the spiral at room temperature. The spiral was heated by either the glow discharge, by passing current through it, or by a combination of the two.

Blank determination.—The gas evolved by the Ni spiral and associated equipment at room temperature after it had been outgassed and conditioned was collected for a 3-min period. This quantity was near 0.01 cc mm and was relatively steady. This figure is also near the limit of sensitivity of the apparatus since it corresponds to 3 min of Hg on the measuring pipet. The blank was frequently checked, not only with the Ni at room temperature but also when it was at much higher temperatures in hydrogen at very low pressure.

Pressures of water vapor.—Four different pressures of water vapor were used during the experimental determinations. A drop of water was placed in the cold trap located near the experimental tube. Liquid Ni was used to attain what is called zero pressure. A $CaCl_2$ bath at −51°C was used to hold the pressure of water vapor at 0.026 mm. An alcohol-ice mixture was used to attain a temperature of −24°C and a vapor pressure of 0.53 mm. Finally an ice water bath at 0°C gave a vapor pressure of 3.8 mm.

Oxide films.—During the course of these studies it was found desirable to oxidize the Ni spiral and later a Ba film which was deposited on the clean Ni. The Ni was heated to about 400°C in air to obtain a visible NiO film. This could be removed by heating in hydrogen. The evaporated Ba was converted to a visible oxide film by admission of air.

Diffusion coefficient.—Exploratory measurements of initial transients gave values from which hydrogen diffusion coefficients were calculated. These were in agreement with Euringer (2), and Hill and Johnson (3). Their values have been used to draw the curve given in Fig. 2 which has been used in the calculations of concentration.

Concentration.—Hydrogen concentration was calculated from the steady state quantity of gas flowing through the tube using Eq. (I). The concentration is

$$C = \frac{1.36 \times 10^{-6} Q}{D} \text{ cc mm/cc Ni} \qquad \text{(II)}$$

where the values $t = 180$ sec, $A = 20.5$ cm^2, $d = 0.0050$ cm have been substituted. Results of measurements made with hydrogen at 0.67 mm of Hg, no bombardment and various temperatures are given in Fig. 2. These are to be compared with values given by Barrer (4), which have been corrected to 0.67 mm of hydrogen by assuming that concentration is proportional to the square root of hydrogen pressure. The authors' values are lower by a factor of about two. The reason for this discrepancy was not discovered. The results were very reproducible and independent of the cleanliness of the Ni tubing.

Results of Hydrogen Bombardment

"Clean" nickel.—After the concentration of normal hydrogen was determined the effect of a glow discharge in dry hydrogen was studied. The results were not reproducible. There was a tendency for large quantities of hydrogen to flow during an initial period of bombardment, but on prolonged bombardment the flow would ultimately drop to that obtained without the discharge. Since the effect of bombardment should be to clean the surface of the Ni by chemical reduction and by sputtering, it was concluded that the initial effects were due to surface contamination and that effects due to bombardment of clean Ni were too small to be measured.

Nickel plus nickel oxide.—Since there was no increase in concentration under hydrogen ion bombardment of clean Ni at temperatures up to 182°C, it was decided to bombard oxidized Ni. An objective was to determine if the initial results could be repeated and made reproducible. Bombardment of oxidized Ni in the same temperature range increased the initial flow but again the flow could not be main-

tained. During these tests liquid nitrogen had been on the cold trap. The liquid nitrogen was removed, a few drops of water were placed in the trap and it was surrounded by an alcohol-ice bath. Hydrogen was admitted to a pressure of 0.67 mm and the glow discharge started. Immediately the quantities collected were much larger than those collected at the same temperature in the absence of the discharge and the results obtained were reproducible. Apparently the two conditions necessary for this higher concentration were the oxide film and enough water vapor or other oxidizing gas to maintain the oxide in the presence of the reducing action of the glow discharge. The flow of hydrogen through the Ni was measured for a range of temperatures and pressures of water vapor as well as different current densities of the glow discharge.

Nickel plus barium oxide.—The tube containing the Ni spiral was opened and two 5-mg Ba getters were attached to the upper electrode with tungsten wires. They were in such a position, one on each side of the tube, that when flashed the Ba evolved coated most of the tubing. The system was pumped and the Ni brought to a clean state. The getters were flashed until there was a visible film of Ba on the glass walls. After oxidation a thin white film of BaO could be seen on the Ni. It was found that the oxide had no effect on the normal flow of hydrogen, but that under bombardment higher concentrations were found than with NiO on Ni. In all these tests with BaO dry hydrogen was used and the results were reproducible.

It was found that a series of cyclic treatments such as heating to 600°-700°C and bombarding at high current densities produced a state resulting in concentrations three to four times greater than those found previously. However, this was an unstable condition and could be maintained for only a few minutes.

Summary of Results

Temperature.—A representative picture of the over-all results is shown in Fig. 3, where the concentration in cc mm/cc of Ni is plotted as a function of the reciprocal of temperature. The lowest curve shows the reference line or the concentration of hydrogen molecules by 0.67 mm of dry hydrogen. The other two curves show the concentrations obtained with bombardment by hydrogen ions under the conditions noted. In the temperature range studied there is a definite increase in concentration as the temperature is lowered. The BaO on Ni resulted in somewhat higher concentration than for NiO on Ni.

Water vapor pressure.—The effect of water vapor on the concentration of hydrogen ions in the system NiO on Ni is shown clearly in Fig. 4 where curves for the increase in concentration (ΔC) are plotted for temperatures of 115° and 182°C. Effects of pressures higher than about 4 mm could not be determined because a proper glow could not be maintained.

The question might be raised as to the effect of the water vapor alone on the Ni. This condition was studied and at 3-4 mm pressure of water vapor and temperatures as high as 450°C, no reaction was observed which resulted in the diffusion of hydrogen through the Ni. At 24 mm pressure of water vapor and 450°C the diffusion of hydrogen was observed but it was completely stopped if the Ni was oxidized visibly.

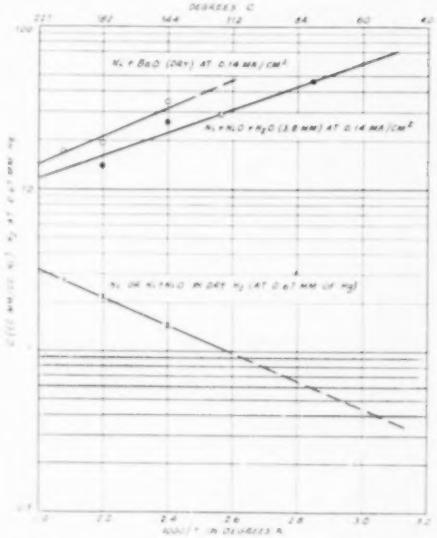

Fig. 3. Concentrations of hydrogen in Ni produced by bombardment compared with normal concentration as a function of temperature.

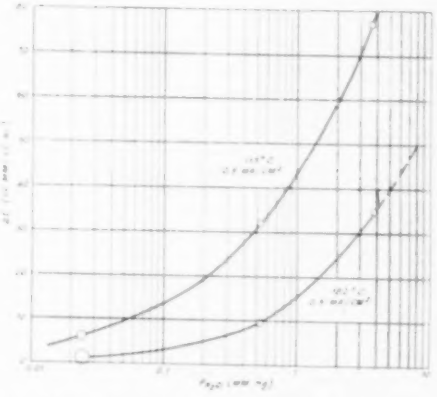

Fig. 4. Effect of water vapor on bombardment enhanced concentration of hydrogen in Ni.

Current density of glow discharge.—The effect of the current density of the discharge on the concentration is shown in Fig. 5. Concentration increased linearly with increasing current density at low current densities but saturated ultimately. For BaO on Ni in dry hydrogen at a pressure of 0.67 mm, saturation was observed in the range from 0.1 to 0.5 ma/cm².

Conclusions

1. In order to relate results obtained by ion bombardment with normal concentration, concentrations are compared for equal numbers of atoms striking the surface. On this basis bombardment has increased the concentration by about four orders of magnitude in the range near 100°C.

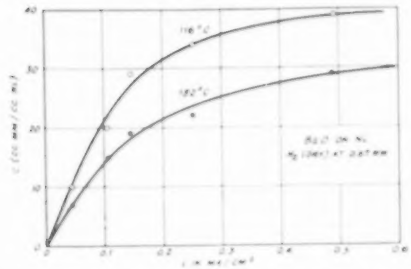

Fig. 5. Effect of current density of the glow discharge on concentration.

2. Bombardment also produces a reversal in the temperature coefficient of concentration. The difference in slopes is a measure of the barrier to escape of hydrogen. This barrier is found to be about 0.35 e.v. for both NiO and BaO on Ni under the conditions of these experiments.

3. Because no effect was observed with clean Ni, it is concluded there is no large barrier to the escape of hydrogen from a clean Ni surface.

4. It is interesting to note that in flowing through the system the hydrogen must pass through the oxide to Ni interface. If a high barrier to flow existed here the very large increases in concentration could not have been obtained.

5. These experiments do not tell the state of hydrogen in the films. It is not unlikely that part or all of the film of BaO was converted to $Ba(OH)_2$ by bombardment, since this is a relatively stable compound under the conditions of these experiments, and because the small amount of oxygen required to form the hydroxide was probably present in the system. Where NiO was the starting material relatively high pressures of water were required to produce the enhanced diffusion rates, and under these conditions $Ni(OH)_2$ is expected to form. Thus the transport mechanism in both surface films is believed to have been proton migration in imperfect hydroxides. It is believed (because of the work with ZnO) that proton migration in the oxides can also take place.

6. These results show conditions for concentrating much larger quantities of hydrogen in Ni than can be obtained by exposure to normal hydrogen. From these data it is clear that normal values of concentration cannot be applied to Ni and probably many other metals operating under hydrogen ion bombardment if their surfaces are contaminated.

Manuscript received Aug. 27, 1957. This paper was prepared for delivery before the Washington Meeting, May 12-16, 1957.

Any discussion of this paper will appear in a Discussion Section to be published in the December 1958 JOURNAL.

REFERENCES

1. J. J. Lander, *J. Phys. and Chem. Solids*, **3**, 87 (1957).
2. G. Euringer, *Z. Physik.*, **96**, 37 (1935).
3. M. L. Hill and E. W. Johnson, *Acta Met.*, **3**, 6 (1955).
4. R. M. Barrer, "Diffusion In and Through Solids," p. 152, Cambridge Press, London (1951).

Iron and Phosphate Slag from Byproduct Ferrophosphorus

J. M. Potts, W. C. Scott, Jr., J. U. Campbell, and J. A. Wilbanks

Tennessee Valley Authority, Wilson Dam, Alabama

ABSTRACT

A process and furnace were developed for converting byproduct ferrophosphorus into high-grade iron for metallurgical purposes and phosphatic slag that might be used as a fertilizer or animal-feed supplement. The process consists in continuously smelting ferrophosphorus with calcined, siliceous iron ore and burnt lime in an electric furnace. The furnace has a two-component lining: walls of graphite, which resist corrosion by molten phosphate slag, and a hearth of magnesite, which resists attack by iron of low phosphorus content. In pilot-plant tests in a 2-meter diameter by 1.5-meter furnace operated at a power input of 350 kw, best results were obtained with about 100 v between the two electrodes. The product iron contained 0.5% P and the slag contained 22% citrate-soluble P_2O_5.

The Tennessee Valley Authority has developed a process and a furnace for the utilization of byproduct ferrophosphorus in the production of high-grade iron for metallurgical purposes and phosphatic slag that should be satisfactory for use as fertilizer or animal-feed supplement. The process involves smelting ferrophosphorus, siliceous iron ore, and burned lime in an electric furnace. The reaction approximates the following equation:

$$6Fe_2P + 5Fe_2O_3 \cdot 3SiO_2 + 15CaO = 22Fe + 3(5CaO \cdot P_2O_5 \cdot SiO_2) \quad (I)$$

This process was identified a number of years ago (5). However, it was not considered technically feasible at that time because of the severe attack of the molten iron and slag on the lining of the furnace. No single refractory material, including rammed magnesite, magnesite brick, chrome ore, zircon brick, and graphite, resisted the corrosive action of both the slag and iron. Work by the Bureau of Mines (2) and others (3) interested in processing ferrophosphorus also failed to define a satisfactory refractory.

In recent work here, the refractory problem was solved through the use of a two-component furnace lining. Graphite, which is resistant to corrosion by molten phosphate slag, was used to line the walls of the furnace, and magnesite, which resists attack by

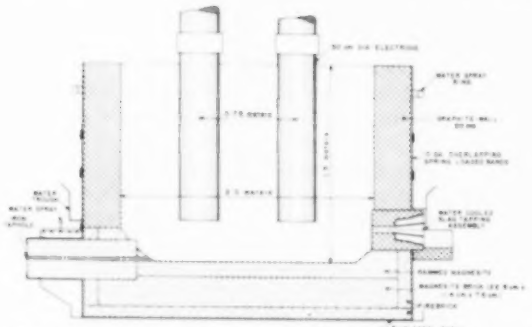

Fig. 1. Furnace crucible used in the production of iron and phosphate slag from byproduct ferrophosphorus.

iron of low-phosphorus content, was used to line the hearth.

This paper briefly describes the new pilot-plant furnace and the results of tests made for the production of iron and phosphate slag.

The Furnace

A sectional view of the new pilot-plant furnace is shown in Fig. 1. The inside diameter of the furnace was 2 meters and the depth was 1.5 meters. The side wall was made of 30-cm thick graphite shapes, which were supported on the hearth with dry joints. Overlapping spring-loaded bands held the shapes in place. A water-spray ring was located around the top of the furnace and a water-collection trough was located just above the hearth section.

The hearth, which was contained in a steel shell, consisted of 7.6 cm of firebrick in the bottom and around the sides of the steel shell, 22.9 cm of magnesite brick, and 15.2 cm of rammed magnesite. At the walls, the rammed magnesite extended 25.4 cm above the floor of the hearth to approximately the slag-tapping level. It was recognized that a small area of the magnesite lining would be exposed to molten slag; however, it was anticipated that the expected high rate of heat transfer to the adjacent graphite would prevent excessive corrosion.

The tapping block for slag was made from a section of 30-cm graphite electrode with a 5-cm taphole in the center. It was fitted with a water-cooled bronze tapping monkey. The tapping block for metal was made from magnesite brick and was water cooled.

Two 30-cm graphite electrodes were located on 76-cm centers an equal distance from the furnace center line. Single-phase power was supplied to the furnace through a voltage regulator, an autotransformer, and a power transformer. The electrodes were connected to opposite ends of the secondary winding of the power transformer. Operation with 50 to about 100 v between electrodes, or 25 to about 50 v between each electrode and ground, was possible. The electrical system used has been described previously in an article on the pilot-plant production of aluminum-silicon alloy (4).

Table I. Compositions of raw materials used in pilot-plant tests

	Analysis, % by weight				
Ferrophosphorus		Lime		Calcined iron ore	
P	24.4	CaO	95.0	Fe_2O_3	78.3
Fe	68.6	CO_2	1.1	FeO	3.8
Mn	3.0	MgO	1.5	SiO_2	13.3
Ti	2.4	SiO_2	0.9	P_2O_5	1.4
Si	1.3	Al_2O_3	0.3	CaO	0.1
S	0.3	Fe_2O_3	0.1	H_2O	<0.1
		Ignition loss	1.1	Other	3.0

Pilot-Plant Tests

Procedure.—Six tests, which totalled 563 hr of operation, were made with the new furnace. The raw materials consisted of ferrophosphorus containing 24.4% P, lime containing 95% CaO, and calcined iron ore containing 59% Fe (Table I). Calcined iron ore was used because, in exploratory tests, uncalcined ore caused boiling of the slag and poor furnace operation. The ore was calcined in a 0.76-meter diameter by 12-meter long gas-fired, pilot-plant rotary kiln at a temperature of 1300°C. The ferrophosphorus and the calcined iron ore were crushed to minus 1½ in. before being used. The lime was purchased as minus 1-in. material. The materials were premixed in the desired proportions before being charged to the furnace.

The power input was kept at about 350 kw. Although this power input may have been somewhat less than optimum, the pilot plant was not equipped to handle the larger quantities of molten slag and iron that would have been produced with more power.

Best results were obtained with about 100 v between electrodes. Operation also was satisfactory with 75 v. When less than 75 v were used, the electrodes rode too low in the furnace and caused boiling of the slag. Also, carbon from the electrodes was absorbed by the iron with the result that dephosphorization was poorer because of preferential oxidation of the carbon.

The furnace operated continuously and was charged through a feed chute as required to keep the level near the top. Molten slag and iron were tapped at 2-hr intervals. The slag, at about 1620°C, was tapped into a cast-iron chill pan in which it was permitted to cool before it was ground to the desired size. The iron was tapped into a preheated crane-type ladle and then was cast into 34-kg pigs.

Effect of Burden Composition

Equation (I) indicates that, for dephosphorization of ferrophosphorus, the stoichiometric requirement of iron oxide is that necessary to oxidize the phosphorus to P_2O_5. Also, the equation calls for 5 moles CaO and 1 mole SiO_2 per mole of P_2O_5, which is the relationship for silicocarnotite (6). Since the proportion of SiO_2 supplied in the charge material was in excess of 1 mole per mole of P_2O_5, it was assumed that 1 mole of CaO should be provided per mole of SiO_2 and 4 moles should be provided per mole of P_2O_5. However, in the pilot-plant tests, excesses of iron ore and lime were required to obtain satisfactory furnace operation and products of the desired chemical composition. Exploratory tests showed that 135% of the stoichiometric proportion of iron ore was required, and this amount was used in most of the subsequent work.

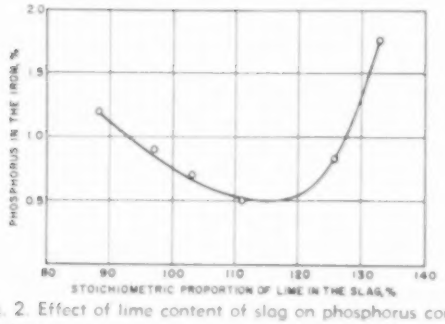

Fig. 2. Effect of lime content of slag on phosphorus content of the iron.

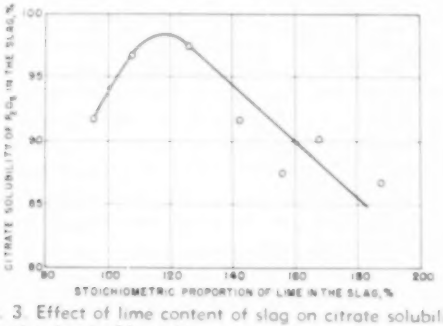

Fig. 3. Effect of lime content of slag on citrate solubility of P_2O_5 in the slag (—80 mesh).

Figure 2 shows that the phosphorus content of the iron decreased to 0.5% as the proportion of lime was increased to about 110% of the stoichiometric requirement. When the proportion of lime was increased to above 120% of stoichiometric, the viscosity of the slag in the furnace increased, with the result that furnace operation was poor and the phosphorus content of the iron increased.

Figure 3 shows that the citrate solubility of the P_2O_5 in the slag was at a maximum of 98% when it contained 120% of the CaO required to form silicocarnotite and was over 95% when the CaO content was in the range 105 to 135% of stoichiometric.

Operating Results

Best results were obtained when the furnace was operated at 75-100 v and 350 kw and the charge was proportioned to contain 110% of the stoichiometric amount of lime required to provide 4 moles of CaO per mole of P_2O_5 and 1 mole of CaO per mole of SiO_2, and 135% of the stoichiometric amount of iron ore required to oxidize the phosphorus present. Data from a typical test are given in Table II. By weight, the charge contained 1.8 metric tons of calcined iron ore (59% Fe) and 1.3 metric tons of lime (95% CaO) per metric ton of ferrophosphorus (24.4% P). From this charge, the products, per ton of ferrophosphorus, were: 1.3 tons of iron containing 0.8% P and 2.5 tons of slag containing 22.1% P_2O_5 of which 99% was soluble in neutral ammonium citrate solution when the slag was ground to pass an 80-mesh screen. Presumably, 0.3 ton was lost as spillage of raw materials and products. Power consumption averaged 1761 kwhr and electrode consumption averaged 29.1 kg per metric ton of ferrophosphorus charged.

The graphite lining of the furnace showed very little attack by molten slag. The magnesite hearth was satisfactorily resistant to attack by molten iron of low phosphorus content. No apparent damage to the hearth was observed after tests in which the iron produced contained less than 1% of phosphorus. However, after one test in which the composition of the charge was not controlled satisfactorily and 12 of 40 taps contained more than 1% phosphorus,

Table II. Summary of data on production of phosphate slag and iron from byproduct ferrophosphorus

Operating Conditions

Length of period, hr	117.5	Electrode voltage (between electrodes)	101.5
Total time of operation, hr	110.4	Current, amp	3644
Operating time, %	94.0	Electrode current density, amp/cm²	5.0
Charge proportions, kg			
Lime	1275	Average kva	369.9
Ore	1800	Average kw	350
Ferrophosphorus	1000	Power factor	0.946

Operating Results

Consumption of charge		Iron composition, %			
Lime, kg/hr	229	Fe	99.0	C	0.07
Ore, kg/hr	322	P	0.8	Cr	0.03
Ferrophosphorus, kg/hr	179	Si	0.01	Mo	0.01
Lime, kg/metric ton of ferrophosphorus charged	1275	Mn	0.07	Sn	<0.10
Ore, kg/metric ton of ferrophosphorus charged	1800	S	0.01	Pb	<0.10
Ferrophosphorus, kg/metric ton of iron produced	760	Cu	<0.10	Zn	<0.40
Iron production rate, kg/hr	236	Ti	<0.02	Ni	<0.10
Slag production rate, kg/hr	443				
Power consumption, kwhr/metric ton of ferrophosphorus charged	1941	Slag composition, %			
Graphite electrode consumption		SiO_2	12.0	MgO	0.9
kg/hr	5.2	Fe_2O_3	12.1	MnO	2.0
kg/metric ton of ferrophosphorus charged	29.1	CaO	49.2	Al_2O_3	2.7
Temperature of iron as tapped, °C	1540	P_2O_5	22.1	TiO_2	1.1
Temperature of slag as tapped, °C	1620	C.I. P_2O_5	0.2	F	0.02
Iron recovery, kg/metric ton of ferrophosphorus charged	1316			As	<0.001
Slag recovery, kg/metric ton of ferrophosphorus charged	2467				

drillings of the hearth showed that it had been penetrated about 8 cm by the metal.

Acknowledgment

The authors wish to acknowledge the advice and encouragement received from M. M. Striplin, Jr., and T. P. Hignett. A. W. Beinlich, Jr., M. R. Burns, H. W. Elder, J. L. Graham, A. B. Harrison, and other members of the TVA Development Branch helped carry out the experimental work.

Manuscript received July 8, 1957.

Any discussion of this paper will appear in a Discussion Section to be published in the December 1958 JOURNAL.

REFERENCES

1. G. L. Bridger, J. W. Moore, and H. M. McLeod, Jr., *Ind. Eng. Chem.*, **41**, 1391 (1949).
2. R. C. Buehl and M. B. Royer, *Bur. Mines Rept. Investigations 5102*, February 1955.
3. Private correspondence.
4. M. M. Striplin, Jr. and W. M. Kelly, *Chem. Eng. Prog.*, **43**, 569 (1947).
5. Tennessee Valley Authority, Chemical Engineering Report No. 10. Analytical Index of Chemical Engineering Publications, Patents, and Reports. Compiled by E. L. Newman and L. D. Copeland. U. S. Government Printing Office, Washington, D. C. (1954).
6. G. Tromel, *Stahl u. Eisen*, **63**, 21 (1943).

Electrolytic Production of Sodium Perchlorate Using Lead Dioxide Anodes

Joseph C. Schumacher, David R. Stern, and Paul R. Graham

American Potash & Chemical Corporation, Whittier, California

ABSTRACT

Lead dioxide was investigated as an anode substitute for platinum in the production of sodium perchlorate. Rod shaped deposits were prepared on nickel and platinum clad tantalum wires. The plate was dense, heavy, metallic-like in appearance and not too fragile for ordinary handling. The first phase of experimentation was performed in small laboratory cells to determine approximate electrolyses data. Larger bench-scale production cells were also run simulating plant operating conditions. Lead dioxide anodes produce sodium perchlorate at high cumulative current efficiencies. One lead dioxide anode was used in cell operation for 3,000 hr. Cumulative current efficiency for a given anodic current density is a function of the cathode material, cathodic current density, and the additive used. Perchlorate can be produced using nickel, copper, stainless steel, and carbon steel cathodes. Energy requirements, under identical experimental conditions, indicate that stainless steel and nickel are the best cathode materials. A current efficiency of 91.5% was obtained with a stainless cathode at anodic and cathodic current densities of 15.5 amp/dm^2 and of 7.25 amp/dm^2, respectively. No unusual metallic contamination could be detected in the ammonium perchlorate prepared from the sodium perchlorate.

Increased demand for $NaClO_4$ as an intermediate for the production of ammonium and potassium perchlorates resulted in a search for a replacement for the Pt anode. Previous investigations have shown that PbO_2 might be a satisfactory substitute for Pt. Lead dioxide electrodes in various sizes and shapes may be prepared from suitable electrolytic baths (1-4). The rod-shaped electrodes used in these experiments were prepared by plating PbO_2 on Ni and Pt clad Ta wires. Platinum clad Ta as a conductor on which to deposit the PbO_2 had the advantage of being corrosion resistant to the HNO_3 liberated during electrolysis from the $Pb(NO_3)_2$ electrolyte. The PbO_2 deposit is dense, heavy, and metallic in appearance. Perchlorates can be produced on PbO_2 deposits from 8-10 mm thick (4). Thin deposits are fragile and erode easily during electrolysis. When a thickness of at least 20 mm is obtained, the electrode is not too fragile for ordinary handling and erosion is not significant.

The over-all chemical equation for the electrochemical oxidation of chlorate to perchlorate has been reported by other investigators (5-9).

The investigation was divided into two phases. The first dealt with exploratory experiments in small laboratory cells designed to determine feasibility, to approximate electrolyses data, and to evaluate different cathodes with small PbO_2 anodes. On the basis of these experiments, larger cells were operated simulating actual plant conditions. The first phase of the investigation is referred to as laboratory cell experimentation and the latter phase as bench-scale production.

Three methods for measuring current efficiencies have been used by other investigators and were used in this study. They were:

Gas collection.—If a standard coulombic cell with Pt electrodes containing a 5% NaOH electrolyte is connected in series with a perchlorate cell, the ratio of gas volumes in the coulombic cell to that of the

perchlorate is 3:2. Thus, the gas volumes from the coulombic and perchlorate cells give an approximate measure of the instantaneous current efficiency. This may not be too accurate if there are appreciable side reactions.

Chlorate depletion.—If side reactions are negligible, then the $NaClO_3$ disappearing can be used as an approximation to current efficiency.

Perchlorate determination.—This measurement is the most accurate determination of current efficiency, but necessitates a time consuming perchlorate analysis. Moreover, this is a cumulative and not an instantaneous current efficiency.

Gas collection and chlorate depletion are easily and rapidly obtained and may indicate the trend of a variable. Gas collection was utilized for the small laboratory cells, recognizing that it was only an approximation, which would be checked by direct analyses later on the bench-scale production cell.

Data obtained by analyses on the bench-scale cell indicate that inefficiencies due to side reactions are of small magnitude with some cathodes and that the current efficiency measurement used for the laboratory cells has some validity.

Laboratory Cell

Cell construction.—Laboratory cells were constructed of $\frac{1}{8}$ in. Lucite. They were cylindrical in shape, $2\frac{1}{2}$ in. I.D. x 5 in. high. The electrodes, a thermometer, and a $\frac{1}{4}$ in. diameter x $1\frac{1}{2}$ in. gas outlet tube were sealed through the cell cover. A rubber gasket was fitted to a $\frac{1}{2}$ in. flange around the top of the cells. Wing nuts through the flange secured the cover, creating a gas-tight fitting.

Evolved gas was directed to 50 ml burets. Volumes were measured by the displacement of water in the burets.

Electrolyte levels in both cells were maintained 1 in. from the top; this gave a small equal volume. Electrolysis time, while the gases were being collected, was short. Since a ratio of volumes was utilized, no corrections for pressure and temperature were necessary; it was assumed that the burets remained under identical conditions, even though volumes of different magnitude were involved.

Lead dioxide was employed as the anode in the laboratory cell except for the initial experiments. A Pt anode was used in these experiments to establish reference data. Two cathodes connected in parallel were used. The initial concentration of the electrolyte was approximately 500 g/l of reagent grade $NaClO_3$ with various additives. New electrolyte was used for each series of experiments.

Temperatures of both cells were controlled with external water cooling within 5°C.

Experimental procedure.—The coulombic and laboratory cell were connected in series to a Se rectifier. Current and voltage across the laboratory cell were measured during electrolysis. These cells were operated until the coulombic cell had evolved 50 ml of gas. Comparison of this volume to that evolved from the laboratory cell gave the current efficiency. Each experiment was made under a controlled current density. The pH of the electrolyte was controlled within a given range and was adjusted with HCl or NaOH.

The cells were operated a sufficient length of time after reaching thermal equilibrium to purge the dead air space. During this time gas was evolved to the atmosphere. When a steady rate of evolution existed, the gas was collected in the burets and data recorded during the collection of the gas samples. Current was varied from 1.33 to 5.30 amp, while the voltage across the laboratory perchlorate cell covered the range of 4.0-6.1 v. A temperature range of 20°-40°C was investigated.

Experimental Results

To establish reference data, the initial experiments utilized a Pt anode in the laboratory perchlorate cell. After this, experiments were conducted using PbO_2 as the anode with Cu, carbon steel, Ni, and stainless steel as the cathodes. Variables observed were current efficiency, current density, cell temperature, electrolyte concentration, pH, cathode material, and additives. Some of these data are presented in Table I. The most satisfactory values of cell operating conditions were selected from these data for subsequent verification in the larger bench-scale production cell.

Table I. Experimental results of laboratory perchlorate cells

Material		Anodic current density (amp/dm²)	Voltage (volts)	Current (amp)	Temp range (°C)	pH	Initial concentration (g/l): Electrolyte	Additive		Current* efficiency (%)
Anode	Cathode						$NaClO_3$	NaF	$Na_2Cr_2O_7$	
Pt	Carbon steel	31.0	5.2	2.90	20-25	6.0	484.5	—	5	92.8
PbO_2	Carbon steel	15.5	4.6	2.46	30-35	6.5	484.5	—	5	37.7†
PbO_2	Copper	15.5	4.4	4.71	30-35	6.0	484.5	—	5	36.3
PbO_2	Copper	15.5	5.0	1.47	35-40	6.5	500.0	0.5	—	92.4
PbO_2	Nickel	7.25	4.0	1.33	35-40	6.5	500.6	0.5	—	93.5
PbO_2	Nickel	15.5	5.0	1.47	35-40	6.5	493.5	—	—	84.8
PbO_2	Nickel	15.5	5.0	1.47	35-40	6.5	493.5	0.5	—	92.3
PbO_2	Nickel	15.5	5.3	1.47	35-40	6.5	493.5	1.5	—	92.7
PbO_2	Nickel	15.5	5.2	1.47	35-40	6.5	493.5	Saturated	—	93.0
PbO_2	Nickel	15.5	4.9	2.65	35-40	6.5	500.6	0.5	—	93.7
PbO_2	Nickel	23.25	5.8	2.21	35-40	6.5	493.5	0.5	—	92.7
PbO_2	Stainless steel (302)	31.0	6.1	5.30	25-30	6.5	495.2	0.5	—	97.5†

* Approximate instantaneous current efficiency based on gas collection technique.
† Discoloration of evolved cell gases during electrolysis indicated that side reactions were taking place.

Conclusions.—Examination of the data in Table I indicates that the following conclusions may be made:

1. Sodium perchlorate can be made by electrolysis using a PbO_2 anode with Cu, carbon steel, Ni, or stainless steel cathodes.
2. Current efficiencies appear to be higher with Ni, stainless steel, and Cu cathodes than with carbon steel.
3. Data obtained with carbon steel are not conclusive because of side reactions.
4. Sodium fluoride appears to be a better additive than sodium dichromate. The minimum effective NaF concentration is 0.5 g/l.
5. Data obtained with a PbO_2 anode, Ni cathodes, and a NaF additive indicate that the current efficiency is practically independent of current density, temperature, and pH in the range of variables investigated. An instantaneous current efficiency of 93.7% was obtained at an anodic current density of 15.5 amp/dm^2.
6. Lower voltages appear to be possible using PbO_2 anodes.

Bench-Scale Production Cell

The first phase of the investigation had set up sufficient design criteria to proceed with the construction of a larger unit which could be operated semicontinuously and for longer periods of time. All the variables could be evaluated based on the current efficiency, which could be determined by a direct chemical analysis. In order to proceed with this unit, larger PbO_2 anodes were made.

Bench-scale cell construction.—The cell was a 4-liter resin reaction kettle with a bottom outlet (Fig. 1). Current was provided by a Se rectifier and voltages and current measurements obtained. Temperature was controlled by circulating water through a glass coil immersed in the electrolyte. When pH control was necessary, 18% HCl was added.

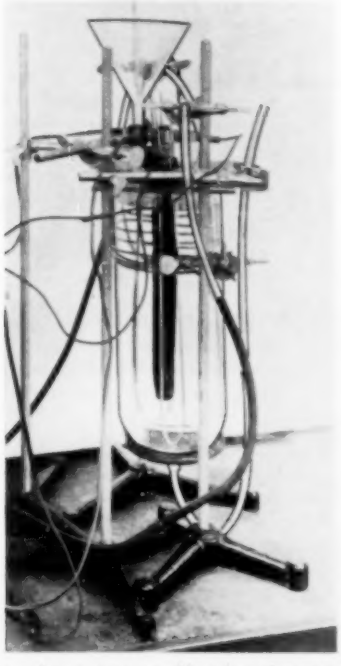

Fig. 1. Internal arrangement of bench-scale production cell

The anode consisted of a rod-shaped, rough surfaced PbO_2 electrode and was immersed in solution so that, at a current of 26 amp, the anodic current density was 15.5 amp/dm^2. This value was maintained constant in all experiments. It proved to be the best value obtained in the smaller laboratory cells and simulates approximate plant operating conditions. Cathodes were U-shaped metal rods of varying diameters by 15 in. in length. The anode, cathodes, cooling coil, and thermometer were inserted through the top of the cell into the electrolyte. An electrical connection was made at the top of the anode with a Ag-plated Cu clamp. Cathodes were on 3 in. center to center spacing, with the anode centered between them or 1½ in. from the cathodes. Figure 2 is a picture of a typical PbO_2 anode with the cathodes used.

Electrolyte could be removed from the bottom of the cell and returned to the top to insure adequate mixing.

Experimental procedure.—At the start, the cell was filled with 4 liters of solution containing approximately 500 g/l $NaClO_3$ plus the additive. The pH and temperature were recorded. A value of 6.9 was considered to be the maximum limiting pH while the temperature was controlled within the range of 30°-45°C. Current was adjusted to the desired anodic current density, and voltage noted.

Electrolyte was removed during electrolysis from the bottom of the cell and returned through the top. About 2 liters were removed in from 2 to 3 min in 500 ml increments. This served to keep the electrolyte well circulated and was repeated every half hour. After recirculation was completed, a 100 ml sample was secured and the pH measured. This sample was returned to the cell and the pH adjusted, if necessary.

A 15 ml sample was taken for chemical analysis every 2 hr after recirculation. Then 15 ml of make-up solution were added to maintain constant volume.

The addition of make-up solution is important, since no drastic concentration changes in the electrolyte could be introduced. During the initial phases of the experiment the make-up solution contained 300 g/l $NaClO_3$. This solution was used until the concentration of the electrolyte in the cell dropped to 150

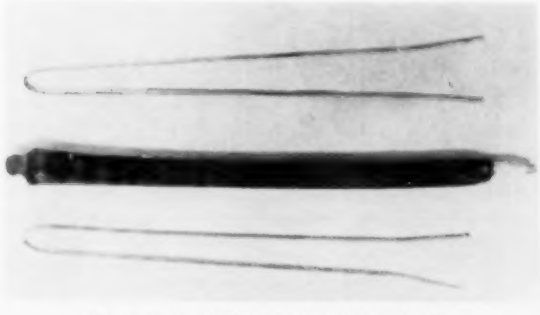

Fig. 2. Typical PbO_2 anode-nickel cathodes

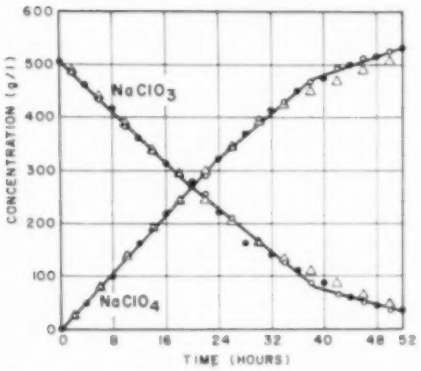

Fig. 3. Effect of PbO_2 conductor wire. Electrolysis conditions: anodic C. D. = 15.5 amp/dm²; cathodic C. D. = 7.25 amp/dm²; temp. range = 30°-45°C; cell voltage = 5.2-5.3 v; pH = 5.2-5.7; NaF conc. = 0.5 g/l. Anode: solid circle, PbO_2 plated on Ni wire; open circle, PbO_2 plated on Pt clad Ta; open triangle, PbO_2 plated on Ni wire.

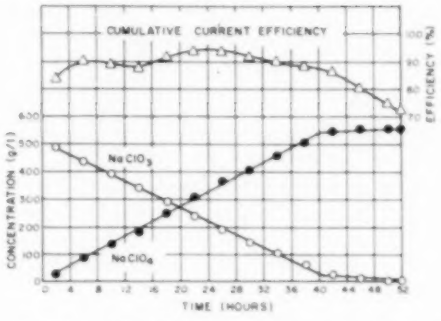

Fig. 4. Effect of nickel cathodes on cumulative current efficiency. Electrolysis conditions: anodic C. D. = 15.5 amp/dm²; cathodic C. D. = 7.25 amp/dm²; temp. range = 35°-45°C; cell voltage = 5.0 v; pH = 5.3; NaF conc. = 0.5 g/l; anode: rough surface rod-shaped, 2.06 cm dia. x 45.72 cm long; cathode: two U-shaped Ni rods, 0.95 cm dia. x 38.10 cm long.

g/l of chlorate. From this point, make-up solution of 150 g/l was added until the concentration dropped to 100 g/l. Then solution adjusted to the chlorate composition of the electrolyte was added until the completion of the experiment.

Every 2 hr a 15 ml sample was analyzed immediately for its sodium chloride and chlorate concentrations. Since the perchlorate determination was time consuming, samples were taken only every 4 hr for analyses.

Experiments were carried out for 52 hr continuously, except when side reactions or chlorate analyses indicated that the obtained efficiencies were too low.

Experimental Results

Two different PbO_2 anodes were used in the experiments with the bench-scale production cell. One

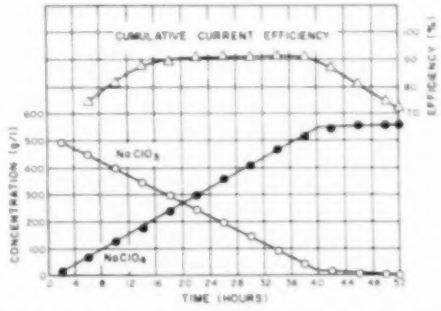

Fig. 5. Effect of stainless steel cathodes on cumulative current efficiency. Electrolysis conditions: anodic C. D. = 15.5 amp/dm²; cathodic C. D. = 7.25 amp/dm²; temp. range = 35°-45°C; cell voltage = 4.75 v; pH = 5.7; NaF conc. = 0.5 g/l; anode: rough surface rod-shaped, 2.06 cm dia. x 45.72 cm long; cathode: two U-shaped stainless steel (302) rods, 0.95 cm dia. x 38.10 cm long.

Table II. Experimental results of bench-scale production cells

Cathode	Cathode current density (amp/dm²)	Additive	Voltage (volts)	Current[a] (amp)	Time, (hr)	Kw-Hr	Final[b] concentration (g/l) $NaClO_4$	Final[b] concentration (g/l) $NaClO_3$	Cumulative current efficiency (%)	Unit energy[c] (kw-hr/lb)
Nickel	21.4	NaF[d]	5.1	26.0	41.6	5.51	510	50	83.0	1.23
Nickel	21.4	NaF and $Na_2Cr_2O_7$[e]	5.3	26.0	52.0	7.16	240	280	31.1	3.38
Nickel	7.25	NaF	5.0	26.0	38.6	5.02	514	50	88.2	1.11
Stainless steel (302)	21.4	NaF	5.2	26.0	49.2	6.52	493	50	68.0	1.50
Stainless steel (302)	7.25	NaF	4.75	26.0	37.6	4.64	505	50	91.5	1.04
Stainless steel (302)	7.25	NaF and $Na_2Cr_2O_7$[f]	4.75	26.0	24.0	2.96	235.5	287.6	66.0	1.43
Copper	21.4	NaF	5.7	26.0	42.8	6.36	492	50	78.5	1.47
Carbon steel	21.4	NaF	5.1	26.0	52.0	6.89	264	214	34.2	2.96
Carbon steel	14.1	$Na_2Cr_2O_7$[g]	4.9	26.0	48.0	6.13	68	445	9.9	10.23

[a] Anodic current density = 15.5 amp/dm².
[b] Volume = 4 liters.
[c] Commercial production requires 1.5-1.9 kw-hr/lb at 6.2-6.8 v, and anodic current densities of 31.1-52 amp/dm² (11).
[d] NaF as an additive = 0.5 g/l concentration.
[e] $Na_2Cr_2O_7$ concentration = 0.5 g/l.
[f] $Na_2Cr_2O_7$ concentration = 0.003 g/l.
[g] $Na_2Cr_2O_7$ concentration = 5.1 g/l.

Table III. Spectrographic analyses of unpurified ammonium perchlorate

Cathode material	Nickel	Stainless steel (302)	Copper
Major constituent* **	Sodium	Sodium	Sodium
Intermediate constituent	Potassium	Potassium	Potassium
Minor constituent	Approximate %	Approximate %	Approximate %
Calcium	0.10	0.10	0.10
Aluminum	0.05	0.05	0.01
Iron	0.05	0.01	0.005
Magnesium	0.01	None found	None found
Silicon	0.01	0.01	None found
Barium	0.01	0.01	0.01
Chromium	0.005	0.001	0.001
Copper	0.005	0.01	0.005
Vanadium	0.005	0.001	0.001
Nickel	0.005	None found	None found
Manganese	0.001	None found	None found
Lead	0.001	Trace	Trace
Wt of Ash (g)	1.62	1.39	3.03

* Mother liquor hold-up.
** Based on spectrographic analyses of ash.

anode consisted of PbO_2 plated on Pt clad Ta and the other was plated on Ni wire. Experimental results obtained when PbO_2 is plated on these two different conductors are presented in Fig. 3. When sodium dichromate was used as an additive, a thin yellow deposit was formed on the surface of the PbO_2 anode. Cathodes were constructed of Ni, Cu, carbon steel, and 302 stainless steel. The effects of cathodic current density and additives were also investigated. Some experimental results are presented in Table II.

A typical result, using Ni cathodes, illustrating the change in electrolyte concentration as a function of time and the cumulative current efficiency is presented in Fig. 4. Figure 5 presents results with stainless steel cathodes.

Sodium perchlorate produced in these bench-scale experiments was converted to ammonium perchlorate to determine purity and for evaluation purposes. Only the first crop of unwashed crystals was selected for chemical and spectrographic analyses. Table III presents spectrographic data on the ammonium perchlorate prepared, and indicates that no unusual quantity of metallic impurities was introduced into the perchlorate.

Conclusions.—The following conclusions may be reached from the experimentation, utilizing PbO_2 anodes as a substitute for Pt in the production of sodium perchlorate:

1. Lead dioxide anodes produce sodium perchlorate at high cumulative current efficiencies.
2. The cumulative current efficiency for a given anodic current density is a function of chlorate concentration, the cathode material, the cathodic current density, and the additive used.
3. The wire on which the PbO_2 was plated for an anode appears to have no effect on the production of sodium perchlorate.
4. Sodium perchlorate can be produced using cathodes of Ni, Cu, stainless steel, and carbon steel. However, efficiencies with carbon steel are very low.
5. Sodium dichromate has a detrimental effect on the current efficiency by forming a thin deposit on the surface of the PbO_2 anode.
6. Decreasing the cathodic current density increased the current efficiency when utilizing Ni and stainless steel cathodes.
7. One PbO_2 anode was used in the cell operation for 3,000 hr.
8. Ammonium perchlorate was prepared from the sodium perchlorate produced in these experiments. No unusual metallic contamination was present and the ammonium perchlorate meets present commercial specifications.
9. Comparison of energy requirements calculated for identical experimental conditions indicates that Ni and stainless steel are the best cathode materials and that PbO_2 offers energy advantages over Pt as an anode.
10. Energy results of 1.04 kw-hr/lb of sodium perchlorate with a cumulative current efficiency of 91.5% were obtained. These results were attained with stainless steel cathodes at a cathodic current density of 7.25 amp/dm^2 and a final sodium chlorate concentration of 50 g/l.

Manuscript received May 6, 1957. This paper was prepared for delivery before the Washington Meeting, May 12-16, 1957.

Any discussion of this paper will appear in a Discussion Section to be published in the December 1958 JOURNAL.

REFERENCES

1. G. Angel and H. Mellquist, *Z. Elektrochem.*, **40**, 702 (1934) (Ger. 140,317; 195,117; 206,329).
2. Y. Kato and K. Koizumi, *J. Electrochem. Assoc. Japan*, **2**, 309 (1934).
3. K. Sugino and Y. Shibazaki, *ibid.*, **16**, 9 (1948).
4. K. Sugino, *Bull. Chem. Soc. Japan*, **23**, 115 (1950).
5. F. Foerster, *Z. Elektrochem.*, **4**, 386 (1898).
6. W. Oechsli, *ibid.*, **9**, 807 (1903).
7. J. G. Williams, *Trans. Faraday Soc.*, **15**, 134 (1919).
8. N. V. S. Knibbs, *ibid.*, **16**, 402 (1921).
9. C. W. Bennett, *ibid.*, **29**, 323 (1916).
10. N. H. Furman, "Scott's Standard Methods of Chemical Analyses," Vol. 1, p. 272-275, D. Van Nostrand Co., Inc., New York (1950).
11. C. L. Mantell, "Industrial Electrochemistry," 3rd ed., p. 135, McGraw-Hill Book Co., Inc., New York (1950).

Dissolution of Metals in Aqueous Acid Solutions

II. Depolarized Dissolution of Mild Steel

A. C. Makrides and N. Hackerman

Department of Chemistry, University of Texas, Austin, Texas

ABSTRACT

Dissolution rates of mild steel cylinders rotated in 2*N* HCl solutions containing ferric chloride, benzoquinone, and tolu-p-quinone are reported. At high velocities the dissolution rate depends linearly on velocity of rotation. The dissolution rate also depends on the roughness of the metal surface.

In a previous paper (1) current-potential relations for dissolution of mild steel in acid solutions containing depolarizers were interpreted on the assumption that dissolution was under diffusion control. A kinetic study of dissolution is presented here. In particular, the dependence of rate on depolarizer concentration, stirring velocity, temperature, and surface roughness of the metal is examined. Results are consistent with the postulate that dissolution is limited by the rate of diffusion of depolarizer to the interface.

Experimental

The experimental arrangement and procedure have been described previously (1). Mild steel cylinders, polished with 2/0 emery paper and degreased with benzene in an extractor, were rotated in 2*N* HCl solutions containing depolarizer at speeds up to 11,000 rpm (1000 cm/sec linear velocity). Only the lateral surface of the cylinder was exposed to the solution, the top and bottom parts as well as the edges being covered with paraffin. All solutions were deaerated by passing nitrogen through the solution before a run.

The reaction vessel was a 600 ml beaker loosely fitted with a Lucite cap. The cap had openings through which the specimen and a calomel electrode with a saturated KCl-agar bridge were inserted. The center of the cylinder was 2 cm from the center of the beaker. This arrangement was chosen to avoid separation of flow along the shaft observed when the cylinder was concentric with the beaker.

The surface of the cylinder was 1.5 cm from the wall of the beaker and 4 cm from the tip of a calomel electrode placed opposite the cylinder and next to the wall of the container. The top of the cylinder was immersed to a depth of 4 cm when the cylinder was stationary. The diameter of the cylinders varied from 1.70 to 1.90 cm and the height of the lateral surface exposed to solution was between 1.8 and 2.1 cm. These last two dimensions were measured for each run.

Ferric chloride was of C. P. grade and was used without further purification. The quinones were of highest commercial purity available and were twice recrystallized from ethanol.

Results and Discussion

Dissolution rates are expressed in terms of the specific rate constant k, given by

$$k = \frac{2.30\ V}{At} \log \frac{x_\infty}{x_\infty - x} \qquad (I)$$

Here V, is the volume of the solution (400 ml), A the projected exposed metal surface area, x the weight loss (mg) in time t (sec), and x_∞ the calculated weight loss for $t \to \infty$.

Generally, the weight loss at the end of a specified time (600 sec) was measured and k calculated from Eq. (I). In some cases the solution was analyzed for iron at measured time intervals and k obtained from a first order kinetic plot.

For purposes of discussion a differentiation is made between results obtained at average dissolution rates less than 0.020 mg/sec/cm² of projected area and those at higher rates. Results for the former interval are given in Tables I and II and are plotted in Fig. 1. In this range, k is independent of initial depolarizer concentration. At greater average dissolution rates, k increases with initial depolarizer concentration. It is shown below that the dependence of k on C_0 in the latter case is caused by excessive surface roughening brought about by dissolution.

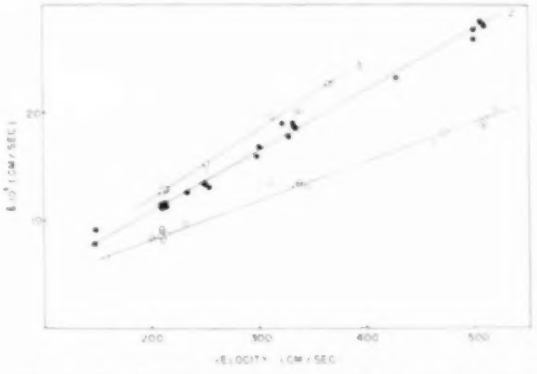

Fig. 1. Specific rate constant as a function of velocity: curve 1, ferric chloride; curve 2, tolu-p-quinone; curve 3, benzoquinone.

Table I. Dissolution rates of mild steel cylinders in 2N HCl solutions containing depolarizers; T = 30 ± 0.5°C

Ferric chloride			Tolu-p-quinone			Benzoquinone		
Velocity (cm/sec)	Conc (moles/l)	$k \cdot 10^2$ (cm/sec)	Velocity (cm/sec)	Conc (moles/l)	$k \cdot 10^2$ (cm/sec)	Velocity (cm/sec)	Conc (moles/l)	$k \cdot 10^2$ (cm/sec)
158	0.0431	6.62	147	0.0100	7.88	209	0.0056	13.0
200	0.0432	8.36	149	0.0100	9.25	210	0.0050	12.6
210	0.0700	8.60	211	0.0050	11.4	211	0.0094	12.6
211	0.0102	9.32	212	0.0100	11.5	211	0.0204	13.3
211	0.0103	9.20	212	0.0200	10.9	211	0.0301	13.1
211	0.0318	8.50	234	0.0100	12.7	212	0.0108	13.0
211	0.0446	8.19	250	0.0100	13.4	212	0.0150	12.3
213	0.0191	8.73	254	0.0100	13.1	213	0.0300	12.6
232	0.0431	9.83	299	0.0100	15.9	245	0.0100	15.3
311	0.0432	13.5	300	0.0100	16.8	251	0.0100	15.3
333	0.0450	13.3	322	0.0049	19.0	253	0.0050	14.6
339	0.0450	13.6	328	0.0046	17.7	253	0.0050	15.1
345	0.0194	13.1	332	0.0092	18.7	305	0.0051	19.8
463	0.0200	17.4	332	0.0098	19.2	312	0.0103	19.6
472	0.0200	18.2	334	0.0200	18.4	312	0.0106	20.4
506	0.0200	18.9	424	0.0100	23.4	335	0.0200	20.1
512	0.0194	18.7	488	0.0050	27.7	339	0.0200	20.2
512	0.0194	19.4	500	0.0050	26.7	364	0.0050	22.7
520	0.0312	20.4	506	0.0100	28.6	368	0.0050	22.6
			510	0.0100	28.0			

Table II. Dependence of rate constant on velocity

Depolarizer* 2N HCl solutions containing depolarizers. T = 30.0° ± 0.5°C.	Slope†	Intercept†	Estimated Deviation†‡
Ferric chloride	3.50×10^{-5}	$+1.38 \times 10^{-3}$	$\pm 0.74 \times 10^{-3}$
Tolu-p-quinone	5.56×10^{-5}	-0.09×10^{-3}	$\pm 0.88 \times 10^{-3}$
Benzoquinone	6.39×10^{-5}	-0.70×10^{-3}	$\pm 0.60 \times 10^{-3}$

Note: * Range of Reynolds numbers: 30,000 to 100,000.
† From results given in Table I. The slope and intercept were calculated by the least squares method.
‡ The estimated deviation is given by $S_k(\text{estim}) = S_k(1-r^2)^{1/2}$ where S_k is the standard deviation and r the correlation coefficient. The average deviation is ±6.0% for ferric chloride, ±4.5% for tolu-p-quinone, and ±4.0% for benzoquinone.

Dependence of the Specific Rate Constant on Velocity

Heat and mass transfer in turbulent flow are of considerable theoretical as well as practical interest and have been the subject of numerous investigations (2). The work of King and collaborators (3), of Agar (4), and of Eisenberg, Tobias, and Wilke (5, 6) is of particular interest since it is directly applicable to the rotating cylinder-turbulent flow system.

Agar (4) has suggested that the effective thickness, δ, of the boundary layer at the solid surface is given by an expression of the form[1]

$$\delta = \frac{L}{B} (R_a)^{-\alpha} (Pr)^{-\beta} \qquad \text{(II)}$$

Here L is the characteristic length, the diameter, d, of the cylinder in this case; B, α, and β are constants; (R_a) is the Reynolds number; and (Pr) Prandtl's number. The last two are given by

$$(R_a) = \frac{Vd}{\nu} \qquad \text{(III)}$$

$$(Pr) = \frac{\nu}{D} \qquad \text{(IV)}$$

[1] The effective thickness of the boundary layer is equivalent to that calculated on the basis of a model of a stationary layer of liquid adjacent to the solid. Through this layer, the concentration of diffusing species is assumed to change linearly with distance from a value of zero, at the surface, to that in the bulk of the solution. δ is not, in general, equal to the physical thickness of the hydrodynamic boundary layer, but it is related to this thickness.

where ν is the kinematic viscosity and D the diffusion coefficient. Equation (II) assumes that for forced convection δ is independent of the concentration of diffusing species and that electrolytic transport is negligible. Agar (4) notes that experimentally

$$\delta = (\text{const})\ V^{-q} \qquad \text{(V)}$$

where $0.5 < q < 1.0$. If a reaction is controlled by diffusion

$$k = D/\delta \qquad \text{(VI)}$$

and Fig. 1 shows that in this case q [and hence α in Eq. (II)] is unity.

Comparison with Results of Previous Investigators

The linear dependence of k on velocity of stirring found with the present system is in agreement with the results of King and co-workers (3) and of Frank-Kamenitskii and co-workers (7), but is, at first sight, in variance with the results of Roald and Beck (8), and of Eisenberg, Tobias, and Wilke (5, 6) who find that the rate of mass transfer increases as the 0.70 power of velocity. The latter authors correlate their results through the function $j'_D = (k/V)(Pr)^{-0.644}$. From a plot of j'_D vs. Reynolds number they find

$$k = 0.0791\ V\ (R_a)^{-0.30}\ (Pr)^{-0.644} \qquad \text{(VII)}$$

The experimental system studied by these authors (6) was oxidation and reduction of the ferri-ferrocyanide couple at inert (nickel) electrodes.

The velocity exponent given in Eq. (VII) is a "best value" for the range of Reynolds number 1,000 to 100,000 (6). Actually, the exponent depends on Reynolds number. Thus, the slope of the correlation curve (j'_D vs R_a) was −0.32 for the interval R_a = 1,000 to 10,000, while it was only −0.23 for R_a = 30,000 to 100,000 [Table II of ref. (6)]. To be exact, therefore, comparisons must be made in the same range of Reynolds numbers.

In the work reported here, Reynolds number varied from 30,000 to 100,000. A least squares' analysis of the data of Eisenberg, Tobias, and Wilke (6)

in this interval shows that the limiting rates for reduction and oxidation depend on the 0.72 and 0.77 power of velocity, respectively.

Table II gives an analysis of the data of Table I by the least squares method. As noted above, a linear relation exists between k and V. The possibility that a log-log function gives a better fit was examined and rejected. In the case of $FeCl_3$, for example, the correlation coefficient was 0.988 for a linear relation and 0.92 for a logarithmic one.

Hydrodynamic considerations, based on a model of a liquid layer of finite thickness through which convective diffusion is absent, show that for the limiting case of large Reynolds and Prandtl's numbers the rate of mass transfer is linearly related to the flow velocity (7). However, it is unlikely that the Reynolds and Prandtl's numbers involved here are sufficiently large to attain this case.[2] In the absence of complicating effects, the dissolution rate is expected to increase as the 0.70 to 0.80 power of velocity (6). The higher value of the velocity exponent must therefore be attributed either to a difference in geometrical arrangement, or to an effect of the dissolution process on the hydrodynamic conditions under which mass transfer occurs.

Hydrodynamic conditions.—The different velocity exponents found in this work and that of Eisenberg, Tobias, and Wilke (5, 6) may be the result of different geometric arrangements. These authors (5, 6) used cylinders concentric with the wall (outer cylinder), a length to diameter ratio from 3.0 to 11.6, and complete end-baffling. In this work the cylinder was not concentric with the vessel and the length to diameter ratio was 1.0 to 1.2.

The differences noted above are probably not responsible for the different velocity exponents observed. The length to diameter ratio, l/d, does not appear to be significant. Eisenberg, Tobias, and Wilke (5, 6) found no effect for an almost fourfold change in this ratio. If, as pointed out below, a correlation exists between dissolution rate and friction factors derived from measurements of the drag on cylinders rotating in fluids, the experiments of Theodorsen and Regier (9) also support the view that the l/d ratio is without influence. These authors (9) found no effect on the dependence of the drag coefficient, $f/2$, on R_r for a change of l/d from 20:1 to 3:1. Further, the functional dependence of $f/2$ on R_r was the same for cylinders and disks,[3] which suggests that even extreme variation of the l/d ratio does not alter the velocity dependence.

The effect of baffling and of concentric arrangement is more difficult to evaluate. Eisenberg, Tobias, and Wilke (5, 6) found no dependence on the gap between the rotating cylinder and the outer tube (gaps of 0.5-12.5 cm). However, all of their experiments were done with a concentric arrangement. It has been suggested (8) that increased baffling gives values of the velocity exponent closer to unity. On this basis, our results should have shown probably a smaller, rather than larger, velocity exponent.

Proposed correlations [*see* (14-17)] between heat or mass transfer and hydrodynamic parameters are based generally on Reynolds' analogy (13) and assume the validity of the momentum transfer theory of turbulence. With other theories, e.g., the vorticity transfer theory (10), there is no direct correlation between the velocity and temperature distributions. It is probable that the success of proposed relations is to be ascribed to the fact that the momentum transfer theory gives the correct velocity distribution near a wall (11).

Even in cases where the velocity distribution in the core of the flow agrees with the vorticity transfer theory, Reynolds analogy may still be applicable. An example is the system of concentric cylinders. Eisenberg, Tobias, and Wilke (5, 6) find that an extended Reynolds' analogy (the Chilton-Colburn analogy) describes correctly the dependence of the mass transfer coefficient on Reynolds number. The work of Taylor (10) and of Pai-Shih I (12) shows that in this case, the momentum transfer theory fails in the core of the flow. However, in the neighborhood of the wall, the momentum transfer theory is valid and the skin friction coefficient is given by a von Kármán logarithmic equation (9, 10, 12). These observations support the view that the type of core flow is of secondary importance when mass transfer is controlled by the hydrodynamic conditions near a wall. If this supposition is correct, the nature of secondary flows, the presence of other surfaces at distances of the order of 1000 times the thickness of the boundary layer, a concentric or eccentric arrangement, and the extent of end-baffling are not expected to influence the rate of mass transfer.

One possible difficulty with dissolution experiments may be mentioned here. Dissolution is frequently accompanied by evolution of hydrogen. Although depolarizers reduce hydrogen evolution, it is unlikely that they suppress it entirely. The stirring effect of bubbles moving in the boundary layer must therefore be considered.

Roald and Beck (8) found for magnesium dissolving in HCl solutions that the stirring effect of bubbles was negligible at small dissolution rates but became dominant at high rates. The dissolution rate at which the stirring effect of hydrogen first becomes detectable increases with stirring velocity. At 150 cm/sec, this rate is equivalent to 1.9 cc H_2/cm^2/min. The maximum rate of hydrogen evolution in the experiments reported here was 0.01 cc H_2/cm^2/min.[4] Since the rate here is 100 times smaller than the rate threshold found by Roald and Beck (8), it may be concluded that stirring by bubbles is negligible.

It is believed that the linear dependence of rate on velocity usually found in dissolution experiments is the result of surface roughening caused by the

[2] These statements refer to smooth surfaces. As shown below, the rate of mass transfer may become a linear function of velocity at relatively small Reynolds numbers if the surface is hydrodynamically rough.

[3] Theodorsen and Regier (9) find for cylinders $1/\sqrt{f} = 4.07 \log\sqrt{f} = -0.6 + 4.07 \log R_r$ and for disks $1/\sqrt{f_x} = 4.07 \log\sqrt{f_x} = -2.05 + 4.07 \log R_x$, where f_x and R_x refer to the drag coefficient and Reynolds number at a distance x from the center of the disk. R_r is Reynolds number based on the radius of the cylinder.

[4] An upper bound for the rate of hydrogen evolution is given by the rate in solutions without depolarizers. This is calculated from the dissolution rate in 2*N* HCl.

dissolution process. Eisenberg, Tobias, and Wilke (6) took special pains to prepare smooth surfaces. In the present study it was impossible to avoid surface roughening during a run. Surface irregularities of height comparable to the thickness of the laminar sublayer give rise to a "hydrodynamically rough" surface. The rate is expected then to be a linear function of velocity when a critical value of Reynolds number is exceeded. The effect of surface roughness on rate of mass transfer is considered below.

Mass transfer in turbulent flow.—Proposed correlations (14-17) between rates of heat or mass transfer and hydrodynamic parameters are generally based on Reynolds' analogy which suggests that in turbulent flow momentum and heat are transferred in the same way (13). Reynolds' analogy fails for fluids for which Prandtl's number is not unity because of the existence of a layer near the wall through which the transfer of heat and momentum by conduction and viscosity is important. Kármán's extension (16) of Reynolds' analogy leads to the following expression for the rate of heat transfer

$$1/k_H = \frac{2}{f} + 5\sqrt{2/f}\,[(Pr-1) + \ln\{1+0.83(Pr-1)\}] \qquad \text{(VIII)}$$

where

$$k_H = \frac{Q_w}{V(T_w - T_m)c\rho}$$

with Q_w the rate of heat transfer per unit area of the wall, T_w the temperature at the wall, T_m the mean temperature for the region of flow considered, c the specific heat capacity, and ρ density.

For small values of Prandtl's number (Pr~1-10), Eq. (VIII) is in reasonably good agreement with experiment (11). At large values of Prandtl's number, however, Eq. (VIII) reduces to

$$\frac{1}{k_H} = \frac{2}{f} + 5\sqrt{2/f}\,(Pr) \qquad \text{(VIIIa)}$$

The indicated linear dependence of $1/k_H$ on (Pr) for constant $f/2$ is contrary to observation (17). Good agreement with experiment is observed with

$$k_H = \frac{f}{2}(Pr)^{-(\beta+1)} \qquad \text{(IX)}$$

where $\beta = 0.35$. Colburn (17) and Chilton and Colburn (18) use $\beta = 1/3$, while Eisenberg, Tobias, and Wilke (5, 6) find from mass transfer experiments with cylinders $\beta = 0.356$.

Theodorsen and Regier (9) find for rotating cylinders with smooth surfaces

$$\frac{1}{\sqrt{f/2}} = -1.72 + 5.76 \log R_s\sqrt{f/2} \qquad \text{(X)}$$

As pointed out by Eisenberg, Tobias, and Wilke (5), Eq. (X) is closely approximated by

$$f/2 = 0.0794\, R_s^{-0.25} \qquad \text{(Xa)}$$

in the range $1000 \leq R_s \leq 100{,}000$. Substitution of this value of $f/2$ in an equation for mass transfer similar to Eq. (IX) gave good agreement with experiment (5, 6).

For rough surfaces, Theodorsen and Regier (9) find $\sqrt{f/2}$ to be a function of relative roughness and independent of R_s once a critical value of R_s is exceeded[5]

$$\frac{1}{\sqrt{f/2}} = 1.25 + 5.76 \log (d/\epsilon) \qquad \text{(XI)}$$

where d is the diameter of the cylinder and ϵ the height of surface irregularities.[6] The value of ϵ at which relation (XI) holds is given by

$$\epsilon/L \geq 3.3$$

where L is the friction length

$$L = \nu/V_* = \nu/\sqrt{\tau_w/\rho}$$

with V_* the friction velocity, τ_w the shear per unit area at the surface, and ρ the density.

But

$$d/L = R_s\sqrt{f/2}$$

and from (Xa)

$$d/L \cong 0.282\, R_s^{0.75}$$

At the lowest R_s used here (30,000) and with $d = 1.8$ cm

$$L \cong 3.55\,(d)\, R_s^{-0.75} \cong 1.0 \times 10^{-3}\ \text{cm}$$

If surface irregularities of height

$$\epsilon \geq 3.3\, L \geq 3.3 \times 10^{-3}\ \text{cm}$$

are present, the Chilton-Colburn analogy predicts a linear dependence on velocity since substitution in

$$k_H = \frac{k}{V} = \frac{f}{2}(Pr)^{-0.667}$$

of Theodorsen and Regier's value for $f/2$ gives

$$k = (1.25 + 5.76 \log [d/\epsilon])^{-2}\,(Pr)^{-0.667}\,V \qquad \text{(XII)}$$

Microscopic examination after polishing of the cylinders used here showed that, on the average, the height of surface irregularities was about 1×10^{-3} cm. Examination after a run revealed irregularities of height 5 to 15×10^{-3} cm. As shown below, it is probable that surface roughening occurs in the first minute of a run. Taking as an average height 10×10^{-3} cm, the value of $f/2$ is 0.00493 and[7]

$$k = 0.00493\,(Pr)^{-0.667}\,V \qquad \text{(XIIa)}$$

An accurate comparison of the present results with Eq. (XIIa) is not possible because reliable values for the diffusion coefficients are lacking. General agreement with Eq. (XIIa) was found using estimated values for the diffusion coefficients (Table III). It should be noted that the calculated

[5] This result refers to a "saturation" condition for the spacing of surface irregularities. In this case the drag coefficient remains constant and equal to its critical value. A saturation condition exists with specimens undergoing dissolution.

[6] A similar equation has been found by Nikuradse (19) from experiments with pipes.

[7] For $\epsilon = 5 \times 10^{-3}$ cm, $f/2 = 0.00392$, while for $\epsilon = 15 \times 10^{-3}$ cm, $f/2 = 0.00580$.

Table III. T = 30.0° ± 0.5°C

Depolarizer	Observed slope	$D \cdot 10^5$ (cm²/sec)	$(\nu/D)^{1/3}$ [1]	Calculated[2] slope
Ferric chloride	3.50×10^{-5}	3.5[3]	2.48×10^{5}	3.2×10^{-5}
Tolu-p-quinone	5.56×10^{-5}	7.0[4]	1.24×10^{5}	5.0×10^{-5}
Benzoquinone	6.39×10^{-5}	8.0[5]	1.09×10^{5}	5.5×10^{-5}

[1] Estimated from the data of King and Weidhenhammer (20). Since $D_{Fe^{+++}}$ depends on the HCl concentration, the estimate given may be in error appreciably.
[2] Estimated from the diffusion coefficient of hydroquinone.
[3] The value given is that for hydroquinone (21). The value for benzoquinone is probably less.
[4] The kinematic viscosity used (0.87×10^{-2} cm²/sec) is for 2*N* HCl solutions. The value of ν for solutions containing depolarizers at concentrations employed here is estimated to deviate less than 2% from this value.
[5] Calculated from Eq. (XIIa).

slopes in Table III are uncertain within rather wide limits.

Surface Roughness and Dissolution Rate

Figure 2 shows weight loss in 600 sec as a function of velocity. The linear increase of weight loss with velocity is contrary to expectation since it suggests that the velocity exponent in Eq. (V) is considerably greater than unity. Examination of the cylinders after each run showed that at the higher velocities, the surface had become exceedingly rough. Numerous elongated pits appeared. Their long dimension was approximately parallel to the axis of the cylinder and their width was about 1/30 to 1/40 their length. Their depth varied, but was generally of the order of tenths of a millimeter. It was apparent that during the run the surface area had increased greatly.

Surface irregularities, in addition to their effect on flow conditions discussed in the previous section, may alter both the (apparent) magnitude and the (apparent) velocity dependence of rate constants calculated with the aid of Eq. (I).

Surface irregularities of height comparable to the thickness of the laminar sublayer may change the effective surface area of the cylinder. In using Eq. (I) it was assumed that the cross-sectional area for diffusion was equal to the projected geometric area. This may not be true for hydrodynamically rough surfaces. Consequently, k's calculated from Eq. (I), which may be termed "apparent rate constants", may be numerically larger than the actual rate constants for rough surfaces.

The extent of surface roughening is, in general, a function of dissolution rate and of the metal specimen and its metallurgical history. If, therefore, in any given velocity and concentration interval, the extent of surface roughness increases with dissolution rate, the effective surface area may be a function of velocity, and the apparent dependence of k on velocity greater than expected from flow conditions alone.

In the velocity interval 150-550 cm/sec, and for the range of concentrations given in Table I, the specific rate constant was independent of initial depolarizer concentration, and, consequently, also independent of dissolution rate. The effective surface area was therefore constant and the surface roughness approximately the same in all cases. The surface roughening observed in this interval probably occurred in approximately the first minute of a run during which time the dissolution rate is greatest.

In general, it was found that for average dissolution rates (in 600 sec) less than 0.020 mg/sec/cm² of projected area, specific rate constants calculated from Eq. (I) were independent of initial depolarizer concentration. The opposite was true for rates greater than 0.025 to 0.030 mg/sec/cm² of projected area. It should be noted that at any given velocity, the average dissolution rate increases with concentration. Accordingly, in compiling Table I, the concentration ranges were restricted to values giving average dissolution rates less than the stated limiting value.

Experiments with roughened cylinders.—The rate of dissolution was determined as a function of time at the higher velocities by withdrawing small portions of the solution and analyzing for iron (Fig. 3). With initially polished cylinders, the specific rate constant, given by the slope of the log $x_i/(x_i - x)$ vs. t curve, increased continuously at small times and eventually became constant (curve 1, Fig. 3). If the

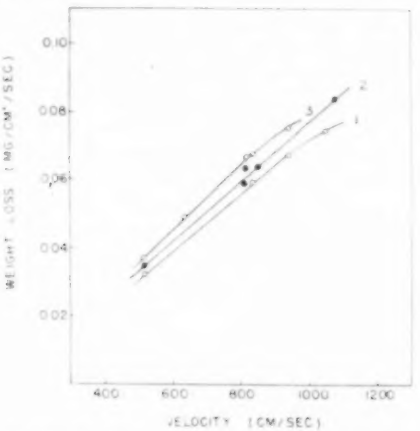

Fig. 2. Weight loss as a function of velocity: curve 1, 0.020M tolu-p-quinone; curve 2, 0.0431M ferric chloride; curve 3, 0.020M benzoquinone.

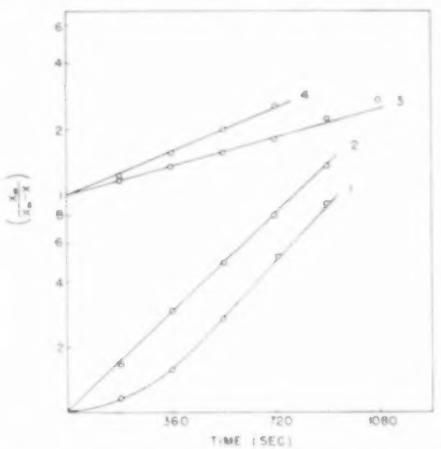

Fig. 3. First order kinetic plot with 0.0431M ferric chloride: curve 1, polished specimen, V = 820 cm/sec; curve 2, roughened specimen, V = 820 cm/sec; curve 3, roughened specimen, V = 200 cm/sec; curve 4, roughened specimen, V = 312 cm/sec. The log $x_i/(x_i - x)$ values have been corrected for volume changes during the run.

cylinder was used again without polishing, curve 2 was obtained. The slope was constant throughout the time interval studied and was equal to the slope of curve 1 at large times. It is apparent that in the former case the effective surface area increased during the course of the run until it attained a constant value. This value was not changed by repeating the run with the roughened cylinder.

Cylinders whose surface had been roughened by runs at 820 cm/sec in 0.0431M $FeCl_3$ were used without repolishing at smaller velocities. Curves 3 and 4 of Fig. 3 gave for the rate constants $k_{av} = 41.0 \times 10^{-3}$ cm/sec and $k_{av} = 61.5 \times 10^{-3}$ cm/sec. The value of k obtained with roughened cylinders at 820 cm/sec (curve 2, Fig. 3) was 140×10^{-3} cm/sec.

Effective surface area for dissolution.—In the velocity interval 150 to 550 cm/sec and for average dissolution rates less than 0.020 mg/sec/cm², observed values of k agree within 20% with those calculated from Eq. (XIIa) (*see* Table IV). It is evident, therefore, that the effective surface area for dissolution is, in this case, essentially equal to the projected surface area used in Eq. (I).

At high velocities and dissolution rates, the apparent values of k are larger than calculated, even after allowance is made for the increase in the friction coefficient because of increased roughness. From Eq. (XI) with $\epsilon = 0.05$ cm,

$$f/2 = 0.01$$

and from (XII)

$$k = 0.01\ (Pr)^{-0.6}\ V \qquad \text{(XIIb)}$$

Values of k calculated from (XIIb) are compared with observed values in Table IV. The observed (apparent) values are from 2.9 to 3.2 times larger than calculated from Eq. (XIIb). This result agrees with the authors' interpretation of the dissolution rate-time curves (Fig. 3).

The suggestion that with roughened specimens the effective surface area is larger than the projected area is not inconsistent with the physical interpretation of the hydrodynamic boundary layer. In Kármán's model (9), the thickness of the laminar sublayer is about $11.5(L)$. While irregularities of the order of $3(L)$ cause the friction coefficient to become independent of R_x, they do not change, apparently, the effective area for dissolution from that of a hydrodynamically smooth surface. Irregularities of height larger than $12(L)$ may alter however the effective surface area. The large apparent values of k observed with roughened cylinders indicate that, in this case, the ratio of the effective to the projected area is about 3.

Table IV. $C_{FeCl_3} = 0.0431M$

Velocity (cm/sec)	Polished cylinders k (obs) (cm/sec)	Polished cylinders k (calc)* (cm/sec)	Roughened cylinders k (obs) (cm/sec)	Roughened cylinders k (calc)** (cm/sec)
200	$8.2 \cdot 10^{-3}$	$6.4 \cdot 10^{-3}$	$41.0 \cdot 10^{-3}$	$12.8 \cdot 10^{-3}$
318	$12.5 \cdot 10^{-3}$	$10.2 \cdot 10^{-3}$	$61.5 \cdot 10^{-3}$	$20.5 \cdot 10^{-3}$
820	——	$(27.2 \cdot 10^{-3})$	$140 \cdot 10^{-3}$	$52.5 \cdot 10^{-3}$

* Calculated from Eq. (XIIa).
** Calculated from Eq. (XIIb).

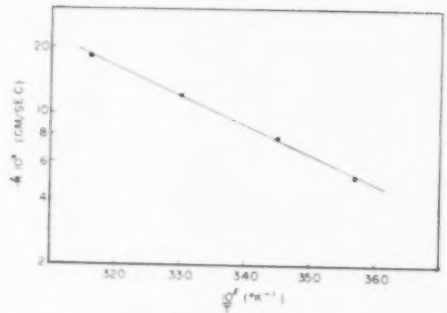

Fig. 4. The specific rate constant as a function of temperature. 0.0431M $FeCl_3$, $V = 312$ cm/sec.

Temperature Coefficient

Figure 4 shows the temperature dependence of the specific rate constant at 312 cm/sec in 0.0431M $FeCl_3$ solutions. The Arrhenius energy of activation is 6100 cal.

The observed temperature dependence is within the range expected for diffusion controlled reactions. It is in good agreement with the values 5500 cal ($V = 33$ cm/sec, 0.050M $FeCl_3$) and 6100 cal ($V = 167$ cm/sec, 0.025M $FeCl_3$) reported by Abramson and King (22).

Conclusions

1. The dependence of dissolution rate on stirring velocity, depolarizer concentration, and temperature indicates diffusion-controlled kinetics.
2. The specific reaction rate constant depends on the stirring velocity to a power close to unity. This is probably a result of the effect of surface irregularities on flow conditions near the surface.
3. When surface irregularities or height comparable to the thickness of the laminar sublayer are present, the effective surface area for dissolution may be larger than the projected geometric area.

Acknowledgment

The authors thank N. Komodromos and J. J. Bordeaux for carrying out some of the measurements given in Table I. The authors also gratefully acknowledge financial assistance from the Office of Ordnance Research under contract DA 23-072-ORD-216 and the Office of Naval Research under contract Nonr-375 (02).

Manuscript received Jan. 9, 1957. This paper was prepared for delivery before the Pittsburgh Meeting, Oct. 9-13, 1955.

Any discussion of this paper will appear in a Discussion Section to be published in the December 1958 JOURNAL.

REFERENCES

1. A. C. Makrides, N. Komodromos, and N. Hackerman, *This Journal*, **102**, 363 (1955).
2. L. Prandtl, "Essentials of Fluid Dynamics," Hafner Publishing Co., New York (1952).
3. C. V. King and W. H. Catchart, *J. Am. Chem. Soc.*, **59**, 63 (1937); C. V. King and P. L. Howard, *Ind. Eng. Chem.*, **29**, 75 (1937).
4. J. N. Agar, *Disc. Faraday Soc.*, **1**, 26 (1947).
5. M. Eisenberg, C. W. Tobias, and C. R. Wilke, *Chem. Eng. Progr.*, **51**, [16] (1955).
6. M. Eisenberg, C. W. Tobias, and C. R. Wilke, *This Journal*, **101**, 306 (1954).

7. D. A. Frank-Kamenitskii, "Diffusion and Heat Exchange in Chemical Kinetics," Princeton University Press, Princeton (1955).
8. B. Roald and W. Beck, *This Journal*, **98**, 277 (1951).
9. T. Theodorsen and A. Regier, *Nat. Advisory Comm. Aeronaut., Rept* **793** (1944).
10. G. I. Taylor, *Proc. Roy. Soc. (London)*, **A151**, 494 (1935).
11. "Fluid Dynamics," S. Goldstein, Editor, Vol. II, p. 650—4, Oxford Press (1938).
12. Pai Shih-I, *Nat. Advisory Comm. Aeronaut., Tech. Note* **892** (1943).
13. O. Reynolds, *Proc. Manchester Lit. and Phil. Soc.*, **14**, 7 (1874).
14. L. Prandtl, *Physik. Z.*, **29**, 487 (1928).
15. G. I. Taylor, *Aeronaut. Res. Comm., Reports and Memoranda*, No. 272 (1919).
16. T. von Kármán, *Proc. 4th Intern. Congress for Applied Mechanics*, p. 77, Cambridge (1934).
17. A. P. Colburn, *Trans. Am. Inst. Chem. Engrs.*, **29**, 174 (1933).
18. T. H. Chilton and A. P. Colburn, *Ind. Eng. Chem.*, **26**, 174 (1933).
19. J. Nikuradse, *Ver. deutsch. Ing., Forschungsheft*, 361 (1933).
20. C. V. King and L. Weidenhammer, *J. Am. Chem. Soc.*, **58**, 602 (1936).
21. International Critical Tables, Vol. V, 70 (1929).
22. M. B. Abramson and C. V. King, *J. Am. Chem. Soc.*, **61**, 2290 (1939).

Anodic Polarization of Titanium in Nonaqueous Base Etching Solutions

Morris Eisenberg[1] and Robert E. DeLaRue

Stanford Research Institute, Menlo Park, California

ABSTRACT

Results of systematic studies of the anodic polarization of titanium in essentially nonaqueous electrolytic etching baths of hydrogen fluoride are described. Solvents included ethylene glycol, dioxane, and tetrahydrofuran. A direct method using nickel reference electrodes was employed. The studies covered a current density range from 0 to 100 ma/cm^2 at temperatures ranging from 25° to 65°C. Plots of current density vs. net anode polarization show an interesting rapid rise of the polarization (by an incremental change ranging from 1.3 to 4.1 v) at a "critical" current density whose value depends on bath composition and temperature. The critical current density, which varied from 6.5 to 15 ma/cm^2 (when working with ascending current densities), has been found, in the course of experiments designed to test the applicability of Faraday's law, to correspond to a point at which chemical (local action) attack by the hydrofluoric acid is essentially eliminated and the linear rate of anode dissolution corresponds to the requirements of Faraday's law.

For a completely nonaqueous solution (including both HF and H_2SO_4) a cathodic polarization curve was also determined. A linear relationship between the polarization and the current density was found and interpreted to be due both to the dissolution of the titanium cathode and to the hydrogen discharge process.

For each of the six solutions studied, the parameter $L/k\ (dE/dI)$ was evaluated and compared with the observed nonuniformity of the etching as manifested by electropolishing in areas of high current density. This parameter was found to be a valuable criterion of the uniformity of current distribution only within the range of conditions at which a desirable anodic process can take place. Anodic polarization and dissolution rate studies offer a valuable method for determination of the optimum conditions for anodic etching of titanium without causing hydrogen embrittlement.

In studies of electrodeposition of protective coatings of Cu and Ni on Ti and Zr, it has been found that the usual methods for removal of the oxide film do not necessarily assure satisfactory adhesion of the coatings to the underlying substrate. Furthermore, the cohesive forces between Ti and coatings of Cu or Ni cannot be expected to be large in view of the different crystal structures of the metals involved. The room temperature stable phase of Ti (alpha) has a hexagonal, close-packed structure with lattice constants $a = 3.228$Å and $c = 5.120$Å. On the other hand, Cu and Ni have face-centered cubic structures with lattice constants of 3.608Å and 3.517Å, respectively. To obtain an acceptable adherence, Colner, Feinleib, and Reding (1) found it necessary to produce electrolytically a pocket-type roughening of the Ti surface in order to assure a mechanical bonding by means of keying and anchoring of the deposit on the Ti substrate. On this basis an essentially mechanical "as-plated" adhesion was sought. Hydrofluoric acid solutions proved necessary for electrolytic etching, and to reduce the local action of the bath Colner and co-workers had to resort to essentially nonaqueous baths with small amounts of water added to increase the d-c conductivity of the

[1] Present address: Lockheed MSD, Palo Alto, California.

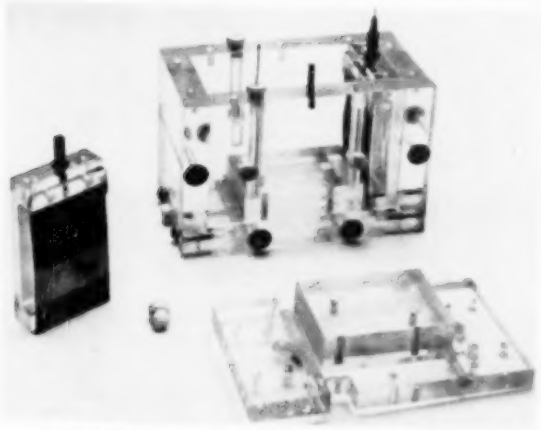

Fig. 1. Cell and electrodes for polarization studies

bath. In ethylene glycol baths containing as little as 6% water, they still found that local action persisted up to current densities of 18 ma/cm². From this point on, a rate of dissolution linear with increasing current was observed.

Earlier work in this laboratory on problems of preparation of Ti surfaces for electrodeposition by means of anodic etching has pointed toward difficulties in obtaining adhesion and toward a necessity for elucidating the mechanism of the anodic etching. It was expected that a study of this mechanism would yield valuable information relating to the optimum conditions for obtaining the type of surface etching most desirable for electrodeposition purposes.

A systematic study was initiated of the anodic polarization of Ti in essentially nonaqueous baths employing ethylene glycol, p-dioxane, and tetrahydrofuran.

Experimental Studies and Results

A Lucite cell was constructed with suitable electrode assemblies designed to allow accurate determination of the polarization of single electrodes as a function of applied current density, without polarizing the reference electrodes (Fig. 1). The reference electrodes were built into the walls of the cell and connected to the main compartment by means of small capillary openings. Nickel wires were found to be quite suitable as reference electrodes. Two were used in the cell walls near the Ti anode and a Ni cathode of the same size was placed parallel to the anode in the cell. Titanium metal Ti 75A[1] cleaned by mechanical abrasion and degreasing was employed throughout these experiments. The electrodes were mounted in special Lucite holders (Fig. 1), and were insulated on the back side by means of epoxy resins. They had an exposed surface area of 50 cm². The cell was thermostated in a large bath. A stirrer with a constant speed of 415 rpm was employed between the cathode and the anode throughout all experiments. Sometimes it was necessary to employ a Ni cathode, which was perforated to facilitate a better heat transfer through the cell when an additional stirrer was placed behind it. This was necessary because in the dissolution of Ti, the anodic

[1] Supplied by Titanium Metals Corporation.

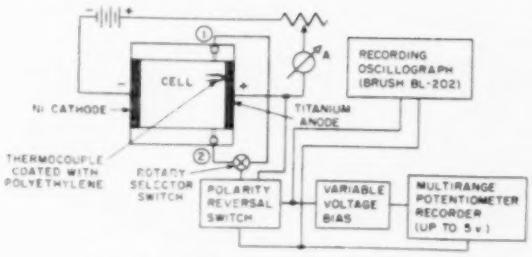

Fig. 2. Schematic diagram of cell and circuit

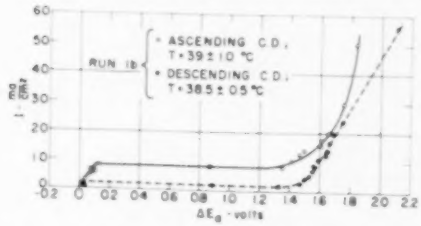

Fig. 3. Net polarization of Ti anode (Ti 75A) as a function of apparent c.d. Solution D-4: 11.9% HF, 6.6% H_2O, 81.5% ethylene glycol

reaction is highly irreversible, with an estimated free energy for reaction of −109 kcal/mole (for the formation of the TiF_6^{-2} ion). The circuit is shown in Fig. 2. By means of a rotary switch it was possible to measure the anode potential vs. reference 1 and also vs. reference 2 successively twice a minute. A variable voltage bias was employed, when necessary, to measure potentials over 5 v. A specially designed multirange potentiometer recorded simultaneously the potentials of a Ti anode against both references and thus provided the basis for calculation of the iR-drop between reference 1 and the anode according to the direct method (2). In addition, a recording oscillograph (Brush BL202) was employed to record rapid potential changes. A small iron-constantan thermocouple with a thin coating of polyethylene was placed in the vicinity of the anode, thus permitting temperature measurements to be made.

The resulting data were used to calculate the net anode polarization, i.e., the departure of anode potential at various set current densities from the zero current potential determined prior to the experiment. Figure 3 shows a typical plot.

Essentially nonaqueous solutions of HF in ethylene glycol were used. The solutions were prepared from a base of pure ethylene glycol in which gaseous HF had been dissolved. Water was added as desired to a maximum content of 10 wt %. The glycol base assured low chemical attack of the Ti by the electrolyte; the water improved the d-c conductivity of the bath. In one case, however, an entirely nonaqueous solution was used successfully with an H_2SO_4 addition serving to improve conductivity. The compositions of all solutions employed are given in Table II.

Polarization runs were carried out with both successively increasing and successively decreasing current densities. Slight changes in the anode potential occurred after each current setting, and within a

Table II. Compositions and Properties of Etching Solutions

	D-4	D-8	K-2	M-5	K-6	N-1
1. Composition:						
% HF	11.9	18.0	11.5	12.0	11.0	15
% KF	—	—	—	—	0.5	—
% H_2O	6.6	6.2	6.2	10.0	6.2	—
% H_2SO_4	—	—	—	—	—	15
% Dioxane	—	—	—	15.0	—	—
% THF	—	—	15.0	—	15	—
(Balance ethylene glycol)						
2. Rate of chem. dissolution at 55°C at no current (415 rpm) $\frac{\text{moles}}{\text{cm}^2\,\text{sec}} \times 10^7$	1.35 1.39	1.81 1.90	1.80 1.87	1.01 1.10	0.0348	0.0157
C.d. at min. anode losses ma/cm²	10.5	5.0	12.0	5.0	—	—
n average (in Faraday's Law)	3.11	3.29	3.50	3.63	3.68	3.73
3. Min. rate of loss by chem. dissolution at 55°C (calc.) $\frac{\text{moles}}{\text{cm}^2\,\text{sec}} \times 10^7$	0.15	0.18	0.20	0.08	—	—

minute or two the values became constant. The rapid rise of potential on ascending current densities or drop in potential on descending current densities were investigated for each run by means of the Brush recording oscillograph. An example of this rise is given in Fig. 4, which shows that practically the entire change took place within about 10 sec. As shown in this figure, such a change could take place with an overshoot of as much as 0.1 v compared to the final value which occurred after an additional 30 sec. The current remained essentially constant during such a rise. In other cases, however, no such overshoot was observed, as shown in Fig. 5 in which solution M-5 containing 15% p-dioxane was employed. Here the bulk of the potential rise occurred within 25 sec. The entire change from the initial constant value to the final constant value rarely exceeded 60 sec. No attempt was made to replot the shape of these potential rise-time curves to the bath composition, as it is believed that the shape of these curves depends, among other factors, on the manner in which the particular applied current density was set.

It should be noted that the current density value at which the sudden potential rise occurred (from here on denoted as the critical c.d.) depended to a small extent on the experimental procedure. Thus in an auxiliary experiment it was found possible to obtain this potential rise at a c.d. somewhat below the one accepted as the critical c.d. However, the time it took to arrive at the rise of potential, as well as the time period for the rise itself, were quite long, in one case as long as 40 min. For this reason it was decided to accept arbitrarily as the critical c.d. the value at which the rise of potential took place within a period not exceeding 5 min after the setting of the

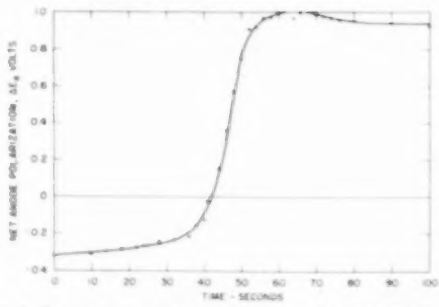

Fig. 4. Rise of net anode polarization of Ti (Ti 75A) at the breakthrough c.d. of 10.5 ma/cm². Solution D-4: 11.5% HF + 6.2% H_2O + glycol. Run 1a, T = 43° ± 1°C.

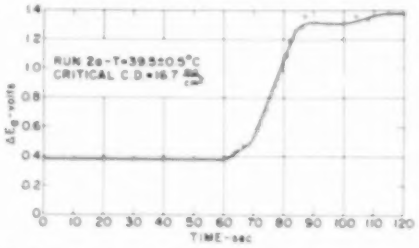

Fig. 5. Rise of net anode polarization of Ti (Ti 75A) at the "critical" c.d. of 16.7 ma/cm² (ascending c.d.'s). Solution M-5: 12% HF, 10% H_2O, 15% dioxane, 63% ethylene glycol.

current. This was justified by the fact that the potential rise usually took place quickly (within less than 1 min) when the critical c.d. was reached or exceeded. By applying small enough increments of current, particularly in the region at which the transition could be expected (on the basis of preliminary experiments), it was possible to determine the critical c.d. in a fairly reproducible manner. This can be seen, for instance, in Fig. 6, in which for a solution containing 18% HF the various branches of the polarization curves are well reproduced. An important feature of these curves is that the critical c.d. obtained with ascending current was always higher than the value obtained with descending currents. Another important feature is the dependence of the critical c.d. on the temperature, illustrated in Fig. 7 for three temperatures: 26°, 39.5°, and 55.5°C. With ascending currents, the corresponding critical c.d. values are 11, 17, and 32 ma/cm², respectively. The values of the critical c.d.'s obtained with descending

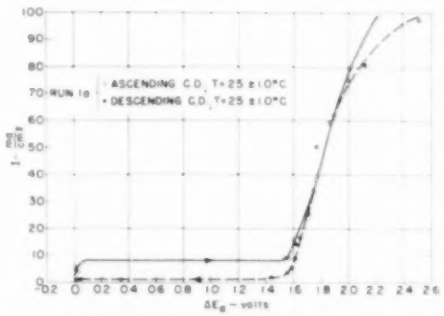

Fig. 6. Net polarization of Ti anode (Ti 75A) as function of apparent c.d. Solution D-8: 18% HF, 6.2% H_2O, 75.8% ethylene glycol.

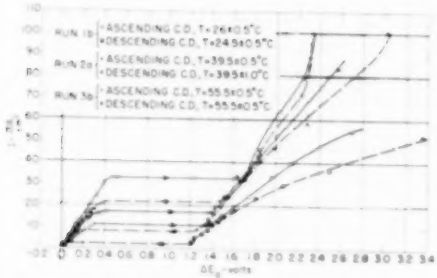

Fig. 7. Net polarization of Ti anode (Ti 75A) as function of apparent c.d. Solution M-5: 12% HF, 10% H_2O, 15% dioxane, 63% ethylene glycol.

applied currents are lower, but remain in approximately the same ratio. The critical c.d. increases generally with the chemical activity of the electrolyte, which depends on its acid and water content as well as the temperature of the bath. For instance, with solution K-2 a change from about 40° to about 55°C accounted for a rise in the critical c.d. (on ascending currents) from 8.5 to about 17 ma/cm².

In the initial phase of these studies, anodic polarization curves were taken up to very high c.d.'s with the result that anodic limiting current plateaus were obtained (usually in the region of 0.05-0.12 amp/cm² depending on the temperature and the solution). The upper part of Fig. 12 illustrates the achievement of such a limiting c.d. plateau at 0.078 amp/cm². Normally the anodic curves were not taken up to the limiting conditions.

Values of critical c.d.'s obtained with ascending and descending applied currents at various temperatures (in the range 25°-55°C) for the six electrolytes covered by this study are given in Table I.

As has already been reported (1), Ti undergoes chemical attack even in glycol solutions of HF when the applied current is too small. Under such conditions chemical etching takes place, resulting in a uniformly roughened surface. However, as pointed out previously, in preparing Ti for electrodeposition purposes a deep pocket-type roughening is desirable. This could be achieved only by electrolytic etching in low-activity, essentially nonaqueous, baths of composition representing a compromise between a desirable low chemical activity and satisfactory d-c conductivity. In such baths Colner and co-workers (1) found it necessary to apply a certain minimum c.d. to suppress the desirable chemical action. This minimum current increased with acid concentration of the bath, its water content, and temperature.

Since the critical c.d.'s obtained from anodic polarization curves showed a similar dependence on temperature and acid concentration it was suggested that these critical c.d.'s are related or equal to the current values required for suppressing local action by chemical attack.

It was thought that studies of the rate of metal dissolution as a function of applied c.d. (with particular attention to the low c.d. range) would lead to the determination of the minimum current required to stop chemical attack as the point beyond which the metal dissolution proceeds according to a

Table I. Critical Current Densities

Solution	Run No.	Critical c.d. Ascending	Critical c.d. Descending	Temperature Ascending	Temperature Descending
		ma/cm²		°C	
D-4	1a	6.89	1.78	41	43
	1b	8.14	1.40	39	38.5
	2a	13.7	3.65	53.5	55
	2b	14.9	3.66	54.5	56
D-8	1a	8.83	0.87	25	25
	1b	8.88	0.65	25	25
	2a	16.6	3.76	55	54.5
	2b	20.2	3.79	55.5	54
K-2	1a	8.60	2.82	40.5	43.5
	1b	8.60	2.79	40.5	42.5
	2a	14.80	4.45	55.5	55
	2b	17.20	4.39	57	55.5
M-5	1a	10.3	1.81	25.5	25.5
	1b	11.5	1.91	26	24.5
	2a	16.7	7.17	39.5	39.5
	2b	20.2	7.43	40	39
	3a	27.2	18.2	55	55
	3b	32.7	17.8	55.5	55.5
K-6	1a	0.033 (15 min*)	0.061	25	25
	2a	0.105 (20 min)	2.76 (14 min)	55	54
N-1	1a	0.028 (18 min)	0.004 (21 min)	23	24
	2a	1.61**	1.25	53	55
	2b	0.925-0.687	—	49.5	—
	2c	0.924-0.656	—	49	—

* Potential transition usually occurred within 150 sec or less. Whenever longer time periods were involved, these are indicated in parentheses.

** This transition required only 53 sec, obviously due to the overrun over the Run 1a current density value. This underscores the importance of relating the critical c.d. to the transition time.

linear Faradaic relationship. With this in mind additional experiments were undertaken in which Ti anodes were subjected to a constant current at a given temperature and for periods ranging from 10 to 20 min. From the resulting weight losses and the known number of coulombs passed, a check on the applicability of Faraday's law was carried out for the six solutions employed in these studies (*see* Table II). The results for solution D-4, containing 11.9% HF, are shown in Fig. 8 in the form of a plot of the rate of dissolution in moles/cm²/sec against the applied c.d. Each point in this plot represents a separate experiment with a new Ti anode. The rate of metal dissolution by local chemical action, which takes place with liberation of hydrogen, gradually

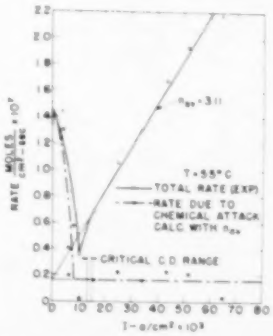

Fig. 8. Rate of Ti anode dissolution vs. c.d. Solution D-4: 11.9% HF, 6.6% H_2O, 81.5% ethylene glycol.

decreases until a minimum is reached at a value of 10 ma/cm². From then on the rate of Ti dissolution follows a linear law increasing with the applied c.d. along a straight line with a slope corresponding to an average number of 3.11 equivalents in Faraday's law. With the value of this slope one can calculate the amount of Ti that should have dissolved if no other process but the anodic dissolution took place. Extrapolation of the straight line portion to the zero current axis gives the value of the residual chemical attack which still persists after the anodic dissolution essentially becomes the major mechanism. The results of such calculations are shown at the bottom of Table II. Using the correction for residual chemical attack, the net total chemical rate can be calculated (as shown in Fig. 8 by a dashed line) with the assumption that the residual chemical rate remains constant once the Ti is anodically polarized. The validity of this assumption is subject to some dispute.

For comparison the range of critical c.d. values obtained with the same solution at the same temperature (55°C) is indicated in Fig. 8. These values generally coincide with the c.d.'s at which the anodic electrochemical dissolution becomes the predominant reaction.

Sometimes (see Fig. 9 and 10), the critical c.d. values, derived from polarization runs, were larger than the c.d. at which reversal in the rate of dissolution curve occurred. Such deviations were due to the different techniques used in the two types of experiments. In the study of dissolution rates, a new specimen was used for each point; however, a single anode was employed in a polarization run with the result that the surface of the anode was already roughened when the critical c.d. point was reached. If, as it happened in some runs, the roughening significantly increased the true anode surface area, the observed (apparent) critical c.d. values were larger than normal.

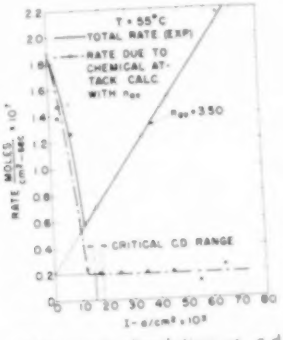

Fig. 9. Rate of Ti anode dissolution vs. c.d. Solution K-2. 11.5% HF, 6.2% H_2O, 15% tetrahydrofuran, 67.3% ethylene glycol.

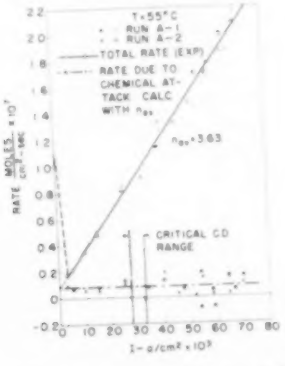

Fig. 10. Rate of Ti anode dissolution vs. c.d. Solution M-5. 12% HF, 10% H_2O, 15% dioxane, 63% ethylene glycol.

The experimental value of 3.11 Faradays per mole of metal, shown in Fig. 8, suggests that Ti dissolves in the form of two ions, the +3 and the +4 titanium ions. It is believed that both of these ions complex readily in solution, forming primarily TiF_6^{-2} and TiF_6^{-3}. Since the solutions employed in these experiments were essentially saturated with air, all Ti would eventually be oxidized to the +4 state. Indeed, preliminary polarographic studies gave only reduction waves for solution samples taken near the anode at the end of a run, thus indicating the presence of reducible species. Reduction potentials of approximately 0.44 v (half-wave potential vs. the mercury pool) were obtained with diffusion currents suggesting Ti^{+4} concentrations ranging from 3 to 8 millimoles per liter. Reduction of Ti^{+3} would require much higher potentials.

It should not be surprising that Ti can dissolve simultaneously in the +3 and the +4 state. If the values for standard potentials in aqueous solutions given by Latimer (3) can be used as an approximation, one finds that the oxidation potential for the formation of the TiF_6^{-2} ion is 1.19 v and that of the Ti^{+3} (and probably of TiF_6^{-3}) formation would be 1.21 v. While these values do not apply directly to the systems employed, they give a fair approximation of the free energy and standard potential relationships that might be involved in the two dissolution reactions. On this basis it can be expected that the actual electrode potentials at which Ti can go into solution in either ionic form are fairly close and the two processes occur simultaneously.

As mentioned above, the extension of the linear portion of the anode dissolution curve to intersection with the zero current intercept should indicate the value of the minimum rate of chemical attack on Ti that still persists, at least at this transition point. In the calculation used for Fig. 8 through 11 this minimum value was assumed to apply throughout up to high c.d.'s. A value of 3.50 Faradays/mole (see Fig. 9) would indicate that half of the Ti dissolves in the +3 and the other half in the +4 state. However, if with increasing c.d. this minimum rate of chemical attack should in reality still decrease, then the actual slope of the line (from which n is calculated) as plotted in Fig. 9 or 10 would increase and therefore would decrease the number of Faradays/mole in the direction of the value of 3.0. It can thus be safely said that in most of the cases studied at least half of the Ti went into solution in the +3 state rather than in the +4 state. Attempts to carry out calculations with the assumption that the +2 state is favored showed the latter reaction to be improbable. The standard oxidation potential estimated by Latimer for the formation of the +2 ion is larger

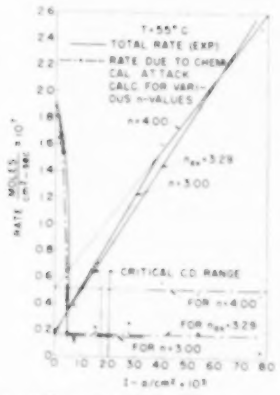

Fig. 11. Rate of Ti anode dissolution vs. c.d. Solution D-8: 18% HF, 6.2% H_2O, 75.8% ethylene glycol.

than for the other ions, namely, about 1.63 v. Figure 10 shows results of similar calculations performed for solution M-5, in which two sets of runs are given; the general agreement is found to be quite satisfactory. It should be noted, however, that in this case the c.d. at which inversion of the rate took place was significantly lower than the critical c.d. range determined through the polarization measurements. A similar discrepancy is shown in Fig. 11 for solution D-8.

It is interesting to note that in all cases (for a given solution and temperature) the critical c.d. values were larger than the c.d. at which the inversion of the dissolution rate occurred.

While these discrepancies cannot be accounted for quantitatively, a satisfactory qualitative explanation becomes available when the difference in the procedures in the two types of experiments is considered. In the dissolution rate vs. c.d. studies, a fixed total current was applied to a new, smooth Ti anode and kept constant. Each point on the plot represents a separate specimen. The apparent c.d. value for inversion in the rate found from such a plot is thus fairly close to that of the true c.d. On the other hand, in the polarization experiments complete curves were taken on one anode, which thus underwent progressive suface roughening (to a major or minor extent depending on the number of coulombs passed) with the result that the measured apparent c.d. values were significantly larger than the true current densities. Thus the observed critical (apparent) c.d. value was also larger than the value one would expect on a new, smooth Ti surface. The latter should obviously be smaller and coincide with the c.d. at which inversion of the rate takes place. The soundness of this explanation was confirmed when a polarization curve was taken with a fresh anode at which current was passed for a short time (compare Fig. 8).

For Solution D-8 (Fig. 11) in addition to the average value of n, slopes corresponding to $n = 3$ and $n = 4$ were found. This shows that in the lower c.d. range the +3 state is favored while at higher c.d.'s the +4 state is predominant.

Another problem investigated was whether a previous or simultaneous anodic treatment of a Ti specimen affects the rate of chemical dissolution itself. This was of interest because it was thought that passage of current removes the protective oxide from the Ti and facilitates the rate of chemical local action. Experiments carried out with specimens treated at 5-40 ma/cm² for 1 min and then left in the same electrolyte with no applied current for 10 min indicated that the rate of chemical action was essentially the same as the one obtained without any previous passage of current. Hence the chemical activity of the electrolytes is sufficiently large to remove any TiO_2 films which might interfere with the metal dissolution process.

In the solutions discussed above, small amounts of water were used to improve their conductivity. It was thought desirable to investigate the behavior of a completely anhydrous electrolyte in which H_2SO_4 (100%) (instead of the water) was used. The ethylene glycol solution of 15% HF and 15% H_2SO_4 (N-1 in Tables III and IV) was found to have the

Table III. Slope of Polarization Curves

Assuming straight line from critical c.d. value on:

Solution	Run No.	Ascending dE/dI volt cm²/a	Ascending Temp, °C	Descending dE/dI volt cm²/a	Descending Temp, °C
D-4	1a	12.1	41	12.6	43
	1b	10.5	39	11.1	38.5
	2a	0	53.5	1.78	55
	2b	0.7	54.5	0.024	56
D-8	1a	6.4	25	6.31	25
	1b	4.5	25	3.28	25
	2a	0	55	2.34	54.5
	2b	0.5	55.5	3.32	54
K-2	1a	6.3	40.5	8.00	43.5
	2a	2.9	55.5	1.11	55
	2b	2.4	57	1.78	55.5
M-5	1a	29.8	25.5	27.3	25.5
	1b	26.8	26	32.7	24.5
	2a	16.8	39.5	19.7	39.5
	2b	16.4	40	17.4	39
	3b	10.4	55.5	11.1	55.5
K-6	1a	33.7	25	35.7	25
	2a	7.37	55	11.9	54
N-1	1a	0	23	0	24
	2a	6.30	53	9.01	55
	2c	0	49	—	49

Table IV. Throwing Power in Etching Baths at 55°C

	D-4	D-8	K-2	M-5	K-6	N-1
Conductivity, k mhos/cm × 10³	4.42	10.7	3.8	6.32	17.9	235
$h_c = k \cdot dE/dI$, $\frac{\text{volt cm}}{\text{amp ohm}} \times 10^3$	1.72	2.70	8.2	99.8	132	740
Parameter: L/h_c (dimensionless) (L = width of electrode = 1.52 cm)	885	565	186	15.2	11.5	2.05
Dimension, a (average electropolished length near edges, i.e., high c.d. area), at applied average c.d. of 45 ma/cm², microns	270	225	50	115	—*	—**

* The value for this solution was excessively large and difficult to determine. The useful etching range was limited and the pit depths were low (up to 15 μ).

** Insufficient and non-uniform etching at 15-25 ma/cm². At 45 ma/cm² complete polishing occurred.

Fig. 12. Net anodic and cathodic polarization of Ti vs. apparent c.d. Solution N-1: 15% HF, 15% H_2SO_4, 70% ethylene glycol.

highest conductivity among the solutions studied (0.235 mhos/cm). Both cathodic and anodic polarization studies were carried out on Ti in this system, as shown in Fig. 12. Several interesting features can be noted. The anodic behavior was analogous to that in the other solutions except that Ti polarized much stronger (by about 4.1 v) already at a very low (critical) c.d. (less than 1 ma/cm^2). This agreed with the practical observations that Solution N-1 gave poor etching of the Ti anodes and tended to cause electropolishing at c.d. values as low as 20 ma/cm^2.

The cathodic polarization of Ti in Solution N-1 was remarkable because the usual logarithmic dependence on the c.d. (as called for by the Tafel equation) was not followed. Instead a perfectly linear relation was found between the cathodic polarization and the applied c.d. From the results shown in Fig. 12, the following relation for the net cathodic polarization is obtained.

$$\Delta E_c = 6\,I \qquad (I)$$

where ΔE_c = total net cathode polarization, volts, and I = current density, amp/cm^2. A similar straight line relationship, although with a different slope value, was observed by Straumanis and co-workers (4) in aqueous solutions of HF. In comparing the behavior of Ti in aqueous solutions of various acids they concluded that the linear dependence takes place if the cathodic metal, Ti, dissolves with hydrogen evolution in the HF acid solution, whereas a logarithmic relation is obtained if it does not dissolve, e.g., in HCl solutions, but behaves as a noble metal. In the nonaqueous solution (N-1) employed in the present study, in addition to the cathodic reduction of hydrogen ($H^+ \rightarrow \frac{1}{2}H_2$), the chemical dissolution of Ti takes place, due to the presence of HF ($Ti + 3H^+ \rightarrow Ti^{+++} + 3/2H_2$), as confirmed by observed weight losses of the electrode.

No cathodic polarization studies were carried out on the solutions containing a small amount of water; however, in view of the behavior of completely aqueous systems (4) and the results of the present study, it is reasonable to expect that linear cathodic polarization curves would result for all of the solutions employed in this study. The slopes of such curves may differ from case to case due to varying HF acid activities.

Discussion and Conclusions

The anodic behavior of Ti in essentially nonaqueous electrolytes is dominated by the presence of a "critical c.d."—a particular value of the apparent c.d. at which the incidental chemical attack of the metal by the electrolyte is suppressed and the anodic reaction becomes the controlling process. Values of the critical c.d. were found to be usually larger when obtained with ascending, than with descending, applied currents. This "hysteresis" can be explained, at least in part, by: (*a*) increased surface roughness, i.e., lowering of the true current density in the descending runs which followed the ascending runs; and (*b*) the natural tendency to overshoot the applied current in ascending runs and to undershoot in descending runs.

In general, the critical c.d. increased with temperature and the chemical activity of the bath. The latter increased with the content of HF and of water in the glycol base solutions. The combined effect of these two is to increase the thermodynamic activity of the acid in the solution and the rate of metal attack with the resulting evolution of hydrogen according to:

$$Ti + 3H^+ \rightarrow Ti^{+++} + 3/2H_2 \qquad (II)$$

This reaction involves a flow of electrons from the metal to the electrolyte and results in discharge of protons; it is thus essentially a cathodic process. When the critical c.d. value is reached the anodic dissolution of the metal becomes the dominant process according to either:

$$Ti \rightarrow Ti^{+++} + 3\bar{e} \qquad (IIIa)$$

or

$$Ti \rightarrow Ti^{++++} + 4\bar{e} \qquad (IIIb)^*$$

and the cathodic reaction (II) is then suppressed. Since reaction (II) involves evolution of atomic hydrogen capable of severe embrittlement of the Ti, the critical c.d. is also an important concept in practical consideration of anodic cleaning or etching of the metal.

The magnitude of the critical c.d. in anodic polarization runs can be considered a measure of the chemical activity of the bath. Comparison of critical c.d. with the compositions of Solutions D-4, D-8, and H-5 (Table II) indicates that an increase in water content (from about 6.4% to 10%) causes a

* The actual form of the metal ions is probably TiF_6^{-3} and TiF_6^{-2}.

much larger increase in critical c.d. values than results from an increase of the acid concentration. The presence of cyclic ethers such as dioxane and tetrahydrofuran apparently does not affect the chemical activity of the solutions.

The rapid potential shift at the critical c.d. represents the onset of the polarization of the Ti electrode associated with the normal electrochemical dissolution reaction. This rise in potential must therefore be clearly differentiated from limiting current plateaus which, incidentally, are rarely observed in such a form for anodic metal dissolution processes. In supplementary experiments it was found that by carrying out the reaction to large enough c.d.'s an actual plateau was obtained. The latter corresponded to the discharge of oxygen. However, such reactions could not be studied very satisfactorily because of the extreme amount of heat involved at very high c.d.'s and because of the difficulty of controlling the current and the temperature.

From the studies of the rate of metal dissolution with and without applied current, the rate was found to decrease from the zero current value to a minimum at a c.d. ($I_{m,i}$) close to the critical c.d. ($I_{c,i}$) obtained from anodic polarization studies in the same solution. From the $I_{m,i}$ value on the rate vs. c.d., plots follow a linear relationship according to Faraday's law. The slopes of the straight line portions correspond to values of n (number of equivalents/mole) ranging from 3.11 to 3.73 (Table II), thus indicating that the relative amounts of Ti^{+} and Ti^{++} formed through anode dissolution depend on the composition of the electrolyte.

Through extrapolation of the straight line portions of the rate vs. c.d. plots the minimum residual rates due to chemical attack (persisting simultaneously with the anodic dissolution) were estimated. These residual minimum rates were found to be, by an order of magnitude, smaller than the zero current rate (compare Table II). The persistence of a residual chemical attack rate and its value are important in determining the suitability of a given electrolyte for anodic treatment of Ti from the hydrogen embrittlement point of view.

Generally in electrolytic etching it is important to obtain as uniform a c.d. distribution as possible. Otherwise, in the high c.d. areas near edges and corners, electropolishing takes place while the central area of the specimen is at the optimum etching conditions. For this reason it was interesting to investigate how the various baths compare in respect to the uniformity of the secondary current distribution, i.e., throwing power. In a special set of experiments Ti specimens were etched at several c.d.'s in the various baths and examined metallographically in cross section. The extent of smoothing due to electropolishing near the edges was measured in terms of an electropolished length adjacent to the outer edge. These values are shown as dimension "a" in Table IV. As is known (5, 6) the throwing power of a bath can be best described in terms of a dimensionless parameter (L/h_c) which represents a ratio of a characteristic length dimension over the product of the conductivity and the slope of the polarization with respect to the applied current. Using the slope values from Table III the values of the dimensionless parameter were calculated at 55°C for the six solutions under study and compared with the measured electropolished length "a". Inspection shows that with decreasing value of the parameter the electropolished length "a" diminishes as the theory would require. Strictly speaking, throwing power should be evaluated experimentally by means of the Haring method or according to the method of sectioned electrodes (7). However, when out of practical considerations one is concerned with a uniform etching of the surface, direct observation and measurement provide a satisfactory way for correlating uniformity of etching with theory and for determining the suitability of a given etching bath.

The criterion that the parameter, L/h_c, should be at a minimum for optimum throwing power cannot be used, of course, without limitations. In some solutions, it is possible to obtain a fairly good secondary current distribution (and low values of L/h_c) without a satisfactory etching. Thus Solutions M-5, K-6, and N-1, which showed the lowest values of L/h_c (*see* Table IV) tended to cause electropolishing even at c.d.'s below 45 ma/cm² (in most cases, dimension "a" could not even be determined). Of the entire group, Solution K-2 was definitely the most suitable for etching purposes on the basis of the most uniform and deep surface roughening. However, Solutions K-6 and N-1 (of low parameter values) were not suitable for etching at all. This demonstrates that the magnitude of the parameter L/h_c is primarily a criterion of the uniformity of the secondary c.d. in a cell and by itself is not sufficient to determine the suitability of a given solution for a desirable anodic process. Its usefulness for prediction of throwing power is thus limited to a range of conditions within which the desirable electrode processes can take place.

The anodic polarization studies for Ti in essentially nonaqueous solutions, coupled with rate studies as a function of c.d., represent a reliable method for determination of the suitability of an electrolyte and of the optimum operational conditions, e.g., temperature and c.d., for anodic etching of Ti without causing a deterimental hydrogen embrittlement of the metal.

Manuscript received July 16, 1956. This paper was prepared for delivery before the Cincinnati Meeting, May 1-5, 1955.

Any discussion of this paper will appear in a Discussion Section to be published in the December 1958 JOURNAL.

REFERENCES

1. W. H. Colner, M. Feinleib, and J. N. Reding, *This Journal*, **100**, 485 (1953).
2. M. Eisenberg, C. W. Tobias, and C. R. Wilke, *ibid.*, **102**, 415 (1955).
3. W. M. Latimer, "Oxidation Potentials," 2nd ed., p. 269, Prentice Hall, New York (1952).
4. M. E. Straumanis, S. T. Shih, and A. W. Schlechten, *J. Phys. Chem.*, **59**, 317 (1955).
5. C. Wagner, *This Journal*, **98**, 116 (1951).
6. T. P. Hoar and J. N. Agar, *Disc. Faraday Soc.*, **1**, 162 (1947).
7. E. Mantzell, *Z. Elektrochem.*, **39**, 10 (1935).

Technical Note

Junction Delineation in Silicon by Gold Chemiplating

S. J. Silverman and D. R. Benn

Allentown Laboratory, Bell Telephone Laboratories, Inc., Allentown, Pennsylvania

In recent years there has been an increased demand for a simple, straightforward technique to analyze junctions in Si. These junctions may occur as an uncontrolled series of striations during the growth of single crystals for raw material evaluations. They may also be created purposely by doping during growth or by alloy or diffusion processes on wafers. In the first case one may wish to determine qualitatively the degree of homogeneity in the single crystal. This observation can be used to appraise the extent of removal of N-type impurities by observing a cross-sectioned single crystal after refining the raw material. In the other two cases junction depths may be measured and the degree of planarity examined.

Several methods have been used for this type of analysis. Originally one used finely divided particles of $BaTiO_3$ (1) which concentrated along a junction barrier under the influence of an external electric field. A second procedure, highly successful in Ge, has been copper electroplating using a pulsed field in an appropriate electrolytic solution of $CuSO_4$ (2). A third process, perfected by Fuller (3), involves staining of the surface using a suitable combination of HNO_3 and HF. A preferential oxidation stains the P-type region darker than the N-type. The gold chemiplating technique is analogous to the Fuller stain. It is believed that this plating action in the vicinity of the junction is accomplished by preferential reduction, gold first appearing on the N-type region relative to a P region. The advantages of this technique lie in the relative simplicity of sample preparation and subsequent processing. The resultant pattern shows excellent definition enabling one to detect junctions readily.

Originally, Au chemiplating was used in making ohmic contacts on Si diodes. A discussion of this process is given in detail by Pudvin (4). During the course of plating disks prior to device fabrication, it was noticed that initially Au did not plate uniformly. This observation prompted a more complete investigation, the results of which are herein described.

Experimental

The sample is prepared by lapping with 600 mesh carborundum powder, rinsing well with deionized water, and drying quickly with an air blast. It is then immersed in the plating solution. Care is taken not to contaminate the surface during handling; otherwise, spurious patterns may develop. The following plating solution is identical to that described by Pudvin (5): (*a*) 10 g $KAu(CN)_2$ (67% Au content); (*b*) 200 g KOH; (*c*) deionized H_2O for one liter of solution.

In order to obtain reproducible results, both heat and light are necessary. This requirement is easily satisfied by using an infrared lamp. A solution temperature range of 30°-70°C is desirable, depending on the type of junction. The reaction is seriously hampered by the precipitation of KOH at temperatures below 5°C. Those junctions having a less pronounced change in the net impurity concentration, $|N_D - N_A|$, across the junction require higher temperatures and longer exposure times in the solution. After the pattern shows sufficient definition the chemical action is stopped by removing the sample from the bath. It is rinsed immediately with tap water and dried with an air blast.

Various surfaces have been examined for the production of an optimum pattern. Attempts to plate an etched surface have been unsuccessful in that the resulting deposit is neither reproducible nor adherent. Although sharply defined striations appeared, the color contrast is decreased and the pattern is easily obliterated by additional Au which soon plates the surface indiscriminately. A delicately adherent film, however, can be plated on a Linde A polished surface. It is felt that this type of surface preparation is more desirable when investigating thin junction depths of the order of 0.5 mil because of better resolution under a microscope. Such a smoothly abraded surface requires a longer plating time than a coarse one. For purposes of rapid, reproducible analyses, however, 600 mesh carborundum powder is satisfactory. Figure 1 shows individual striations whose widths have been measured to be about 1 mil on a single crystal lapped in the latter manner.

Mechanism

The over-all process may be classified as a displacement reaction described by the following reaction:

$$2KAu(CN)_2 + 4KOH + Si \rightarrow 2Au + K_2SiO_3 + 4KCN + H_2 + H_2O$$

Although the electrochemical action causes Au to plate on a Si surface according to this equation, it is

Fig. 1. Striations in a single-crystal cross section

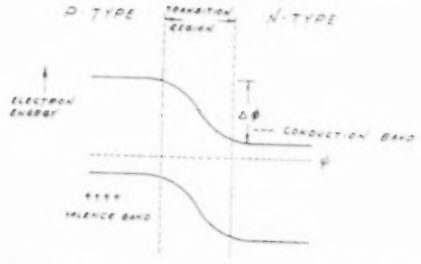

Fig. 2. Potential distribution in a typical PN junction

only in the presence of light that one can obtain consistently predictable results in which the Au plates first on the more negative side of a junction (6). A brief explanation of the possible mechanism responsible for this phenomenon is presented.

If one considers the simplified energy diagram of a typical P-N junction, one notes the potential difference associated with the difference in carrier concentration on either side, as indicated in Fig. 2. Psi represents the Fermi level and $\Delta\phi$ is the change in electron energy when going from the N region to the P. Neglecting possible complications due to surface states, one can, by the following equation, represent $\Delta\phi$ as a function of p and n, where p is the density of excess holes in the P region; n is the density of excess electrons in the N region; and n_i represents the density of intrinsic carriers.

$$\Delta\phi = \phi_n - \phi_p = \frac{KT}{q} \ln \frac{pn}{n_i^2}$$

This equation then represents conditions in the vicinity of the junction which satisfy requirements of thermal equilibrium and charge neutrality throughout the specimen.

If, now, one shines light on the junction, hole-electron pairs are created. The minority carriers in either region diffuse across the transition region under the influence of the built-in field created by $\Delta\phi$. A photovoltage then is created on the surface near the junction. Positive Au ions resulting from dissociation of the $Au(CN)_2^-$ complex in the solution above the surface are attracted to the more negative region and plate on the N side. The photovoltage is more pronounced the greater the potential difference across the junction. It has been observed that the rate of plating increases with this difference; the greater the concentration of excess carriers in the P and N regions, respectively, the faster the Au plates onto the more negative region.

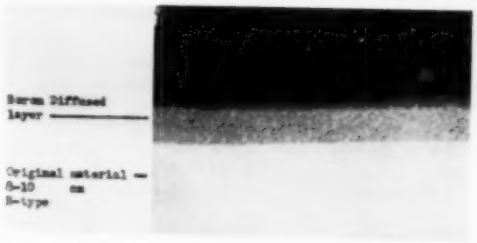

Fig. 3. NP^+ junction. Magnification 30X before reduction for publication.

In order to approximate conditions wherein one could vary the deposition rate with the potential difference across a junction, several single conductivity crystals with different N-type concentrations were prepared. These were measured by standard two-probe resistivity techniques, cut into samples of equal size, and diffused simultaneously with the same amount of P^+ type (boron) diffusant to form the junctions ($^+$ denotes the high concentration in the diffused layer). After diffusion the specimens were prepared by the previously described experimental procedure and simultaneously immersed in the plating solution. Figure 3 is a typical example of an NP^+ junction. Measurements were made of the average times required for the Au to become sufficiently thick that the junction became delineated. Table I shows that those specimens with the higher N-type concentration and, hence, the larger potential difference across the junction exhibited the faster deposition rate.

An additional experiment illustrated the effect of the potential difference of the junction on the deposition rate. Part of a grown NP junction was cut in half. The N region and the P region were separated and then immersed in the plating solution together with the original junction. The plating times were observed as follows: (a) the N region of the junction, 30 sec; (b) the isolated N region, 4 min; (c) the isolated P region, 7 min; (d) and the P region of the junction, 40 min. These results indicated that, although one can plate Au on any Si surface, the presence of a junction can be detected more rapidly, thus making this technique a very positive method of junction delineation.

Table II is a summary of the relative ease in getting positive results for various types of junctions. It can be seen that this technique is applicable to all types of junctions with varying degrees of suc-

Table I. A comparison of plating times for the same junction types

Group	Specimen	Cond. type	N_D-N_A in at./cc	Junction type	Avg. plating time, min
I	A	N	1.1×10^{15}	NP^+	3.8
	B	N	5.2×10^{15}	NP^+	1.8
II	C	N	1.6×10^{15}	NP^+	5.8
	D	N	5.8×10^{15}	NP^+	2.4

Table II. A comparison of the plating times for different junction types

Junction type	Avg. plating time, min	Reproducibility
PN	6	Excellent
$PN^{\cdot}$	6	Excellent
$NP^{\cdot}$	6	Excellent
$PN^{\cdot}P^{\cdot}$	7	Good
$PP^{\cdot}$	20	Good
$NP^{\cdot}N^{\cdot}$	120	Fair
$NN^{\cdot}$	10	Questionable

cess. The reason for the poor reproducibility on $NN^{\cdot}$ is not known. It is possible that surface states so alter the potential difference as to render the effect undetectable.

When one attempts to duplicate these general observations at the same temperature without exposing the samples to the light source, the results are not reproducible. A simple experiment was devised to compare the plating action on a given junction in the light and then in the dark. The same specimens were immersed for equal times in the same plating solution, first in the light and then in the dark. In the light Au always deposited on the more negative regions first. In the dark, however, several of the previously examined junctions plated in the opposite manner, on the P-type regions first; whereas, on the other surfaces Au plating was randomized. Therefore, it has been concluded that the photovoltaic effect is essential to obtain results that can be predicted reliably from theory.

Examination of the foregoing results leads one to suggest that Au chemiplating, essentially a reduction process, complements the Fuller etch (3), an oxidation process. Whereas Pudvin (4) has adequately described the chemistry for Au chemiplating in the dark, the present study offers a model to explain the reaction in the presence of light.

Conclusions

It has been shown that the Au chemiplating technique has been highly successful for simple, rapid qualitative analyses of junctions in Si. The results are permanent until the Au is removed by dissolving or lapping.

Acknowledgment

The authors are indebted to B. Sawyer, J. F. Pudvin, and other members of the staff for their interest and encouragement in this study.

Manuscript received June 10, 1957. This paper was prepared for delivery before the Cleveland Meeting, Sept. 30-Oct. 4, 1956.

Any discussion of this paper will appear in a Discussion Section to be published in the December 1958 JOURNAL.

REFERENCES

1. "Transistor Technology," Vol. I, Chap. 12, p. 290, D. VanNostrand Co. (1958).
2. P. R. Camp, *J. Appl. Phys.*, **25**, 459 (1954).
3. C. S. Fuller, *ibid.*, **27**, 553 (1956).
4. J. F. Pudvin, "Transistor Technology," Vol. II, Chap. 15, D. VanNostrand Co. (1958).
5. J. F. Pudvin and J. E. McNamara, Semiconductor Symposium, Electrochemical Society, Pittsburgh, October 1955.
6. D. R. Turner, Private communication.

Technical Review

A Review of the Measurement of the Quantum Efficiency of Inorganic Phosphors

J. Tregellas-Williams

Research Laboratories, The General Electric Company, Limited, Wembley, England

The importance of the knowledge of the quantum efficiency of any phosphor is widely accepted; apart from its theoretical importance in the consideration of the mechanism of the processes involved in luminescence, it is a valuable guide to the luminous efficiency which may be expected from a phosphor when incorporated in a lamp. Discrepancies between the precise values given by various authors for particular phosphors are still rather wide, as are the differences in the methods of measurement. This paper is intended to review both the published data and the methods used, in the light of original work on various phosphors by some of these methods.

The quantum efficiency of a phosphor is defined as the ratio of the number of quanta emitted to the number absorbed; it is thus a measure of the energy loss due to the failure of all absorbed photons to lead to emission. In general, this includes emission in the near infrared, since it is absolute quantum efficiency rather than the quantum efficiency in the visible which is under consideration. When measurements of emitted radiation are taken only in the range of about 4000-7000 Angström units, that is, when the ratio of the number of quanta of visible radiation emitted to the number of quanta absorbed is quoted, a fall in quantum efficiency might be observed when a range of phosphors is examined, if the spectral energy distributions overlap increasingly into the ultraviolet or infrared regions. This observation might imply a change in the process leading to luminescence although, in fact, the quantum efficiency, as defined above, may be unaltered. The value corresponding to the more precise definition may be rather more difficult to measure in some cases, due to the difficulties involved in changing photocells at the ends of the spectrum in optical methods, but this would seem to be overcome when the determination of the non-emitted energy is made thermally, when no differentiation occurs between visible and near visible radiation.

The quantum efficiency of a phosphor may vary both with the wave length (1, 2) and the intensity of the exciting radiation; for example, some phosphors have broad excitation spectra and are strongly excited by both 2537Å and 3650Å radiation, but most phosphors have a comparatively narrow excitation spectrum. For certain sulfide phosphors, the quantum efficiency is reported (2) to be constant at the fundamental absorption frequency, thereafter falling as the anti-Stokes region is entered. Most measurements have been made at the wave lengths of the strong mercury lines, e.g., at 3650Å for sulfides and at 2537Å for halophosphates. A nonlinear dependence of quantum efficiency on the intensity of excitation has been observed in sulfide phosphors (3-6); the effect is more marked when nickel is present and varies with temperature and the concentration of the nickel. The intensity of the source in use is rarely, if ever, quoted when quantum efficiency results are published, however, and in comparing results, one must assume that the conditions of excitation do not differ widely in intensity.

The measurement of quantum efficiency has been carried out in four different ways: by direct optical measurements, from measurements of lamp efficiencies, by comparison with a fluorescent powder having a known quantum efficiency, and by a calorimetric method. These are discussed below.

Methods

Direct optical measurement.—In the method used by Fonda (7), the spectral energy distribution of the phosphor emission under monochromatic radiation was determined by the use of a spectrophotometer, the intensity of the emitted lines being compared with that of a standardized tungsten lamp. The efficiency of excitation, given by the ratio of visible fluorescence energy to the energy of the exciting radiation, was obtained, the fluorescence energy being measured in an integrating sphere with a photovoltaic cell and correcting filter. Conversion to lumens was achieved by calibrating the sphere for light of known wave lengths, and measuring the radiant energy with a thermopile. Values for the quantum yield were obtained for zinc and cadmium silicates, zinc sulfide and zinc cadmium sulfide, but quantum efficiences were not derived in the absence of data on the absorption of the exciting radiation by the phosphor. However, since

$$\text{Quantum yield, } \phi, = \frac{\text{No. of quanta of radiant energy falling on sample}}{\text{No. of quanta of fluorescent energy emitted}}$$

$$\text{and Quantum efficiency } \eta = \frac{\text{No. of quanta emitted by sample}}{\text{No. of quanta absorbed by sample}}$$

$$\eta = 1/\phi \cdot \frac{1}{1-r}$$

where r is the reflection coefficient for exciting light. Values of $1/\phi$ give minimum values of quantum efficiency of 0.77 for zinc silicate:Mn, 0.36 for zinc sulfide:Cu and 0.24 for zinc cadmium sulfide:Cu. A similar method has been used by Kröger (21).

In a later paper (8) the quantum efficiency of magnesium tungstate, measured by a similar method, was reported to be unity. This is higher than other published values from 0.70 to 0.90 (9-11).

The quantum efficiency of zinc sulfide:Cu and zinc silicate:Mn has been determined by Antonov-Romanovsky and Epstein (12); the phosphor occupied the space between two concentric quartz spheres, fitted with ports for the exciting and emitted radiation. The energy of the former was measured by interposing a calibrated thermopile and the latter by a photocell. The energy absorbed was determined by comparing the brightness of a luminescent screen when exposed to the incident radiation with that obtained when the screen was placed at the exit port of the sphere.

The quantum efficiency of ZnS:Cu was found to be a maximum of 0.50 at 3600A; Zn_2SiO_4:Mn had a maximum value of 0.60 from 2200A to 2600A, falling to zero at 3100A. This is lower than the minimum efficiency computed above and may be due to the particular sample used.

This method, which is capable of giving absolute values of quantum efficiency, involves measuremental difficulties and other, more convenient methods have been used for the determination of quantum efficiency.

Comparison method.—The method (13) consists of evaluating the quantum output of a phosphor relative to magnesium tungstate by integrating the product of fluorescence energy and wave length over the visible range and expressing this as a percentage of the quantum output of magnesium tungstate obtained under identical conditions. Division of this value by the phosphor absorption for the exciting radiation gives the quantum efficiency related to magnesium tungstate. Since, as mentioned above, a quantum efficiency of unity has been reported for this phosphor (8), the relative quantum efficiency is taken to equal the absolute value.

Results were reported (13) for calcium halophosphate phosphors containing optimum amounts of manganese and antimony and antimony alone: the reported value of 0.85 for the former is somewhat lower than most published values.

The measurements required by this method take much less time than in the previous method, but a disadvantage may lie in the reliance on the value for magnesium tungstate. The method is very useful, however, where series of phosphors are to be compared, although it leads to a "visible quantum efficiency" rather than the absolute quantum efficiency as defined above. A variant of this method has been used by the author for the determination of the quantum efficiency of four standard phosphors. From spectral energy distributions, plots were made of the variation of the energy function $E\lambda$ and the luminosity function $\bar{y}$ with wave length and integrating over the wave-length range from 3600A to 7300A, thus including the whole spectral emission. Since the measurements were made over a period, values of E were not necessarily consistent; the curves were normalized by determining the brightness of the phosphors relative to magnesium tungstate in a simple powder photometer which employed a circular quartz lamp and selenium cell with correcting filter.

The observed integral $\int E\lambda d\lambda$ is normalized by the application of the factor F

$$F = \frac{B}{B_s} \cdot \frac{\int E_s \bar{y} d\lambda}{\int E \bar{y} d\lambda}$$

where B = brightness and subscript $_s$ refers to $MgWO_4$. Then

$$\text{Q.E.} = F \cdot \frac{\int E\lambda d\lambda}{\int E_s \lambda d\lambda}$$

Values obtained are given in Table I. The fact that the general level of these figures is rather high may be attributable to the assumption of a higher efficiency for magnesium tungstate than is justifiable; the agreement with published data for halophosphate is within ±5% which is the expected variation although, when phosphors are compared under the same conditions, as in normal use, the results might be expected to have a smaller spread, say ±2%. The last column in Table I shows values computed for a quantum efficiency of 0.90 for magnesium tungstate as deduced from lamp efficiency measurements.

If, as seems reasonable, spectral energy distributions can be assumed to vary little with small variations in composition, the relative brightness of a phosphor becomes a useful measure of the quantum efficiency.

Lamp efficiencies.—The method of deducing quantum efficiencies of lamp phosphors from the luminous performance of fluorescent lamps was introduced by Thayer and Barnes (9); it is based on correcting the theoretical maximum performance of a lamp for losses incurred in the phosphor during processing and for lamp losses, e.g., at the ends, then relating the observed initial luminous efficiency to

Table I. Quantum efficiencies by comparison method

Phosphor	Q.E. ($MgWO_4$ = 1.0)	Q.E. ($MgWO_4$ = 90)
Warm white halophosphate	0.96	0.87
Daylight halophosphate	0.99	0.89
Cadmium borate	0.73	0.66
Zinc silicate	1.02	0.92

this, the ratio giving the quantum efficiency of the phosphor. The method gave efficiencies of 0.53 and 0.70 for zinc beryllium silicate and magnesium tungstate, respectively. Later, more exhaustive corrections were applied (11), resulting in new values of 0.9 in both cases. This was partially attributed to improved manufacturing techniques. The corrections considered included coating absorption, end losses, utilization of 2537Å radiation, bulb absorption, and the approximate brightness loss on milling; of these, the latter is greatest and varies from lamp to lamp according to the method of lamp manufacture used. The method has been applied to halophosphates and blended phosphors, using a single factor of 75% for the corrections above.

The theoretical efficiency then became

$$\text{lpw} = \frac{K\int \bar{E}_\lambda d\lambda}{\int E_\lambda / 2537 \cdot d\lambda} + C$$

where $K = 281$ and includes the above corrections, and $C = 5$ lpw which is the contribution to the output by the visible mercury lines. Quite good agreement with values from the tungstate comparison method were obtained, although this phosphor was found to be only 84% efficient which was thought to be due to a higher loss in lampmaking than in the case of halophosphates.

This method has been used by the author and comparison with the published data is interesting (*see* Table II). It will be seen that there is good agreement for daylight halophosphate, and that for warm white halophosphate, the value obtained approaches more nearly the figure for the comparison method. The use of factor K for phosphors other than halophosphate may cause some error, since the corrections are computed for halophosphates. The value obtained for magnesium tungstate is higher than the previous figure, which is due, perhaps, to the measurement of the quantum output over the whole of the emission spectrum, including, in this case, the ultraviolet. Results obtained by this method for zinc silicate are likely to be somewhat unreliable due to the difficulties in obtaining accurate initial luminous efficiencies with this phosphor.

The method is attractive to the lamp-maker since, when results are compared with those obtained by the comparison method, a direct measure of the efficiency of the lamp manufacturing process is made available; if the values are close, improvements should be sought in the phosphor, but if the efficiency by the comparison method is greater, then improvements should be possible in the lamp making process. For accurate measurements, the method suffers from the disadvantage that some of the corrections accumulated into the factor K apply to a particular phosphor made into one batch of lamps; extension to include other phosphors, even within the same general class, e.g., the halophosphates, may lead to inaccuracies.

Table II. Quantum efficiency of phosphors from lamp efficiencies

	Daylight	Warm white	Blue halophosphate	Magnesium tungstate	Cadmium borate	Zinc silicate
QE (G.E.C.)	92	91	95	90	79	83
QE (Jerome)	92	86		84		
QE (Comparison)	90	94		100		
QE (Bodó)	84				58	71

Calorimetric method.—The measurement of the light absorbed by a layer of phosphor may be made (14) by measuring the temperature change of the layer on irradiation. By repeating the experiment with a similar layer of carbon black, a measure of the total light falling on the phosphor is obtained, which, combined with reflection measurements, makes possible the calculation of the quantum efficiency of a phosphor. Since the exciting and emitted radiation are both determined in terms of heat energy, the quantum output obtained includes radiation emitted in the near visible regions of the spectrum, and the quantum efficiency deduced conforms to the definition in absolute terms given in the introductory paragraphs above.

The apparatus used by Bodó consisted of two copper disks, coated with phosphor and carbon black, respectively, supported on a tray which was thermally isolated from a massive base, in an insulated enclosure, the temperature of the tray being measured with respect to the base by a series of 40 thermocouples. Radiation from germicidal lamps was admitted through a water filter with a quartz window.

A modified version of the microcalorimeter is shown in Fig. 1. A copper disk, D, which is coated with phosphor on one side and blackened on the other, rests on a copper tray, T, which is supported in a cylindrical copper box, B, internally blackened, in an evacuable enclosure, E, by insulators A and G. Cooled water is circulated over the quartz disk, Q, to remove heat radiated by the source. The difference in temperature between the tray and the box is measured by the current flowing in three germanium-copper thermocouples, C, connected in par-

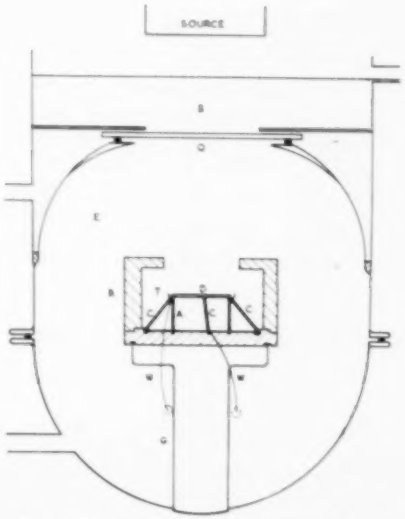

Fig. 1. Modified version of microcalorimeter

allel, which passes out of the enclosure through fine copper wires.

Measurements on phosphors excited by 2537A radiation are difficult to make since, ideally, a compact monochromatic source of high power is required for imaging onto the phosphor-coated disk. In the practical case, very high sensitivity is required to measure the temperature rise obtained when an efficient phosphor is irradiated by a practical, extended source.

For experiments on long wave u.v. excited phosphors a 125W H.P.M.V. lamp with Woods glass outer bulb, suspended in a reflector very close to the water surface, raises the temperature of the disk and the maximum current flowing in the thermocouples is recorded. Emitted or reflected light leaving the disk is absorbed by the blackened box and spurious heating effects caused by reflection onto the disk are avoided. The disk is then reversed and the procedure repeated. From the maximum values, and from separate reflection measurements, the luminous efficiency and hence the quantum efficiency may be found.

After Bodó, the quantum efficiency η'_z uncorrected for absorption by the phosphor of its own radiation is

$$\eta'_z = \frac{1}{\eta_i}\left[1 - p/b \cdot \frac{(1 - r_b)}{(1 - r_z)}\right]$$

where η_i is the quantum conversion (the ratio of the mean absorbed wave length to the mean emitted wave length); p and b, respectively, are the galvanometer readings for phosphor and black surface uppermost; r_z and r_b are the respective reflection coefficients for ultraviolet radiation.

The true quantum efficiency is given by

$$\eta_z = \eta'_z \cdot \frac{2}{r + 1}$$

(where r is the reflection coefficient of the phosphor for light of the same spectral composition as its emission), which makes correction for the absorption of emitted radiation by the phosphor.

The low quantum efficiency of the sulfide phosphor (Table III) is in agreement with published values; higher efficiencies may be expected for oxygen-dominated phosphors excited by long wave ultraviolet and have been reported for many of this class. The higher quantum efficiency of barium strontium lithium silicate is in accord with results obtained for oxygen-dominated phosphors.

Conclusion

The relative merits of the methods outlined above vary according to what use is to be made of the information obtained. For fundamental work of high accuracy it seems probable that a painstaking series of measurements by a direct optical method would be preferred, since all the other methods require subsidiary optical measurements. For routine evaluation of phosphors, a rapid and simple method is required and the comparison method would seem to be suitable, provided that the quantum efficiency of the standard phosphor chosen had been measured by as many methods as possible. It is important that the whole spectral emission of the phosphors and standard be measured; otherwise errors may arise due to the energy emitted at the extremes of the spectral energy distribution curves. Magnesium tungstate is perhaps the most suitable primary standard since its characteristics are independent of activator concentration.

The lamp efficiency method is useful for determining the quantum efficiency of a phosphor, but some of the factors involved are variable, even within one class of phosphors, and one should be cautious in extending the method to purely experimental phosphors.

The novel principle applied in the calorimetric method makes it attractive for confirmation of results obtained by more conventional methods and for measurements on phosphors emitting in the near visible regions; the limitations on sensitivity are not easily surmounted especially for very efficient phosphors excited by short u.v. radiation.

Table IV summarizes the reported values of quantum efficiencies for various phosphors. It will be noted that existing figures for sulfide phosphors appear to be variable but that, in general, efficiencies of about 50% appear to be the rule. In oxygen-dominated phosphors the agreement between various authors is much better; figures obtained by the calorimetric method are sometimes at variance with those obtained from more conventional techniques; this may be due to the difference in principle involved.

Much more work remains to be done to clarify the position; the only group where agreement is reasonable is the halophosphates; other phosphors require further study to resolve anomalies.

Table III. Quantum efficiencies by calorimetric method (3650A)

	p	b	r_z	r_b	η_i	η'_z	r	η_z
Zinc cadmium sulfide: Cu	72	129	0.12	0.01	0.61	0.61	0.95	0.63
Barium, strontium lithium silicate Ce, Mn	75	155	0.08	0.01	0.57	0.84	0.8	0.93

Acknowledgment

Acknowledgment is due to J. Fryer, who made the measurements of spectral energy distributions and reflection coefficients.

Manuscript received June 3, 1957. This paper was prepared for delivery before the Washington Meeting, May 12-16, 1957.

Any discussion of this paper will appear in a Discussion Section to be published in the December 1958 JOURNAL.

REFERENCES

1. R. Nagy, R. W. Wollentin, and C. K. Lui, *J. (and Trans.) Electrochem. Soc.*, **95**, 187 (1949).
2. V. V. Antonov-Romanovsky, *J. phys. radium*, **17**, 694 (1956).
3. N. Riehl, *Z. Tech. Physik.*, **20**, 152 (1939).
4. J. H. Gisoff and F. A. Kröger, *Physica*, **6**, 1101 (1939).
5. N. R. Nail, D. Pearlman, and F. Urbach, Cornell Symposium of Amer. Phys. Soc., p. 190, John Wiley & Sons, Inc., New York (1948).

Table IV. O-Dominated phosphors

Phosphor	Excited by	Q.E.	Method	Reference
Aluminum oxide: Cr	3650	0.35		Leverenz 1950 (20)
(Ca,Mg) Aluminum oxide: Mn	3650	0.39	Direct	Kröger 1948 (21)
Barium strontium lithium silicate: Ce,Mn	3650	0.93	Calorimeter	This paper
Cadmium borate: Mn	2537	0.58	Calorimeter	Bodó 1953 (14)
		0.73	Comparison	This paper
		0.79	Lamp efficiency	This paper
Cadmium silicate: Mn	2537	0.79	Lamp efficiency	Shklover 1947 (26)
		0.56	Direct	Fonda 1939 (7)
		0.55	Lamp efficiency	Thayer and Barnes (9)
Calcium halophosphate: Sb	2537	0.87-0.96	Comparison	Fonda, 1954 (13)
		0.95	Lamp efficiency	This paper
:Sb,Mn	2537	0.52-0.76	Comparison	Fonda, 1954 (13)
		0.85	Comparison	Fonda, 1954 (16)
(Warm white)		0.86	Lamp efficiency	Jerome, 1953 (11)
		0.91	Lamp efficiency	This paper
		0.94	Comparison	Jerome, 1953 (11)
(Daylight)		0.92	Lamp efficiency	Jerome, 1953 (11)
		0.92	Lamp efficiency	This paper
		0.90	Comparison	Jerome, 1953 (11)
		0.84	Calorimeter	Bodó, 1953 (14)
Calcium molybdate: Sm	2537	0.26	Direct	Botden, 1951 (22)
Calcium phosphate: Ce	2537	0.7	Lamp efficiency	Froelich, 1947 (23)
:Tl	2537	0.9	Lamp efficiency	Froelich, 1947 (23)
:Ce,Mn	2537	0.74	Lamp efficiency	Froelich, 1951 (24)
		0.65	Direct	Botden and Kröger, 1948 (17)
		0.50		Ouweltjes, 1952 (15)
:Ce,Th	2537	ca. 0.8	Lamp efficiency	Froelich, 1947 (23)
Calcium silicate: Pb,Mn	2537	0.55	Lamp efficiency	Thayer and Barnes, 1939 (9)
		>0.8	Lamp efficiency	Froelich, 1948 (25)
Calcium tungstate:	2537	0.7	Lamp efficiency	Thayer and Barnes, 1939 (9)
		0.7	Direct	Kröger, 1948 (21)
:Sm		0.28	Direct	Kröger, 1948 (21)
		0.58	Direct	Botden, 1951 (22)
Magnesium arsenate: Mn	2537-3650	0.85		Ouweltjes et al, 1952 (19)
Magnesium tungstate	2537	0.7	Lamp efficiency	Thayer and Barnes, 1939 (9)
		1.0	Direct	Fonda, 1944 (8)
		0.9	Lamp efficiency	Thayer, 1945 (10)
		0.84	Lamp efficiency	Jerome, 1953 (11)
		0.90	Lamp efficiency	This paper
		0.82-0.98	Lamp efficiency	Shklover, 1947 (26)
Zinc beryllium silicate: Mn	2537	0.53	Lamp efficiency	Thayer and Barnes, 1939 (9)
		0.9	Lamp efficiency	Thayer, 1945 (10)
		0.53-0.74	Lamp efficiency	Shklover, 1947 (26)
		0.77-0.84		Schulman, 1946 (27)
Zinc silicate: Mn	2537	≈0.77	Direct	Fonda, 1939 (7)
		0.71	Calorimeter	Bodó, 1953 (14)
		0.83	Lamp efficiency	This paper
		0.92	Comparison	This paper
		0.91	Lamp efficiency	Shklover, 1947 (26)
	2200-2600	0.60	Direct	Antonov-Romanovsky, 1949 (12)

Sulfide phosphors

Phosphor	Exciting wave length	Q.E.	Method	References
Zinc sulfide: Ag (Hex)	3650	0.90-0.94	Calorimeter	Gergely, 1956 (18)
(Cub)	3650	0.89	Calorimeter	Gergely, 1956 (18)
:Cu	2200->3650	0.50 (Max) at 3600Å	Direct	Antonov-Romanovsky, 1949 (12)
	3600-4000	0.6	Direct	Antonov-Romanovsky, 1956 (2)
	3650	0.36 (Min)	Direct	Fonda, 1939 (7)
:Zn	3400	0.6	Direct	Antonov-Romanovsky, 1956 (2)
Zinc Cadmium Sulfide	3650	0.24 (Min)	Direct	Fonda, 1939 (7)
:Cu		0.50	—	Ouweltjes, 1952 (15)
	2537	0.25	—	Ouweltjes, 1952 (15)
	3650	0.63	Calorimeter	This paper
	3650	0.55	Calorimeter	Gergely, 1956 (18)

6. N. R. Nail, F. Urbach, and D. Pearlman, *J. Opt. Soc. Amer.*, **39**, 690 (1949).
7. G. R. Fonda, *J. Phys. Chem.*, **43**, 574 (1939).
8. G. R. Fonda, *ibid.*, **48**, 303 (1944).
9. R. N. Thayer and B. T. Barnes, *J. Opt. Soc. Amer.*, **29**, 131 (1939).
10. R. N. Thayer, *Trans. Electrochem. Soc.*, **87**, 413 (1945).
11. C. W. Jerome, *This Journal*, **100**, 586 (1953).
12. V. V. Antonov-Romanovsky and M. T. Epstein, *C. R. Acad. Sci. U.R.S.S.*, **64**, 483 (1949).
13. G. R. Fonda, *Brit. J. Appl. Phys. Suppl.*, **4**, S69 (1954).
14. Z. Bodó, *Acta. Phys. Acad. Sci. Hung.*, **3**, 23 (1953).
15. J. L. Ouweltjes, *Phillips Tech. Rev.*, **13**, 346 (1952).
16. G. R. Fonda, *Brit. J. Appl. Phys. Suppl.*, **4**, S17 (1954).
17. P. J. Botden and F. A. Kröger, *Physica*, **14**, 553 (1948).
18. Gy. Gergely, *J. phys. radium*, **672**, 698 (1956).
19. J. L. Ouweltjes, W. Elenbaas, and K. R. Labberté, *Phillips Tech. Rev.*, **13**, 109 (1952).
20. H. W. Leverenz, "An Introduction to the Luminescence of Solids," John Wiley & Sons, Inc., New York (1950).
21. F. A. Kröger, "Some Aspects of the Luminescence of Solids," Elsevier Publishing Co., New York (1948).
22. P. J. Botden, *Phillips Res. Repts.*, **6**, 425 (1951).
23. H. C. Froelich, *Trans. Electrochem. Soc.*, **91**, 241 (1947).
24. H. C. Froelich, *This Journal*, **98**, 402 (1951).
25. H. C. Froelich, *J. (and Trans.) Electrochem. Soc.*, **93**, 101 (1948).
26. A. A. Shklover, *J. Tech. Phys. (USSR)*, **7**, 1239 (1947).
27. J. H. Schulman, *J. Appl. Phys.*, **17**, 902 (1946).

New York Program

THE ELECTROCHEMICAL SOCIETY

One Hundred and Thirteenth Meeting

Sunday through Thursday

April 27, 28, 29, 30, and May 1, 1958

CONDENSED TECHNICAL PROGRAM

Monday, April 28, 1958

Electric Insulation (Abs. 1-8) 9:30-11:30 A.M.; 2:00-4:00 P.M. (Hartford Room, Mezzanine)
Electronics-Semiconductors (Abs. 40-51) 9:30 A.M.-12:15 P.M.; 2:00-4:45 P.M. (Penn Top, 18th floor)
Electrothermics and Metallurgy (Abs. 77-81) 9:30 A.M.-12:00 M.; (Skytop, 18th floor)
Electrothermics and Metallurgy—Corrosion (Abs. 82-87) 1:30-4:30 P.M. (Skytop, 18th floor)
Industrial Electrolytic (Abs. 120-124) 10:00-11:00 A.M.; 2:00-3:30 P.M. (Washington Room, Mezzanine)
Theoretical Electrochemistry (Abs. 125-132) 9:30-11:50 A.M.; 2:00-4:50 P.M. (Gold Ballroom, Mezzanine)
Richards Memorial Lecture 5:00 P.M. (Penn Top, 18th floor)

Tuesday, April 29, 1958

Electric Insulation (Abs. 9-13) 9:00-11:30 A.M.; 2:00-4:00 P.M. (Hartford Room, Mezzanine)
Electronics-Luminescence (Abs. 20-31) 9:00-11:30 A.M.; 2:00-4:55 P.M. (Washington Room, Mezzanine)
Electronics-Semiconductors (Abs. 52-63) 9:00-11:45 A.M.; 2:00-5:00 P.M. (Penn Top, 18th floor)
Electrothermics and Metallurgy (Abs. 88-99) 9:00 A.M.-12:00 M.; 2:00-5:00 P.M. (Skytop, 18th floor)
Theoretical Electrochemistry (Abs. 133-142) 9:00-11:40 A.M.; 2:00-4:45 P.M. (Gold Ballroom, Mezzanine)

Wednesday, April 30, 1958

Electric Insulation (Abs. 14-19) 9:00 A.M.-12:00 M.; 2:00-5:00 P.M. (Hartford Room, Mezzanine)
Electronics-Luminescence (Abs. 32-39) 9:00 A.M.-12:00 M.; 2:00-4:30 P.M. (Washington Room, Mezzanine)
Electronics-Semiconductors (Abs. 64-76) 9:00 A.M.-12:00 M.; 2:00-5:00 P.M. (Penn Top, 18th floor)
Electrothermics and Metallurgy (Abs. 100-107) 9:00-11:00 A.M.; 2:00-4:00 P.M. (Skytop, 18th floor)
Theoretical Electrochemistry (Abs. 143-151) 9:00-11:20 A.M.; 2:00-4:50 P.M. (West Room, Mezzanine)

Thursday, May 1, 1958

Electrothermics and Metallurgy—Electronics-Semiconductors (Abs. 108-119) 9:00 A.M.-12:00 M.; 2:00-5:00 P.M. (Penn Top, 18th floor)
Theoretical Electrochemistry (Abs. 152-156) 9:00 A.M.-12:00 M (Skytop, 18th floor)

GENERAL INFORMATION

Convention Headquarters will be at the Hotel Statler, 7th Ave. and 33rd St., New York 1, N. Y.

Rates per day for rooms (with bath) are: single room $8.00, 9.00, 10.00, 11.00, 12.00, 13.00, 14.00; double-bed room $11.00, 12.00, 13.00, 14.00, 15.00, 16.00, 17.00, 18.00; twin-bed room, $15.00, 16.00, 17.00, 18.00, 19.00, 20.00, 21.00, 22.00; suite-living room, bed room, and bath $36.00, 37.00.

Requests for room reservations at the Headquarters Hotel should be mailed to the Front Office Manager, Hotel Statler, 7th Ave. and 33rd St., New York 1, N. Y. BE SURE to state your intention to attend The Electrochemical Society meeting.

Other hotels within a few blocks of the Headquarters Hotel and their minimum rates are:

Hotel Governor Clinton, 7th Ave. at 31st St., single room $9.00 and up; double-bed room from $14.00; twin-bed room from $15.00.

Hotel New Yorker, 8th Ave. at 34th St., single room $8.00 and up; double-bed room from $11.50; twin-bed room from $14.50.

Sheraton-McAlpin Hotel, Broadway at 34th St., single room starts at $8.35; double-bed or twin-bed room from $12.35.

Sloane House, YMCA, 356 W. 34th St., single room starts at $2.20, double room from $3.40.

Requests for room reservations should include mention of The Electrochemical Society.

The Office of the Secretary will be in the Hudson Room on the Mezzanine Floor.

The Local Committee Office will be in the Sutton Room on the Mezzanine Floor.

Ladies' Headquarters will be in the Boston Room on the Mezzanine Floor.

All technical sessions will be held on either the Mezzanine or 18th floor.

REGISTRATION

The registration desk will be in the Writing Lounge, Mezzanine Floor, except on Thursday when it will be in Penn Top Foyer (18th floor). Following is the registration schedule:

Sunday, April 27—3:00 to 9:00 P.M.
Monday, April 28—8:00 A.M. to 4:00 P.M.
Tuesday, April 29—8:00 A.M. to 4:00 P.M.
Wednesday, April 30—8:30 A.M. to 4:30 P.M.
Thursday, May 1—8:30 A.M. to 12:00 M.

Registration fees are:

Members	$ 8.00
Ladies	5.00
Nonmembers	14.00*
Thursday only	5.00
Students	2.00

*If a nonmember fills out an application blank and is subsequently elected to membership in the Society, the difference between the nonmember and member registration fee will be applied to his first year's dues.

INFORMATION ABOUT NEW YORK

The Hotel Statler is centrally located for all activities. Information about places of interest, theatrical and other attractions, restaurants, and night clubs will be available at the registration desk, or you can write to the New York Visitors Bureau, 90 E. 42 St., New York, N.Y.

SYMPOSIA AND ROUND TABLES

The Electric Insulation Division has scheduled symposia on Ceramics, Plastic Insulation, including a round-table discussion; Chemical Aspects of Printed Wiring, including a round-table discussion.

The Electronics Division-Luminescence Group has scheduled four sessions.

The Electronics Division—Semiconductor Group has scheduled symposia on Semiconductor Materials Research, Transport Phenomena, Diffusion, Physics and Chemistry of Semiconductor Surfaces, and Process Technology. The group has scheduled a joint symposium with the **Electrothermics and Metallurgy Division** on Preparation, Evaluation, and Uses of High Purity Metals on Thursday, May 1.

The Electrothermics and Metallurgy Division has scheduled symposia on Stress Corrosion Cracking of Stainless Steels jointly with the **Corrosion Division** Monday afternoon; Preparation, Evaluation, and Uses of High Purity Metals Monday morning, all day Tuesday, and jointly with the **Electronics Division, Semiconductor Group** all day Thursday; and an all-day Wednesday symposium on High Temperature Property Measurements.

The Industrial Electrolytic Division has scheduled a symposium on

Fused Salt Electrolysis and another general session.

The Theoretical Electrochemistry Division has scheduled a symposium on Electrokinetic and Membrane Phenomena all day Monday and Tuesday, with a general session starting Tuesday afternoon, continuing through Thursday morning.

GENERAL FUNCTIONS

Symposia Chairmen Breakfasts

On **Monday, Tuesday, Wednesday,** and **Thursday,** April 28, 29, 30, and May 1, special breakfasts for symposia chairmen will be held. On the day on which he presides at a symposium, each chairman should be at the Office of the Secretary (Hudson Room) *by 7:45 A.M.*

Richards Memorial Lecture

Monday, April 28, 5:00 P.M.

Dr. Abner Brenner, of the National Bureau of Standards, Washington, D.C., will deliver the Richards Memorial Lecture at 5:00 P.M. on Monday, April 28, in the Penn Top (18th floor). He will speak on "Electrolysis of Nonaqueous Solutions."

Monday Evening

On Monday, April 28, all those registered at the meeting are invited to attend the get-acquainted mixer in the Gold Ballroom, Mezzanine Floor, from 8:00 P.M. on. Beer, soft drinks, and snacks will be served on a complimentary basis; a bar will be available for the purchase of other beverages.

Admission is by registration badge. This will be a good opportunity to meet old friends, make new ones, and plan your convention activities.

Tuesday Society Luncheon

The Electrochemical Society Luncheon and Business Meeting will be held on Tuesday, April 29, at 12:15 P.M. in the Penn Top North (18th floor). An outstanding speaker will be featured.

Tuesday Evening Reception and Banquet

A reception for President and Mrs. Norman Hackerman will be held at 6:30 P.M. on Tuesday, April 29, in the Penn Top North (18th floor). Cocktails will be served from 6:30 to 7:30 P.M., followed by dinner at 7:30 P.M. in Penn Top South (18th floor). President Hackerman will deliver the Presidential Address. (Dress optional.)

Wednesday Electronics Division Cocktail Mixer

The Electronics Division will hold a Cocktail Mixer from 5:15 to 6:30 P.M. on Wednesday, April 30, in the Washington Room (Mezzanine Floor).

LADIES' PROGRAM

Ladies' Headquarters will be in the Boston Room, Mezzanine Floor, throughout the meeting. A member of the Ladies' Committee will be in the Ladies' Headquarters on Sunday from 3:00 to 9:00 P.M. to welcome and assist the ladies in every way.

Monday morning, April 28—From 9:00 to 10:30 A.M. coffee and rolls will be served in the Boston Room (complimentary).

Monday noon, April 28—Luncheon at the Plaza at 12:30 P.M. (complimentary). Gather at Ladies' Headquarters (Boston Room) at 12:00 M. During the afternoon there will be guided shopping tours.

Monday evening, April 28—The ladies are invited to attend the Mixer at 8:00 P.M. in the Gold Ballroom (*see* general program).

Tuesday morning, April 29—From 9:00 to 10:30 A.M. coffee and rolls will be served in the Boston Room (complimentary).

Tuesday noon, April 29—The ladies are invited to attend the Society Luncheon at 12:15 P.M. in the Penn Top North (18th floor). Tickets should be purchased at the registration desk. Tuesday afternoon is open.

Tuesday evening, April 29—The ladies are invited to attend the Reception and Banquet at 6:30 P.M. in the Penn Top (18th floor). Tickets should be purchased at the registration desk.

Wednesday morning and afternoon, April 30—From 9:00 to 10:30 A.M. coffee and rolls will be served in the Boston Room (complimentary). At 11:30 A.M. the ladies will gather in the Boston Room for a yacht cruise around Manhattan Island; sandwiches and coffee will be served (cruise and refreshments complimentary). The cruise will be followed by a visit to the observatory of the Empire State Building which commands an excellent view of New York City. Transportation involved will be an individual responsibility; otherwise these functions are complimentary. Return to the Hotel Statler will be about 5:00 P.M.

Wednesday evening, April 29—Open.

Thursday, May 1—Open for individual arrangements. Guides will be available to suit varied requirements.

LUNCHEONS AND BUSINESS MEETINGS OF DIVISIONS

Electric Insulation Division Luncheon and Business Meeting, Monday, April 28, at 12:15 P.M. in the Buffalo Room (Mezzanine).

Industrial Electrolytic Division Luncheon and Business Meeting, Monday, April 28, at 12:15 P.M. in Penn Top North (18th floor).

Electronics Division Business Meeting at 5:00 P.M. on Tuesday, April 29, in the Washington Room (Mezzanine).

Theoretical Electrochemistry Business Meeting, Wednesday, April 30, at 11:20 A.M. in Penn Top North (18th floor).

Electrothermics and Metallurgy Luncheon and Business Meeting, Wednesday, April 30, at 12:15 P.M. in the Buffalo Room (Mezzanine).

BOARD AND COMMITTEE MEETINGS

Sunday, April 27, 2:00 P.M.—Meeting of the **Board of Directors** in the Buffalo Room (Mezzanine).

Sunday, April 27, 7:30 P.M.—Meeting of the **Investment Advisory Panel** in the Schuyler Room (18th Floor).

Tuesday, April 29, 5:00 P.M.—Meeting of the **Editorial Staff** of the JOURNAL in the Hudson Room (Mezzanine).

Tuesday, April 29, 5:00 P.M.—Meeting of the **Membership Committee** in the Schuyler Room (18th floor).

Wednesday, April 30, 5:00 P.M.—Meeting of the **Council of Local Sections** in the Schuyler Room (18th floor).

Thursday, May 1, 12:00 M.—Meeting of **General Chairmen of Future Meetings.** Meet at the Office of the Secretary (Hudson Room) at 12:00 M. Luncheon will be arranged.

COST OF VARIOUS FUNCTIONS

(other than registration)

Please buy tickets as early as possible.

Symposia Chairmen breakfasts	
Standard menu prices	
Division Luncheon	$ 4.25
Society Luncheon	4.75
Monday Evening Mixer	
Complimentary	
Tuesday Reception and Banquet	
Single	$ 9.00
Couple	16.00
Wednesday Electronics Division	
Cocktail Mixer	3.00
Ladies' Functions	
Coffee and rolls, Monday, Tuesday, Wednesday	Complimentary
Monday luncheon at the Plaza	Complimentary
Monday Evening Mixer	Complimentary
Tuesday Society Luncheon	$4.75
Tuesday Reception and Banquet	
Couple	$16.00
Wednesday Yacht trip and Empire State Building visit	Complimentary
(except for transportation to and from hotel)	

JOURNALS

Copies of the January, February, March, and April issues of the "Journal of The Electrochemical Society" will be available at the registration desk. The price of a single copy of the JOURNAL is $1.25 to members and $1.75 to nonmembers of the Society.

EXTENDED ABSTRACTS

The Electronics Division Extended Abstracts booklet should be available about April 15, 1958 from Martin F. Quaely, Research Dept., Lamp Div., Westinghouse Electric Corp., Bloomfield, N.J., at the price of $2.50. Copies will also be on sale at the registration desk at the New York Meeting.

MESSAGES

Members and guests attending the meeting should check occasionally at the bulletin board near the registration desk to see if there are messages for them. Phone calls received in Society Headquarters Office will be posted on the bulletin board.

DISCUSSION

No recordings will be made of oral discussions. Those contributing to the discussion of a paper and desiring their remarks to be published will be supplied by the symposium chairman with a printed form on which any discussion may be written. These forms should be given to the Secretary-Treasurer of the Division or to the Managing Editor of the JOURNAL after the session; they can be mailed

to the Managing Editor of the JOURNAL, 1860 Broadway, New York 23, N.Y. The discussion will then be referred to the author for reply. Publication of the discussion and the comments of the author depends on publication of the article in the JOURNAL.

Written discussion should be submitted within two months following publication of the article in the JOURNAL. A Discussion Section is published semiannually in the JOURNAL.

EMPLOYMENT POSTERS

Companies which desire to recruit employees at the New York Meeting will have posters to this effect on a bulletin board near the registration desk.

Technical Program

Monday, April 28, 1958

9:00 A.M.—Formal opening of the 113th Meeting with Introduction by General Chairman Frederick A. Lowenheim and Response by President Norman Hackerman in Penn Top (18th floor).

ELECTRIC INSULATION

Monday, April 28, 1958
Ceramics
with L. J. Frisco presiding
(HARTFORD ROOM)

9:30 A.M.—"Effect of Temperature and Thickness on the Electrical Resistivity of Ceramic Coatings" by W. H. Fischer (Abstract No. 1)

10:00 A.M.—"High Temperature Aluminum Oxide Insulation for Wire and Strips" by Henry Walker (Abstract No. 2)

10:30 A.M.—"Progress in High Frequency Ceramic Dielectric Insulation" by E. J. Smoke and S. DiVita (Abstract No. 3)

11:00 A.M.—"Ultra Low Loss, High Frequency Dielectric Insulators" by E. J. Smoke and S. DiVita (Abstract No. 4)

12:15 P.M.—Electric Insulation Division Luncheon and Business Meeting in the Buffalo Room (Mezzanine). Guest Speaker, H. H. Chapman, Jr., Owens-Corning Fiberglas Corp., New York, N.Y.

Electric Insulation (cont'd)

Monday, April 28, 1958
Ceramics
with Hans Thurnauer presiding
(HARTFORD ROOM)

2:00 P.M.—"Boron Nitride, a Machinable High Temperature Insulation Material" by J. J. McGahan (Abstract No. 5)

2:30 P.M.—"The Effect of the Crystalline and Glassy Phases on the Dielectric Properties of Ceramic High Frequency Insulation" by B. R. Eichbaum (Abstract No. 6)

3:00 P.M.—"Some Current Problems in the Production of Magnetic Ceramics" by George Economos (Abstract No. 7)

3:30 P.M.—"D.T.A. Characteristics of Barium Titanate" by K. G. Skinner (Abstract No. 8)

5:00 P.M.—Richards Memorial Lecture—"Electrolysis of Nonaqueous Solutions" by A. Brenner (Penn Top)

Electric Insulation (cont'd)

Tuesday, April 29, 1958
Plastic Insulation
with A. J. Sherburne presiding
(HARTFORD ROOM)

9:00 A.M.—"Flammability Testing of Plastics" by L. V. Larsen (Abstract No. 9)

9:30 A.M.—"Damage to Plastic Insulation Caused by Heavy Forming Die Pressures" by F. H. Wells and J. H. Whitley (Abstract No. 10)

10:00 A.M.—"Flashover Strength of Plastic Insulation" by L. J. Frisco and J. J. Chapman (Abstract No. 11)

10:30 A.M.—"Results of Reinforced and Laminated Plastics Survey" by L. R. Samelson (Abstract No. 12)

11:00 A.M.—"LEXAN Polycarbonate Resin" by G. C. Calderwood (Abstract No. 13)

12:15 P.M.—The Electrochemical Society Luncheon and Business Meeting in the Penn Top North (18th floor)

Electric Insulation (cont'd)

Tuesday, April 29, 1958
Plastic Insulation
with A. J. Sherburne presiding
(HARTFORD ROOM)

2:00 P.M.—Round-table discussion of the Recent Developments and Problems Associated with the Use of Plastic Insulation at High Temperatures.

Electric Insulation (cont'd)

Wednesday, April 30, 1958
Chemical Aspects of Printed Wiring
with E. J. Lorenz presiding
(HARTFORD ROOM)

9:00 A.M.—"Processing Effects on High Pressure Thermosetting Laminates Used in the Manufacture of Printed Wiring Boards" by St. John Bain (Abstract No. 14)

9:45 A.M.—"Environmental Conditioning" by Elmer Varga (Abstract No. 15)

10:45 A.M.—"Organic Coatings in Printed Wiring" by B. G. Brand (Abstract No. 16)

11:30 A.M.—"Etching Control" by D. Alnutt (Abstract No. 17)

Electric Insulation (cont'd)

Wednesday, April 30, 1958
Chemical Aspects of Printed Wiring
with E. J. Lorenz presiding
(HARTFORD ROOM)

2:00 P.M.—"Plating Considerations for Printed Wiring" by W. H. Hannahs (Abstract No. 18)

2:40 P.M.—"Improved High Temperature Resistance of Copper Clad Teflon-Fiberglas Laminate" by A. H. Haroldson (Abstract No. 19)

3:30 P.M.—Round-table discussion on Printed Wiring

ELECTRONICS—LUMINESCENCE

Tuesday, April 29, 1958
with H. C. Froelich presiding
(WASHINGTON ROOM)

9:00 A.M.—Keynote Address—"Use of Polarized Light in the Study of Luminescent Systems" by C. C. Klick (Abstract No. 20)

9:45 A.M.—"Effect of Impurities on the Plaque Brightness of a 3000°K Calcium Halophosphate Phosphor" by A. Wachtel (Abstract No. 21)

10:10 A.M.—"The System ZnO.CdO.B_2O_3. Phase Relationships and Fluorescence" by D. E. Harrison and F. A. Hummel (Abstract No. 22)

10:35 A.M.—"Phase Equilibria in the System ZnO-P_2O_5" by F. L. Katnack and F. A. Hummel (Abstract No. 23)

11:00 A.M.—"Phosphors in the System Magnesia-Cadmium Oxide-Zinc Oxide-Silica" by P. G. Herold (Abstract No. 24)

12:15 P.M.—The Electrochemical Society Luncheon and Business Meeting in the Penn Top North (18th floor)

Electronics—Luminescence (cont'd)

Tuesday, April 29, 1958
with C. W. Jerome presiding
(WASHINGTON ROOM)

2:00 P.M.—"Some Observations on Aluminum Nitride" by C. Buhrer and E. Banks (Abstract No. 25)

2:25 P.M.—"Applications of Luminescence in Glass" by R. J. Ginther,

MEETING ROOM SCHEDULES

Meeting	Monday A.M.	Monday P.M.	Tuesday A.M.	Tuesday P.M.	Wednesday A.M.	Wednesday P.M.	Thursday A.M.	Thursday P.M.
Electric Insulation	B	B	B	B	B	B		
Electronics—Luminescence			A	A	A	A		
Electronics—Semiconductors	C	C	C	C	C	C		
Electrothermics and Metallurgy—Semiconductors							C	C
Electrothermics and Metallurgy—Corrosion		E						
Electrothermics and Metallurgy	E		E	E	E	E		
Industrial Electrolytics	A	A						
Theoretical Electrochemistry	F	F	F	F	D	D	E	

A = Washington Room (Mezzanine)
B = Hartford Room (Mezzanine)
C = Penn Top (18th floor)
D = West Room (Mezzanine)
E = Skytop (18th floor)
F = Gold Ballroom (Mezzanine)

J. H. Schulman, and G. W. Arnold (Abstract No. 26)

2:50 P.M.—"Oxygen As A Factor in Electroluminescence Maintenance" by W. A. Thornton (Abstract No. 27)

3:15 P.M.—"Electroluminescence of ZnS Single Crystals" by D. R. Frankl (Abstract No. 28)

3:40 P.M.—"Image Forming Devices Using Sintered Photoconductors" by K. H. Butler (Abstract No. 29)

4:05 P.M.—"Particle Size Effects and the Distribution of Barriers in Electroluminescent Zinc Sulfide Phosphors" by Paul Goldberg (Abstract No. 30)

4:30 P.M.—"The Influence of Activator and Coactivator Concentrations on the Photoconductivity of Cadmium Sulfide Powders" by B. E. Bartels and M. S. Wasserman (Abstract No. 31)

5:00 P.M.—Electronics Division Business Meeting in the Washington Room (Mezzanine)

Electronics—Luminescence (cont'd)

Wednesday, April 30, 1958
with H. F. Ivey presiding
(WASHINGTON ROOM)

9:00 A.M.—"Luminescent Properties of ZnS Phosphors with Ga and In Coactivators" by E. F. Apple (Abstract No. 32)

9:30 A.M.—"ZnS:Cu Phosphor Produced by Radioactive Decay of Neutron-Irradiated ZnS" by J. Kastner, R. M. Potter, and M. Aven (Abstract No. 33)

10:05 A.M.—"Self-Activated Luminescent Center in ZnS Phosphors" by J. S. Prener and D. J. Weil (Abstract No. 34)

10:30 A.M.—"Energy Levels of Activators in Zinc Sulfide Phosphors" by C. F. Wahlig (Abstract No. 35)

10:55 A.M.—"Optical Anisotropy and Birefringence Banding in ZnS Crystals" by L. W. Strock, V. A. Brophy, and T. E. Peters (Abstract No. 36)

11:30 A.M.—"The Lead Oxide-Lead Sulfate and Lead Oxide-Lead Selenate Systems" by R. O. Jones and S. Rothschild (Abstract No. 37)

Electronics—Luminescence (cont'd)

Wednesday, April 30, 1958
with Luke Thorington presiding
(WASHINGTON ROOM)

2:00 P.M.—"Infrared Stimulation and Quenching of Photoconduction in Single-Crystal ZnS:Cu" by F. G. Ullman and J. J. Dropkin (Abstract No. 38)

2:25 P.M.—"Sintered CdS Photoconductors" by M. J. B. Thomas (Abstract No. 39)

3:00-4:30 P.M.—Round-table discussion

ELECTRONICS—SEMICONDUCTORS

Monday, April 28, 1958
Semiconductor Materials Research
with N. B. Hannay presiding
(PENN TOP)

9:30 A.M.—Keynote Address—"Present State of Semiconductor Materials Research" by D. K. Hartman (Abstract No. 40)

10:20 A.M.—"Solid Solubilities and Electrical Properties of Aluminum and Gallium in Germanium" by F. A. Trumbore and E. M. Porbansky (Abstract No. 41)

10:35 A.M.—"Solid Solubility of Tin in Silicon" by F. A. Trumbore, C. R. Isenberg, and E. M. Porbansky (Abstract No. 42)

10:50 A.M.—"A Sensitive Method of Measuring Optical Scattering in Silicon" by G. H. Schwuttke, O. A. Weinreich, and P. H. Keck (Abstract No. 43)

11:15 A.M.—"On the Crystal Chemistry of Semiconductors" by E. Mooser and W. B. Pearson (Abstract No. 44)

11:30 A.M.—"The Electronic Structure of Compounds Formed between Group VB to VIIB Elements" by E. Mooser and W. B. Pearson (Abstract No. 45)

11:45 A.M.—Recent News Papers. Short Abstracts of these papers will be available at the meeting.

Electronics—Semiconductors (cont'd)

Monday, April 28, 1958

Semiconductor Materials Research (cont'd)

(Compound Semiconductors)
with H. P. R. Frederikse presiding
(PENN TOP)

2:00 P.M.—Keynote Address—"Semiconducting Compounds—A Challenge in Applied and Basic Research" by A. C. Beer (Abstract No. 46)

2:50 P.M.—"Recent Studies of the Properties of PbS, PbSe, and PbTe" by W. W. Scanlon (Abstract No. 47)

3:10 P.M.—"Interdiffusion by the Vacancy Mechanism in Binary Ionic Semiconductors" by R. F. Brebrick (Abstract No. 48)

3:25 P.M.—"Production of 1/f Noise by Radiation in Lead Sulfide Cells" by R. L. Williams (Abstract No. 49)

3:50 P.M.—"Preparation of Crystals of Hexagonal SiC" by D. R. Hamilton (Abstract No. 50)

4:05 P.M.—"High Pressure, High Temperature Growth of Cadmium Sulfide Crystals" by W. E. Medcalf and R. H. Fahrig (Abstract No. 51)

4:20 P.M.—Recent News Papers. Short abstracts of these papers will be available at the meeting.

5:00 P.M.—Richards Memorial Lecture—"Electrolysis of Nonaqueous Solutions" by A. Brenner in the Penn Top (18th floor)

Electronics—Semiconductors (cont'd)

Tuesday, April 29, 1958
Transport Phenomena
with H. F. Mataré presiding
(PENN TOP)

9:00 A.M.—Keynote Address—"Carrier Transport Phenomena in Semiconductor Crystals" by E. M. Conwell (Abstract No. 52)

9:50 A.M.—"Electron Mobility in Indium Phosphide" by M. Glicksman and K. Weiser (Abstract No. 53)

10:05 A.M.—"Recombination of Carriers in InSb" by R. N. Zitter, A. J. Strauss, and A. E. Attard (Abstract No. 54)

10:20 A.M.—"Avalanche Breakdown and Collector-Voltage-Saturation of Diffused Intrinsic Power Transistors" by C. Huang (Abstract No. 55)

10:45 A.M.—"Effects of Radiation on Germanium and Silicon" by G. C. Messenger and J. P. Spratt (Abstract No. 56)

11:00 A.M.—"Two New Transistor Switching Types" by C. S. McCarthy, Jr. (Abstract No. 57)

11:15 A.M.—Recent News Papers. Short abstracts of these papers will be available at the meeting.

12:15 P.M.—The Electrochemical Society Luncheon and Business Meeting in the Penn Top North (18th floor)

Electronics—Semiconductors (cont'd)

Tuesday, April 29, 1958
Diffusion
with I. A. Lesk presiding
(PENN TOP)

2:00 P.M.—Keynote Address—"Factors Influencing Diffusion Processes" by F. Smits (Abstract No. 58)

2:50 P.M.—"Diffusion Concentration Profiles by Analog Computation" by Worden Waring (Abstract No. 59)

3:05 P.M.—"Diffusion Control in Silicon by Carrier Gas Composition" by C. J. Frosch and L. Derick (Abstract No. 60)

3:20 P.M.—"Diffusion of Radioactive Antimony in Silicon" by J. J. Rohan, J. K. Kennedy, and N. E. Pickering (Abstract No. 61)

3:45 P.M.—"Diffusion into Silicon from Glassy Layers" by J. E. Cline and R. G. Seed (Abstract No. 62)

4:00 P.M.—"Effects of Heat Treatment on Diffused Silicon Material" by A. L. MacDonald and W. J. Heinecke (Abstract No. 63)

4:15 P.M.—Recent News Papers. Short abstracts of these papers will be available at the meeting.

5:00 P.M.—Electronics Division Business Meeting in the Washington Room (Mezzanine)

Electronics—Semiconductors (cont'd)

Wednesday, April 30, 1958
Physics and Chemistry of Semiconductor Surfaces
with J. W. Faust presiding
(PENN TOP)

9:00 A.M.—Keynote Address—"Semiconductor Surface Phenomena" by A. Many (Abstract No. 64)

9:50 A.M.—"Effects of Certain Chemical Treatments and Ambient Atmospheres on Surface Properties of Silicon" by T. M. Buck and F. S. McKim (Abstract No. 65)

10:05 A.M.—"Effect of Various Etches on Recombination Centers at Germanium Surfaces" by G. Wallis and Shyh Wang (Abstract No. 66)

10:20 A.M.—"Saturation Current in Germanium and Silicon Electrodes" by J. B. Flynn (Abstract No. 67)

10:45 A.M.—"Theory of Electron Transfer Reactions at Semiconductor Electrodes" by J. F. Dewald (Abstract No. 68)

11:00 A.M.—"Experiments on Electron Transfer Reactions at the ZnO Electrode" by J. F. Dewald (Abstract No. 69)

11:15 A.M.—"Chemical Etching of Silicon, I. The System HF, HNO_3, H_2O" by B. Schwartz and H. Robbins (Abstract No. 70)

11:30 A.M.—Recent News Papers. Short abstracts of these papers will be available at the meeting.

Electronics—Semiconductors (cont'd)

Wednesday, April 30, 1958

Process Technology
with H. Pollack presiding
(PENN TOP)

2:00 P.M.—Keynote Address—"Status of Semiconductor Process Technology" by F. Biondi (Abstract No. 71)

2:50 P.M.—"On the Jet Etching of Germanium and Silicon" by P. F. Schmidt and D. A. Keiper (Abstract No. 72)

3:05 P.M.—"Determination of Crystal Orientation by High Intensity Reflectograms" by G. H. Schwuttke (Abstract No. 73)

3:20 P.M.—"Some Properties of Electroless Nickel Contacts to Silicon" by E. Matovich, P. J. Heinle, and J. E. McNamara (Abstract No. 74)

3:45 P.M.—"The Use of Organo-Substituted Hydrolyzable Silanes on Silicon Devices" by B. Schwartz (Abstract No. 75)

4:00 P.M.—"Photolithographic Techniques as Applied to Semiconductor Devices" by J. R. Nall and J. W. Lathrop (Abstract No. 76)

4:15 P.M.—Recent News Papers. Short abstracts of these papers will be available at the meeting.

Electronics—Semiconductors and Electrothermics and Metallurgy Joint Symposium

Thursday, May 1, 1958

Preparation, Evaluation, and Uses of High Purity Metals
Zone Refining Methods
with Morris Steinberg presiding
(PENN TOP)

9:00 A.M.-12:00 M.—*See* Electrothermics and Metallurgy Program for Thursday, May 1.

Preparation, Evaluation, and Uses of High Purity Metals (cont'd)

Iodide Processes
with John M. Blocher, Jr., presiding
(PENN TOP)

2:00 P.M.-5:30 P.M.—*See* Electrothermics and Metallurgy Program for Thursday, May 1.

ELECTROTHERMICS AND METALLURGY

Monday, April 28, 1958

Preparation, Evaluation, and Uses of High Purity Metals
Criteria of Purity
with Donald Wilkins presiding
(SKYTOP)

9:30 A.M.—Review Paper—"Review of Various Analytical Methods for Determination of Trace Impurities" by L. Pepkowitz (Abstract No. 77)

10:00 A.M.—"Spectrochemical Methods for Analyzing High Purity Hafnium" by T. A. Sullivan, R. W. Lewis, and J. L. Potter (Abstract No. 78)

10:30 A.M.—"X-Ray Fluorescent Analysis of Tin in Titanium in the Range of 0.03-0.50% Tin" by T. A. Sullivan, R. W. Lewis, and L. Carpenter (Abstract No. 79)

11:00 A.M.—"Determination of Hydrogen in Titanium and Its Alloys—A Critical Review" by T. D. McKinley (Abstract No. 80)

11:30 A.M.—"Some Applications and Methods for Low Level Analysis of Specific Impurities in Metals" by R. A. Wallace, Thomas Polanyi, and John Roboz (Abstract No. 81)

Electrothermics and Metallurgy—Corrosion

Monday, April 28, 1958

Stress Corrosion Cracking of Stainless Steels
with William Tragert presiding
(SKYTOP)

1:30 P.M.—"Stress Corrosion Cracking of Austenitic Stainless Steel" by J. J. Harwood (Abstract No. 82)

2:00 P.M.—"Mechanism of Stress Corrosion of Type 304 Stainless Steel" by H. L. Logan (Abstract No. 83)

2:30 P.M.—"Stress Corrosion Cracking of Some Homogeneous Alloys Containing Nickel" by H. R. Copson (Abstract No. 84)

3:00 P.M.—"Stress Corrosion of Austenitic Stainless Steel in High Temperature Water" by M. G. Fontana (Abstract No. 85)

3:30 P.M.—"Caustic Stress Corrosion of Type 347 Stainless Steel" by G. C. Wheeler and E. Howells (Abstract No. 86)

4:00 P.M.—"Cracking of Martensitic Stainless Steel under Conditions of Stress and Corrosion" by F. Brown (Abstract No. 87)

5:00 P.M.—Richards Memorial Lecture—"Electrolysis of Nonaqueous Solutions" by A. Brenner in the Penn Top (18th Floor)

Electrothermics and Metallurgy (cont'd)

Tuesday, April 29, 1958

Preparation, Evaluation, and Uses of High Purity Metals (cont'd)
Electrorefining and Electrowinning
with H. H. Kellogg presiding
(SKYTOP)

9:00 A.M.—Review Paper—"Review of Aqueous Electrolytic Techniques and Methods for Preparation of High Purity Metals" by A. Brenner (Abstract No. 88)

9:30 A.M.—Review Paper—"Fused Salt Electrowinning and Electrorefining Methods" by M. E. Sibert (Abstract No. 89)

10:00 A.M.—"Fused Salt Electrorefining of Hafnium Metal" by D. H. Baker, Jr., J. R. Nettle, and J. Heigel (Abstract No. 90)

10:30 A.M.—"Elemental High Purity Boron Preparation with Emphasis on Fused Salt Electrolytic Methods" by E. W. Fajans (Abstract No. 91)

11:00 A.M.—"Fused Salt Electrorefining of Columbium Metal" by E. Hirakis and M. E. Sibert (Abstract No. 92)

11:30 A.M.—"Electrorefining of Titanium" by B. C. Raynes (Abstract No. 93)

12:15 P.M.—The Electrochemical Society Luncheon and Business Meeting in the Penn Top North (18th floor)

Electrothermics and Metallurgy (cont'd)

Tuesday, April 29, 1958

Preparation, Evaluation, and Uses of High Purity Metals (cont'd)
Chemical Purification Methods
with Morris Kolodney presiding
(SKYTOP)

2:00 P.M.—Review Paper—"The Hydrogen Reduction Method for the Preparation of High Purity Tungsten and Rhenium" by C. Toensing (Abstract No. 94)

2:30 P.M.—"Aqueous Methods for the Preparation of High Purity Metals" by G. B. Wood (Abstract No. 95)

3:00 P.M.—"Preparation of Pure Chromium by a Vacuum Distillation Technique" by W. H. Smith and R. L. Hadley (Abstract No. 96)

3:30 P.M.—"Metallurgy of Uranium Refining" by B. Blumenthal (Abstract No. 97)

4:00 P.M.—"Phase Equilibrium Study of the System Na_2WO_4-Na_2CO_3-H_2O" by R. L. Pilloton and G. E. Crawley, Jr. (Abstract No. 98)

4:30 P.M.—"Methods for Preparing Pure Scandium Oxide" by F. H. Spedding, J. E. Powell, A. H. Daane, M. A. Hiller, and W. H. Adams (Abstract No. 99)

Electrothermics and Metallurgy (cont'd)

Wednesday, April 30, 1958

High Temperature Property Measurements
General Methods
with G. M. Butler presiding
(SKYTOP)

9:00 A.M.—"On the Measurement of the Temperatures of Unenclosed Objects by Radiation Methods" by A. Emslie and H. Blau (Abstract No. 100)

9:30 A.M.—"Thermal Conductivity Measurement in the Temperature Range 1000°-3000°F" by T. E. Waterman and I. B. Fieldhouse (Abstract No. 101)

10:00 A.M.—"Micro Furnace for Thermal Microscopy and Studies at High Temperatures" by W. A. Lambertson and G. Lewis (Abstract No. 102)

10:30 A.M.—"Water-Stabilized Arc Tests on Nonmetallic Materials" by M. Dank, R. A. Nelson, W. R. Sheridan, and W. H. Sutton (Abstract No. 103)

12:30 P.M.—Electrothermics and Metallurgy Luncheon and Business Meeting in the Buffalo Room (Mezzanine)

Electrothermics and Metallurgy (cont'd)

Wednesday, April 30, 1958

High Temperature Property Measurements (cont'd)
Metallic Materials
with Robert Carlson presiding
(SKYTOP)

2:00 P.M.—"Rigidity Relaxation in Recrystallized Tungsten Wires at Elevated Temperatures" by I. Berlec (Abstract No. 104)

2:30 P.M.—"Strength of Titanium at 1300°-1600°C" by E. Scala (Abstract No. 105)

3:00 P.M.—"The Activities of Refractory Metal Systems" by Rudolph Speiser and George St. Pierre (Abstract No. 106)

3:30 P.M.—"Vapor Pressure of Columbium" by Rudolph Speiser, Paul Blackburn, and Herrick Johnston (Abstract No. 107)

Electrothermics and Metallurgy and Electronics-Semiconductors Joint Symposium

Thursday, May 1, 1958

Preparation, Evaluation, and Uses of High Purity Metals (cont'd)
Zone Refining Methods
with Morris Steinberg presiding
(PENN TOP)

9:00 A.M.—Review Paper—"Contributions of Zone Melting to High Purity Materials" by F. H. Horn (Abstract No. 108)
10:00 A.M.—"Application of the Floating Zone Technique to Metals" by R. L. Smith, J. L. Rutherford, and M. Herman (Abstract No. 109)
10:30 A.M.—"Tungsten Zone Melting by Electron Bombardment" by R. G. Carlson (Abstract No. 110)
11:00 A.M.—"Techniques and Results of Zone Refining Some Metals and Semiconducting Compounds" by J. H. Wernick, K. E. Benson, D. Dorsi, and J. J. Gillich (Abstract No. 111)
11:30 A.M.—"Continuous Multistage Zone Melting of Silicon Tetraiodide" by G. H. Moates and B. Rubin (Abstract No. 112)

Electrothermics and Metallurgy and Electronics-Semiconductors Joint Symposium

Thursday, May 1, 1958

Preparation, Evaluation, and Uses of High Purity Metals (cont'd)
Iodide Processes
with John M. Blocher, Jr., presiding
(PENN TOP)

2:00 P.M.—"Principles and Application of the Iodide Process" by A. C. Loonam (Abstract No. 113)
2:25 P.M.—"The Iodide Process for High Purity Silicon Preparation" by F. B. Litton (Abstract No. 114)
2:50 P.M.—"Some Aspects of the Decomposition of Silicon Tetraiodide" by A. F. Armington and B. Rubin (Abstract No. 115)
3:15 P.M.—"Zirconium Coating of Uranium by the Iodide Process" by W. L. Robb (Abstract No. 116)
3:40 P.M.—"High Purity Silicon from Silicon Tetraiodide Purified by Solvent Recrystallization and Distillation" by L. V. McCarty (Abstract No. 117)
4:05 P.M.—"Plating of Tungsten with Titanium and Zirconium by the Van Arkel-de Boer Process" by H. T. Stephenson (Abstract No. 118)
4:30 P.M.—"High Purity Crystalline Boron" by D. R. Stern and Lahmer Lynds (Abstract No. 119)

INDUSTRIAL ELECTROLYTIC

Monday, April 28, 1958

Fused Salt Electrolysis
with M. Janes presiding
(WASHINGTON ROOM)

10:00 A.M.—"Electrodeposition of Adherent Titanium Coatings on Induction Heated Cathodes in Fused Salts" by J. G. Wurm, B. J. Fortin, L. Gravel, and R. J. A. Potvin (Abstract No. 120)
10:30 A.M.—"Refining of Titanium Scrap by Fluoride Electrolysis" by S. S. Carlton and B. C. Raynes (Abstract No. 121)
12:15 P.M.—Industrial Electrolytic Division Luncheon and Business Meeting in the Penn Top North 18th floor)

Industrial Electrolytic (cont'd)

Monday, April 28, 1958

General Industrial Electrolytic
with J. C. Cole presiding
(WASHINGTON ROOM)

2:00 P.M.—"Report of the Chlor-Alkali Committee" by J. C. Cole and R. B. MacMullin (Abstract No. 122)
2:30 P.M.—"Effect of Gas Evolution on Current Distribution and Cell Resistance" by C. W. Tobias (Abstract No. 123)
3:00 P.M.—"Investigations on the Structure of the Color Compound in Caustic" by S. Wawzonek and D. S. P. Eftax (Abstract No. 124)
5:00 P.M.—Richards Memorial Lecture—"Electrolysis of Nonaqueous Fluids" by A. Brenner in the Penn Top (18th floor)

THEORETICAL ELECTROCHEMISTRY

Monday, April 28, 1958

Electrokinetic and Membrane Phenomena
with Paul Delahay presiding
(GOLD BALLROOM)

9:30 A.M.—"Relative Rates of Electromigration of Different Ions of the Same Charge across Permselective Membranes" by Rex Neihof, Ruth McClintock, and Karl Sollner (Abstract No. 125)
10:00 A.M.—"Improved Protamine Collodion Membranes of Extreme Ionic Selectivity" by Marc Lewis and Karl Sollner (Abstract No. 126)
10:50 A.M.—"Transport Processes in Ionic Membranes" by K. S. Spiegler (Abstract No. 127)
11:20 A.M.—"Transport in Ion-Selective Membranes" by M. A. Peterson and H. P. Gregor (Abstract No. 128)

Theoretical Electrochemistry (cont'd)

Monday, April 28, 1958

Electrokinetic and Membrane Phenomena (cont'd)
with R. Hurd presiding
(GOLD BALLROOM)

2:00 P.M.—"Transport against the Chemical or Electrochemical Gradient in Charged Porous Membranes" by Richard Schlögl (Abstract No. 129)
2:50 P.M.—"Membrane Potentials in Isothermal and Nonisothermal Systems; A Detailed Investigation of a Single Membrane System" by G. J. Hills and P. W. M. Jacobs (Abstract No. 130)
3:40 P.M.—"Electro-Osmosis and Electro-Convection in Ionic Membranes; Relation between Electro-Osmotic Transport, Ionic Conduction, Ionic Self-Diffusion, and the Degree of Counter-Ion Solvation" by G. J. Hills and P. W. M. Jacobs (Abstract No. 131)
4:20 P.M.—"Phenomenological Electrochemistry of Membranes" by George Scatchard (Abstract No. 132)
5:00 P.M.—Richards Memorial Lecture—"Electrolysis of Nonaqueous Solutions" by A. Brenner in the Penn Top (18th floor)

Theoretical Electrochemistry (cont'd)

Tuesday, April 29, 1958

Electrokinetic and Membrane Phenomena (cont'd)
with Ralph Roberts presiding
(GOLD BALLROOM)

9:00 A.M.—"Streaming Potentials of Corundum in Organic Electrolyte Solutions" by H. J. Modi and D. W. Fuerstenau (Abstract No. 133)
9:30 A.M.—"Interpretations of Experimental Donnan Equilibria Obtained with Polyphosphates" by U. P. Strauss (Abstract No. 134)
10:00 A.M.—"Direct Determination of Adsorption of Organic Molecules at Solid Electrodes" by B. E. Conway and R. G. Barradas (Abstract No. 135)
10:40 A.M.—"Electrokinetic Measurements on Stainless Steel Capillaries" by B. Levy and A. R. Fritsch (Abstract No. 136)
11:10 A.M.—"Surface Conductance of Clays" by H. van Olphen (Abstract No. 137)
12:15 P.M.—The Electrochemical Society Luncheon and Business Meeting in the Penn Top North (18th floor)

Theoretical Electrochemistry (cont'd)

Tuesday, April 29, 1958

Electrokinetic and Membrane Phenomena (cont'd)
with Ralph Roberts presiding
(GOLD BALLROOM)

2:00 P.M.—"Membrane Phenomena in Applied Geophysics" by M. Gondouin (Abstract No. 138)
2:30 P.M.—"Influence of Firing Conditions, Composition, and Screening Media on the Zeta Potentials of ZnS Phosphors as Related to Adherence to Glass Surfaces" by B. Levy (Abstract No. 139)
3:00 P.M.—"The Electrokinetic Potential and Some Surface Tension Phenomena" by L. B. Robinson (Abstract No. 140)

General Session
with Paul Delahay presiding

3:45 P.M.—"Overvoltage and Catalysis" by Paul Ruetschi (Abstract No. 141)
4:15 P.M.—"Cathodic and Anodic Properties of Chlorine on Carbon and Graphite Surfaces" by John Aylward, Ernest Yeager, and Frank Hovorka (Abstract No. 142)

Theoretical Electrochemistry (cont'd)

Wednesday, April 30, 1958

General Session (cont'd)
with A. J. de Bethune presiding
WEST ROOM

9:00 A.M.—"Electrode Potentials of Titanium-Oxygen Alloys" by R. S. Dean, I. Hornstein, and W. W. Gullett (Abstract No. 143)

9:30 A.M.—"Mechanisms of Hydrogen Producing Reactions on Palladium, V. The Deuterium-Palladium System" by Sigmund Schuldiner and J. P. Hoare (Abstract No. 144)

10:00 A.M.—"Double Layer Structure and Electrode Processes, I. Salt Effect" by Manfred Breiter, Marcos Kleinerman, and Paul Delahay (Abstract No. 145)

10:40 A.M.—"Double Layer Structure and Electrode Processes, II. Discharge of Certain Metallic Complexes" by Paul Delahay and Carl Weis (Abstract No. 146)

11:20 A.M.—Theoretical Electrochemistry Division Business Meeting in the Penn Top North (18th floor)

Theoretical Electrochemistry (cont'd)

Wednesday, April 30, 1958

General Session (cont'd) with C. W. Tobias presiding

WEST ROOM

2:00 P.M.—"Schlieren Studies of Concentration Gradients at a Cu HCl Anode" by R. S. Cooper (Abstract No. 147)

2:30 P.M.—"The Nature of the Current Flow at or between Cylindrical Electrodes" by R. D. Barnard and S. M. Skinner (Abstract No. 148)

3:00 P. M.—"Electromotive Force Measurements in Cerium-Cerium Chloride Liquid Systems" by S. Senderoff and G. W. Mellors (Abstract No. 149)

3:50 P.M.—"Activities of NiCl$_2$ from EMF Measurements in Molten LiCl-KCl" by R. D. Walker, Jr., and D. E. Danly (Abstract No. 150)

4:20 P.M.—"Electropolishing Silicon in Hydrofluoric Acid Solutions" by D. R. Turner (Abstract No. 151)

Theoretical Electrochemistry (cont'd)

Thursday, May 1, 1958

General Session (cont'd) with S. Schuldiner presiding

(SKY TOP)

9:00 A.M—"Thermodynamics of Electron Atmospheres at Interfaces" by S. M. Skinner (Abstract No. 152)

9:30 A.M.—"Codeposition of Nickel and Hydrogen from Simple Aqueous Solutions" by John Yeager, J. P. Cels, Ernest Yeager, and Frank Hovorka (Abstract No. 153)

10:00 A.M.—"Effect of Addition Agents on Tungsten Codeposition" by J. S. Sallo and R. D. Fisher (Abstract No. 154)

10:00 A. M.—"Anodic Oxidation of Zinc and a Method of Altering the Characteristics of the Anodic Films" by H. Fry and Marjorie Whitaker (Abstract No. 155)

11:20 A.M.—"Anodic Dissolution of Magnesium in Aqueous Solution" by Richard Glicksman (Abstract No. 156)

ABSTRACTS

In the Index to Authors the Abstract Number is the number listed in the right-hand column.

ELECTRIC INSULATION

Abstract No. 1

Effect of Temperature and Thickness on the Electrical Resistivity of Ceramic Coatings

W. H. Fischer, General Engrg. Lab., General Electric Co., 1 River Rd., Schenectady 5, N. Y.

Tests show that the electrical resistivity of ceramic coatings less than 3 mils thick varies with thickness, although the variation of resistivity with temperature is normal. It is believed that the resistivity-thickness variation is due to surface irregularities and metal-ceramic interface factors which together produce nonuniform, nonhomogenous coatings. Consequently, electrical characteristics of ceramic coatings intended for electrical insulation use should be evaluated only from measurements made on coatings closely approximating actual service thicknesses.

Abstract No. 2

High Temperature Aluminum Oxide Insulation for Wire and Strips

Henry Walker, Permaluster, Inc., Burbank, Calif.

The Permaluster Process (electrochemical anodic oxidation) creates a very thin film which has the properties to protect against corrosion, is highly insulating, and provides great heat resistance up to approximately 3650°F. The film is flexible and can be furnished in colors. It is aluminum oxide, created from the aluminum to which it is applied. It can be provided on other metals such as Cu, Ag, and Pt, provided they are Al clad.

Abstract No. 3

Progress in High Frequency Ceramic Dielectric Insulation

E. J. Smoke, School of Ceramics, Rutgers, The State University, New Brunswick, N. J., and **S. DiVita**, U. S. Army Signal Engineering Lab., Fort Monmouth, N. J.

U. S. Army Signal Corps sponsored research on high frequency ceramic dielectric insulation at Rutgers, The State University, has resulted in many interesting findings. The project is divided into several problems, namely, ultra low loss, thermal shock resistance, impact resistance, thermal conductivity, nonshrinking ceramics, etc. These are discussed in terms of the problem, the basic principles involved, and progress to date.

Abstract No. 4

Ultra Low Loss, High Frequency Dielectric Insulators

E. J. Smoke, School of Ceramics, Rutgers, The State University, New Brunswick, N. J., and **S. DiVita**, U. S. Army Signal Engineering Lab., Fort Monmouth, N. J.

The best ultra low loss electrical properties at high frequencies are attained with pure oxide single crystals and pure single oxide glasses and polycrystalline ceramics. However, these have limited use because of fabricating difficulties, particularly in making larger specimens. When the size factor is important and refractoriness is not, polycrystalline fluxed bodies, maturing at relatively low temperatures, become important. Wollastonite and quartz-type bodies fluxed with lead and alkaline earth compounds are discussed, including physical and electrical properties, and compared to single crystals.

Abstract No. 5

Boron Nitride, a Machinable High Temperature Insulation Material

J. J. McGahan, Carborundum Co., Niagara Falls, N. Y.

(No abstract received)

Abstract No. 6

The Effect of the Crystalline and Glassy Phases on the Dielectric Properties of Ceramic High Frequency Insulation

B. R. Eichbaum, Research Lab., International Business Machines Corp., Poughkeepsie, N. Y.

The method of tailor making ceramic insulation for specific purposes has not been used because the effect of both the glass and crystalline phases on the fired body composition was not known. This investigation of the effect of the glass and crystalline phases of ceramic insulation (operating at megacycle) should aid in developing bodies with specific requirements.

In this study the dielectric constant and power factor of the crystal phases of wollastonite, quartz, and alumina and of a bonding glass were determined and calculations (using Niesel's, Lichtenecker's and Maxwell's Law of Mixtures) were used to determine the properties of such ceramic bodies. Special techinques were used to determine the properties of these materials and to determine the volume per cent of each phase present in the fired bodies in order to check the theory with practical results.

The findings of this investigation were used to develop a very low loss quartz-type ceramic body.

Abstract No. 7

Some Current Problems in the Production of Magnetic Ceramics

George Economos, Lab. for Insulation Research, Massachusetts Institute of Technology, Cambridge, Mass.

Reproducibility of the electrical and magnetic properties is still the main difficulty in quantity production of magnetic ceramics. In addition, the mechanical tolerances of the user must be met. These two major problems are discussed from a developmental viewpoint with suggestions for improving present methods. Current efforts at standardizing acceptable testing specifications for the various applications are outlined also.

Abstract No. 8

D. T. A. Characteristics of Barium Titanate

K. G. Skinner, U. S. Naval Research Lab., Washington, D. C.

Differential thermal analyses (d. t. a.) were made of barium titanate samples and of sized-fractions obtained from them. The samples included both commercially available and laboratory-prepared materials. The d. t. a. characteristics showed not only the differences between as-received samples but also

between sized-fractions of the same sample. These differences included (*a*) completeness of chemical reactions between components, (*b*) presence of undesired compounds, from a purity or a piezo-electric standpoint, such as Ba_2TiO_4, $BaTi_2O_5$, and $BaTi_4O_9$, (*c*) phase change temperatures, such as the tetragonal-cubic transition of $BaTiO_3$, and (*d*) approximate temperature at which coalescence (shrinkage) begins. The observed differences in chemical character have been related to ceramic fabrication behavior and to electrical properties of finished bodies.

Abstract No. 9

Flammability Testing of Plastics

L. V. Larsen, Laminated Products Div., General Electric Co., Coshocton, Ohio

This paper discusses a severe test for flammability in which the specimen is exposed to a high temperature source of heat with a spark present to ignite gaseous products of combustion. The results obtained in this test are in terms of the ignition time and the burning time.

A number of the factors influencing the precision and reproducibility of the test procedure are discussed. These include mass of specimen, temperature of source of heat, and rate of ventilation.

Abstract No. 10

Damage to Plastic Insulation Caused by Heavy Forming Die Pressures

F. H. Wells and **J. H. Whitley,** AMP Incorporated, Harrisburg, Pa.

Plastic insulation used on crimp-type electric wire terminations must maintain high dielectric strength after severe mechanical abuse suffered in the crimping operation. Elementary mechanical properties of the plastics often fail to predict their performance in this application. A notable example is reported here, where peculiar stress-relaxation effects were observed in polyvinyl chloride-acetate. The dielectric strength of tubular specimens remained high while under heavy die pressure, but fell sharply after pressure was removed.

Abstract No. 11

Flashover Strength of Plastics

L. J. Frisco and **J. J. Chapman,** Dielectrics Lab., The Johns Hopkins University, Baltimore, Md.

Surface flashover strength has been measured at impulse and d-c voltage and at alternating voltages over the frequency range from 60 cps to 100 mc. Data on the effects of frequency, ambient temperature, moisture absorption, material properties, and electrode configuration demonstrate the influence of these factors on surface failure.

Abstract No. 12

Results of Reinforced and Laminated Plastics Survey

L. R. Samelson, Lake Publishing Co., Lake Forest, Ill.

More than 2200 individuals have cooperated in a mail questionnaire survey on reinforced and laminated plastics used in the electrical and electronic industries. Topics covered include: forms used, applications, improvements desired, information required, standards and specifications, volume used, grades used, etc. Survey results serve as a guide to common problems needing solution in connection with these plastics.

Abstract No. 13

LEXAN Polycarbonate Resin

G. C. Calderwood, Chemical Development Dept., General Electric Co., Pittsfield, Mass.

LEXAN molding compound is a polycarbonate resin developed by the General Electric Co. Its unusual chemical composition offers a combination of toughness and heat stability not previously available in thermoplastic materials. LEXAN resin is a completely new thermoplastic molding compound which is characterized by the following unique properties: (*a*) high impact strength; (*b*) excellent dimensional stability; (*c*) superior heat resistance; (*d*) good electrical properties.

Abstract No. 14

Processing Effects on High Pressure Thermosetting Laminates Used in the Manufacture of Printed Wiring Boards

St. John Bain, Formica Corp., Cincinnati, Ohio

This paper discusses: (*a*) electrical and physical properties of various laminates pertinent to printed wiring board; (*b*) effects of various processing chemicals on copper-clad laminates, including chemical and dimensional changes experienced as a result of degreasing, baking, etching, electroplating, fluxing, and soldering; and (*c*) effects of environmental aging on printed wiring boards, presenting data on the variation in electrical properties as a function of several accelerated aging conditions.

Abstract No. 15

Environmental Conditioning

Elmer Varga, Hughes Systems Development Labs., Culver City, Calif.

A major requirement for military equipment is that it will operate properly under extremes of environmental conditions.

This paper discusses the use of environmental conditioning for the purpose of building into etched circuit assemblies the necessary resistance to environment.

This conditioning finds important use in (*a*) qualification of raw material; (*b*) acceptance tests of incoming raw materials; (*c*) evaluation of the effect of individual processes on the quality of the finished board; (*d*) control of the manufacturing operations; (*e*) inspection tests of finished etched circuit boards.

The application of environmental tests to determine manufacturing capabilities, solder joint reliability, surface contamination, and effectiveness of protective coatings is presented.

Abstract No. 16

Organic Coatings in Printed Wiring

B. G. Brand, Battelle Memorial Institute, Columbus 1, Ohio

The paper presents a brief review of the main methods of production of printed circuits and the role of organic coatings in this production. Requirements of coating materials for the different applications as well as places where improvements are desired are discussed. Attention must be given to mechanical, chemical, electrical properties in the choice of proper materials.

Abstract No. 17

Etching Control

D. Alnutt, Philip A. Hunt Co., Palisades Park, N. J.

A discussion is given on the chemistry of etching, especially when using iron chloride and nitric acid solutions. The effects of temperature, Baume free acid content, etc., on the quality and speed of etching are discussed also. In addition, a new powderless method of etching copper as used for halftone work is explained. The method may have application for printed wiring work.

Abstract No. 18

Plating Considerations for Printed Wiring

W. H. Hannahs, Automatic Production Research, Mount Vernon, N. Y.

The effects of plating solutions, especially cyanide baths, on laminated base materials are discussed as well as special consideration of plating baths used for printed wiring work and control of plating baths, considering that organic substances are immersed in the bath.

Abstract No. 19

Improved High Temperature Resistance of Copper Clad Teflon-Fiberglas Laminate

A. H. Haroldson, Continental-Diamond Fibre Div., Budd Co., Inc., Newark, Del.

At elevated temperatures the surface of the copper foil next to the substrate oxidizes and causes a loosening of the bond. A number of methods have been studied to prevent deterioration of the copper surface. The best results have been attained with a nickel plated copper foil. When the copper surface has been treated to prevent oxidation the laminate can be subjected to 500°F continuously, without any loss of bond strength.

ELECTRONICS—LUMINESCENCE

Abstract No. 20

Use of Polarized Light in the Study of Luminescent Systems

C. C. Klick, U. S. Naval Research Lab., Washington, D. C.

(No abstract received)

Abstract No. 21

Effect of Impurities on the Plaque Brightness of a 3000°K Calcium Halophosphate Phosphor

A. Wachtel, Research Dept., Westinghouse Electric Corp., Bloomfield, N. J.

The killing action of 27 elements on a specially purified 3000°K calcium halophosphate phosphor has been investigated. At 1% addition,

the observed reduction in output increases in the order: Al, Zr, Ce, La, Pb, Y, In, Sm, Cs, S, Pr, Nd, Na, Ag, Sn, W, Si, Mo, U, Ga, Cr, Ni, Fe, Cu, Co, V, and Ti. In the neighborhood of 100 ppm, the first five elements listed showed a slight enhancing effect. None of the elements tested had an appreciable effect on the color of fluorescence, except where killing of the luminescence became very pronounced. The use of capped silica tubes enabled firings with a reproducibility of ±0.3%.

Abstract No. 22

The System ZnO.CdO.B_2O_3, Phase Relationships and Fluorescence

D. E. Harrison, Luminescent Materials Lab., Lamp Wire and Phosphors Dept., General Electric Co., Cleveland, Ohio, and **F. A. Hummel,** Dept. of Ceramic Technology, Pennsylvania State University, University Park, Pa.

The subsolidus phase relationships were investigated using x-ray and petrographic methods. Two compounds were isolated: $2ZnO.CdO.B_2O_3$ which fuses at ca. 860°C and $ZnO.2CdO.2B_2O_3$ which melts congruently at 797° ±3°C. Excitation by either 2537Å or cathode rays produces an orange fluorescence in $2ZnO.CdO.B_2O_3$ with 0.004 wt% Mn and a red fluorescence in $ZnO.2CdO.2B_2O_3$ with 0.082 wt% Mn. The fluorescence of $ZnO.2CdO.2B_2O_3$ was examined using Ag, Sn, Tl, Pb, and Sb as single activators, as well as sensitizers in conjunction with Mn.

Abstract No. 23

Phase Equilibria in the System ZnO-P_2O_5

F. L. Katnack and **F. A. Hummel,** Dept. of Ceramic Technology, Pennsylvania State University, University Park, Pa.

Phase relationships in the system ZnO-P_2O_5 were determined in the range between ZnO and $Zn(PO_3)_2$. Three congruently melting compounds exist, $Zn_3(PO_4)_2$, $Zn_2P_2O_7$, and $Zn(PO_3)_2$. The orthophosphate has a sluggish, reversible inversion at 942° and melts at 1060° ±8°. The pyrophosphate undergoes a rapid, reversible inversion at 132° and melts at 1017°. An irreversible inversion in the metaphosphate takes place in air in the range between 600° and 700°. Simple eutectic relationships exist between ZnO and $Zn_3(PO_4)_2$, $Zn_3(PO_4)_2$ and $Zn_2P_2O_7$, and $Zn_2P_2O_7$ and $Zn(PO_3)_2$.

Abstract No. 24

Phosphors in the System Magnesia-Cadmium Oxide-Zinc Oxide-Silica

P. G. Herold, Electron Tube Div., Radio Corp of America, Lancaster, Pa.

This paper describes four new compounds which are tentatively identified as: *(a)* $5MgO.2CdO.ZnO.7SiO_2$, *(b)* $2CdO.ZnO.SiO_2$, *(c)* $2MgO.4CdO.3SiO_2$, and *(d)* $MgO.2CdO.SiO_2$. The first of these compounds shows good cathodoluminescent properties. When it is activated with 4 mole % Mn and fluxed with $CdCl_2$, it has a peak wave length of 6380Å, a peak efficiency equal to 85% that of Mn-activated Zn orthophosphate, and very little saturation at high current densities.

Abstract No. 25

Some Observations on Aluminum Nitride

C. Buhrer and **E. Banks,** Polytechnic Institute of Brooklyn, Brooklyn, N. Y.

Aluminum nitride has been prepared by several methods. The purest material is obtained by the thermal decomposition of an aluminum chloride-ammonia complex. This material is nonluminescent, while a less pure material prepared from the metal has a blue luminescence. Conductivity data on a sample of the impure material and the diffuse reflectance spectrum of the pure material are presented. It is suggested tentatively that the blue fluorescence is associated with a stoichiometric excess of aluminum.

Abstract No. 26

Applications of Luminescence in Glass

R. J. Ginther, J. H. Schulman, and **G. W. Arnold,** U. S. Naval Research Lab., Washington, D. C.

Luminescent glasses are currently being explored for possible application as scintillators, cathode ray screens, or light sources. For scintillation counting purposes Ce-activated glasses appear to be most promising. Cathode ray screens composed of Mn-, Cu-, and Ce-activated vycor have been prepared. The screen brightness of the Mn-activated glass is about one-third that of a ZnS(Mn) film. Cerium- and Sm-activated vycor are high temperature phosphors and may find application as light sources.

Abstract No. 27

Oxygen As A Factor in Electroluminescence Maintenance

W. A. Thornton, Research Dept., Westinghouse Electric Corp., Bloomfield, N. J.

The assumption that oxygen enters zinc sulfide phosphor crystals during electroluminescence, and thereby introduces electron traps which are considerably deeper than those found in good electroluminescent phosphors containing no added oxygen, is sufficient to explain the extensive experimental data; such traps are expected to have a quenching effect on the electroluminescence light output.

Abstract No. 28

Electroluminescence of ZnS Single Crystals

D. R. Frankl, Sylvania Electric Products Inc., Bayside, N. Y.

Studies of emission from certain ZnS:Cu crystals under pulsed voltage excitation suggest the following mechanisms: *(a)* excitation occurs by impact of electrons which enter the crystal by tunneling and are accelerated to several ev energy in the strong electric field in a barrier; *(b)* emission occurs by capture either of these electrons or of slow electrons that return to the barrier region on removal of the voltage. These mechanisms are shown to be capable of accounting qualitatively for the observed behavior under sinusoidal excitation.

Abstract No. 29

Image Forming Devices Using Sintered Photoconductors

K. H. Butler, Sylvania Electric Products, Inc., Salem, Mass.

Two image-forming devices using sintered photoconductive layers in conjunction with electroluminescent layers are described. One device employs feedback of light to allow indefinite holding of an image, while the second device eliminates all feedback to permit reproduction of a moving image. Equivalent circuits of the devices are used to explain their characteristics.

Abstract No. 30

Particle Size Effects and the Distribution of Barriers in Electroluminescent Zinc Sulfide Phosphors

Paul Goldberg, Central Research Labs., Sylvania Electric Products Inc., Bayside, N. Y.

The particle size of electroluminescent phosphors is found to be a significant factor in empirical equations describing brightness-voltage relationships. These observations can be understood by considering *(a)* distribution of barriers in an electroluminescent particle, *(b)* division among the barriers of the voltage drop per particle, and *(c)* dependence on the particle size of the voltage drop per particle. Equations are derived which permit a meaningful comparison of the brightness of different phosphors.

Abstract No. 31

The Influence of Activator and Coactivator Concentrations on the Photoconductivity of Cadmium Sulfide Powders

B. E. Bartels and **M. S. Wasserman,** Sylvania Electric Products Inc., Flushing 54, N. Y.

Analyses of photoconductive CdS powders reveal an interdependence between the activator and coactivator concentrations retained after synthesis. In powders prepared with controlled amounts of activator (Cu) and excess coactivator (Cl), the amount of retained coactivator is found to be closely related to the activator content, and independent of the excess coactivator present during preparation. As the copper content is increased, the mole ratio Cu/Cl increases, passing unity in the range in which photoconductive sensitivity is a maximum. In the same range there are marked changes in spectral response and dark conductivity. Optical and electrical data are related to the analyses of the powders in such a way that tentative conclusions can be drawn.

Abstract No. 32

Luminescent Properties of ZnS Phosphors with Ga and In Coactivators

E. F. Apple, Research Lab., General Electric Co., Schenectady, N. Y.

In ZnS:(Cu,Ag,Au)(Ga,In) the luminescence observed depends on structure, activator concentration, and coativator identity. Cubic phosphors containing 10^{-4} g/atoms activator and coativator/mole ZnS show green, blue, and yellow-

green emissions typical of Cu, Ag, Au, respectively. In hexagonal materials the emission is yellow with Ag, orange with Cu, and orange-red with Au. These effects, which are observed at room temperature with In and at lower temperatures with Ga, can be interpreted qualitatively by means of the Schön-Klasens theory of hole migration.

Abstract No. 33

ZnS:Cu Phosphor Produced by Radioactive Decay of Neutron-Irradiated ZnS

J. Kastner, R. M. Potter, and **M. Aven,** Lamp Development Dept., General Electric Co., Cleveland, Ohio

ZnS powder was irradiated in a high density thermal neutron flux to form radioactive Zn-65, Zn-69, and S-35. These radioisotopes decay to randomly distributed Cu-65, Ga-69, and Cl-35, respectively. Approximately one week after removal from the nuclear reactor the sample was fired at 900°C. The optical properties of the sample were determined during the ensuing ten-month decay period. Experimental findings are presented and interpreted in the light of current theories of luminescence in ZnS.

Abstract No. 34

Self-Activated Luminescent Center in ZnS Phosphors

J. S. Prener and **D. J. Weil,** Research Lab., General Electric Co., Schenectady, N. Y.

A model for the ground state of the self-activated luminescent center in ZnS phosphors proposed by Prener and Williams in 1956 has been confirmed experimentally. It is shown that a Zn vacancy is involved in the blue luminescence and that the spectrum depends on whether the required coativator can occupy a Zn or S site near the vacancy. The calculated energy levels of the center using a simple model are in qualitative agreement with the observed spectra.

Abstract No. 35

Energy Levels of Activators in Zinc Sulfide Phosphors

C. F. Wahlig, Photo Products Dept., E. I. du Pont de Nemours & Co., Experimental Station, Wilmington, Del.

Measurements of the decrease of emission peak intensity under 3650A u.v. excitation with increasing temperature tend to confirm the existence of two basic levels in self-activated ZnS identical with those proposed by Browne.* Changes in the position of the basic levels, 0.9 ev and 1.6 ev above the valence band, upon including Ag, Cu, or Mn activator in the phosphor formulation have also been investigated.

* P. F. Browne, *J. Electronics*, 2, 154 (1956).

Abstract No. 36

Optical Anisotropy and Birefringence Banding in ZnS Crystals

L. W. Strock, V. A. Brophy, and **T. E. Peters,** Research Lab., Sylvania Electric Products Inc., Bayside, N. Y.

Electroluminescent ZnS crystals with 3-layer x-ray structure and banded birefringence exhibit strong anisotropy in light emission—fields applied perpendicular to the [c] direction producing brightest emission. Crystals with 2-layer structure also show similar banding. Experiments on the decay of the birefringence at elevated temperatures have shown that the decay time is at least two orders of magnitude slower for the 2-layer compared with the 3-layer structure crystals. These data, combined with parallel x-ray studies of structural changes accompanying the birefringence decay, provide a useful means of determining the role of structural disorder in the host crystal of electroluminescent phosphors.

Abstract No. 37

The Lead Oxide-Lead Sulfate and Lead Oxide-Lead Selenate Systems

R. O. Jones and **S. Rothschild,** Mullard Research Labs., Cross Oak Lane, Salfords, Nr. Redhill Surrey, England

The lead oxide-lead sulfate and lead oxide-lead selenate systems have been investigated using the room temperature x-ray powder method. The two systems are very similar and the preparation and x-ray powder patterns are given of lead sulfate $PbSO_4$, and lead monoxysulfate $PbO.PbSO_4$, lead tetroxysulfate $4PbO.PbSO_4$, lead selenate $PbSeO_4$, lead monoxyselenate $PbO.PbSeO_4$, and lead tetroxyselenate $4PbO.PbSeO_4$. The lead oxyselenates are isomorphous with the corresponding lead oxysulfates and the pattern of lead monoxyselenate has been indexed on the basis of a monoclinic unit cell of dimensions. $a=13.94$°A, $b=5.78$°A, $c=7.25$°A, $\beta=115.9°$.

Abstract No. 38

Infrared Stimulation and Quenching of Photoconduction in Single-Crystal ZnS:Cu

F. G. Ullman and **J. J. Dropkin** Polytechnic Institute of Brooklyn, Brooklyn, N. Y.

The photoconduction of laboratory grown single crystals of Zns:Cu in the near infrared has been studied as a function of light intensity and electric field with and without simultaneous 3650Å radiation. Infrared alone produces photocurrents even in an unexcited crystal. This photocurrent quenches the u.v. photocurrent. The stimulation and quenching spectrum for infrared photocurrent has been determined and compared to published luminescence quenching spectra and excitation spectra for infrared emission and to previously postulated mechanisms.

Abstract No. 39

Sintered CdS Photoconductors

M. J. B. Thomas, Sylvania Electric Products Inc., Salem, Mass.

The effects of composition and firing procedure on the optical and electrical properties of thin photoconductive layers, formed by sintering cadmium sulfide powder, are described. Photocurrent, dark current, decay rate, and spectral sensitivity data are included. These characteristics are compared with those of films formed from unsintered powders.

ELECTRONICS—SEMICONDUCTORS

Abstract No. 40

Present Status of Semiconductor Materials Research

D. K. Hartman, General Electric Co., Syracuse, N. Y.

It was just a decade ago that transistor action was first announced by Bardeen and Brattain. No small part of the advances made in transistor technology during the ensuing period have been credited to materials research in processing and purification. Today, because of these advances, both germanium and silicon are finding wide acceptance in the semiconductor industry. There are still problems associated with these materials but it is the general consensus of many of the semiconductor manufacturers that present-day devices are not materials limited. It is the intent of this paper to review pertinent work in technological advancement that has made this materials position possible and to give some insight as to the present status of semiconductor materials research.

Abstract No. 41

Solid Solubilities and Electrical Properties of Aluminum and Gallium in Germanium

F. A. Trumbore and **E. M. Porbansky,** Bell Telephone Labs., Inc., Murray Hill, N. J.

The distribution coefficients of Al and Ga in Ge, determined from crystal pulling experiments, fall from 0.08-0.09 at the melting point of Ge (937°C) to 0.04-0.05 at 900°C. The most heavily doped crystals, with acceptor concentrations of 2×10^{20} atoms/cc, had room temperature resistivities of 0.0003 ohm-cm corresponding to hole mobilities of about 70 $cm^2/v\text{-}sec$. Solid solubilities and resistivities were also obtained on crystals grown at lower temperatures by thermal gradient crystallization.

Abstract No. 42

Solid Solubility of Tin in Silicon

F. A. Trumbore, C. R. Isenberg, and **E. M. Porbansky,** Bell Telephone Labs., Inc., Murray Hill, N. J.

The distribution coefficient of Sn in Si, as determined by crystal pulling and thermal gradient crystallization techniques, falls from a value of 0.015 at the melting point of Si to a value of about 7×10^{-4} at lower temperatures. Resistivity and lifetime measurements indicate that Sn is electrically neutral in Si. The observed lattice parameter for crystals grown at 800°C is in agreement with the calculated lattice expansion assuming Vegard's law.

Abstract No. 43

A Sensitive Method of Measuring Optical Scattering in Silicon

G. H. Schwuttke, O. A. Weinreich, and **P. H. Keck,** Sylvania Electric Products Inc., Bayside, N. Y.

Radiation scattering in the high transparency infrared region of silicon can be utilized effectively to

study the perfection of single crystals. A novel optical arrangement has been developed which is suitable for detecting extremely small amounts of scattered radiation. This method is sensitive enough to study minute inhomogeneities, e.g., fluctuations in concentration of impurities (oxygen).

Abstract No. 44

On the Crystal Chemistry of Semiconductors

E. Mooser and **W. B. Pearson**, National Research Council, Ottawa, Ont., Canada

On the basis of the valence bond theory a relationship is derived between the position in the Periodic Table of the chemical components of semiconductors and their crystal structures. Rules are given with which the coordination configurations in a semiconductor can be predicted with some certainty. We also examine the influence of the presence in the valence shell of empty d orbitals on the crystal structure and the results of this investigation are applied to the discussion of semiconductors containing groups VB to VIIB elements only.

Abstract No. 45

The Electronic Structure of Compounds Formed between Group VB to VIIB Elements

E. Mooser and **W. B. Pearson**, National Research Council, Ottawa, Ont., Canada

Crystal structures and properties of compounds of the types $A_2^{V}B_3^{VI}$ and $A^{I}B_2^{VII}$ are discussed on the basis of the valence bond theory of semiconductors. A consistent bond scheme is proposed for these substances and the band structures derived from it show some interesting features deviating, in many cases, from the usual semiconductor band structure. Thus, in Bi_2Te_3, for instance, it is found that the energy gap between valence and conduction band is bridged by a d band of low state density, the electrons in this band showing a low mobility. A series of new ternary semiconductors of the type $A^{I}B^{III}C_2^{VI}$ is predicted.

Abstract No. 46

Semiconducting Compounds—A Challenge in Applied and Basic Research

A. C. Beer, Battelle Memorial Institute, Columbus, Ohio

The use of a number of semiconducting compounds in device applications are discussed for categories defined by the external field which produces a modulation of the carrier density or mobility. Included are applications based on response to electric fields, magnetic fields, thermal fields, photon energy, and thermal energy. The implications of recent investigations as regards band structure, states densities, charge carrier mobilities, crystal imperfections, and other basic characteristics are presented.

Abstract No. 47

Recent Studies of the Properties of PbS, PbSe, and PbTe

W. W. Scanlon, U. S. Naval Ordnance Lab., White Oak, Md.

The solid phase of PbS is shown to exist only over a composition range from about 10^{19} excess sulfur atoms to 10^{20} excess lead atoms. Controlled composition within this range is discussed. Optical absorption edges in the three compounds have been established. Direct and indirect transition energies, radiative recombination rates, and radiative recombination lifetimes have been evaluated. The lifetime is shown to be limited by lattice recombination processes in PbS with the lifetime varing inversely within the concentration of dislocations.

Abstract No. 48

Interdiffusion by the Vacancy Mechanism in Binary Ionic Semiconductors

R. F. Brebrick, Naval Ordnance Lab., Silver Spring, Md.

Interdiffusion in a binary ionic semiconductor is considered starting from the phenomenological equations of Wagner. A consistent kinetic treatment of the vacancy mechanism establishes the composition dependence of the ion mobilities. Using chemical potentials recently given by the author, an expression for the complete composition dependence of the interdiffusion constant is derived. This expression agrees with the asymptotic values given by Wagner. The theory is applied to the available data on lead sulfide.

Abstract No. 49

Production of 1/f Noise by Radiation in Lead Sulfide Cells

R. L. Williams, Defense Research Board, Canadian Armament Research and Development Establishment, Quebec, Canada

The noise spectrum of a lead sulfide cell can be changed from one which is dominantly generation-recombination to 1/f by irradiating the cell with short wave-length radiation. The surface properties of lead sulfide along with the depth of penetration of short wave-length radiation are used to explain the effect. The change in spectral form can be produced at room temperature and dry ice temperatures. The experiments indicate that the use of the term "radiation noise" is too restrictive.

Abstract No. 50

Preparation of Crystals of Hexagonal SiC

D. R. Hamilton, Research Lab., Westinghouse Electric Corp., Pittsburgh 35, Pa.

Crystals of hexagonal SiC have been prepared by a method similar to that of Lely.* In particular means of controlling crystal habit and nucleation have been introduced. Methods of preparation of relatively pure material are outlined, and some experiments on the growth of electroluminescent p-n junctions described. Some data are presented on the photoluminescence characteristics of a number of samples.

* J. A. Lely, *Ber. deut. keram. Ges.*, **32**, 229 (1955).

Abstract No. 51

High Pressure, High Temperature Growth of Cadmium Sulfide Crystals

W. E. Medcalf and **R. H. Fahrig**, Eagle-Picher Co., Miami, Okla.

A method was developed for growing cadmium sulfide crystals from the melt. Melting was carried out at pressures in excess of 100 atm and at temperatures greater than 1500°C. Single crystals weighing in excess of 100 g were grown. The crystals had desirable photovoltaic properties. High purity cadmium sulfide powder was produced by synthesis from elemental cadmium and sulfur which had been purified by zone refining and other metallurgical techniques.

Abstract No. 52

Carrier Transport Phenomena in Semiconductor Crystals

E. M. Conwell, Sylvania Electric Products Inc., Bayside, N. Y.

This paper reviews some of the recent developments relating to carrier transport, mainly in Ge and Si. The dependence of lattice mobility on temperature and electric field intensity has been found to disagree with theory. Proposed explanations for the disagreement, as well as other effects of high electric field, are discussed. Properties peculiar to relatively impure samples and/or low temperatures, such as impurity band conduction and anomalously large thermoelectric power, are considered also.

Abstract No. 53

Electron Mobility in Indium Phosphide*

M. Glicksman and **K. Weiser**, RCA Labs., Princeton, N. J.

The Hall mobility of electrons in InP has been observed as a function of temperature and of carrier concentration. A lattice mobility of 5000 $cm^2/v\text{-}sec$ at 290°K is calculated from these results, varing with temperature at least as rapidly as $T^{-2.1}$. The observations have been fitted by assuming a combination of lattice and ionized impurity scattering with an effective mass of the order of 0.05 m_e.

* This work was supported in part by the Air Force.

Abstract No. 54

Recombination of Carriers in InSb*

R. N. Zitter, **A. J. Strauss**, and **A. E. Attard**, Midway Labs., University of Chicago, Chicago, Ill.

Recombination of excess carriers in n- and p-type InSb below 200°K is shown to take place primarily via bound states in the forbidden gap. Activation energies, concentrations, and recombination parameters associated with these states are estimated from measurements of the dependence of photoconductive and photoelectromagnetic lifetimes on temperature, impurity concentration, and light intensity.

* This research was supported by the U.S. Air Force, through the Office of Scientific Research of the Air Research and Development Command.

Abstract No. 55

Avalanche Breakdown and Collector-Voltage-Saturation of Diffused Intrinsic Power Transistors

C. Huang, Sylvania Electric Products Inc., Woburn, Mass.

A theory is presented on the collector-voltage-saturation of a diffused intrinsic power transistor. Calculations are made for the distributions of carrier density, current density, and electrical potential in the emitter, base, and collector regions. The avalanche breakdown of this transistor is calculated based on Miller's data.* It is shown that a collector breakdown voltage of 1000 v is not incompatible with a saturation voltage of 1 v at a collector current of 10 amp.

* S. L. Miller, *Phys. Rev.*, 105, 1246 (1957).

Abstract No. 56

Effects of Radiation on Germanium and Silicon

G. C. Messenger and **J. P. Spratt,** Philco Corp., Philadelphia, Pa.

The effects of radiation-introduced defects on Ge and Si were obtained by irradiating transistors with neutrons from several different sources. The variation of transistor parameter with accumulated neutron dose shows that

$$\frac{1}{\tau_{eff}} = \frac{1}{\tau_{initial}} + \frac{\phi[\text{Neutrons/cm}^2]}{K}$$

	Lifetime damage constant K [neutrons/cm^2 $\times$ μ]
N Ge	$4.2 \pm 0.8 \times 10^{13}$
P Ge	$3.0 \pm 1.0 \times 10^{13}$
N Si	$1.1 \pm 0.4 \times 10^{13}$
P Si	$2.0 \pm 0.8 \times 10^{13}$

The recombination mechanism is of the Schottky-Read type with the important recombination site in p-Ge located 0.2 e.v. below the conduction band.

Abstract No. 57

Two New Transistor Switching Types

C. S. McCarthy, Jr., Philco Corp., Philadelphia, Pa.

This paper describes two new types of *P-N-P* Ge switching transistors. The first type is a symmetrically fabricated, homogeneous-base device, having large-area microalloy contacts. It is designed as a switch for core matrices in computer circuits. The second type (low-injection efficiency collector) was designed to minimize the minority-carrier storage time in the base region. This was accomplished by a surface-barrier-type collector. Pertinent design, fabrication, and performance data are presented.

Abstract No. 58

Factors Influencing Diffusion Processes

F. M. Smits, Bell Telephone Labs., Murray Hill, N. J.

Diffusion processes for the controlled introduction of impurities into semiconductors are determined by certain factors. A summary is given of these factors followed by a discussion of the experimental and theoretical knowledge about them. Included are the diffusion constant and its possible dependence on concentration, the effect of the initial conditions and the boundary conditions on the impurity distribution, and the role of undesirable impurities. Particular processes are mentioned only as representative for basic methods with emphasis placed on inherent advantages and limitations of such methods.

Abstract No. 59

Diffusion Concentration Profiles by Analog Computation

Worden Waring, Semiconductor Div., Raytheon Mfg. Co., Newton, Mass.

Use of an analog computer (REAC) to solve the diffusion equations gives solutions which take account of "out-diffusion" following initial "in-diffusion", "slumping" on reheating, and variation of the diffusion coefficient. The effects of such phenomena on junction locations and base widths of devices are found to be significant.

Abstract No. 60

Diffusion Control in Silicon by Carrier Gas Composition

C. J. Frosch and **L. Derick,** Bell Telephone Labs., Murray Hill, N. J.

A single heating process is described for producing controlled double diffused *n-p-n* structures in Si by changing the carrier gas type or composition during the diffusion. The process is shown to depend on the large changes in the volatility of compounds such as Ga_2O_3 at a given temperature in carrier gases of different type and composition. Data are presented for As_2O_3-Ga_2O_3 and Sb_2O_3-Ga_2O_3 diffusions to illustrate the control of layer thickness by heating first in wet N_2 and then in wet H_2. These diffused structures are shown to be suitable for the fabrication of high alpha transistors.

Abstract No. 61

Diffusion of Radioactive Antimony in Silicon

J. J. Rohan, J. K. Kennedy, and **N. E. Pickering,** Air Force Cambridge Research Center, Bedford, Mass.

Diffusion coefficients of Sb in Si obtained at several temperatures between 1200° and 1400°C are compared to values obtained via *p-n* junction techniques. A method is described for determining diffusion coefficients and surface concentrations from the integrated residual count rates of the 0.602 mev gamma of Sb-124, measured before and after removing successive 2-4 micron layers of Si perpendicular to the diffusion path. Low surface concentrations and relatively short anneal times minimize surface erosion.

Abstract No. 62

Diffusion into Silicon from Glassy Layers

J. E. Cline and **R. G. Seed,** Sylvania Electric Products Inc., Woburn, Mass.

The diffusion of boron into silicon from glassy layers containing the system K_2O-SiO_2-B_2O_3 was investigated. These glassy layers can be formed by dehydrating aqueous solutions; they are fluid at the diffusion temperature of 1200°C. Methods were developed for obtaining controllable initial concentrations and penetrations of diffusant. Uniformly flat junctions were obtained, apparently due to the solvent action of the glassy layers in preventing masking by silicon dioxide.

Abstract No. 63

Effects of Heat Treatment on Diffused Silicon Material

A. L. MacDonald and **W. J. Heinecke,** Raytheon Mfg. Co., Newton, Mass.

Two series of experiments are discussed which show the changes in bulk lifetime, resistivity, and diode characteristic as a function of heat treatment. All samples were heated at 1300°C for 20 hr. One series was cooled at a rate of 100°/hr to the desired temperature (1000°-300°C), and then quenched. The second series was quenched to the desired annealing temperature (700°-300°C) and the properties studied as a function of time. Attendant changes are presented.

Abstract No. 64

Semiconductor Surface Phenomena

A. Many, Sylvania Electric Products Inc., Bayside, N. Y. (On leave of absence from Hebrew University, Jerusalem, Israel)

This paper reviews recent results on the surface structure of semiconductors, especially Ge and Si, obtained from measurements of surface conductance, surface recombination velocity, field effect, etc. It is now well established that there are two distinct types of surface states referred to as slow and fast states. The characteristics of these states, such as their distribution in energy in the forbidden gap and their hole or electron capture cross section, for different surfaces are summarized and discussed.

Abstract No. 65

Effects of Certain Chemical Treatments and Ambient Atmospheres on Surface Properties of Silicon

T. M. Buck and **F. S. McKim,** Bell Telephone Labs., Murray Hill, N. J.

Measurements of surface conductivity, recombination velocity (S), and field-effect mobility were made on Si. The choice of chemical treatments and ambient atmospheres made it possible to explore a wide range in surface potential and S. With the treatments used, low S occurs when the surface is either strongly p-type or strongly *n*-type; S is increased by atmospheres which shift surface potential in toward the middle from these extreme conditions.

Abstract No. 66

Effect of Various Etches on Recombination Centers at Germanium Surfaces

George Wallis and **Shyh Wang,** Sylvania Electric Products Inc., Woburn, Mass.

Germanium samples were etched with CP-4, hydrogen peroxide, iodine A, silver, and electrolytic etches. The density, energy levels,

and capture probabilities of the surface recombination centers were measured before and after the etched samples were baked. Iodine A and electrolytic etch produce centers of type I; the remaining etches, centers of type II. On surfaces etched with iodine A, baking changes the type of centers to II. On surfaces etched otherwise, baking merely increases the density of the initial type of centers.

Abstract No. 67

Saturation Current in Germanium and Silicon Electrode

J. B. Flynn, Sylvania Electric Products Inc., Woburn, Mass.

The saturation currents observed in *n*-type Si and Ge anodes and *p*-type Si and Ge cathodes in certain aqueous electrolytic cells have been studied. With *n*-type Ge anodes in 1.35*N KOH*, the current is limited by bulk generation of carriers. *N*-type Si anodes in 5% HF shows that generation from the surface region is dominant. The cathodes (p-Si and Ge) show poorer saturation, but indicate contribution from surface generation.

Abstract No. 68

Theory of Electron Transfer Reactions at Semiconductor Electrodes

J. F. Dewald, Bell Telephone Labs., Murray Hill, N. J.

A general theory of electron transfer reactions at semiconductor electrodes is developed. Semiconductor electrodes are shown to differ from metal electrodes most importantly in (a) the ability of the electric fields to penetrate deep into the electrode, and (b) the existence of two, readily distinguishable kinds of electrons, i.e., valence and conduction band. Assuming nonradiative transitions, operation of the Franck-Condon principle and the absence of surface states, a relatively simple picture of the electron transfer processes is derived which gives the kinetic parameters for the hole and election currents in terms of the equilibrium properties of the electrode system.

Abstract No. 69

Experiments on Electron Transfer Reactions at the ZnO Electrode

J. F. Dewald, Bell Telephone Labs., Murray Hill, N. J.

Measurements of the kinetic parameters of several electron transfer reactions at single crystal zinc-oxide electrodes (*n*-type) are reported. Major dependences on semiconductor doping and on u.v. illumination are observed. The kinetics are similar in some respects to those observed on "valve" electrodes like Ta_2O_5, exhibiting strong dissymmetry between the anodic and cathodic processes. Interpretation of the data is made in terms of theory previously presented.

Abstract No. 70

Chemical Etching of Silicon, I. The System HF, HNO_3, N_2O

B. Schwartz and **H. Robbins,** Semiconductor Lab., Hughes Products, Los Angeles 45, Calif.

The kinetics of the dissolution of silicon in HF-HNO_3-H_2O solutions at 25°C are discussed. Experimental data cover the entire range of etching compositions which show measurable attack on a 111 silicon surface in a given time interval. Interpretation of the reaction mechanisms is discussed in relation to the data.

Abstract No. 71

Status of Semiconductor Process Technology

F. Biondi, Bell Telephone Labs., Murray Hill, N. J.

(No abstract received)

Abstract No. 72

On the Jet Etching of Germanium and Silicon

P. F. Schmidt and **D. A. Keiper,** Research Div., Philco Corp., Philadelphia, Pa.

The rate of jet-electropolishing of low resistivity *n*-Si is controlled by two factors: supply of injected minority carriers, and rate of dissolution of the SiO_2 film. On low resistivity *n*-Ge the applied electrostatic field can generate its own hole supply. Under certain conditions electropolishing is possible in complete darkness. Ge can also be jet-etched cathodically, the reaction product being GeH_4. This reaction does not take place on Si.

Abstract No. 73

Determination of Crystal Orientation by High Intensity Reflectograms

G. H. Schwuttke, Sylvania Electric Products Inc., Bayside, N. Y.

An instrument based on the light figure technique for optical orientation of Ge and Si is described which fulfills all requirements for a fast precision orientation of single crystals. The dependence of high intensity reflectograms on etching conditions is shown and standard etching specifications are given.

Abstract No. 74

Some Properties of Electroless Nickel Contacts to Silicon

Edwin Matovich, P. J. Heinle, and **J. E. McNamara,** Semiconductor Research Dept., Motorola, Inc., Phoenix, Ariz.

Electroless Ni contacts to Si were evaluated with respect to solderability, adherence, specific contact resistance, and ohmic character. These properties were investigated for *n*- and p-type Si having resistivities between 0.005 and 400 ohm-cm and various degrees of surface roughness. The effects on contact properties of plating in an ultrasonic bath and of annealing at temperatures up to 1000°C are discussed.

Abstract No. 75

The Use of Organo-Substituted Hydrolyzable Silanes on Silicon Devices

B. Schwartz, Semiconductor Lab., Hughes Products, Los Angeles, Calif.

Surface treating silicon devices with organo-substituted hydrolyzable silanes of the form R_{4-i} Si X_i (where R can be CH_3 C_2H_5, etc., and X can be Cl, OC_2H_5, and i = 1, 2, 3) results in improved characteristics of the device. Data are presented on the effect of "silaning" on reverse saturation current and channeling.

Abstract No. 76

Photolithographic Techniques as Applied to Semiconductor Devices

J. R. Nall and **J. W. Lathrop,** Diamond Ordnance Fuze Labs., Washington, D. C.

Techniques are described for the use of photosensitive coatings in the fabrication of semiconductor devices. The chemical, optical, thermal, and electrical characteristics of the coating are outlined and techniques of exposing and developing patterns are given. Application of photolithographic techniques to the specific problems of masking, vacuum deposition, electrodeposition, etching, and electrical insulation are discussed. Specific devices fabricated by photolithographic techniques are illustrated and their electrical characteristics presented.

ELECTROTHERMICS AND METALLURGY

Abstract No. 77

Review of Various Analytical Methods for Determination of Trace Impurities

L. Pepkowitz, Nuclear Materials and Equipment Co., Pittsburgh, Pa.

(No abstract received)

Abstract No. 78

Spectrochemical Methods for Analyzing High Purity Hafnium

T. A. Sullivan, R. W. Lewis, and **J. L. Potter,** Electrometallurgical Experimental Station, U. S. Bureau of Mines, Boulder City, Nev.

The Electrometallurgical Experiment Station of the United States Bureau of Mines at Boulder City, Nev., has been engaged in research for the production of high purity hafnium metal from off-grade hafnium sponge by electrolytic means. This paper deals with the spectrochemical methods developed for the analysis of this high purity metal. The metal is first converted to the oxide and the impurity elements are then determined spectrographically, using a silver chloride carrier technique.

Abstract No. 79

X-Ray Fluorescent Analysis of Tin in Titanium in the Range of 0.03-0.50% Tin

T. A. Sullivan, R. W. Lewis, and **L. Carpenter,** Electrometallurgical Experimental Station, U. S. Bureau of Mines, Boulder City, Nev.

The Analytical Laboratory of the Boulder City Station of the United States Bureau of Mines as a testing laboratory for compliance of titanium sponge to meet General Services Administration purchase specifications was faced with the problem of determining tin in titanium by a fast, accurate method. An x-ray fluorescent spectrographic method was developed, using the hardness button as a sample, that is both fast and accurate.

Abstract No. 80

Determination of Hydrogen in Titanium and Its Alloys—A Critical Review

T. D. McKinley, Research Div., Pigments Dept., E. I. du Pont de Nemours & Co., Inc., Experimental Station, Wilmington, Del.

Theory, operational characteristics, and indicated precision and accuracy of analytical methods based on vacuum extraction, equilibrium pressure, and combustion approaches are reviewed. At the present time vacuum extraction at 1400°C and the equilibrium pressure method are recommended for determination of hydrogen in titanium and titanium-rich alloys.

Abstract No. 81

Some Applications and Methods for Low Level Analysis of Specific Impurities in Metals

R. A. Wallace, T. G. Polanyi, and **John Roboz,** Central Research Labs., Sylvania Electric Products Inc., Bayside, N. Y.

Results on the mass-spectrometric analysis of tungsten and cathode nickel for potassium, and on silicon for boron, are presented. Data on preliminary work, using isotope-dilution techniques, are described. The relative ion yields for several chemical compound-surface ionizing systems were investigated in a single-filament surface ionization source. One system, at the relatively slow temperature of 650° ± 50°C, yields its major ionic species as singly charged, positive, elemental boron ions.

Abstract No. 82

Stress Corrosion Cracking of Austenitic Stainless Steels

J. J. Harwood, Office of Naval Research, Washington, D. C.

The factors influencing the susceptibility of austenitic stainless steels to stress corrosion cracking and the mechanisms which have been proposed are reviewed briefly. Environment, metallurgical structure, composition, temperature, time, surface condition, and stress are considered. General agreement exists about the conditions necessary to nucleate the crack, but the mechanism by which the crack propagates remains to be resolved. Methods of prevention are discussed and recent findings indicate the benefits of composition and impurity control.

Abstract No. 83

Mechanism of Stress Corrosion of Type 304 Stainless Steel

H. L. Logan, National Bureau of Standards, Washington, D. C.

(No abstract received)

Abstract No. 84

Stress Corrosion Cracking of Some Homogeneous Alloys Containing Nickel

H. R. Copson, Research Lab., International Nickel Co., Inc., Bayonne, N. J.

The results of some laboratory tests on the stress corrosion cracking of Fe-Cr-Ni alloys, or Fe-Ni alloys, and of Ni-Cu alloys are described. In each of these systems susceptibility to stress corrosion cracking seems to be present when the atomic percentage of the more noble constituent is between 0 and 50%, with the maximum susceptibility occurring at some intermediate percentage. Some thoughts on mechanism are included. Presumably susceptible alloys resist cracking in many environments because crack initiation is prevented by protection films, by rapid uniform attack, or in some other way.

Abstract No. 85

Stress Corrosion of Austenitic Stainless Steel in High Temperature Water

M. G. Fontana, Ohio State University, Ohio

(No abstract received)

Abstract No. 86

Caustic Stress Corrosion of Type 347 Stainless Steel

G. C. Wheeler and **E. Howells,** Knolls Atomic Power Lab., Schenectady, N. Y.

Stress corrosion tests of Type 347 stainless steel were made in mixtures of caustic-in-water and caustic-in-sodium at temperatures between 488° and 850°F, using various types of specimens. Transgranular cracking of the specimens occurred in both solvents over a wide range of temperatures and concentrations. In miniature boiler tests cracking was prevented by adding disodium phosphate to the boiler water at the rate of 1 part PO_4 to 4 parts caustic-anion.

Abstract No. 87

Cracking of Martensitic Stainless Steel under Conditions of Stress and Corrosion

F. Brown, Naval Research Lab., Washington, D. C.

(No abstract received)

Abstract No. 88

Review of Aqueous Electrolytic Techniques and Methods for Preparation of High Purity Metals

A. Brenner, National Bureau of Standards, Washington, D. C.

(No abstract received)

Abstract No. 89

Fused Salt Electrowinning and Electrorefining Methods

M. E. Sibert, Horizons Inc., 2891 E. 79 St., Cleveland, Ohio

A variety of metals which cannot be prepared by conventional smelting or aqueous reduction methods may be prepared in a high state of purity by fusion electrolysis. These include transition metals of Groups IV, V, and VI. Processing may be carried out by electrolytic decomposition of a metallic compound or by electrolytic refining of an impure metal through its employment as an anode. General process principles are described and illustrated. Advantages and limitations of these process types are discussed.

Abstract No. 90

Fused Salt Electrorefining of Hafnium Metal

D. H. Baker, Jr., J. R. Nettle, and **J. Heigel,** U. S. Bureau of Mines, Boulder City, Nev.

The U.S. Bureau of Mines Electrometallurgical Experiment Station at Boulder City, Nev., has, under the Atomic Energy Commission's sponsorship, attempted to apply the fused salt electrorefining techniques developed for titanium to off-grade hafnium sponge. This paper deals with the various electrolytes studied, and types and quality of deposits produced from these electrolytes. Hafnium metal with hardnesses as low as 130 BHN has been produced by this technique.

Abstract No. 91

Elemental High Purity Boron Preparation with Emphasis on Fused Salt Electrolytic Methods

E. W. Fajans, U. S. Borax and Chemical Corp., Anaheim, Calif.

(No abstract received)

Abstract No. 92

Fused Salt Electrorefining of Columbium Metal

E. C. Hirakis and **M. E. Sibert,** Horizons Inc., 2891 E. 79 St., Cleveland, Ohio

Attempts to purify crude columbium sponge by soluble anode electrolysis in fused salt electrolytes are described. Since small concentrations of oxygen are transported quantitatively to the cathode, the composition of the carbon reduced sponge is regulated so that a small excess of carbon is present. The crude anode material then contains a minimum of oxygen and a number of contaminants including carbon which are not transported electrolytically. The refined columbium is recovered as a crystalline powder.

Abstract No. 93

Electrorefining of Titanium

B. C. Raynes, Horizons Inc., 2891 E. 79 St., Cleveland, Ohio

(No abstract received)

Abstract No. 94

The Hydrogen Method for the Preparation of High Purity Tungsten and Rhenium

C. H. Toensing, Lamp Wire & Phosphors Dept., Lamp Div., General Electric Co., 21800 Tungsten Rd., Cleveland 17, Ohio

A brief review of the historical aspects of hydrogen reduction applied to tungsten oxides with emphasis on purity as well as the chemical equilibra, the thermodynamic properties and the kinetics of the reduction reactions are presented. The application of these data to the commercial production of pure tungsten metal powders along with process variables are discussed. The technical methods currently employed to produce pure rhenium metal powder are reviewed.

Abstract No. 95

Aqueous Methods for the Preparation of High Purity Metals

G. B. Wood, National Bureau of Standards, Washington, D. C.

The preparation of high purity metals by electrorefining from aqueous solutions is discussed. Specific cases where metals of high purity have been obtained by electrodeposition are reviewed, such as Cu, Fe, Cr, Ni, Ag, Au, etc. Reference

is made to high purity Al obtained from organic solutions.

Abstract No. 96

Preparation of Pure Chromium by a Vacuum Distillation Technique

W. H. Smith and **R. L. Hadley**, General Electric Co., Schenectady, N. Y., and Louisville, Ky., respectively.

Very high purity chromium was prepared by distillation in high vacuum. Alloys of Cr and Zr were prepared by arc melting, with Zr content ranging up to 10%. The Zr was added to tie up oxygen, nitrogen, sulfur, and carbon as nonvolatile impurities. During the evaporation of Cr from these alloys some reduction in metallic impurities was also effected. The Cr deposits obtained had an average hardness of 100 VPN. Most deposits were brittle at room temperature.

Abstract No. 97

Metallurgy of Uranium Refining

B. Blumenthal, Argonne National Lab, Lemont, Ill.

Metallurgical refining methods for uranium have been developed for three grades of uranium, each one meeting a specific purpose: reactor grade uranium, irradiated uranium, and high purity uranium. The various refining methods—vacuum melting, liquidation, oxidation, carburization, formation of intermetallic compounds, molten metal and salt extraction, bomb reduction, vapor decomposition, and fused salt electrolysis—are evaluated with respect to the efficacy which each operation permits for the preparation of a pure product. The evaluation is based on thermodynamic considerations, experimental data, and practical factors.

Abstract No. 98

Phase Equilibrium Study of the System Na_2WO_4-Na_2CO_3-H_2O

R. L. Pilloton and **G. E. Crawley, Jr.**, Metals Research Labs., Electro Metallurgical Co., Division of Union Carbide Corp., Niagara Falls, N. Y.

A phase equilibrium diagram representing the binary system Na_2WO_4-H_2O between −7.5° and +35°C was constructed. This curve shows the regions of stability of the dihydrate and decahydrate of sodium tungstate. There is a eutectic ice-$Na_2WO_4 \cdot 10H_2O$ at −7.5°C, a transformation point $Na_2WO_4 \cdot 10H_2O$-$Na_2WO_4 \cdot 2H_2O$ at 6.2°C, and a metastable eutectic point ice-$Na_2WO_4 \cdot 2H_2O$ at −13°C.

Phase equilibria for the ternary system Na_2CO_3-Na_2WO_4-H_2O between −8° and +35°C are represented by a tridimensional diagram. Polythermal projections showing temperature contours and crystallization paths are given. The regions of stability of the various salts are presented. Applications of the diagram for fractional crystallizations are discussed.

Abstract No. 99

Methods for Preparing Pure Scandium Oxide

F. H. Spedding, J. E. Powell, A. H. Daane, M. A. Hiller, and **W. H. Adams**, Institute of Atomic Research, Iowa State College, Ames, Iowa.

A review of the techniques for isolating scandium in a pure state is presented, including the newest cation-exchange methods. These methods include elution with ethlyenediaminetetraacetate and *N*-hydroxyethylethylenediaminetriacetate solutions and the use of copper and lead ions, respectively, as retaining ions which permit passage of scandium but retain rare earth ions. A new approach to opening thortveitite ore by treating with ammonium bifluoride and reducing the mixed metal fluorides to the metallic state with calcium is presented.

Abstract No. 100

On the Measurement of the Temperatures of Unenclosed Objects by Radiation Methods

A. Emslie and **H. Blau**, Arthur D. Little, Inc., Cambridge, Mass.

Both relative and absolute temperature measurement techniques that utilize emitted radiation are discussed and evaluated in terms of their application to the measurement of the temperature of nonplankian radiators. The accuracy of the various techniques is determined both under ideal and practical operating conditions. It is shown that accurate temperatures can be determined by using a two-color, two-temperature pyrometer without recourse to absolute measurement even when the spectral emissivity of the sample is unknown.

Abstract No. 101

Thermal Conductivity Measurement in the Temperature Range 1000°-3000°F

T. E. Waterman and **I. B. Fieldhouse**, Armour Research Foundation of Illinois Institute of Technology, Chicago, Ill.

A method is described for determining thermal conductivity of metallic and ceramic materials in the temperature range 1000°-3000°F. The method is one of unidirectional heat flow through a 6-¾ in. diameter, 1-½ in. thick disk of the material mounted between a heat source and a heat sink which also serves as a calorimeter. The rate of heat flow through the disk is obtained by collecting and weighing the condensed vapor which results from the boiling of a liquid in the calorimeter. The energy required to produce boiling is transferred through the disk to the calorimeter from a Mo heater. Temperature measurements are made with Pt-Pt 10% Rh butt welded thermocouples. Since numerous investigators have measured the thermal conductivity of Armco iron and show good agreement, it was used to calibrate the equipment. As a result of this calibration, the accuracy of the results obtained by the method are believed to be within ±2%.

Abstract No. 102

Micro Furnace for Thermal Microscopy and Studies at High Temperatures

W. A. Lambertson and **G. Lewis**, Research and Development Div., The Carborundum Co., Niagara Falls, N. Y.

A small laboratory furnace is described for use in microscopy and for determining chemical compatibility, wetting, sintering, and temperatures of apparent melting up to 3000°C (5430°F). The furnace shell is a water-cooled, 5-in. copper tee and is of such construction as to afford a controlled atmosphere. Water-cooled electrodes are designed to hold refractory metal strip heaters (either plain or with a wedge for better black body conditions) or special machined graphite heaters. Stepless power input is provided by a variac-controlled, saturable core reactor.

Abstract No. 103

Water-Stabilized Arc Tests on Nonmetallic Materials

M. Dank, R. A. Nelson, W. R. Sheridan, and **W. H. Sutton**, Missiles and Ordnance Systems Dept., General Electric Co., Philadelphia, Pa.

Preliminary evaluation of erosion rates on possible high temperature resistant materials have been carried out in a water-stabilized arc. General classes of materials tested include: graphites and impregnated graphites; ceramics, principally oxides; plastic-ceramic composites; and reinforced ceramics. Results on erosion rates as a function of power dissipated in the arc and time are given and a general ranking of these materials for high temperature use is discussed.

Abstract No. 104

Rigidity Relaxation in Recrystallized Tungsten Wires at Elevated Temperatures

I. Berlec, Lamp Development Dept., General Electric Co., Cleveland, Ohio

Rigidity relaxation of recrystallized tungsten filaments has been measured as a function of temperature and grain structure. Measurements were performed on various commercial grades of tungsten in the temperature range between 1000° and 3000°K. The apparatus is essentially a torsion pendulum operated in vacuum. The specimen under study is used as the suspension, and is heated by its own resistance.

Abstract No. 105

Strength of Titanium at 1300°-1600°C

E. Scala, Avco Corp., Lawrence, Mass.

Stress rupture data has been obtained for titanium at the nominal temperatures of 1300°, 1500°, and 1600°C. A linear relationship of log time vs. log stress was obtained for three different grades of unalloyed titanium; namely, RC-55 with 0.137% and 0.053% oxygen and Foote iodide titanium. The lower the original impurity content, the lower the stress rupture values. The slope of log time vs. log stress, however, remains essentially the same for all three grades of titanium at the three test temperatures. The equipment and techniques were established for operating creep and stress rupture tests at temperatures above 1500°C for materials affected by the absorption of oxygen, nitrogen, and carbon.

Abstract No. 106

The Activities of Refractory Metal Alloy Systems

Rudolph Speiser and **George St. Pierre**, Dept. of Metallurgical Engrg., Ohio State University, Columbus, Ohio

Under favorable circumstances the activities of the components of refractory metal alloy systems can be ascertained from the composition of the vapor effusing from the Knudsen cell containing the alloy. It can be shown that the absolute partial pressures need not be determined if sufficient experimental data are obtained to make a satisfactory extrapolation of the data to the pure component. This method can be used to determine the phase diagram of an n-ary alloy system.

Abstract No. 107

Vapor Pressure of Columbium

Rudolph Speiser, Dept. of Metallurgical Engrg., Ohio State University, Columbus, Ohio, **Paul Blackburn**, Westinghouse Research Lab., Pittsburgh, Pa., and **Herrick Johnston**, Herrick Johnston Associates, Columbus, Ohio

(No abstract received)

Abstract No. 108

Contributions of Zone Melting to High Purity Materials

F. H. Horn, Research Lab., General Electric Co., Schenectady, N. Y.

(No abstract received)

Abstract No. 109

Application of the Floating Zone Technique to Metals

R. L. Smith, J. L. Rutherford, and **M. Herman**, The Franklin Institute Labs. for Research and Development, Philadelphia 3, Pa.

The application of the floating zone method of purification to some crucible reactive metals is discussed. The use of RF melting in which the induction coil is placed either inside or outside of the protecting envelope is described. The advantages and disadvantages of purifying in a reducing or in an inert atmosphere and in a vacuum are discussed. The results of some mechanical properties of zone refined Fe, Ti, and Zr are presented.

Abstract No. 110

Tungsten Zone Melting by Electron Bombardment

R. G. Carlson, General Electric Co., Cleveland, Ohio

An apparatus for refining tungsten by the floating zone method is described. It consists of four components: vacuum system, power supply, cathode traversal assembly, and anode support. Power requirements for melting ⅛ in. diameter rods are found to be in the order of 500 w. As many as ten passes at different rates of travel have been made. Tungsten rods that are refined by this techique have relatively high ductility at room temperature, as determined by tensile and bend tests, and are of very high purity.

Abstract No. 111

Techniques and Results of Zone Refining Some Metals and Semiconducting Compounds

J. H. Wernick, K. E. Benson, D. Dorsi, and **J. J. Gillich**, Bell Telephone Labs., Inc., Murray Hill, N. J.

Techniques and results for zone refining Ag, Al, Sb, Au, Cu, Ni, Ti, V, and ternary semiconducting compounds are given. Boat and floating zone methods are discussed.

Abstract No. 112

Continuous Multistage Zone Melting of Silicon Tetraiodide

G. H. Moates and **B. Rubin**, Air Force Cambridge Research Center, Bedford, Mass.

A continuous multistage apparatus which separates purified and impurity-enriched silicon tetraiodide into separate receivers has been constructed. The continuous operation of this apparatus is based on the introduction of voids which travel the length of the enriching and stripping arms and which are filled in as they reach a reservoir. The design characteristics are based on the segregation coefficients of the impurities in the silicon tetraiodide, the length of the molten zones, the length of the voids, and the length of the arms.

Abstract No. 113

Principles and Application of the Iodide Process

A. C. Loonam, 70 E. 45th St., New York 17, N. Y.

The origin of the process, its development, and the elements to which it has been applied are reviewed; some of the fundamentals and methods of operation are discussed.

Abstract No. 114

The Iodide Process for High Purity Silicon Preparation

F. B. Litton, Research and Development Labs., Foote Mineral Co., Berwyn, Pa.

(No abstract received)

Abstract No. 115

Some Aspects of the Decomposition of Silicon Tetraiodide

A. F. Armington and **B. Rubin**, Air Force Cambridge Research Center, Bedford, Mass.

Silicon tetraiodide has been decomposed to silicon and iodine *in vacuo* with deposition on a single-crystal silicon substrate heated inductively. Effects of rate of passage of the vapor, vapor pressure of the iodide, and temperature of the substrate have been studied and results have been correlated with yield of silicon and rate of deposition.

Abstract No. 116

Zirconium Coating of Uranium by the Iodide Process

W. L. Robb, Knolls Atomic Power Laboratory, Schenectady, N. Y. (Present address: Research Lab., General Electric Co., Schenectady, N. Y.)

A method for coating uranium metal with a bonded layer of crystalline zirconium metal has been developed. It consists of thermally decomposing ZrI_4 vapors on the surface of uranium metal heated to about 1100°C in a good vacuum. Prior to coating, the uranium metal surface is cleaned by iodiding it. In this way a diffusion bond between the uranium and zirconium is obtained. Several methods for improving the bond and reducing the porosity of the crystalline zirconium coating are also reported.

Abstract No. 117

High Purity Silicon from Silicon Tetraiodide Purified by Solvent Recrystallization and Distillation

L. V. McCarty, Lamp Development Dept., General Electric Co., Cleveland, Ohio

This paper deals with the electrical properties of silicon prepared from silicon tetraiodide purified by recrystallization from solvents, by distillation in an all-quartz column, and by a combination of the two techniques. The silicon was deposited on hot tantalum or quartz at reduced pressure, and single crystals were prepared in quartz crucibles. Portions of the better samples have resistivities which correspond to a minimum of five to seventeen boron atoms per ten billion silicon atoms.

Abstract No. 118

Plating of Tungsten with Titanium and Zirconium by the Van Arkel-de Boer Process

H. T. Stephenson, Strong-Cobb Co., Cleveland, Ohio

(No abstract received)

Abstract No. 119

High Purity Crystalline Boron

D. R. Stern and **Lahmer Lynds**, American Potash & Chemical Corp., Whittier, Calif.

Vapor phase reduction of boron trichloride with hydrogen on electrically heated filaments in flow systems was investigated as a potential method for the preparation of high purity boron. Massive deposits of crystalline boron analyzing as high as 99.6% by direct chemical analyses were obtained. Purity of boron appeared to be a function of both filament diffusion and boron trichloride purity. Titanium filaments were found to be most satisfactory, since contamination due to titanium could be removed by chlorination at 300°C. X-ray diffraction studies indicated that titanium existed in solid solution with boron rather than as a boride.

INDUSTRIAL ELECTROLYTIC

Abstract No. 120

Electrodeposition of Adherent Titanium Coatings on Induction Heated Cathodes in Fused Salts

J. G. Wurm, B. J. Fortin, L. Gravel, and **R. J. A. Potvin**, Laval University, Quebec, Que., Canada

A new electrolytic method for the deposition of adherent coatings of titanium on steel cathodes is described. The procedure involves the use of fused alkali-halide baths com-

posed of eutectic mixtures of lithium, potassium or sodium iodides, bromides, chlorides, and fluorides, with a high frequency heated cathode and a soluble titanium anode. The bath composed of KI-KF performed best and deposited a very smooth and uniform titanium coating. Conversely, the bath composed of KI-NaI and TiI_4 (2-5%) yielded pure dendritic Ti and is therefore considered more suitable for an electrorefining process. Equipment and operating conditions are described and the microstructure of the coating produced is reported. A series of decomposition voltage curves are included and discussed, and the mechanism of the electrolytic reactions is studied in detail.

Abstract No. 121

Refining of Titanium Scrap by Fluoride Electrolysis

S. S. Carlton and **B. C. Raynes,** Horizons Inc., Cleveland 4, Ohio

The electrolytic recovery and purification of unalloyed titanium scrap by a semicontinuous operation is described. The process employs titanium scrap or off-grade primary metal as the soluble anode in an electrolytic cell containing a fused electrolyte of K_2TiF_6 in NaCl. Interstitial and metallic impurities remain as an inactive sludge and refined titanium is cathodically deposited as crystalline powder. Refined titanium with as-cast hardness of 80 Brinell has been produced in a pilot operation carried out at Horizons Inc.

Abstract No. 122

Report of the Chlor-Alkali Committee of the Industrial Electrolytic Division for the Year 1957

J. C. Cole, Diamond Alkali Co., Cleveland, Ohio, and **R. B. MacMullin,** R. B. MacMullin Associates, Niagara Falls, N. Y.

Production facilities for chlorine and alkali are reviewed with indications of market and end use patterns. New plants and expansions during the year and technical and outstanding commercial developments are noted.

Abstract No. 123

Effect of Gas Evolution on Current Distribution and Cell Resistance

C. W. Tobias, Dept. of Chemical Engrg., University of California, Berkeley, Calif.

It is known that when gaseous products are liberated at one or both electrodes of an electrolytic cell the effective resistance of electrolyte is larger than in the gas-free cell, and the volume concentration of gas generally increases in the direction of flow of gas. The resulting variation in effective conductance can cause nonuniform distribution of current density. Using a simple parallel vertical electrode arrangement as a model, theoretical predictions are made for gas holdup in the cell and current distribution along the electrodes.

Abstract No. 124

Investigations on the Structure of the Color Compound in Caustic

S. Wawzonek and **D. S. P. Eftax,** Dept. of Chemistry, State University of Iowa, Iowa City, Iowa

The material isolated by Heller from stubs of graphite anodes used in chlorine-caustic soda cells and shown by him to give the color in concentrated caustic soda has been reinvestigated. An extract from the stubs after treatment with nitric acid was found to consist of mellitic acid, pentacarboxychlorobenzene, a tetracarboxychlorobenzene of unknown configuration, and material of unknown structure which is the source of the color. The acids were formed during the treatment with nitric acid. The color forming material seems to be of high molecular weight and structurally more complex than proposed by Heller.

THEORETICAL ELECTROCHEMISTRY

Abstract No. 125

Relative Rates of Electromigration of Different Ions of the Same Charge across Permselective Membranes

Rex Neihof, Ruth McClintock, and **Karl Sollner,** Lab. of Physical Biology, National Institute of Arthritis and Metabolic Diseases, National Institutes of Health, Public Health Service, Bethesda, Md.

The theory of polyionic potentials permits the prediction of the ratios of the rates of electromigration across permselective membranes of any two species of critical ions coexisting in solution. These ratios are calculated from the bi-ionic potentials arising with the same pair of ions across the same membrane. This prediction was approximately confirmed in experiments with various combinations of critical ions in systems with cation selective and with anion selective membranes.

Abstract No. 126

Improved Protamine Collodion Membranes of Extreme Ionic Selectivity

Marc Lewis and **Karl Sollner,** Lab. of Physical Biology, National Institute of Arthritic and Metabolic Diseases, National Institutes of Health, Public Health Service, Bethesda, Md.

The use of purified protamine makes possible the preparation of permselective protamine collodion membranes of extreme ionic selectivity, the anion permeabilities in 0.1*N* KCl being 300-500 times greater than the cation permeabilities, and 4,000-11,000 times greater in 0.01*N* solution. Concentration potentials across these membranes agree with the calculated maximum potentials in potassium chloride cells up to 0.1*N*/0.05*N* within the meaningfulness of the method.

Abstract No. 127

Transport Processes in Ionic Membranes

K. S. Spiegler, Gulf Research & Development Co., Pittsburgh, Pa.

A simple molecular model representing an ion-exchange membrane in equilibrium with a salt solution is described. The transport processes caused by pressure, electrical, and osmotic forces are computed in terms of the volume concentrations of ions, water, and solid, and certain "friction coefficients" between these components. This analysis suggests approximations which reduce the number of the experiments needed for describing the transport properties of the membrane. Some applications of the theory are illustrated.

Abstract No. 128

Transport in Ion-Selective Membranes

M. A. Peterson and **H. P. Gregor,** Dept. of Chemistry, Polytechnic Institute of Brooklyn, Brooklyn, N. Y.

The exchange and transport of gegenions and of nebenions (excluded ions) in ion-selective membranes was measured as a function of the solution phase concentration, stirring at the membrane interface, and applied current density. From these results the thickness of the unstirred film and diffusion coefficients of ionic species were calculated. The boundary conditions which define film, membrane, or coupled film-membrane transport mechanisms as being rate controlling were determined.

Abstract No. 129

Transport against the Chemical or Electrochemical Gradient in Charged Porous Membranes

Richard Schlögl, Max-Planck-Institut für Physikalische Chemie, Bunsenstr. 10, Goettingen, Germany

Investigations on membranes of ion exchange material have shown that the essential types of transport mechanism are: diffusion, convection, and electrical transference. A quantitative treatment of a simple membrane model confirms the empirical laws governing negative and anomalous positive osmosis. It is also possible to construct a working model based on these three mechanisms which imitates the concentration of K^+ and dilution of Na^+ in living cells compared with the surrounding body fluid. The source of free energy required for this stationary state of non-equilibrium is the continuous production of an acid within the cell.

Abstract No. 130

Membrane Potentials in Isothermal and Nonisothermal Systems; A Detailed Investigation of a Single Membrane System

G. J. Hills and **P. W. M. Jacobs,** Dept. of Chemistry, Imperial College of Science and Technology, Imperial Institute Rd., London, S. W. 7, England

Results are presented of measurements of a number of interrelated properties of a single membrane system, cross-linked polymethacrylic acid. The properties include ionic and solvent transport numbers, isothermal and nonisothermal membrane potentials, ionic self-diffusion coefficients, and ionic conductances for a number of alkali metal counter-ions. These observations are correlated and interpreted in terms of both classical theory and the thermodynamics of irreversible processes.

Abstract No. 131

Electro-Osmosis and Electro-Convection in Ionic Membranes; Relation between Electro-Osmotic Transport, Ionic Conduction, Ionic Self-Diffusion, and the Degree of Counter-Ion Solvation

G. J. Hills and **P. W. M. Jacobs,** Dept. of Chemistry, Imperial College of Science and Technology, Imperial Institute Rd., London, S.W. 7, England

Accurate measurements of the electro-osmotic transport through a number of membranes have been made as a function of ion-type and of current density. The limiting equivalent electro-osmotic flow is discussed in terms of the difference between the two derived mobilities and the probable degree of counter-ion solvation.

Abstract No. 132

Phenomenological Electrochemistry of Membranes

George Scatchard, Massachusetts Institute of Technology, Cambridge 39, Mass.

The electrochemical study of membranes, particularly of physiological membranes, has been seriously hampered by the use of unrealistic models such as right-circular-cylindrical pores. An important contribution of the thermodynamics of irreversible processes is to show what parameters can be determined and which measurements are most suitable for determining them. To be useful the description must be simple. Most living membranes must be studied through over-all transport properties. Synthetic membranes may serve as models for which detailed mapping is possible.

Abstract No. 133

Streaming Potentials of Corundum in Organic Electrolyte Solutions

H. J. Modi and **D. W. Fuerstenau,** Dept. of Metallurgy, Massachusetts Institute of Technology, Cambridge, Mass.

The effect of certain 12-carbon anionic and cationic surface-active compounds on the zeta potential of corundum at different pH values has been evaluated from streaming potential measurements. These measurements, made under conditions of both positive and negative surface charge, indicate that long-chained ions are adsorbed appreciably only when the solid and organic ions are oppositely charged. An adsorption mechanism involving electrostatic attraction and hydrocarbon chain association is discussed.

Abstract No. 134

Interpretations of Experimental Donnan Equilibria Obtained with Polyphosphates

U. P. Strauss, School of Chemistry, Rutgers, The State University, New Brunswick, N. J.

The distribution of electrolyte across a semipermeable membrane has been measured for long-chain polyphosphates in aqueous solutions of lithium, sodium, potassium, and tetramethylammonium bromide. The conventional interpretation of the results in terms of an effective degree of ionization, α, leads to an increase of α with increasing electrolyte concentration. A more satisfactory interpretation is obtained by considering the Donnan equilibrium as arising from the volume excluded by the polyelectrolyte.

Abstract No. 135

Direct Determination of Adsorption of Organic Molecules at Solid Electrodes

B. E. Conway and **R. G. Barradas,** University of Ottawa, Ottawa 2, Canada

The necessity for development of a thermodynamically rigorous method for determination of adsorption of ions and molecules at *solid* electrodes is stressed. For molecules which absorb in a convenient spectral region, adsorption may be followed directly under thermodynamically reversible conditions at solid electrodes in a cell in which absorbance and potential measurements are made simultaneously. Results obtained with benzacridine, acridine, quinoline, pyridine, poly-4-vinyl pyridine, and their quaternary ions at Ag, Cu, and Ni, electrodes are described.

Abstract No. 136

Electrokinetic Measurements on Stainless Steel Capillaries

B. Levy and **A. R. Fritsch,** Radiation & Nucleonics Lab., Materials Engineering Dept., Westinghouse Electric Corp., East Pittsburgh, Pa.

Electrokinetic potentials of stainless steel in HCl, H_2SO_4, and $K_2Cr_2O_7$ solutions have been measured by the streaming current technique. Negative zeta potentials are obtained in H_2O and in low acid concentrations. The isoelectric acid concentrations occur between 10^{-4} and $10^{-3}N$. At higher concentrations positive potentials are obtained. $K_2Cr_2O_7$ adsorbs irreversibly at its isoelectric concentration of 10^{-4}M as evidenced by the inability of water washing to return the sample to its original negative zeta potential.

Abstract No. 137

Surface Conductance of Clays

H. van Olphen, Exploration and Production Research Div., Shell Development Co., 3737 Bellaire Blvd., Houston 25, Texas

On the basis of a particle network picture, the specific surface conductance of a clay may be calculated from the conductance of the clay gel. Since the charge density is known, the ion mobility parallel to the surface may be calculated. From particle interaction studies, it has been concluded that the counter ions are strongly adsorbed. Nevertheless, the surface mobility of the ions is relatively high, indicating a small barrier for lateral movement of the ions.

Abstract No. 138

Membrane Phenomena in Applied Geophysics

M. Gondouin, Schlumberger Well Surveying Corp., Ridgefield, Conn.

Natural membrane potentials and electrokinetic phenomena play an important role in oil exploration. These potentials observed in wells filled with mud result from the ion exchange properties of clays in shales and muds. From laboratory results an approximate expression for the shale membrane potential with mixed electrolytes is derived using simplifying assumptions. Data on shale electrokinetic properties are given and related to ionic transport numbers. Dependence of shale conductivity on frequency and polarization effects are discussed.

Abstract No. 139

Influence of Firing Conditions, Composition, and Screening Media on the Zeta Potentials of ZnS Phosphors as Related to Adherence to Glass Surfaces

B. Levy, Electron Tube Div., Radio Corporation of America, Lancaster, Pa. (Present Address: Radiation and Nucleonics Lab., Materials Engrg. Dept., Westinghouse Electric Corp., East Pittsburgh, Pa.)

Zeta potentials of ZnS phosphors were determined by the streaming potential technique as a function of firing conditions, flux, activation, phosphor coating, and type and concentration of screening media. Either positive or negative potentials are obtained depending on the type of coating. Certain firing conditions change the sign of the zeta potential. In all of these experiments a trend toward enhanced wet adherence with decreasing negative and increasing positive zeta potentials has been noted.

Abstract No. 140

The Electrokinetic Potential and Some Surface Tension Phenomena

L. B. Robinson, Ramo-Wooldridge Corp., P.O. Box 45144 Airport Station, Los Angeles 45, Calif.

The Onsager-Samaras theory (without adjustable constants) allows one to calculate the surface tension of an aqueous electrolyte solution as a function of concentration. It predicts that an electrolyte added to water would increase the surface tension. Precise measurements of the surface tension by the capillary rise method give an initial decrease and a minimum in the surface tension-concentration wave. Theory and experiment can be reconciled by taking the electrokinetic effects into account.

Abstract No. 141

Overvoltage and Catalysis

Paul Ruetschi, Research Dept., The Electric Storage Battery Co., Philadelphia, Pa.

Rate equations describing the kinetics of electrode reactions have hitherto been formulated without taking into account the activity of intermediate species on the electrode surface. The interaction of adsorbed species is shown to be of importance on overvoltage characteristics. Adsorbed species induce a contact potential change proportional to their concentration which is accompanied by a corresponding change in adsorption energy. The meaning of exchange currents is discussed and the rate equations are reformulated. The electronic or catalytic properties of the electrode material are reflected in these rate equations.

Abstract No. 142

Cathodic and Anodic Properties of Chlorine on Carbon and Graphite Surfaces*

John Aylward, Ernest Yeager, and **Frank Hovorka,** Dept. of Chemistry, Western Reserve University, Cleveland, Ohio

The cathodic and anodic polarization of the chlorine electrode have been measured on graphite and carbon surfaces in HCl solutions saturated with chlorine gas. Mechanisms for the anodic and cathodic processes are proposed on the basis of the experimentally determined Tafel slopes and the stoichiometric number calculated from polarization measurements at low current densities. The mechanism of the anodic process appears to be complex as indicated by a change in the Tafel slope with changing HCl concentration.

* Research supported by the Office of Naval Research under Contract Nonr 581(00).

Abstract No. 143

Electrode Potentials of Titanium-Oxygen Alloys

R. S. Dean, I. Hornstein, and **W. W. Gullett,** Chicago Development Corp., Riverdale, Md.

The value of electrode potentials of titanium-oxygen alloys as measured against standard titanium samples in molten salt electrolytes have a definite relation to the oxygen content of the alloy. The smooth relationship between emf and oxygen content in the beta phase indicates that the technique may be used to determine oxygen contents of alloys containing less than 0.15% oxygen. The effects of alloying elements and impurities on the emf measurements have also been investigated.

Abstract No. 144

Mechanisms of Hydrogen-Producing Reactions on Palladium, V. The Deuterium-Palladium System

Sigmund Schuldiner and **J. P. Hoare,** Naval Research Laboratory, Washington, D. C.

Anodic and cathodic polarization curves for the α-D-Pd system were determined on a Pd bi-electrode. The experimental equilibrium potential of the $(Pd\text{-}D)_x/D^+$ electrode was found to be 0.029 ± 0.001 v. The rate $(-di/d\eta)$ of the over-all deuterium-producing reaction on an α-Pd-D electrode surface in the linear η vs. i region was found to be about one-half that of the hydrogen-producing reaction on α-Pd-H. At constant overvoltage, the rate of diffusion of hydrogen through the bi-electrode ranged from 2.2 to 1.06 times faster than deuterium, depending on the polarizing current density. It was also found that at low current densities 90% of the deuterium formed on the cathode side diffused through the bi-electrode and was ionized on the anode side.

For a β-deuterium-palladium cathode-diaphragm, it was shown that the reaction mechanisms were the same as for a β-hydrogen-palladium diaphragm. A calculation was made which showed that, at a given atomic concentration gradient, the rate of diffusion of hydrogen through a β-Pd diaphragm was $2^{1/2}$ times faster than that of deuterium.

Abstract No. 145

Double Layer Structure and Electrode Processes, I. Salt Effect

Manfred Breiter, Marcos Kleinerman, and **Paul Delahay,** Dept. of Chemistry, Louisiana State University, Baton Rouge, La.

Ideas originally advanced by Frumkin and co-workers on the effect of the double layer structure on electrode processes are applied and extended to the following problems: (a) influence of foreign salts on the exchange current for slow and fast reactions; (b) complications resulting from control of ionic strength rather than ionic charges; (c) possible error in the determination of transfer coefficients for reactions occurring near the point of zero charge. Detailed experimental results are presented.

Abstract No. 146

Double Layer Structure and Electrode Processes, II. Discharge of Certain Metallic Complexes

Paul Delahay and **Carl Weis,** Dept. of Chemistry, Louisiana State University, Baton Rouge, La.

Experimental determination of kinetic data by electrochemical relaxation methods for chemical reactions coupled with electrochemical reactions is affected by the double layer structure when ions having charges of the same sign are involved. Correction can be made when the chemical reaction occurs essentially in a layer which is appreciably thinner than the diffuse double layer. The effect of foreign salts on kinetic data can then be interpreted quantitatively. Experimental data are presented for the study of the reduction of several complexes by the current-step (galvanostatic) method.

Abstract No. 147

Schlieren Studies of Concentration Gradients at a Cu/HCl Anode

R. S. Cooper, University of Illinois, Urbana, Ill. (Present Address: University of California, Los Alamos Scientific Lab., Los Alamos, N. Mex.).

Schlieren optical techniques were applied to the study of the anolyte at a Cu/HCl anode during current transients. Both the space and time dependence of the concentration gradients were observed quantitatively and correlated to the electrochemical processes occurring at the anode. The development and relative importance of ionic diffusion and natural as means of mass transport was studied under various conditions.

Abstract No. 148

The Nature of the Current Flow at or Between Cylindrical Electrodes*

R. D. Barnard and **S. M. Skinner,** Case Institute of Technology, Cleveland 6, Ohio

Solid-state thermodynamic equations of electrical current flow of the majority carrier in nonmetallic materials are solved in cylindrical coordinates for the case in which external potential is applied to the electrodes. Current, charge transfer at boundary, and inner potential are dependent both on the nature and separation of electrodes and on the electrode curvature. Current is nonlinear with voltage, and rectification is possible. Mechanical and electrical quantities related to the current are considered.

* With the support of the Office of Ordnance Research.

Abstract No. 149

Electromotive Force Measurements in Cerium-Cerium Chloride Liquid Systems

S. Senderoff and **G. W. Mellors,** Chemistry Div., Research Labs., National Carbon Corp., A Division of Union Carbide Corp., P.O. Box 6116, Cleveland 1, Ohio

The emf of the cell $Ce|CeCl_3(1\text{-}x)\ Ce(x)||CeCl_3|Cl_2$ (graphite) has been measured over a temperature range from the melting point of $CeCl_3$ to about 950°C. Preliminary conductance measurements indicate that the saturated solution of cerium in cerium chloride is an ionic conductor. The potential results indicate the presence of a subhalide, $Ce^+[CeCl_4]^-$, in which both monovalent and trivalent cerium exist. Further, it is suggested that cerium chloride may exist in a highly associated state in which the following formula may represent the dominant species, viz., $[CeCl_3]^+[CeCl_4]^-$. The addition of cerium to this system may result in the reduction of the less highly complexed cation as follows:

$$[Ce^{3+}Cl_3]^+\,[Ce^{3+}Cl_4]^- + Ce \rightarrow 3/2\ Ce^+\,[Ce^{3+}Cl_4]^-$$

In the course of the work a reversible chlorine electrode, satisfactory at temperatures up to 950°C, was developed.

Abstract No. 150

Activities of $NiCl_2$ from EMF Measurements in Molten LiCl-KCl

R. D. Walker, Jr., and **D. E. Danly,** Dept. of Chemical Engrg., University of Florida, Gainesville, Fla.

Activities of $NiCl_2$ dissolved in fused LiCl-KCl have been estimated from emf measurements in the temperature range 500°-700°C. Activity coefficients based on a standard state of pure liquid $NiCl_2$ increase with both temperature and solute concentration, and indicate strong complexing of $NiCl_2$. Emf and x-ray evidence indicate that the solid separating from a melt of LiCl-KCl-$NiCl_2$ differs from the original components; the compound K_2NiCl_4 is postulated.

Abstract No. 151

Electropolishing Silicon in Hydrofluoric Acid Solutions

D. R. Turner, Bell Telephone Labs., Inc., Murray Hill, N. J.

Silicon is electropolished in HF solutions if a critical current density is exceeded. Below the critical c.d., Si dissolution is largely divalent and a thick solid layer forms. This film is unstable and reacts slowly with the electrolyte to form tetravalent Si and H_2. In the electropolishing region, Si dissolution is mainly tetravalent with the formation of a very thin high resistance type of film. Experimental results on the effect of HF concentration and temperature indicate that elec-

tropolishing begins when the HF concentration at the Si becomes diffusion limited.

Abstract No. 152

Thermodynamics of Electron Atmospheres at Interfaces*

S. M. Skinner, Case Institute of Technology, Cleveland 6, Ohio

The thermodynamics of the final charge equilibrium at the interface between two different materials is discussed in terms of the chemical and electrical properties of the materials. The kinetics of the attainment of equilibrium is developed, and a number of practical applications are treated in detail, including the charging of dielectric and polymer surfaces, destaticization, and charge transfer during frictional sliding contact.

* With the support of the Office of Ordnance Research.

Abstract No. 153

Codeposition of Nickel and Hydrogen from Simple Aqueous Solutions

John Yeager, (Present address: National Carbon Research Labs. Parma Ohio), **J. P. Cels,** (Present address: The Kemet Co., Cleveland, Ohio), **Ernest Yeager,** and **Frank Hovorka,** Dept. of Chemistry, Western Reserve University, Cleveland, Ohio

The codeposition of nickel and hydrogen has been studied in chloride and sulfate solutions and the individual polarization curves determined. Nickel polarization has a Tafel slope of 0.10 and is independent of pH and anion type at constant nickel ion activity. Hydrogen overvoltage at constant pH is independent of anion type with a Tafel slope of 0.12. Hydrogen and nickel deposition exhibit no appreciable interdependence. Nickel polarization data are explained in terms of the transfer of a nickel ion from the solution across an unsymmetrical potential energy barrier to the metal phase.

Abstract No. 154

Effect of Addition Agents on Tungsten Codeposition

J. S. Sallo and **R. D. Fisher,** Research Div., National Cash Register Co., Dayton 9, Ohio

Trace amounts of certain compounds containing the C-S functional group prevent the codeposition of tungsten with Fe, Ni, or Co. Results indicate that the addition agents act through a complexation mechanism. The structure of the nickel-tungsten deposit, as determined by x-ray diffraction, does not agree with the structure predicted by the catalytic reduction mechanism of codeposition. Both the x-ray data and the prevention of codeposition can be explained by either a complexation mechanism of codeposition or by a modified form of the catalytic reduction mechanism.

Abstract No. 155

Anodic Oxidation of Zinc and a Method of Altering the Characteristics of the Anodic Films

H. Fry and **Marjorie Whitaker,** British Non-Ferrous Metals Research Assoc., Euston St., London N. W. 1, England

Preliminary work on anodizing zinc in a variety of alkaline solutions led to some smooth white or gray films. A detailed study was made of the anodic oxidation of zinc and zinc alloys in one electrolyte, the results of which suggest similarities but also some differences between anodic films on Al and on Zn. Autoclaving in silicate solutions improved the resistance to corrosion and abrasion and changed the chemical composition of the anodic films without altering their appearance greatly.

Abstract No. 156

Anodic Dissolution of Magnesium in Aqueous Solution

Richard Glicksman, RCA Labs., Princeton, N. J.

(No abstract received)

FALL MEETING

at the

Chateau Laurier

OTTAWA, ONT., CANADA

September 28, 29, 30, and October 1 and 2, 1958

Sessions probably will be scheduled on

Batteries
Corrosion
Electrodeposition (including symposia on "Electrodeposition on Uncommon Metals" and "Chemical and Electropolishing")

Electronics—Semiconductors
Electro-Organics
Electrothermics and Metallurgy

Abstracts for the Fall Meeting (*not exceeding 75 words in length*) must reach the Secretary's Office, 1860 Broadway, New York 23, N. Y., *not later than June 2, 1958* in order to be included in the program.

Indicate on abstract for which Division's symposium the paper is to be scheduled.

INDEX TO AUTHORS

(The number in the right hand column is the abstract number used in the Technical Program and in the Abstracts.)

	Abstract No.
Adams, W. H.	99
Alnutt, D.	17
Apple, E. F.	32
Armington, A. F.	115
Arnold, G. W.	26
Attard, A. E.	54
Aven, M.	33
Aylward, John	142
Bain, St. John	14
Baker, D. H., Jr.	90
Banks, E.	25
Barnard, R. D.	148
Barradas, R. G.	135
Bartels, B. E.	31
Beer, A. C.	46
Benson, K. E.	111
Berlec, I.	104
Biondi, F.	71
Blackburn, Paul	107
Blau, H.	100
Blumenthal, B.	97
Brand, B. G.	16
Brebrick, R. F.	48
Breiter, Manfred	145
Brenner, A.	88
Brophy, V. A.	36
Brown, F.	87
Buck, T. M.	65
Buhrer, C.	25
Butler, K. H.	29
Calderwood, G. C.	13
Carlson, R. G.	110
Carlton, S. S.	121
Carpenter, L.	79
Cels, J. P.	153
Chapman, J. J.	11
Cline, J. E.	62
Cole, J. C.	122
Conway, B. E.	135
Conwell, E. M.	52
Cooper, R. S.	147
Copson, H. R.	84
Crawley, G. E., Jr.	98
Daane, A. H.	99
Dank, M.	103
Danly, D. E.	150
Dean, R. S.	143
Delahay, Paul	145, 146
Derick, L.	60
Dewald, J. F.	68, 69
DiVita, S.	3, 4
Dorsi, D.	111
Dropkin, J. J.	38
Economos, George	7
Eftax, D. S. P.	124
Eichbaum, B. R.	6
Emslie, A.	100
Fahrig, R. H.	51
Fajans, E. W.	91
Fieldhouse, I. B.	101
Fischer, W. H.	1
Fisher, R. D.	154
Flynn, J. B.	67
Fontana, M. G.	85
Fortin, B. J.	120
Frankl, D. R.	28
Frisco, L. J.	11
Fritsch, A. R.	136
Frosch, C. J.	60
Fry, H.	155
Fuerstenau, D. W.	133
Gillich, J. J.	111
Ginther, R. J.	26
Glicksman, M.	53
Glicksman, Richard	156
Goldberg, Paul	30
Gondouin, M.	138
Gravel, L.	120
Gregor, H. P.	128
Gullett, W. W.	143
Hadley, R. L.	96
Hamilton, D. R.	50
Hannahs, W. H.	18
Haroldson, A. H.	19
Harrison, D. E.	22
Hartman, D. K.	40
Harwood, J. J.	82
Heigel, J.	90
Heinecke, W. J.	63
Heinle, P. J.	74
Herman, M.	109
Herold, P. G.	24
Hiller, M. A.	99
Hills, G. J.	130, 131
Hirakis, E.	92
Hoare, J. P.	144
Horn, F. H.	108
Hornstein, I.	143
Hovorka, Frank	142, 153
Howells, E.	86
Huang, C.	55
Hummel, F. A.	22, 23
Isenberg, C. R.	42
Jacobs, P. W. M.	130, 131
Johnston, Herrick	107
Jones, R. O.	37
Kastner, J.	33
Katnack, F. L.	23
Keck, P. H.	43
Keiper, D. A.	72
Kennedy, J. K.	61
Kleinerman, Marcos	145
Klick, C. C.	20
Lambertson, W. A.	102
Larsen, L. V.	9
Lathrop, J. W.	76
Levy, B.	136, 139
Lewis, G.	102
Lewis, Marc	126
Lewis, R. W.	78, 79
Litton, F. B.	114
Logan, H. L.	83
Loonam, A. C.	113
Lynds, Lahmer	119
MacDonald, A. L.	63
MacMullin, R. B.	122
Many, A.	64
Matovich, E.	74
McCarthy, C. S., Jr.	57
McCarty, L. V.	117
McClintock, Ruth	125
McGahan, J. J.	5
McKim, F. S.	65
McKinley, T. D.	80
McNamara, J. E.	74
Medcalf, W. E.	51
Mellors, G. W.	149
Messenger, G. C.	56
Moates, G. H.	112
Modi, H. J.	133
Mooser, E.	44, 45
Nall, J. R.	76
Neihof, Rex	125
Nelson, R. A.	103
Nettle, J. R.	90
Pearson, W. B.	44, 45
Pepkowitz, L.	77
Peters, T. E.	36
Peterson, M. A.	128
Pickering, N. E.	61
Pilloton, R. L.	98
Polanyi, T. G.	81
Porbansky, E. M.	41, 42
Potter, J. L.	78
Potter, R. M.	33
Potvin, R. J. A.	120
Powell, J. E.	99
Prener, J. S.	34
Raynes, B. C.	93, 121
Robb, W. L.	116
Robbins, H.	70
Robinson, L. B.	140
Roboz, John	81
Rohan, J. J.	61
Rothschild, S.	37
Rubin, B.	112, 115
Ruetschi, Paul	141
Rutherford, J. L.	109
Sallo, J. S.	154
St. Pierre, G.	106
Samelson, L. R.	12
Scala, E.	105
Scanlon, W. W.	47
Scatchard, George	132
Schlögl, Richard	129
Schmidt, P. F.	72
Schuldiner, Sigmund	144
Schulman, J. H.	26
Schwartz, B.	70, 75
Schwuttke, G. H.	43, 73
Seed, R. G.	62
Senderoff, S.	149
Sheridan, W. R.	103
Sibert, M. E.	89, 92
Skinner, K. G.	8
Skinner, S. M.	148, 152
Smith, R. L.	109
Smith, W. H.	96
Smits, F. M.	58
Smoke, E. J.	3, 4
Sollner, Karl	125, 126
Spedding, F. H.	99
Speiser, Rudolph	106, 107
Spiegler, K. S.	127
Spratt, J. P.	56
Stephenson, H. T.	118
Stern, D. R.	119
Strauss, A. J.	54
Strauss, U. P.	134
Strock, L. W.	36
Sullivan, T. A.	78, 79
Sutton, W. H.	103
Thomas, M. J. B.	39
Thornton, W. A.	27
Tobias, C. W.	123
Toensing, C.	94
Trumbore, F. A.	41, 42
Turner, D. R.	151
Ullman, F. G.	38
van Olphen, H.	137
Varga, Elmer	15
Wachtel, A.	21
Wahlig, C. F.	35
Walker, Henry	2
Walker, R. D., Jr.	150
Wallace, R. A.	81
Wallis, George	66
Wang, Shyh	66
Waring, Worden	59
Wasserman, M. S.	31
Waterman, T. E.	101
Wawzonek, S.	124
Weil, D. J.	34
Weinreich, O. A.	43
Weis, Carl	146
Weiser, K.	53
Wells, F. H.	10
Wernick, J. H.	111
Wheeler, G. C.	86
Whitaker, Marjorie	155
Whitley, J. H.	10
Williams, R. L.	49
Wood, G. B.	95
Wurm, J. G.	120
Yeager, Ernest	142, 153
Yeager, John	153
Zitter, R. N.	54

Perkin Medal Award to W. J. Kroll

William J. Kroll, consulting electrochemist and metallurgist, Corvallis, Ore., has been awarded the Perkin Medal, one of the highest honors in American industrial chemistry. Announcement of the award was made by Monroe E. Spaght, Chairman of the Award Jury and Executive Vice-President of the Shell Oil Co. Formal presentation of the medal took place on January 1, 1958, following a dinner in Dr. Kroll's honor at the Waldorf-Astoria Hotel, New York City.

The Jury of Award of the Perkin Medal consists of representatives of the American Chemical Society, the American Institute of Chemical Engineers, The Electrochemical Society, and the American Section of the Société de Chimie Industrielle, in addition to officers of the American Section of the Society of Chemical Industry, under whose auspices the medal is awarded.

The Perkin Medal was founded in 1906 in honor of Sir William Perkin, in recognition of his discovery, 50 years before, of the first synthetic dye. It is awarded annually to a member of the chemical profession residing in the United States, for outstanding work in applied chemistry.

Dr. Kroll is eminently suited as a Perkin medalist because he embodies all the qualifications which are the prerequisite. By his own creative work, functioning almost as a one-man research team, he has made real contributions to the technical aspect of applied chemistry. His qualifications can best be expressed in his own words*:

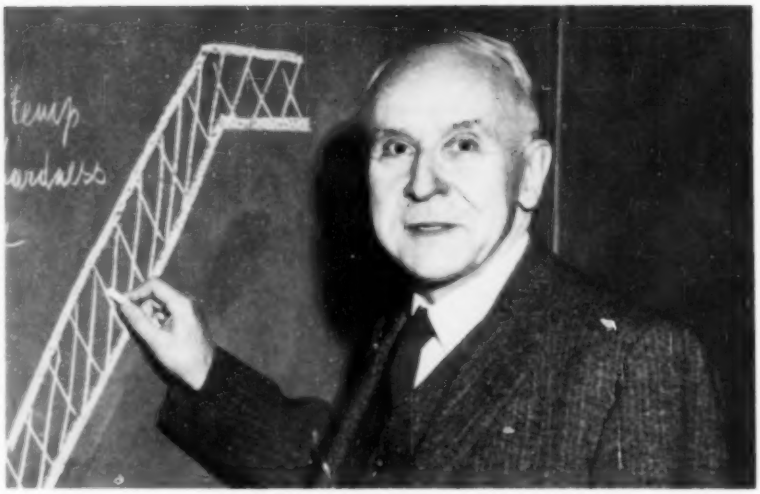

W. J. Kroll, 1958 Perkin Medalist

"When in 1937 I set out alone with my rather limited means to solve the big problem of finding a cheap process of production for ductile titanium, I was a visionary, and I was considered as such by the outstanding metallurgists of the United States when I visited this country a year later. It was the enjoyment of discovery, the curiosity to know what is around the corner, which motivated my action and let me get over hardships and relative poverty, until final success was achieved. This example should refute all those who claim that today individual research—as was done by Pasteur or Fleming—is dead, and that it has been replaced by the collectivist planned work of teams or groups of salaried men, who operate the scientific machinery in private and government laboratories in hopes of discovering something under the command of a director who, although usually removed from the observation of the experiments, is supposed to do the thinking. I do not agree with this claim. The free individual who accepts risks and years of sacrifice and who is driven by religious devotion to his task and by the spiritual joy which invention procures, in much the same way as is the artist by aesthetic achievements, can still today defy and outsmart the captive salaried research performed at extravagant cost in palatial laboratories where frequently nothing else is wanting but ideas. Money alone does not create or invent and the free individual still has great chances of success because his ideas originate in that same mind that commands the activity of his hands, while his thoughtful eyes watch the things that happen. This is the philosophy behind the invention of ductile titanium."

Dr. Kroll stands out as one of the

* W. J. Kroll, "How Commercial Titanium and Zirconium Were Born," *J. Franklin Inst.*, 260, No. 3, September 1955.

great original chemists and metallurgists of our time. His best-known contribution is the titanium process which bears his name. With limited means and without encouragement from industry, he worked out the process of economical production of ductile titanium. Present investments in titanium industries, totaling hundreds of millions of dollars, are based on his process.

Equally impressive are his numerous accomplishments in other fields of nonferrous metallurgy. His work in charge of the zirconium project of the U. S. Bureau of Mines resulted in large-scale production of zirconium metal for atomic reactor applications. The same process was adapted to the commercial production of titanium in large quantities. Among his developments in earlier years are: a calcium-barium lead alloy for bearings, known by the name "Lurgimetall"; methods for debismuthizing lead; a hyper-eutectic 23% Si-Al alloy, known as "Alasil" in Germany, used for pistons in combustion engines; a magnesium base alloy used in super chargers to aviation motors. Hundreds of ideas destined to have an effect in all metallurgy were reduced by Dr. Kroll to patents and writings. Some of these are: vacuum dezincing of lead; age hardening of aluminum-silver alloys; aging of lithium-aluminum zinc alloys; age hardenable-aluminum alloys; reduction of anhydrous beryllium fluoride with magnesium. The forerunner of the present transistor was Dr. Kroll's discovery that germanium crystals could replace silicon for radio detectors.

He has a long list of accomplishments in the field of vacuum metallurgy. He was one of the first to make high purity calcium. His knowledge of vacuum purification was extended to the purification of silicon, copper, iron, chromium, beryllium, and alloys of copper, tin, and lead.

His numerous papers and patents are distributed through Germany, France, England, and the United States.

Dr. Kroll was born in Esch, Luxembourg, in 1889. He studied at the Technische Hochschule in Charlottenburg, Germany, where he received the Doctor of Engineering Degree in 1917. His thesis was written on the preparation of pure boron.

In 1940 he immigrated to the United States, becoming a consultant for Union Carbide Research Labs. in Niagara Falls, N. Y., and from 1945 to 1950 he was associated with the U. S. Bureau of Mines in Albany, Ore. In 1950 he established a home and private consulting practice in Corvallis, Ore.

Other awards to Dr. Kroll include: the Francis J. Clamer Medal, The Franklin Institute of Philadelphia, 1954; the James Douglas Medal, American Institute of Mining Engineers, 1954; the Heyn Award, Deutsche Gesellschaft für Metallkunde; the Albert J. Sauveur Award, American Society for Metals, 1955; Honorary Degree, University of Grenoble, 1955.

He has been active in The Electrochemical Society since 1929.

Section News

Boston Section

At the ninth meeting of the Boston Section, on November 19, Dr. Abner Brenner, Chief of the Electrodeposition Section, National Bureau of Standards, spoke on "Electrodepcsition Research in Progress at the National Bureau of Standards."

He discussed results from a series of interesting research projects, including electroless plating, hydrogen embrittlement of steel, concentration polarization, the protection of molybdenum oxidation at elevated temperatures, and electrochemical calorimetry.

The talk, illustrated by slides, was followed by questions from the floor and discussions of the various topics.

Worden Waring,
Secretary-Treasurer

San Francisco Section

The second Section meeting for 1957-58 was held on November 27, 1957 at the University of California Faculty Club. The technical program featured a talk by Dr. Harold T. Fullam, Stauffer Chemical Co., on the Production of Metal Borides and Silicides by Fused Salt Electrolysis.

Most of the emphasis was on the electrolytic production of TiB_2. The speaker first reviewed various methods used to prepare compounds of this type, including an electrolysis of oxide melts which he found impossible to duplicate. However, TiB_2 can be deposited from melts containing K_2TiF_6, KBF_4, and KCl, using either graphite or stainless steel cathodes. Depending on conditions, the cathodic product may take the form of loose crystals or thin, adherent deposits.

Dr. Fullam measured decomposition potentials of the individual melt components and of selected mixtures, in an effort to get at the cathode mechanism. From his studies, he deduced that the titanium component of TiB_2 comes from K_2TiF_6 by direct cathodic reduction, whereas the boron is made by a secondary reaction involving potassium. As further support for the proposed mechanism, he pointed out that no TiB_2 can be obtained if Na salts are used instead of the K compounds.

The speaker discussed the effects of temperature, melt composition, and current density upon current efficiency and product composition. Highest cathodic efficiencies (about 50%) were obtained from melts containing about 70% KCl, 15% K_2TiF_6, and 15% KBF_4 by weight, at 720°-730°C. Purity of the TiB_2 often exceeded 99%.

By the use of appropriate salts, the borides of Zr, Cr, and Th were also prepared. When KBF_4 was replaced by K_2SiF_6, the corresponding silicides were obtained at the cathode.

Morris Feinleib

Washington-Baltimore Section

The second regular meeting of the 1957-58 year was held on November 7, 1957 at the National Bureau of Standards. The speaker was Herbert B. Reed, Jr., of the Naval Ordnance Lab., and his topic was "The Theory and Application of the Solion."

The solion is an electrochemical device which may replace vacuum tubes and transistors for direct-current or low-frequency applications. Its operation depends on the movements of ions through a solution and it is based on concentration polarization. There are five elementary types of solions depending on the use to which they are put. Phys-

ically, the solion consists of a small, plastic cylinder divided into sections and containing a solution and electrodes. When the unit is stimulated by light, heat, sound, pressure, or movement, the resultant hydraulic flow within the cell produces a current output. Any reversible redox system can be used in the solion. The speaker described a system consisting of platinum electrodes immersed in a solution of iodine in potassium iodide. Extremely pure materials are essential. The solion is extremely sensitive and it may be very small. It is simple in construction, it is easy to maintain, and it requires very low power.

David Schlain, *Secretary*

News from India

Ferromanganese in India—Demag-Elektrometallurgie, Germany, is working on an electric reducing furnace of closed-top type, for the production of carburized ferromanganese for India. It is to be provided with a transformer capacity of 7500 kva and will be capable of producing 40 tons of the alloy per day. The firm will also carry out extensive tests with Indian manganese ore fines to determine their suitability for smelting by the Lubatti process.

Nickel-Free Stainless Steel—The National Metallurgical Lab., Jamshedpur, has evolved a nickel-free stainless steel containing 21% Cr, 12.6% Mn, and 0.8% nitrogen. It is austenitic in structure and can replace the standard 18/8 steel for a number of applications including the fabrication of utensils.

De Nora Electrolyzers for Nangal Project—Oronzio De Nora, Milan, Italy, will supply electrolyzers for the Nangal Fertilizer and Heavy Water Project. This forms part of a 300-million-rupees project to develop the agricultural and industrial resources of the Punjab. Production is expected to commence early in 1960—80,000 tons of nitrogen in the form of ammonium nitrate and nitro limestone, and 15 tons of heavy water per year. Some 6500 cells grouped in 60 De Nora hydrogen and oxygen electrolyzers of the filter press type, each rated at 10,000 amps, will be installed. This will produce more than 25,000 cubic meters of hydrogen per hour. The normal purity of the products is hydrogen 99.9% and oxygen 99.7%. The plant will be bigger than any other comparable unit completed or under construction anywhere in the world, including that envisaged under the Aswan development scheme. The power required by the electrolyzers will be about 140,000 kw and will be made available from the Bhakra Nangal power station.

Symposium on Rare Metals—A Symposium on Rare Metals was held under the auspices of the Atomic Energy Establishment, Government of India, the UNESCO, and the Indian Institute of Metals at Bombay during December 1957. Twenty-four papers were presented covering the following topics: resources of rare metals, beneficiation of uranium ores and of beach sands, treatment of uranium ores and ore concentrates, treatment of monazite, production and application of rare earth metals, present status of zirconium and beryllium metallurgy, production of metallic uranium and thorium, treatment of irradiated fuel elements and breeder blankets, physical metallurgy and fabrication of uranium and plutonium, physical metallurgy of thorium, technology of rare metal oxides and carbides, powder metallurgy in reactor applications.

Ferrosilicon Plant in Mysore—The Government of India has approved the Rs. 1.3 crore* ferrosilicon scheme forming part of the development program of the state-owned Mysore Iron and Steel Works, Bhadravathi. The new plant is expected to go into production by the end of 1959 and will manufacture 20,000 tons of ferrosilicon per annum as against the present output of 5000 tons. Bhadravathi will then be the sole producer in India of ferrosilicon, an essential ingredient in steel manufacture. This project is expected to reduce substantially the import of the material.

* Thirteen million rupees.

Corrosion of Metals Symposium—A Symposium on Corrosion of Metals was held at Madras in January by the Section of Engineering and Metallurgy, 45th Indian Science Congress. Ten papers were presented: Corrosion and Its Prevention, Inhibition of the Corrosion of Aluminum, Corrosion Inhibitors with Special Reference to Oil Soluble and Vapor Phase Inhibitors, Corrosion Control Measures on Submarine Pipe Lines Carrying Petroleum Products, Conversion Coatings, Behavior of Metals and Metallic Coatings Exposed to Atmosphere, Some Aspects of Cathodic Protection, Corrosion in the Tropics, Anodic Corrosion of Metals and Alloys in Pyrophosphate Solutions, and Corrosion-Resisting Properties of the Austenitic Chromium-Nickel Stainless Steels.

T. L. Rama Char,
Regional Editor, India

Theoretical Division Extended Abstracts

The Theoretical Electrochemistry Division is making available a booklet of extended abstracts of the papers to be presented at the Annual Spring Meeting of the Society in New York, April 27 to May 1. Extended abstracts of general papers and the papers of the Symposium on Electrokinetic and Membrane Phenomena are included. Copies will be available at the meeting, or they can be obtained, at $3.00 each, from:

Dr. Ralph Roberts
3309 Camalier Drive
Washington 15, D. C.

Division News

E & M Division High Purity Metals Symposium Scheduled

The Electrothermics and Metallurgy Division of The Electrochemical Society has organized a symposium, entitled "The Preparation, Evaluation, and Uses of High Purity Metals," to be held in conjunction with the Annual Spring Meeting of the Society at the Statler Hotel, New York City, from April 27 through May 1, 1958.

The Electrothermics and Metallurgy Committee, in preparation for the 1958 Spring Meeting has chosen a subject for a symposium that will be of widespread interest to a large number of scientists and engineers engaged in the preparation and utilization of high purity metals for a variety of uses in the electronic, chemical, metallurgical, and associated fields.

Key discoveries in chemical and metallurgical technology, as well as widespread advances in engineering, have increased the need and utilization of high purity materials in many fields.

It was therefore the opinion of the committee that such a symposium covering the rapidly advancing technology of high purity metal preparation, the methods for the determination of purities obtainable, and the potential uses of such high purity

materials would be timely and of high scientific interest.

The symposium consists of five sessions: (*a*) Zone Refining Methods for the Preparation of High Purity Metals, (*b*) Iodide Type Processes for the Preparation of High Purity Metals, (*c*) Electrorefining and Electrowinning Methods, (*d*) Chemical Purification Methods for Compound Preparation in Production of High Purity Metals, and (*e*) Criteria of Purity in Preparation of High Purity Metals. A total of approximately 28 papers have been scheduled for this meeting. Some of the subjects to be covered include boat and floating zone refining techniques for some metals, semiconductors, floating zone refining of tungsten by electron beam melting, continuous multistage zone refining of silicon tetraiodide. A number of papers on the preparation of silicon and refractory metals by iodide processes are also included.

Electrowinning and electrorefining using fused salt methods for the preparation of high purity hafnium, boron, columbium, uranium, and titanium are included in the papers.

Reduction methods for the preparation of tungsten, rhenium, and methods for preparation of high purity scandium and boron are also being covered.

A number of analytical techniques utilized for the determination of impurity levels in high purity metals will be described.

E & M—Corrosion Joint Symposium

A symposium entitled "Stress Corrosion Cracking of Stainless Steel" will be presented at the Annual Meeting of the Society, to be held in New York, April 27 to May 1. The program, under the joint sponsorship of the Electrothermics and Metallurgy and the Corrosion Divisions, has been formulated by W. E. Tragert and will consist of six papers in one session.

The symposium will be keynoted by J. J. Harwood who will review recent progress in this research area. Critical experiments directed toward obtaining a better understanding of the failure mechanism in austenitic stainless steel will be described by H. L. Logan, while the effect of composition will be the subject of a paper by H. R. Copson. The influence of corrosive environment will be presented in two papers: M. G. Fontana will discuss failure in high temperature water, and G. Wheeler will evaluate performance in caustic solutions. The stress corrosion of martensitic stainless steels comprises the third element of the program and a paper by F. Brown will be presented on this subject.

Brief prepared discussions have been solicited from several investigators who are active in the field and will be presented as time permits.

New Members

In December 1957 the following were approved for membership in The Electrochemical Society by the Admissions Committee:

Active Member Sponsored by a Sustaining Member

Ardrey M. Bounds, Superior Tube Co., P. O. Box 191, Norristown, Pa. (Electrothermics & Metallurgy)

Active Members

Arthur F. Butler, E. I. du Pont de Nemours & Co.; Mail add: 1320 Quincy Dr., Wilmington, Del. (Electronics)

Edward J. Cook, U. S. Naval Academy and Chesapeake Instrument Corp.; Mail add: 138 Gibson Rd., Annapolis, Md. (Battery, Corrosion)

John C. Cutt, Research & Development, Carborundum Co., Niagara Falls, N. Y. (Electrothermics & Metallurgy)

Timothy J. Desmond, Delco Radio Div., G.M.C.; Mail add: 325 Magnolia Dr., Kokomo, Ind., (Electronics)

Harold T. Fullam, Stauffer Chemical Co.; Mail add: 2601 Parker St., Berkeley, Calif. (Electrodeposition, Electrothermics & Metallurgy, Theoretical Electrochemistry)

Charles L. Gravel, Minneapolis-Honeywell Regulator Co.; Mail add: 359 Cabot St., Newtonville 60, Mass. (Electronics)

Edward E. Hucke, University of Michigan, Dept. of Chemical & Metallurgical Engrg., Ann Arbor, Mich. (Electrothermics & Metallurgy)

Nicolas Inchauspe, Physics Dept., University of Illinois, Urbana, Ill. (Electronics—Semiconductors)

Sol S. Jaffe, McGraw-Edison; Mail add: 7 Nance Rd., West Orange, N. J. (Battery)

A. Albert Johnson, Metal & Thermit Corp.; Mail add: 22030 Dante, Oak Park 37, Mich. (Corrosion, Electrodeposition)

Thomas I. Kidd, Reading Battery Div., Electric Auto-Lite Co., 4700 5th St., Highway, Reading, Pa. (Battery)

William A. McNeish, Universal-Cyclops Steel Corp., Bridgeville, Pa. (Electrothermics & Metallurgy)

Gordon E. Moore, Fairchild Semiconductor Co., 844 Charleston Ave., Palo Alto, Calif. (Electronics)

Sven H. Persson, Uddeholms Aktiebolag, Skoghallsverken Elektrokemiska Fabriken, Skoghall, Sweden (Industrial Electrolytic)

William G. Renshaw, Allegheny Ludlum Steel Corp., Brackenridge, Pa. (Corrosion)

William H. Richards, Jr., Stromberg-Carlson Co.; Mail add: 106 Greenaway Rd., Rochester 10, N. Y. (Electronics)

Guy Roberts, Canadian Carborundum Co., Ltd., Niagara Falls, Ont., Canada (Electrothermics & Metallurgy)

Electronics Division Enlarged Abstracts

The Electronics Division will again publish an "Enlarged Abstracts" booklet for the Spring 1958 convention of the Society in New York City. The booklet will have 1000-word abstracts of the papers to be presented before the Electronics Division in its symposia on

Luminescence
Semiconductors.

The abstracts will contain pertinent information and experimental data given in the papers and will provide these details before publication, thus aiding workers in the field. The abstracts will be "printed but not published."

The abstract booklets should be available by mid-April; the price will be $2.50 per copy.

Checks should be made payable to: Electronics Division, The Electrochemical Society.

Orders and checks should be sent to:

Martin F. Quaely
c/o Westinghouse Electric Corp.
Lamp Div., Research Dept.
Bloomfield, N. J.

By action of the Board of Directors of the Society, all prospective members must include first year's dues with their applications for membership.

Also, please note that, if sponsors sign the application form itself, processing can be expedited considerably.

Jay W. Thornhill, Texas Instruments Inc.; Mail add: 3212 Hedgerow Dr., Dallas 35, Texas (Electronics)

Alfred M. Weisberg, Technic Inc., 7001 N. Clark, Chicago 26, Ill. (Electrodeposition)

Transfer from Student Associate to Active Membership

Julius Klerer, Brooklyn College: Mail add: 880 Summit Ave., Jersey City, N. J. (Theoretical Electrochemistry)

Reinstatements to Active Membership

Harold D. Stanley, K. W. Battery Co., 3555 Howard St., Skokie, Ill. (Battery)

Andrew B. Black, Cobalt Chemicals, Box 350, Cobalt, Ont., Canada (Electrodeposition, Electrothermics & Metallurgy)

Deceased—Reported in November 1957

A. J. Liebmann, New York, N. Y.
Paul L. Asnis, Pequannock, N. J.
H. E. Haring, Murray Hill, N. J.

Personals

Lee J. Droege, of Calif., recently has been placed in charge of the Semiconductor Materials Processing Section of the Semiconductor Div., Hughes Aircraft Co.

Robert B. Holden, formerly with Sylvania Electric Products Inc., Bayside, N. Y., is now chief of the Chemistry and Ceramics Section, Nuclear Fuel Research Dept., Metallurgical Labs., Olin Mathieson Chemical Corp., New Haven, Conn.

Justus H. Bower of Berkeley Heights, N. J., recently retired from Bell Telephone Labs., Inc., Murray Hill, N. J.

A. D. Spillman, Philadelphia Electric Co., Philadelphia, Pa., is now assistant manager of the Sales Applications Dept.

N. R. Fasken, who had been with the Shawinigan Water & Power Co., is now with Shawinigan Chemicals Ltd., Stainless Steel and Alloys Div., Shawinigan Falls, P. Q., Canada.

Douglas W. Rowed recently joined the staff of Union Carbide Australia Ltd., Mascot, N.S.W., Australia. Previously he was associated with Eveready (Australia) Pty. Ltd.

Arthur L. Ginsburg is no longer connected with the Cartoucherie Francaise in Paris. At present he is with the Laboratoire de Physique, Institut Textile de France, Paris.

John F. Gall, supervisor of research of the Pennsalt Chemicals Corp.'s Whitemarsh Labs., Philadelphia, has been elected chairman of the American Chemical Society's Div. of Inorganic Chemistry for 1958.

Arthur Fleischer has been appointed senior scientist of electrochemistry at the Thomas A. Edison Lab., McGraw-Edison Co., West Orange, N. J. Dr. Fleischer was formerly director of research at Gould-National Batteries, Nicad Division, Inc.

V. S. de Beausset, who had been project manager of the Taipei, Formosa, Field Office of the J. G. White Engineering Corp., has returned to the United States as manager of the corporation's Process Div. in New York City.

H. V. K. Udupa has been appointed assistant director, Central Electrochemical Research Institute, Karaikudi, India.

S. Ramaswamy has returned to India after a brief visit to Europe and the United Kingdom in connection with the expansion program of the Mettur Chemical and Industrial Corp., Mettur Dam.

Capitol Records cuts costs and simplifies plating of record masters with "Plus-4" Anodes

Capitol RECORDS

In its big, modern plant at Scranton, Pa., Capitol Records, Inc., produces record masters by acid-copper electroplating. To improve and simplify this critical step in making its high-quality popular and classical records, Capitol tried "Plus-4"* Anodes, Anaconda's phosphorized copper anodes. Chemical Engineer T. Melioris reports these operating results:

1. Material savings. Because there are no free particles of copper in the solution from "Plus-4" Anodes—sludge losses were cut 90%—copper sulfate build-up in the solution was drastically reduced. There has been an annual saving of several thousand pounds of salts and a big reduction in the amount of acid required.

2. Maintenance savings. In tanks using "Plus-4" Anodes, solutions are tested only every other week compared with twice a week for ordinary anodes. "Plus-4" Anodes need not be removed from the tank after plating is completed, as they do not continue to give off copper crystals to the solution after the current is stopped. Less frequent cleaning of tanks to remove sludge.

3. Smoother, denser deposits in tanks with "Plus-4" Anodes because there are relatively few finely divided copper particles suspended in solution.

Write for information on how you can obtain a test quantity to supply one tank. Address: The American Brass Company, Waterbury 20, Conn. In Canada: Anaconda American Brass Ltd., New Toronto, Ont.

ANACONDA®

"PLUS-4" ANODES Phosphorized Copper

Made by The American Brass Company for use under Patent No. 2,689,216

Edward Orban recently was named manager of inorganic product development for the development department of Monsanto Chemical Co.'s Research and Engineering Div. at St. Louis after serving as project specialist in the development department of the company's Inorganic Chemicals Div. since 1955.

Willis R. Whitney

Willis R. Whitney, dean of industrial research in America, died on January 9, 1958 at the age of 89.

In 1900 Dr. Whitney founded the General Electric Research Lab. He served as its director for 32 years, a period during which scientists under his leadership made many of the major discoveries that helped bring electricity into homes and factories throughout the world. He was an honorary vice-president of the General Electric Co.

He was born at Jamestown, N. Y., on August 22, 1868. He was graduated from the Massachusetts Institute of Technology with the degree of B.S. in 1890 and received his Ph.D. in chemistry from the University of Leipzig, Germany, in 1896.

Following his graduation, Dr. Whitney held several positions at M.I.T. While there, he did important research work in electrochemistry, proposing the electrochemical theory of corrosion, now universally accepted as the basis for explanation of corrosion reactions.

Dr. Whitney was an Honorary Member of The Electrochemical Society which he joined in April 1902; he served as Society President in 1912. He was also a member of the National Academy of Sciences, National Research Council, American Chemical Society, American Institute of Mining and Metallurgical Engineers, American Institute of Electrical Engineers, American Society for the Advancement of Science, American Academy of Arts and Sciences, American Physical Society, The Franklin Institute, American Philosophical Society, British Institute of Metals, and the French Legion of Honor.

Many colleges and universities awarded honorary degrees to Dr. Whitney, including the University of Pittsburgh, Union College, Syracuse University, University of Michigan, University of Rochester, and Lehigh University. Other honors bestowed on Dr. Whitney both here and abroad include: The Willard Gibbs Medal, Chandler Medal, Perkin Medal, Franklin Medal, Edison Medal, decoration of Chevalier of the Legion of Honor (France), gold medal of the National Institute of Social Sciences, 1943 John Fritz Medal, distinguished service gold key of the American Congress of Physical Therapy, the Marcellus Hartley Gold Medal, and the medal of the Industrial Research Institute.

He was the author of many scientific publications in such fields as the corrosion of iron, solubility determinations, colloids, alloys, chemistry of light, carbon brushes, catalysis phenomena, vacua, and electrochemistry.

He is survived by his wife, the former Evelyn Jones, and a daughter, Mrs. Van Alstyne Schermerhorn, of Glenville, N. Y.

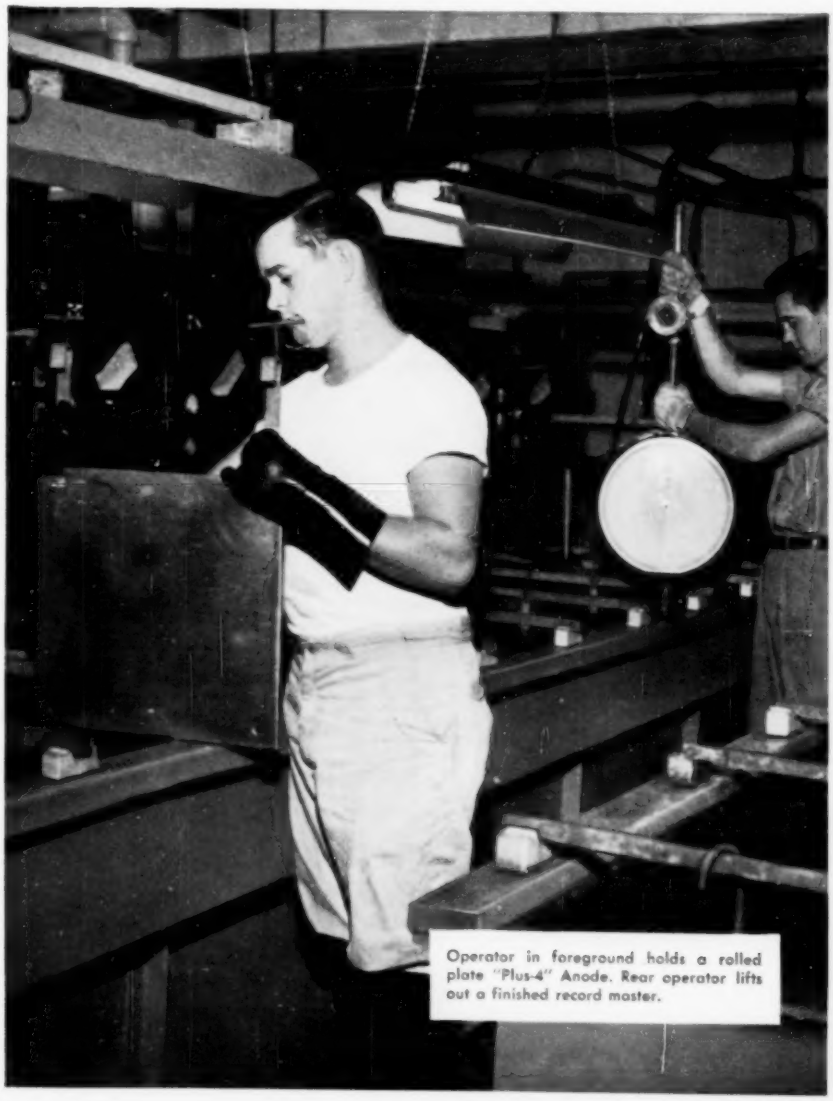

Operator in foreground holds a rolled plate "Plus-4" Anode. Rear operator lifts out a finished record master.

James H. Critchett

James H. Critchett, retired vice-president of several divisions of Union Carbide Corp., died at his home in Orleans, Mass., on December 18, 1957.

Mr. Critchett was born in Watertown, Mass. He attended the Massachusetts Institute of Technology, receiving the B.S. degree in 1909.

He joined the Union Carbide organization in 1914 on the metallurgical staff of two corporation divisions in Niagara Falls, N. Y. Later he moved to New York as part of the corporation's research organization, subsequently coordinating the activities of the research organization at Niagara Falls with those of the manufacturing and sales divisions. He became a vice-president of Electro Metallurgical Co. in 1939 and

of several other divisions in 1944, which positions he held when he retired.

During World War II, Mr. Critchett was a member of a number of Government metallurgical committees of the War Production Board and the National Academy of Science.

He was an Emeritus Member of The Electrochemical Society which he joined in 1919. He was also a member of Theta Delta Chi, American Welding Society, American Foundrymen's Association, American Society for Testing Materials, American Iron and Steel Institute, Uptown Club, Newcomen Society, the Masonic Order, and the Douglaston Yacht Club, and was on the executive board of the Welding Research Committee of The Engineering Foundation.

Mr. Critchett is survived by his wife, Ruth Walton Critchett, and two daughters, Ruth C. Boyer and Doris W. Rainey.

News Items

New Sustaining Members

The following recently became Sustaining Members of The Electrochemical Society: Basic Incorporated, Cleveland, Ohio; Columbian Carbon Co., New York, N. Y.; K. W. Battery Co., Skokie, Ill.; Libbey-Owens-Ford Glass Co., Toledo, Ohio; Pittsburgh Metallurgical Co., Inc., Niagara Falls, N. Y.; Sumner Chemical Co., Div. of Miles Laboratories, Inc., Elkhart, Ind.; Upjohn Co., Kalamazoo, Mich.

1957 Annual Index

The Annual Index for Vol. 104 (1957) of the JOURNAL appeared in the February issue, pp. i-ix. Reprints of the Index can be obtained about the middle of this month by writing to The Electrochemical Society, 1860 Broadway, New York 23, N. Y.

J. C. Bailar, Jr., Chosen President-Elect of ACS

Dr. John C. Bailar, Jr., professor of inorganic chemistry at the University of Illinois, has been chosen president-elect of the American Chemical Society. He will head the society in 1959.

President for 1958 is Dr. Clifford F. Rassweiler, vice-chairman of the board and vice-president for re-

(Continued on page 65C)

ECS Membership Statistics

The following three tables give breakdown of membership as of Jan. 1, 1958. The Secretary's Office feels that a regular accounting of membership will be very stimulating to membership committee activities. In Table I it should be noted that the totals appearing in the right-hand column are *not* the sums of the figures in that line since members belong to more than one Division and, also, because Sustaining Members are not assigned to Divisions. But the totals listed are the total membership in each Section. In Table I, Sustaining Members have been credited to the various Sections.

Table I. *ECS Membership by Sections and Divisions*

Section	Division: Battery	Corrosion	Electric Insulation	Electrodeposition	Electronics	Electro-Organic	Electrothermics & Met	Industrial Electrolytic	Theoretical Electrochem	No Division	Total as of 1/1/58	Total as of 4/1/57	Net Change
Boston	14	28	6	34	49	8	18	13	22	8	131	117	+14
Chicago	12	36	4	42	18	8	12	15	20	12	111	113	− 2
Cleveland	58	37	2	49	41	11	26	31	40	15	203	195	+ 8
Columbus, Ohio	1	13	0	14	4	2	22	3	8	5	45	0	+45
Detroit	7	17	5	44	7	10	5	5	20	20	84	80	+ 4
India	9	7	2	19	8	6	9	14	11	3	36	27	+ 9
Indianapolis	11	8	3	11	10	4	5	3	6	2	40	0	+40
Midland	8	17	0	5	2	2	7	17	10	3	45	41	+ 4
Mohawk-Hudson	5	15	14	9	11	1	7	3	11	5	51	0	+51
New York	78	102	24	133	123	33	67	66	94	45	482	447	+35
Niagara Falls	13	22	1	23	5	5	75	63	27	23	175	156	+19
Ontario-Quebec	12	23	1	14	2	3	33	25	7	15	75	64	+11
Pacific Northwest	4	14	0	11	2	1	7	10	8	10	47	47	0
Philadelphia	24	30	4	37	56	16	20	18	50	29	174	155	+19
Pittsburgh	4	46	3	29	27	5	35	16	36	9	130	117	+13
San Francisco	5	14	2	18	12	3	14	23	21	4	64	60	+ 4
Southern Calif.-Nevada	15	20	2	24	24	3	13	18	22	10	95	87	+ 8
Washington-Baltimore	34	41	8	39	23	3	10	11	28	7	128	117	+11
U. S. Non-Section	54	90	13	87	65	42	56	72	109	35	395	486	−91
Foreign Non-Section	41	58	6	63	29	27	38	59	70	53	224	212	+12
Total as of Jan. 1, 1958	409	638	100	705	518	193	479	485	620	313	2735		
Total as of April 1, 1957	377	618	86	680	411	183	426	454	578	321		2505	

Table II. *ECS Membership by Grade*

	Total as of 1/1/58	Total as of 4/1/57	Net Change
Active	2448	2142	+306
Delinquent	61	146	− 85
Active Representative Patron Members	8	8	0
Active Representative Sustaining Members	70	60	+ 10
Total Active Members	2587	2356	+231
Life	16	15	+ 1
Emeritus	54	44	+ 10
Associate	31	28	+ 3
Student	42	57	− 15
Honorary	5	5	0
	2735	2505	+230

The figures pertaining to Patron and Sustaining Member Representatives have been added to reflect reclassifications and changes in membership status.

Table III. *ECS Patron and Sustaining Membership*

	Total as of 1/1/58	Total as of 4/1/57	Net Change
Patron Member Companies	4	4	0
Sustaining Member Companies	127	119	+ 8

search and development of the Johns-Manville Corp., New York, who took office January 1, succeeding Professor Roger J. Williams of the University of Texas.

Dr. Bailar's election as president for 1959 is the second ACS honor he has received in 1957. Earlier he was chosen as first chairman of the society's new Division of Inorganic Chemistry. He headed the Division of Physical and Inorganic Chemistry in 1950 and the Division of Chemical Education in 1947.

The new president-elect is known for his achievements in chemical research as well as in teaching. He has carried out important investigations in inorganic chemistry.

A native of Golden, Colo., Professor Bailar received the B.A. degree in 1924 and the M.A. in 1925 from the University of Colorado. He earned the Ph.D. in 1928 at the University of Michigan. He was a research fellow at Michigan in 1925-26 and a teaching assistant there for the following two years before joining the University of Illinois faculty in 1928. He was named assistant professor in 1935, associate professor in 1939, and full professor in 1943.

Professor Bailar is a member of The Electrochemical Society, Phi Beta Kappa, Sigma Xi, Phi Lambda Upsilon, and Alpha Chi Sigma. He also is active on several committees of the National Research Council.

B. D. Thomas Appointed President of Battelle Memorial Institute

Dr. B. D. Thomas, scientist and research administrator, has been named to the presidency of Battelle Memorial Institute to succeed Dr. Clyde Williams, whose retirement as president was announced recently by the Institute's Board of Trustees.

Active head of Battelle since being named director a year ago, Dr. Thomas has been a member of the Battelle organization for many years. He joined the staff as a research engineer in 1934, was appointed assistant director in 1942, and vice-president in July 1955.

Transparent Magnetic Oxides

A new class of magnetic oxides, structurally distinct from ferrites, has recently been discovered. These materials, known as rare-earth-iron garnets, are transparent, permitting the internal magnetic domain structure to be seen with a polarizing microscope.

The discovery of ferrimagnetism in these garnets was made first at the Laboratoire Electrostatique et De Physique du Metal of the Institute Fourier in Grenoble, France, and independently by S. Geller and M. A. Gilleo of Bell Telephone Labs., where the optical and magnetic resonance behavior of the garnets is being studied by J. F. Dillon, Jr., employing single crystals grown by J. W. Nielsen.

Most magnetic materials, metals and ferrites alike, are opaque to visible light. Thus, their internal magnetic structure is not visible, and the way magnetic domains are oriented within them has been inferred from reflection of polarized light by their surfaces or by delineating domain boundaries at these surfaces with colloidal magnetic oxides.

Yttrium iron garnet, $Y_3Fe_2(FeO_4)_3$, is the most completely studied member of this new garnet family. Of great interest is that fact that yttrium-iron garnet contains magnetic ions with but a single valence. Both x-ray and neutron diffraction studies have shown clearly that, unlike the ferrites, the interactions between identical magnetic ions wholly occupying two different crystallographic sites are responsible for ferrimagnetism in the garnet structure.

A polarized light beam passing through the transparent magnetic domains in rare-earth-iron garnets has its plane of polarization rotated in one direction in one domain but in the opposite direction in an adjacent and oppositely magnetized domain. This Faraday rotation is wavelength-dependent and amounts to several degrees per mil of thickness; it makes the domains within the crystals clearly visible. The internal domain structure can therefore be studied over a wide range of temperatures and magnetic field conditions. Thus, for the first time, it is now possible to correlate Faraday rotation in a magnetic material with spectroscopic data over a broad temperature range.

Chemstrand Corp. Establishes Scholarship Fund

The Chemstrand Corp., Decatur, Ala., has recently established a fund to provide undergraduate scholarships and grants-in-aid at 30 U. S. colleges and universities.

The scholarships are for upperclass students, preferably seniors, in the fields of chemistry, physics, chemical, mechanical, electrical and textile engineering, business administration, industrial management, and the liberal arts.

The scholarships are awarded and administered by the individual colleges. The purpose of this program is to assist financially in the academic training and development of scientists, engineering and management personnel.

The grants-in-aid will be used by the institutions for the purchase of equipment or to supplement salaries.

A. D. Little, Inc., Sponsors Science Explorers Club

In a move to encourage more science careers, Arthur D. Little, Inc., has made a $5000 gift to the Museum of Science in Boston, Bradford Washburn, museum director, announced recently.

The gift will be used to sponsor the Science Explorers Club—a lively program that has been developing young people's taste for science learning for the past six years.

The Science Explorers Club meets on Saturday mornings at the Museum; 280 boys and girls between 10 and 18 years are enrolled, and there is a long waiting list. Dramatic experiments and demonstrations, use of Museum collections, and field trips give the young people a broad view of the various areas of scientific knowledge.

A new activity of the Science Explorers Club, which began December 1957, is its own television program. Telecast Thursdays at 6:00 P.M. over Channel 5, the show features Mr. Merrill and some of his Explorers as they delve into fascinating facts about science.

Newark College of Engineering Names New Laboratory

Newark College of Engineering has announced that its new facilities at 240-250 High St. will be named the Martin F. Tiernan Laboratory Building, in honor of the man who made its acquisition possible.

The three-story brick structure, once the Maltbie Labs. plant, was acquired by the college in 1956 from Wallace & Tiernan, Inc., Belleville, N. J., manufacturers of water purification systems, for use by NCE's departments of Chemical and Civil Engineering.

The chemical engineering facilities, according to NCE president Robert W. Van Houten, are probably the most modern and up-to-date educational laboratories of their type in the country. Completed in time for use by students in 1957, they are matched by separate facilities for civil engineering students, which are located in the south wing of the building and which were to be ready for occupancy in February 1958.

According to Dr. Van Houten, the new building has enabled the Chemical Engineering Department to centralize its activities and to add much-needed facilities for research and graduate work.

The ground floor contains a Unit Operations Lab., machine shop, storage area for pipes and fittings, and a separate room for dust-free size reduction operations. The first floor contains the Physical Chemistry Lab., Chemical Instrument Lab., commons and locker rooms, and main stock room.

On the second floor are the Organic Chemistry Labs., graduate and staff research laboratories, classrooms, and offices. The third floor includes several specialized laboratories for instrumentation, electrochemical engineering, adsorption, organic research, and small-scale investigation. The area also includes four more classrooms and a design room.

The Tiernan Building brings to six the number of buildings owned by the college, including its new Cullimore Hall, which was to open in February, and Weston Hall, which will be torn down and replaced by a new six-story laboratory building starting next year.

Announcements from Publishers

"Ideas, Inventions, and Patents: How to Develop and Protect Them," by Robert A. Buckles. Published by John Wiley & Sons, Inc., New York City, 1957. 270 pages; $5.95.

"Electroforming of Waveguide Components for the Millimeter-Wavelength Range," by Albert A. Feldmann. National Bureau of Standards Circular 587, issued Nov. 15, 1957. 16 pages; 15 cents. (Order from Superintendent of Documents, U. S. Government Printing Office, Washington 25, D. C. NOTE: Foreign remittances must be in U. S. exchange and should include an additional ¼ of the publication price to cover mailing costs.)

"Investigation of Freezing as a Means of Obtaining Fresh Water from Salt Water," by E. N. Kemler and others, University of Minnesota, for U. S. Naval Civil Engineering Research and Evaluation Lab., Jan. 1955. 55 pages; $1.50. (Order Report PB 121959 from OTS, U. S. Dept. of Commerce, Washington 25, D. C.)

"Opportunities in Research at Mellon Institute," new publication offered by Mellon Institute to prospective applicants. (Available on request from Office of Professional Relations, Mellon Institute, 4400 Fifth Ave., Pittsburgh 13, Pa.)

Translated Digests of Current Soviet Literature

Translated digests of the current Soviet literature of electronics, automation, and physics have been announced for publication in early 1958. Designated as "Express" services, these digests will be tailored to the present-day research and development needs of American laboratories.

Fast and thorough coverage of new Soviet developments in each special field will be achieved by expert scanning of more than 60 leading Russian-language professional journals—many of which have never before been available to an American audience.

Coverage of the "Electronics Express" service will include wave propagation and antenna design, electron tubes and microwave devices, solid state devices and semiconductors, audio systems and acoustics, circuits and circuit elements, communication systems (radio, TV, etc.), electron physics and electron optics, and research and control instrumentation.

Coverage by the "Automation Express" service will include information theory and noise problems, network theory and telemetering, digital and analog computer systems, control systems and data handling, servomechanisms and components, magnetic amplifiers, and circuits.

Precise areas to be covered by the "Physics Express" are soon to be announced.

Each monthly service will include 2 to 4 significant articles translated completely, 20 to 30 articles that are summarized by extensive excerpts in the author's words, 30 or more descriptive abstracts of articles, as well as an estimated 100 or more annotated titles of other currently published articles.

Sample copies and additional information may be obtained from International Physical Index Inc., 1909 Park Ave., New York-35, N. Y.

Notice to Members

According to the Constitution of the Society, Article III, Section 9, "Any member delinquent in dues after April 1 of each year shall no longer receive the Society's publications . . . ." Such delinquents will not receive the May issue of the JOURNAL. A reminder notice will be mailed to delinquents about the middle of February and a final notice about the middle of March.

Book Reviews

Rectifying Semi-Conductor Contacts, by H. K. Henisch. Published by Oxford University Press, New York City, 1957. 372 pages; $11.20.

The field of solid state physics is already so extended that description of one specific aspect in the form of a monograph is the preferred treatment for books on solid state or even on semiconductors only. This monograph is a well-written historical and introductory general survey of contact phenomena in the semiconductor field, although quite a number of pertinent problems, such as crystal structure and orientation, surface chemistry, crystal perfection, pulse technology, and fluctuation phenomena are either ignored or else not dealt with sufficiently. Even for the informed reader, chapters such as those on the unipolar rectification theories are a practical compilation of useful material.

The defects of the book are chiefly those of omission rather than commission. An example of this is the introduction. The rectifying system is defined by the asymmetry of the current-voltage ratio, and the difference between plate and point-contact rectifiers is outlined. The author specifically excludes *p-n* junctions. This is difficult to understand since rectification theory is most easily explained for *p-n* junctions in monocrystals where the local continuity of the Fermi level in thermal equilibrium immediately gives a picture of what in other cases must be deduced from a work function difference. Furthermore, most formed point contacts, especially on *n*-type germanium, are definitely *p-n* junctions.

Other omissions include cyclotron resonance and its results in discussing the temperature dependence of the forbidden gap and the effective mass ratio, the u.h.f. network analysis in discussing the high frequency equivalent network of diodes, and space charge repression and high injection efficiency from high to low forbidden gaps.

H. F. Mataré

Microwave Measurements, by Edward L. Ginzton. Published by McGraw-Hill Book Co., Inc, New York City, 1957. 515 pages; $12.00.

This book offers a clear and competent discussion of the methods of making measurements in microwave circuits. It contains not only a concise review of the fundamental concepts but also a review of many of the recent techniques and devices such as backward wave tubes and the dynamic presentation of impedance data. While different in detail, its general level and scope reminded the reviewer of the widely used Vol. 11 of the M. I. T. Radiation Lab. Series, "Technique of Microwave Measurements," edited by C. G. Montgomery. It might be regarded as a modernized replacement of that book.

This reviewer attempted to visualize what type of laboratory worker would be benefited most by the existence of this book. Such a person, he concluded, would be the employee of a new laboratory, charged with the responsibility of setting up facilities for making exhaustive tests on a large shipment of microwave components to be delivered some months hence. This book would give such a worker good advice regarding what measuring equipment to buy and how to use it, including how to make necessary calibrations and corrections. For complete understanding, the reader needs a general knowledge of physics, especially Maxwell's equations, but no previous knowledge of microwave techniques.

The chapters dealing with signal sources, power measurement, and measurements upon resonant cavities seem particularly strong. No doubt this strength represents the specialized interest of the author, who is director of the Microwave Lab. at Stanford University, which has been devoted to a large extent to the design of high powered klystrons and linear accelerators.

Workers whose interest lies partially or completely in the field of chemistry, mainly through spectroscopy, would find this book of use. However, since obviously it was not planned especially for them, they should not feel disappointed that it does not satisfy all their needs. For one thing, no mention is made of the signal-to-noise problem in spectroscopy, in which one is concerned with the detection of a small change in a large signal rather than a small signal in the presence of noise. Second, Section 1.13, dealing with frequency stabilization of oscillators, is much too brief, as greater knowledge of such circuits is necessary for work in modern high-resolution spectroscopy. Finally, such workers cannot be dependent entirely upon components which can be purchased because individual experiments require the construction of specialized absorption cells and other components. For such workers it would be most imperative to include a discussion of impedance matching methods. Also, more practical information on design would be desired. For example, while the book mentions plungers with rf chokes, it never discusses their principle or design.

This reviewer did not detect any significant errors. The text is aided greatly by a profusion of clear diagrams. It fulfills its intended purpose, and it does honor to the memory of the late W. W. Hansen, to whom it is properly dedicated.

Yardley Beers

Underground Corrosion, by Mervin Romanoff. National Bureau of Standards Circular 579, issued April 1957. 227 pages; $3.00.

The circular is a condensed summary of the Bureau's investigations of Corrosion of Metals in Soils over a period of 45 years (1910-1955.) This research was carried on with the cooperation of several public utilities, technical associations, and manufacturers who supplied material, labor, test sites, and assistance in planning the tests. The Bureau of Standards' investigation has been an important contribution to a better understanding of the subject theoretically and the practical application of preventive measures.

On the whole, contrary to traditional notions, little, if any, difference in rate of pitting was found between the common commercial varieties of wrought ferrous metals, such as low-carbon steel, copper-bearing steel, and wrought iron. The author points out the fact that the irregular condition of soils in contact with buried metals often produces marked pitting which is one of the characteristics of soil corrosion. The important controlling factors and the mechanism of this type of corrosion are described.

A detailed description of field tests of pipe materials and bituminous coatings is given with the sections on laboratory studies and accelerated laboratory tests. The section (pp. 149-165) on accelerated soil-corrosion testing and the evaluation of such tests based on comparison with field tests should be quite useful. Quick tests that give an approximate indication of the corrosiveness of soil are highly desirable. The limitations and value of such tests are indicated in this section.

Cathodic protection of metals underground, which now is relied on so generally for protection under these conditions, is treated briefly (pp. 179-194).

The discussion of anaerobic bacterial effects is scattered. In one section (p. 154) the important oxidation-reduction potential (Redox) is defined, and on p. 13 a brief general description of anaerobic corrosion will be found. Considering the wide-spread damage caused indirect-

Manuscripts and Abstracts for Fall 1958 Meeting

Papers are now being solicited for the Fall Meeting of the Society, to be held at the Chateau Laurier in Ottawa, Canada, September 28, 29, 30, October 1, and 2, 1958. Technical sessions probably will be scheduled on Batteries, Corrosion, Electrodeposition (including symposia on "Electrodeposition on Uncommon Metals" and "Chemical and Electropolishing"), Electronics (Semiconductors), Electro-Organics, and Electrothermics and Metallurgy.

To be considered for this meeting, triplicate copies of abstracts (*not to exceed 75 words in length*) must be received at Society Headquarters, 1860 Broadway, New York 23, N. Y., *not later than June 2, 1958. Please indicate on abstract for which Division's symposium the paper is to be scheduled.* Complete manuscripts should be sent in triplicate to the Managing Editor of the JOURNAL at the same address.

* * *

The Spring 1959 Meeting will be held in Philadelphia, Pa., May 3, 4, 5, 6, and 7, 1959, at the Sheraton Hotel. Sessions will be announced in a later issue.

ly by anaerobic bacteria, the treatment of this subject is rather inadequate.

This Bureau of Standards publication affords a useful introduction to the subject of Underground Corrosion and its historical development.

Frank N. Speller

Fundamentals of Electronic Devices, by Karl R. Spangenberg. Published by McGraw-Hill Book Co., Inc., New York, 1957. 505 pages; $10.00.

This excellent book grew out of the attempt to develop an undergraduate text to serve as an introduction to electronic studies and, although pitched to the level of college seniors in physics or electrical engineering, it would make a good text for a first-year graduate course. Also covering as it does the physics of all electronic devices, instead of merely vacuum tubes, the book offers excellent background material for those who, while not electronics engineers, are nevertheless involved with electronics; chemists concerned with instrumentation, for example.

One outstanding merit in the treatment is the presentation of basic theory in the first third of the book, prior to the introduction of the main topic. Some 50 pages are devoted to a review of the properties of electrons, ions, electric and magnetic fields, and ions in motion in a vacuum. This is followed by a brief but pertinent survey of atomic theory, the solid state, and conduction in solids from the modern quantum mechanical point of view. The theoretical aspects of electron emission, vacuum tubes, and transistors comprise the middle third of the book, and the final portion utilizes these theoretical principles in generalized circuit applications. The latter section is in itself an excellent review of fundamental circuits for those already familiar with the subject. Separate chapters are devoted to photoelectricity and noise in electronic devices.

The author is to be commended for his correlating energy level theory of solids and its bearing on the practical aspects of emission, junction effects, and semiconductors. The analogous features of vacuum tubes and transistors are emphasized and the latest forms of transistors and photoelectric devices discussed.

The bibliography contains 242 references through February 1956. There are also 13 brief appendixes for the derivation of fundamental relationships such as the Fermi-Dirac distribution function. There are 229 excellent problems to which answers are not given. Format and presentation are up to the standard of the other books in the McGraw-Hill Electrical and Electronic Engineering Series.

Walter E. Miller

Inorganic Syntheses, Vol. V, by Therald Moeller. Published by McGraw-Hill Book Co., Inc., New York, 1957. 265 pages; $6.00.

The books in this series are not only invaluable to the researcher interested in obtaining a specific compound but are detailed enough to be used as lab manuals for an undergraduate course in inorganic preparations. The policy of having each procedure checked in an independent laboratory cannot be recommended too highly.

H. W. Salzberg

Thermodynamics for Chemical Engineers, Second Edition, by H. C. Weber and H. P. Meisner. Published by John Wiley & Sons, Inc., New York, 1957. 507 pages, $8.50.

This book has only 11 pages devoted to electrochemical topics, and the material in these pages is covered in greater detail in any good elementary physical chemistry text.

David Lewis

Handbook of Chemical Data. Edited by F. W. Atack. Published by Reinhold Publishing Corp., New York, 1957. 627 pages, $6.75.

This pocket-size handbook falls into the category of good ideas that do not quite work out. By cutting down on the page size, type size, and number of pages, the author achieves convenience, but only at the expense of completeness. Actually, a pocket-size handbook, like a pocket dictionary, while superficially attractive is not of much use to a professional chemist. Anyone with either laboratory or library space has room for a full-size handbook.

H. W. Salzberg

Literature from Industry

New Edition of Dow Products Catalog

Publication of the new 1957-58 edition of its general products catalog is announced by The Dow Chemical Co. This revision includes latest information on properties and uses of some 375 of Dow's basic industrial, pharmaceutical, and agricultural chemicals.

Copies of the general products catalog are available from Technical Service and Development, The Dow Chemical Co., Midland, Mich.

New Booklet on Peracetic Acid and Derivatives

A new 48-page booklet on "Peracetic Acid and Derivatives" has been issued by Union Carbide Chemicals Co., Div. of Union Carbide Corp. This booklet includes a treatise on peracetic acid, reactions of epoxides, and an extensive bibliography supporting these sections. It also lists properties and possible uses of 12 epoxides now available in research samples.

For copies of this booklet (Peracetic Acid and Derivatives; F-40,-108), write Union Carbide Chemicals Co., 30 E. 42 St., New York 17, N. Y.

Advertiser's Index

American Brass Company	62C-63C
Baker & Adamson, General Chemical Division, Allied Chemical & Dye Corporation	33C
Bell Telephone Laboratories, Inc.	32C
Enthone, Incorporated	Cover 4
Great Lakes Carbon Corporation	Cover 2
Stackpole Carbon Company	36C

Employment Situations

Please address replies to box shown, c/o The Electrochemical Society, Inc., 1860 Broadway, New York 23, N. Y.

Position Wanted

Chemist, inorganic, 11 years' experience: Electroplating (copper-acid, alkali; tin-acid, alkali; nickel; chromium), batteries, gelatines, glues, pyrotechny, general physical and chemical commercial testing, seeks position in New Jersey and environs; has held supervisory positions, experienced in analysis, capable of producing new ideas, anxious to forge ahead. *Reply to Box 363.*

Position Available

Required—Chemist with experience in fundamental research on electrode processes to lead battery research in industrial organization. *Reply to Box 999.*

The Electrochemical Society

Patron Members

Aluminum Co. of Canada, Ltd., Montreal, Que., Canada
International Nickel Co., Inc., New York, N. Y.
Olin Mathieson Chemical Corp., Niagara Falls, N. Y.
  Industrial Chemicals Div., Research and Development Dept.
Union Carbide Corp., Divisions:
  Electro Metallurgical Co., New York, N. Y.
  National Carbon Co., New York, N. Y.
Westinghouse Electric Corp., Pittsburgh, Pa.

Sustaining Members

Air Reduction Co., Inc., New York, N. Y.
Ajax Electro Metallurgical Corp., Philadelphia, Pa.
Allied Chemical & Dye Corp.
  General Chemical Div., Morristown, N. J.
  Solvay Process Div., Syracuse, N. Y. (3)
Alloy Steel Products Co., Inc., Linden, N. J.
Aluminum Co. of America, New Kensington, Pa.
American Machine & Foundry Co., Raleigh, N. C.
American Metal Co., Ltd., New York, N. Y.
American Platinum Works, Newark, N. J. (2)
American Potash & Chemical Corp., Los Angeles, Calif. (2)
American Zinc Co. of Illinois, East St. Louis, Ill.
American Zinc, Lead & Smelting Co., St. Louis, Mo.
American Zinc Oxide Co., Columbus, Ohio
Auto City Plating Co. Foundation, Detroit, Mich.
Bart Manufacturing Co., Bellville, N. J.
Basic Incorporated, Cleveland, Ohio
Bell Telephone Laboratories, Inc., New York, N. Y. (2)
Bethlehem Steel Co., Bethlehem, Pa. (2)
Boeing Airplane Co., Seattle, Wash.
Burgess Battery Co., Freeport, Ill. (4)
C & D Batteries, Inc., Conshohocken, Pa.
Canadian Industries Ltd., Montreal, Que., Canada
Carborundum Co., Niagara Falls, N. Y.
Catalyst Research Corp., Baltimore, Md.
Chrysler Corp., Detroit, Mich.
Columbian Carbon Co., New York, N. Y.
Columbia-Southern Chemical Corp., Pittsburgh, Pa.
Consolidated Mining & Smelting Co. of Canada, Ltd., Trail, B. C., Canada (2)
Continental Can Co., Inc., Chicago, Ill.
Cooper Metallurgical Associates, Cleveland, Ohio
Corning Glass Works, Corning, N. Y.
Cramet, Inc., Chattanooga, Tenn.
Crane Co., Chicago, Ill.
Diamond Alkali Co., Painesville, Ohio (2)
Dow Chemical Co., Midland, Mich.
Wilbur B. Driver Co., Newark, N. J. (2)
E. I. du Pont de Nemours & Co., Inc., Wilmington, Del.
Eagle-Picher Co., Chemical Div., Joplin, Mo.
Eastman Kodak Co., Rochester, N. Y.
Eaton Manufacturing Co., Stamping Div., Cleveland, Ohio
Electric Auto-Lite Co., Toledo, Ohio
Electric Storage Battery Co., Philadelphia, Pa.
The Eppley Laboratory, Inc., Newport, R. I. (2)
Federal Telecommunication Labs., Nutley, N. J.
Food Machinery & Chemical Corp.
  Becco Chemical Div., Buffalo, N. Y.
  Westvaco Chlor-Alkali Div., South Charleston, W. Va.
Ford Motor Co., Dearborn, Mich.
General Electric Co., Schenectady, N. Y.
  Chemistry & Chemical Engineering Component, General Engineering Lab.
  Chemistry Research Dept.
  Metallurgy & Ceramics Research Dept.
General Motors Corp., Guide Lamp Div., Anderson, Ind.
  Research Laboratories Div., Detroit, Mich.
  Brown-Lipe-Chapin Div., Syracuse, N. Y. (2)
Gillette Safety Razor Co., Boston, Mass.
Gould-National Batteries, Inc., Depew, N. Y.
Graham, Crowley & Associates, Inc., Chicago, Ill.
Great Lakes Carbon Corp., New York, N. Y.
Hanson-Van Winkle-Munning Co., Matawan, N. J. (3)
Harshaw Chemical Co., Cleveland, Ohio (2)
Hercules Powder Co., Wilmington, Del.
Hooker Electrochemical Co., Niagara Falls, N. Y. (3)
Houdaille-Hershey Corp., Detroit, Mich.
Hughes Aircraft Corp., Culver City, Calif.
International Business Machines Corp., Poughkeepsie, N. Y.
International Minerals & Chemical Corp., Chicago, Ill.
Jones & Laughlin Steel Corp., Pittsburgh, Pa.
K. W. Battery Co., Skokie, Ind.
Kaiser Aluminum & Chemical Corp.
  Chemical Research Dept., Permanente, Calif.
  Div. of Metallurgical Research, Spokane, Wash.
Keokuk Electro-Metals Co., Keokuk, Iowa
Libby-Owens-Ford Glass Co., Toledo, Ohio
P. R. Mallory & Co., Indianapolis, Ind.
McGean Chemical Co., Cleveland, Ohio
Merck & Co., Inc., Rahway, N. J.
Metal & Thermit Corp., Detroit, Mich.
Minnesota Mining & Mfg. Co., St. Paul, Minn.
Monsanto Chemical Co., St. Louis, Mo.
Motorola, Inc., Chicago, Ill.
National Cash Register Co., Dayton, Ohio
National Lead Co., New York, N. Y.
National Research Corp., Cambridge, Mass.
Norton Co., Worcester, Mass.
Olin Mathieson Chemical Corp., Niagara Falls, N. Y.
  High Energy Fuels Organization (2)
Pennsalt Chemicals Corp., Philadelphia, Pa.
Philips Laboratories, Inc., Irvington-on-Hudson, N. Y.
Pittsburgh Metallurgical Co., Inc., Niagara Falls, N. Y.
Poor & Co., Promat Div., Waukegan, Ill.
Potash Co. of America, Carlsbad, N. Mex.
Radio Corp. of America, Harrison, N. J.
Ray-O-Vac Co., Madison, Wis.
Raytheon Manufacturing Co., Waltham, Mass.
Reynolds Metals Co., Richmond, Va. (2)
Shawinigan Chemicals Ltd., Montreal, Que., Canada
Speer Carbon Co., International Graphite & Electrode Div., St. Marys, Pa. (2)
Sprague Electric Co., North Adams, Mass.
Stackpole Carbon Co., St. Marys, Pa. (2)
Stauffer Chemical Co., Henderson, Nev., and New York, N. Y. (2)
Sumner Chemical Co., Div. of Miles Laboratories, Inc., Elkhart, Ind.
Superior Tube Co., Norristown, Pa.
Sylvania Electric Products Inc., Bayside, N. Y. (2)
Sarkis Tarzian, Inc., Bloomington, Ind.
Tennessee Products & Chemical Corp., Nashville, Tenn.
Texas Instruments, Inc., Dallas, Texas
Titanium Metals Corp. of America, Henderson, Nev.
Udylite Corp., Detroit, Mich. (4)
Upjohn Co., Kalamazoo, Mich.
Victor Chemical Works, Chicago, Ill.
Wagner Brothers, Inc., Detroit, Mich.
Weirton Steel Co., Weirton, W. Va.
Western Electric Co., Inc., Chicago, Ill.
Wyandotte Chemicals Corp., Wyandotte, Mich.
Yardney Electric Corp., New York, N. Y.

How to make metal blackening an exact science: What metal do you have to blacken? Steel, copper, brass, zinc? There are seven Ebonol® compounds in Enthone's specially developed series of blackeners for you to call on for jet blackness, maximum wear resistance and adhesion. Enthone is exceptionally well equipped and qualified to assist you in all phases of metal finishing. Years of practical experience, extensive research and service laboratory facilities manned by a team of specialists in the finishing field are at your service. Write us about your needs or problems. Send a sample of your product in question, if possible. Enthone, Inc., 442 Elm St., New Haven 11, Conn.

ENTHONE

ENTHONE, INC. IS A SUBSIDIARY OF AMERICAN SMELTING AND REFINING COMPANY

58-2